NAUTICAL AND RISK STUDIES FOR THE DELIMARA LNG TERMINAL IN MARSAXLOKK PORT, MALTA

Additional metocean analysis

Final report

Report No. : 27689-7-MSCN-rev.2
Date : December 18, 2015

Signature management :

MARIN
P.O. Box 28

6700 AA Wageningen
The Netherlands

T +31 317 47 99 11
F +31 317 49 32 45

E mscn@marin.nl
I www.marin.nl

NAUTICAL AND RISK STUDIES FOR THE DELIMARA LNG TERMINAL IN MARSAXLOKK PORT, MALTA

Additional metocean analysis

Final report

Ordered by : ElectroGas Malta
Level 3, Portomaso Business Tower
Portomaso
STJ 4011 St Julian's
Malta

Document History

Revision	Status	Date	Reported by	Reviewed by
0	Draft	14 August 2015	ARCADIS	Jaap de Groot (ARCADIS) Johan Dekker (MARIN)
1	2nd Draft	16 September 2015	ARCADIS	Jaap de Groot (ARCADIS) Johan Dekker (MARIN)
2	Final	18 December 2015	ARCADIS	Jaap de Groot (ARCADIS) Johan Dekker (MARIN)

NAUTICAL AND RISK STUDIES FOR THE DELIMARA LNG TERMINAL IN MARSAXLOKK PORT, MALTA

ADDITIONAL METOCEAN ANALYSIS

MARIN

15 December, 2015
078630641:E - Final
C03051.000014.0200

ARCADIS

Contents

1 Introduction

1.1 PROJECT BACKGROUND

Enemalta is developing a new gas-fired power station near the existing Delimara Power Station on the north-eastern shore of Marsaxlokk Bay. The gas for the power plant will be imported through a new to build LNG terminal in Marsaxlokk Bay. Figure 1-1 shows the approximate position of the new terminal.

Figure 1-1: Marsaxlokk Port and approximate position of LNG terminal (source: Google Earth)

Enemalta has awarded the contract for design, construction and operation of the new power plant and LNG terminal to Electrogas Malta. The LNG terminal proposed by Electrogas consists of a jetty from the shore south of the power plant to a berth that is positioned where the bay is deeper, so that no or only limited dredging is required. On the jetty a converted LNG carrier will be permanently moored as Floating Storage Unit (FSU), delivering LNG through a cryogenic line over the jetty to the regasification unit onshore. The FSU berth has a conventional layout consisting of a platform, breasting dolphins and mooring dolphins (Figure 1-2). LNG will be imported by LNG carriers (further shortened to LNGCs) that will moor alongside the FSU.

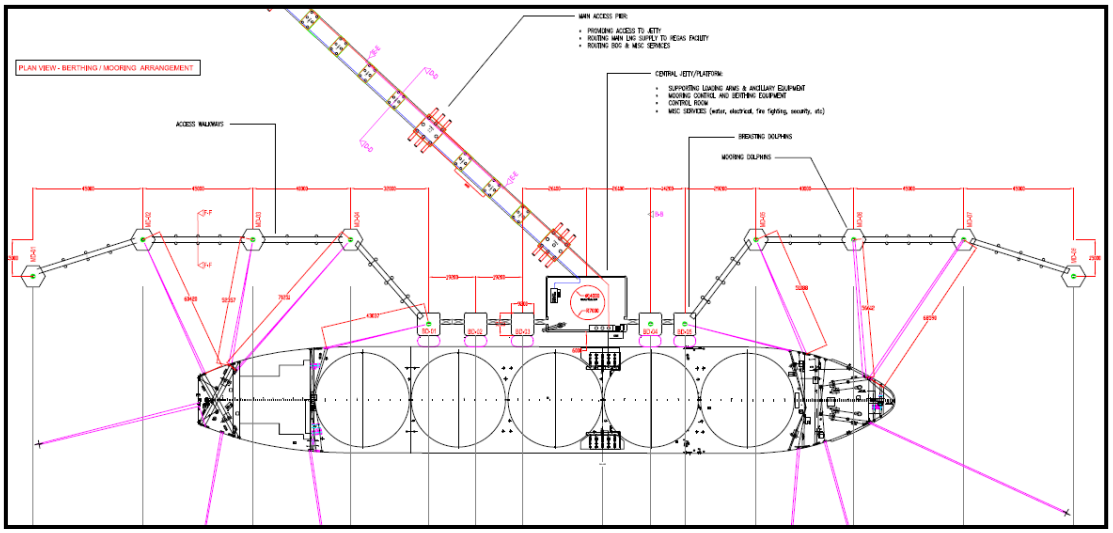

Figure 1-2: Proposed jetty configuration

To verify the design and evaluate safety aspects related to the permanent presence of the FSU in the port and to the regular call of LNGCs to the new LNG terminal, Enemalta has commissioned MARIN to carry out nautical and safety studies for the new LNG terminal. The study addresses a number of items raised by Transport Malta, the authority responsible for the port, who required:

1. Validation of proposed jetty/berth layout
2. Nautical and safety study
    a. Determine the required minimum navigation channel/fairway
    b. Determine the risk involved in the handling of an FSU and LNG carriers when navigating to the terminal
    c. Determine the nautical procedures for the handling of the FSU and LNGC during routine procedures and emergency situations
3. Site specific risk (safety) assessment including
    a. Cargo release
    b. Collision
    c. Fire and explosion
    d. Grounding

The contract for the study (Ref: DPS-GEN-1190) was signed on 25 August 2014 and is based on MARIN's proposal of 24 March 2014.

1.2 OBJECTIVES, APPROACH AND SCOPE OF WORK

Objective

The objectives of the present nautical and risk study for the Delimara LNG terminal are:

- To evaluate the dimensions of the manoeuvring area and port approach
- To determine the operational envelope for ship manoeuvres (input for nautical procedures);
- To evaluate the proposed jetty layout and to determine the limiting operational conditions for safe offloading and for staying safely at the berth (input for nautical procedures);
- To determine the risk involved in the LNG operations in the port regarding grounding of LNGCs and collisions involving FSU or LNGC,
- To determine the consequences (cargo release, fire and explosion) of incidents involving the FSU or an LNGC.

Approach

The above mentioned items are evaluated in this dedicated nautical and safety study for the Delimara LNG terminal. The study consists of the following items:

1. Wave climate study to determine the normal and extreme wave climate outside Marsaxlokk port (frequency of occurrence of directions and wave heights)
2. Wave penetration calculations to determine the wave conditions at the terminal
3. Numerical moored ship response simulations to validate the jetty/berth layout and determine operational limits for the moored FSU;
4. Real-time manoeuvring simulations to verify dimensions of the fairway and determine operational limits for sailing with LNG carriers;
5. Nautical risk study to determine the risks of grounding and collisions involving the FSU or LNG carrier
6. Quantitative Risk Assessment to determine the consequences of collisions in terms of cargo release and risk of fire and explosion

The wave studies (items 1 and 2), which serve as input for the nautical studies (items 3 and 4) were carried out by ARCADIS. Items 3 and 5 were carried out by MARIN. Item 4 was carried out by MARIN in cooperation with MMP (Malta Maritime Pilots) and MMRTC (Malta Maritime Research and Training Centre). SGS Tecnos SA carried out the QRA in item 6.

To support the design of the modifications to the FSU and the storm mooring for the FSU, some additional analysis was carried out for ElectroGas Malta on the data from the wave climate and wave penetration studies. This has been reported directly to EGM.

The additional metocean analysis is presented in this report and concerns the items presented in Table 1-1:

Joint occurrence extreme data for swell, wind sea, wind, and current (100-year extreme associated extremes) 95% confidence: ▪ 100 year Winter Storm - wind dominant ▪ 100 year Winter Storm – wind sea wave dominant ▪ 100 year Winter Storm – swell wave dominant ▪ 100 year Winter Storm - current dominant ▪ Separation of wind sea and swell with defined appropriate wave spectral model for each wave or swell component and associated spectral parameters ▪ Relative direction of wind sea, wind, swell, and current (at least an assessment of collinearity) ▪ Tp ranges (Hs-Tp envelopes) for more precise sensitivity assessment otherwise +/-15% of current design Tp's will be used. ▪ Precise current information and clarification of a current profile at the project site ▪ Fatigue sea-states

Table 1-1: Requested data

In this study only wave conditions at the location of the bow are evaluated. This location was selected because the conditions are most severe compared to other output locations. The coordinates of this location are 459712, 3964687 (UTM33) and the local water depth is 17.0 m +MSL. An exception is the wind data. The only available wind data is the offshore Oceanweather time series. The additional analysis of wind conditions is therefore performed on the offshore Oceanweather wind data [1].

Figure 1-3: Output locations

ARCADIS used the separation between wind sea and swell, as given in the offshore Oceanweather time series, as input for the wave studies carried out. Wind sea and swell were propagated separately to the project site. At the project site, the operational wind sea and swell waves have been combined into a total sea state for the entire offshore time series. The time series of wind sea and swell waves separately (i.e. before combination), will be used as input for the wave analyses in this report.

To obtain information on the current velocities, a desk study is performed in which a review of available sources on current conditions inside Marsaxlokk Bay is made and compared to the wave orbital velocities. Since during the desk study it was found that no information was available on the water circulation (current velocities) inside the bay during extreme events, some Delft3D computations were carried out to get a first estimate on the magnitude of the current velocities.

Note
In the wave penetration report [2], results were presented at various output locations along the jetty (see Figure 1-3). During extreme storm conditions the FSU will be shifted to a location 70 m west of the jetty. At this location the height and direction of the wave and thus forces on the spread mooring system may be different. Based on the wave simulation effort already carried out the spatial variation has been qualitatively evaluated based on figures showing the spatial distribution of the significant wave height.

1.3 REPORTS

The total study is presented in a series of reports, each one treating one of the above mentioned study items. Table 1-2 gives an overview of the reports presenting the results of the study.

Volume	Title	Main author
27689-1-MSCN	Item 1: Wave climate study	ARCADIS
27689-2-MSCN	Item 2: Wave penetration study	ARCADIS
27689-3-MSCN	Item 3: Moored ship response study	MARIN
27689-4-MSCN	Item 4: Real-time manoeuvring simulations	MARIN
27689-5-MSCN	Item 5: Nautical risk study	MARIN
27689-6-MSCN	Item 6: Nautical Quantitative Risk Assessment	SGS Tecnos

Table 1-2: Overview of reports

To support the design of the modifications to the FSU and the storm mooring for the FSU, some additional analysis was carried out for ElectroGas Malta on the data from the wave climate and wave penetration studies. This analysis is presented in this report.

1.4 THIS REPORT

This report describes the approach and results of the additional metocean analysis carried out. The structure of the report is as follows:

- Chapter 1 provides the project background, objectives and scope of work;
- Chapter 2 discusses the study approach and the different types of wave loads;
- In Chapter 3 the directional extremes of offshore all-year wind speed, wind sea and swell significant wave height are determined;
- Then, for each of these parameters, the most likely values of a series of associated parameters are derived in Chapter 4;
- In Chapter 5 the difference between wind sea waves penetrating through the entrance of Marsaxlokk Bay and waves generated by wind inside Marsaxlokk Bay, are discussed;
- Chapter 6 gives a description of the spectral shape of the waves;
- Chapter 7 presents the results of the collinearity analysis.
- Fatigue sea states are presented in Chapter 8;
- Chapter 9 discusses the current velocities and directions inside Marsaxlokk Bay and at the location of the jetty;
- The variation of wave heights between the location of the jetty and the spread mooring system is given in Chapter 10;
- Finally, in Chapter 11 the conclusions and recommendations are given.

1.5 CONVENTIONS AND DEFINITIONS

Units

All parameters and variables have units according to the international SI conventions except where explicitly stated.

Coordinate Systems

All the coordinates given in this report are provided in Universal Transverse Mercator zone 33N (WGS 84) unless otherwise stated. The vertical datum used for the bathymetry and different levels is Chart Datum unless otherwise stated.

Notations

The following notations are used in this report:

. Decimal point; 1.5 means "one and a half".

, Digit grouping symbol; 12,000,000 means "12 million".

E Scientific notation with the exponent of 10; 1.2E-2 means "twelve thousandth"

Directions

Unless otherwise stated, wind and wave directions are given according to the nautical convention. For winds and waves, they refer to the direction from which they are coming in degrees, measured clockwise with respect to the North. For example, a wave direction of 90 degrees means the waves are coming from the East. Directional sectors have a width of 30° and are indicated by their middle directions. The directional sector 30°N for instance indicates directions between 15°N and 45°N.

Directional spreading

The directional spreading is given in terms of the (model free) directional spreading in degrees or in terms of the directional spreading factor m based on the $\cos^m(\theta/2)$ model. See Appendix 1 for definitions.

Current conditions

Current conditions are expressed as orthogonal components of the speed vector. The u component is defined as positive eastwards and the v component as positive northwards.

Wind and wave parameters

The definitions of the wind and wave parameters are listed in Appendix 1.

Locations

Unless otherwise stated, the offshore is the location near the entrance of the bay.
Unless otherwise stated, the nearshore is the location at the bow of the FSU moored at the jetty.

2 Design environmental conditions

2.1 DESIGN CONDITIONS IN PREVIOUS REPORTS

In the previous metocean study [1], yearly averaged directional extreme wind and wave design conditions have been established at the offshore location. At this location (35°45'N, 14°37'30''E), a 33 year time series of 1-hourly wind and wave parameters was purchased from Oceanweather based on their GROW FINE MED database. Extreme offshore all-year wind speeds and significant wave heights were established for directional sectors of 30° width and return periods of 1 in 1, 5, 10, 25, 50 and 100 years. Associated integral wave parameters (peak wave period) and spectral parameters (spectral peakedness and directional spreading) were determined.

The extreme conditions were propagated towards the entrance of Marsaxlokk Bay using the wave model SWAN [1] and consequently into Marsaxlokk Bay with the wave model MIKE21BW [2]. The corresponding nearshore wave conditions are presented as representative 100 year design conditions. In these computations, the effect of locally generated waves in the bay was not included. In this approach, it is assumed that the 1/100 year wind speed and 1/100 year significant wave height for a specific directional sector occur simultaneously. This is a pragmatic, but conservative assumption because the probability of both extreme conditions occurring simultaneously is expected to be less than 1/100 years.

For the determination of less conservative joint extreme conditions, it is advised to determine them on the basis of the nearshore time series which have been established in the previous studies using the wave transformation matrix approach. More details on this approach can be found in Chapter 3.3.1 of the ARCADIS wave climate study report [1]. In the previous wave penetration study [2], it was found that the results of both methodologies (transformation of offshore extreme or extreme analysis based on transformed time series) provide similar results for the extreme wave conditions. Therefore, the present study is based on an analysis of the nearshore time series at the bow location.

In the wave penetration report [2], the omnidirectional nearshore extreme values for the combined (wind sea and swell) significant wave heights at the bow are presented. These results are conservative as it is assumed that different extreme conditions occur simultaneously. More realistic design conditions can be derived by accounting for joint probabilities. This approach is outlined in the following sections.

2.2 STUDY APPROACH

The objective of the present additional metocean analyses (this report) is to provide a detailed description of the results that can be used to determine environmental conditions for the design of the mooring system. Key to selecting suitable (viz. less conservative) design environmental conditions is representing the entire range of possibly occurring conditions for a restricted set of loading cases.

To reduce conservativism (introduced by assuming that different extremes occur simultaneously) we followed a different approach in which we determined the most probable relation between simultaneously occurring wind, wave and current conditions. Firstly, the directional extremes of offshore all-year wind speed, wind sea and swell significant wave height (marked by black outlines around their boxes in Figure 2-1) are determined (Chapter 3). In the following we consider these parameters as primary parameters. Secondly, for each of these parameters, the most likely values of a series of associated parameters are subsequently determined. For instance for the extreme wind speeds, the associated wind sea and swell significant wave height and peak wave period are determined. In this manner, a larger set of extreme conditions is obtained since the extrapolated extremes are no longer assumed to occur at the same moment in time.

In Figure 2-1, a schematic overview is presented of the various environmental conditions which are evaluated in this study. Each of the environmental conditions is described by a series of parameters. Wind conditions are described in terms of wind speed and direction. Wave conditions are expressed in terms of significant wave height, peak wave period and mean wave direction. Current conditions are described by orthogonal components of the speed vector.

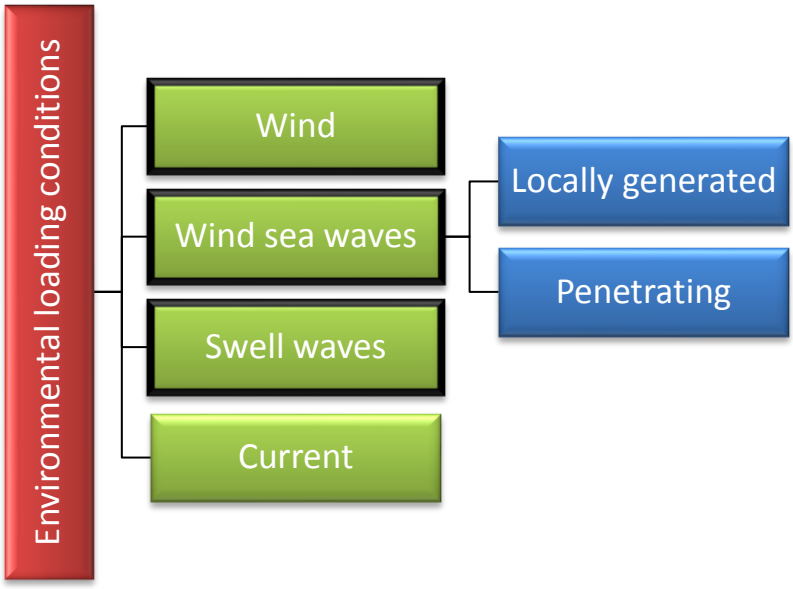

Figure 2-1: Schematic presentation of environmental parameters.

Between some of the evaluated environmental parameters, a distinct correlation exists. Wind sea directions are for example closely related to the wind conditions because it reflects their physical relationship. For such parameters, the full range of occurring conditions can be described by a restricted set of loading cases. For poorly related parameters, more combinations should be evaluated to investigate the full range of occurring conditions. Swell waves for instance are, by definition, not related to the wind and wind sea wave conditions.

The relation between parameters is initially investigated in Chapter 4. In this chapter a general methodology is followed which involves making scatter plots of combinations of parameters and fitting a suitable function to the scattered data. In the subsequent chapters (Chapters 5 - 8) various relations between parameters are investigated in more detail. Finally, in Chapter 10, the results are combined and recommendations for their application are made.

2.3 DIFFERENT TYPES OF WAVE LOADS

It is noted that three types of wave loads are discerned in this report. The first distinction is made between wind sea and swell waves. A further distinction for wind sea wave conditions at the project site is made into locally generated and penetrating wind sea waves. For a proper representation of the combined impact of all types of wave loads, the contributions of all types of wave loads should be included in the evaluation of the design of the mooring system. This can be done for instance by using a multi-peaked wave spectrum.

All throughout the report, a distinction is made between swell and wind sea waves, consistent with the previous wave studies [1], [2]. In Chapter 5, a detailed analysis of the separate components of locally generated and penetrating wind sea waves is presented. All other chapters in this report are concerned with the combined wind sea significant wave height.

3 Nearshore extreme conditions

3.1 INTRODUCTION

In this chapter, the derivation of extreme offshore wind and nearshore wind sea and swell wave conditions is presented. In Chapter 3.2, the followed methodology is explained in detail. In Chapters 3.3 the results for all-year directional extreme conditions are presented. In Chapter 3.4 the monthly omnidirectional extreme conditions are presented.

3.2 METHODOLOGY

To determine directionally extreme conditions and their confidence intervals from a time series the following steps are taken:

1. Data selection to obtain peak values
2. Fitting an extreme value probability distribution
3. Estimation confidence intervals using a bootstrap method

1. Data selection

First, all data in the considered directional sector (based on the wind or mean wave direction) and/or period (year, season, month, etc.) are selected.

A peak-over-threshold (POT) approach is then used for the selection of independent storm peaks in the time series. For the POT method, the maximum (wind speed or significant wave height) peaks above a selected threshold value are selected. To ensure independence of storm peaks only the highest peak in a time window of 96 hours, centred on this peak, is selected. As an example, the selected peaks for wind speeds exceeding 10 m/s in the year 2003 (omnidirectional) are presented in Figure 3-1.

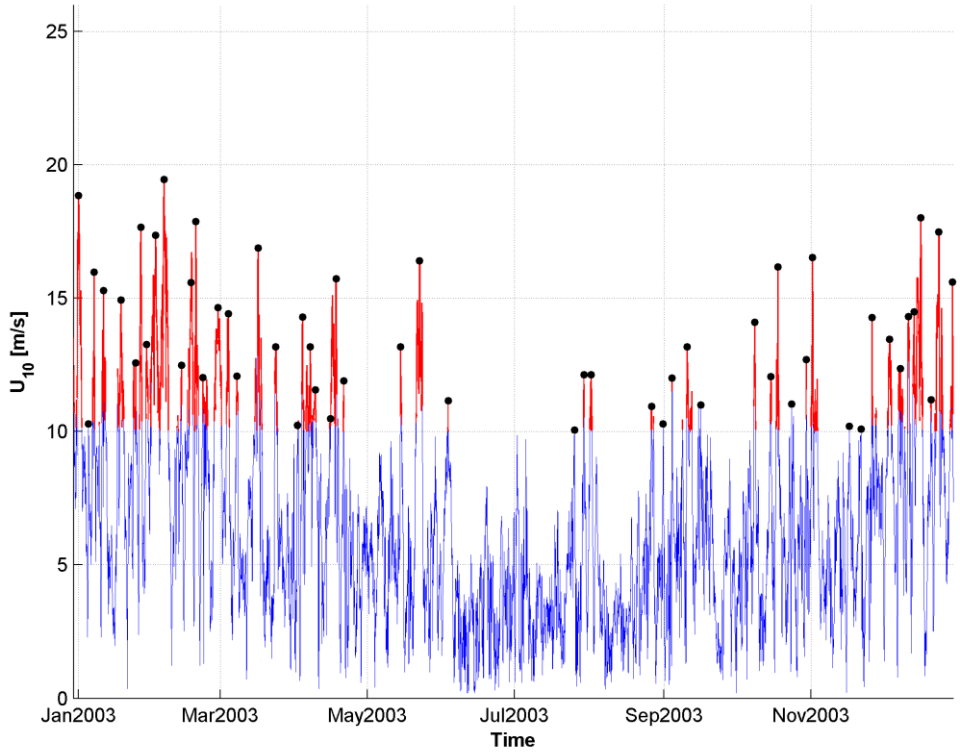

Figure 3-1: Example of peak-over-threshold filtering of wind speeds in m/s

The threshold value is chosen such that the only the most severe storm conditions are included in the data selection, while sufficient data is included to establish a reliable fitting of the probability of exceedance. As most of the peaks are related to winter storms, applying a threshold makes the resulting extreme conditions representative for winter events.

If less than 20 peaks are available in the considered directional sector and period, given the selected threshold value, no reliable estimate of the extreme values can be determined and no results are presented. This is for instance the case for nearshore significant wave height in directional sectors 0°N – 150°N. A lower threshold is selected in some occasions to increase the number of selected peaks to allow fitting. The selected thresholds for significant wave heights are between 1.50 and 0.75 m (increments of 0.25 m). The threshold value for wind speeds is 10 m/s.

The time window of 96 hr is based on an evaluation of a series of storms. In Figure 3-2, the build-up of the ten storms with the highest wind speeds in the offshore Oceanweather time series are presented. The wind speed during a period of 96hr around the maximum is divided by the maximum value. In this manner, the build-up of large storms can be easily compared. The figure shows that the selected time window is appropriate for storms in the project area, as the storm evolution from build up to subsequent decay is observed within this time frame.

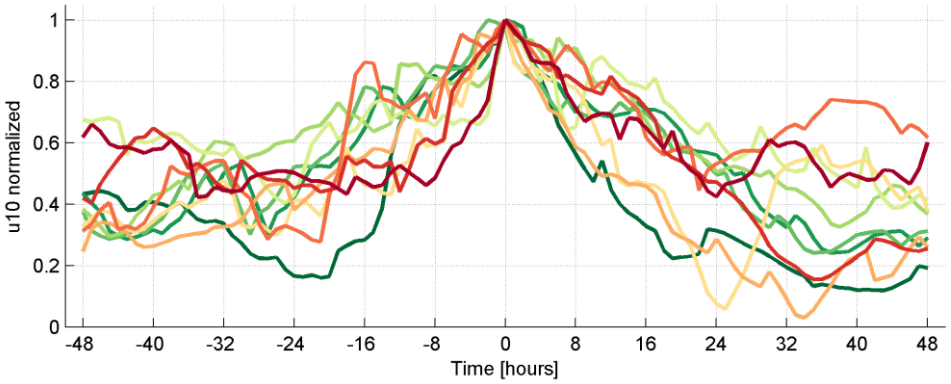

Figure 3-2: Build-up of the ten offshore storm conditions with the highest wind speeds in the offshore time series

2. *Fitting an extreme value probability distribution*

The extreme conditions are derived based on a statistical extrapolation of the selected peaks in the OCEANWEATHER time series. This is done by fitting a Weibull probability distribution function to the selected data. From our previous studies, the Weibull distribution has been proven to be a robust model for fitting the extreme event distributions. The Weibull distribution has the following formulation:

$$p(\bar{x} > x|\theta) = p_0 e^{-\left(\frac{x-a}{b}\right)^c}$$

With:

x = parameter to be extrapolated, such as wind speed or significant wave height
θ = wave direction
p_0 = normalisation parameter
a = location parameter
b = scaling parameter
c = shape parameter

The Weibull distribution fit is optimized for three parameters: b, c and p_0. The location parameter (a) is considered fixed and is assigned a value 0.

3. *Bootstrap*

Bootstrapping is a resampling method which allows assessing confidence intervals of return periods, making use of the original data. Bootstrapping can be applied in different ways. For instance, regular bootstrapping randomly takes samples with replacement from the dataset until a new set is created of the same size as the original dataset. This process is repeated until a large number of bootstrap-datasets is created, after which a statistical analysis is performed on the meta-data.

Instead of using the regular bootstrap, we applied the parametric bootstrap method as this method is more suited to estimate confidence bands. This is because the number of redrawn samples is not restricted to the number of samples in the original data, thus creating more accurate estimates of confidence intervals.

In the parametric bootstrap samples are drawn based on the Weibull distribution fitted on the original dataset. For each bootstrap-dataset a new Weibull fit is made. This process is repeated 10.000 times resulting in 10.000 bootstrap-Weibull fits. For each of the Weibull fits the values are calculated for several requested return periods, returning 10.000 values for each return period. As boundaries of the 95%

confidence interval, the 2.5% and 97.5% percentile scores are selected. This process is illustrated in Figure 3-3 for an all-year wind sea significant wave height. For higher the return periods the confidence band is wider.

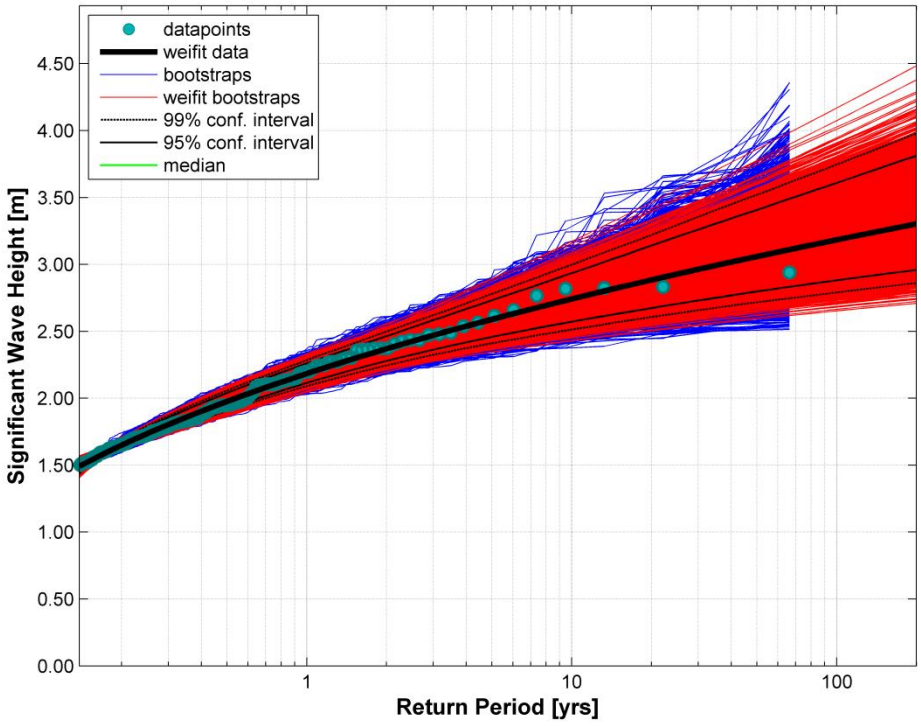

Figure 3-3: Example figure showing the original selected peaks (green dots) and fitted Weibull distribution (thick black line), 10000 bootstrap-datasets (blue lines) with corresponding Weibull fits (red lines) and resulting confidence intervals (thin black lines).

3.3 ALL-YEAR DIRECTIONAL EXTREMES

3.3.1 WIND SPEED

The offshore all-year extreme wind speeds are determined per directional bin using a threshold of 10 m/s. The corresponding number of peaks and the numerical results for a 1/100 year return period are presented in Table 3-1. In Figure 3-4 the directional variation of the results for a return period of 1/100 years and their 95% confidence values are presented.

Offshore direction [°N]	Threshold [m/s]	Nr of peaks [-]	best fit [m/s]	low 95% conf [m/s]	high 95% conf [m/s]
0	10.0	148	25.9	20.7	31.2
30	10.0	181	25.2	21.7	30.2
60	10.0	220	23.1	20.6	26.5
90	10.0	228	21.1	19.4	23.5
120	10.0	303	20.4	19.0	22.2
150	10.0	332	21.9	20.1	24.2
180	10.0	269	20.0	18.1	22.3
210	10.0	197	20.7	17.8	23.5
240	10.0	297	21.4	19.7	23.6
270	10.0	572	25.4	23.8	27.3
300	10.0	1212	25.0	23.9	26.2
330	10.0	760	24.4	22.8	26.4
omni	10.0	1950	26.1	25.1	27.2

Table 3-1: Applied threshold values, corresponding number of peaks and the offshore all-year extreme wind speeds in m/s for a return period of 1/100 years for various directional sectors.

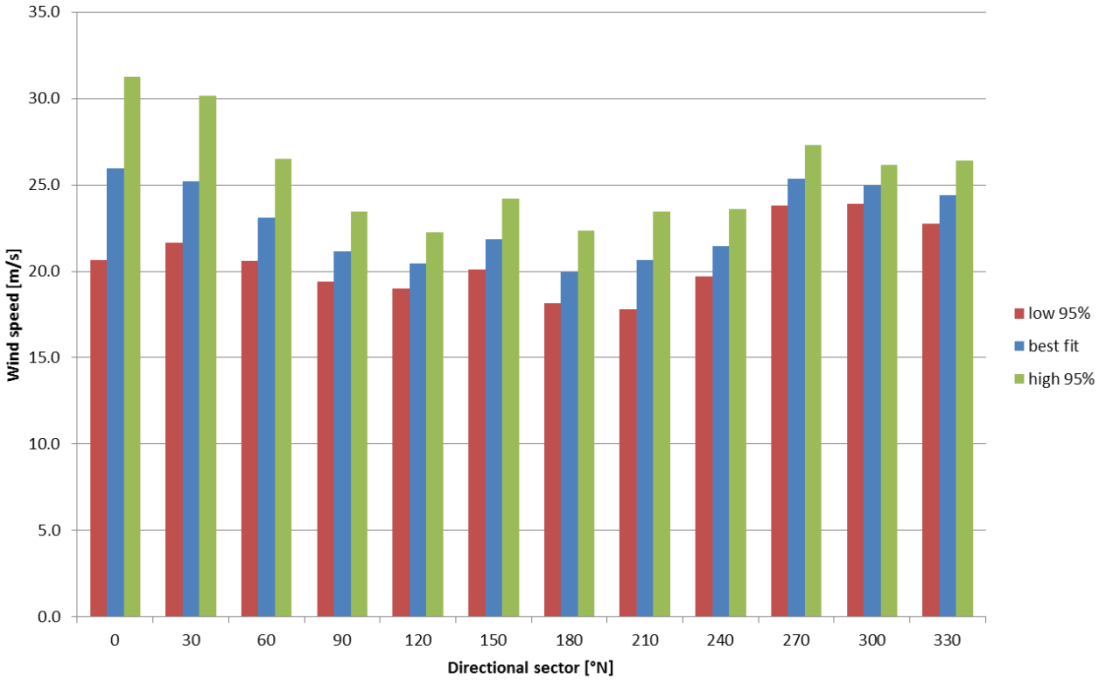

Figure 3-4: Offshore all-year extreme wind speeds in m/s and corresponding 95% confidence interval limits for various directional sectors and 1/100 year return period.

The largest extreme wind speeds occur in directional sector 0°N, being 25.9 m/s for a 1/100 year return period. The width of the confidence intervals is also largest for this direction sector. This is due to the relative low number of peaks that is selected for the Weibull fit. The lowest extreme wind speeds are expected in directional sector 180°N.

The results for the best fit are identical to those in the prior wave climate study [1][1] but now the confidence intervals have been added. The extreme wind speed conditions and their confidence intervals for all directional sectors and return periods are presented in Appendix 2.1. The figures showing the selected data, fitted Weibull functions and confidence intervals graphically are also presented in Appendix 2.1.

[1] The results for directional sector 0°N are slightly different from those presented in the Wave climate study report [1]. This is due to a minor improvement in our post-processing routines. This improvement increases the accuracy of the Weibull fits while it results in slightly more conservative results. The modification only affects the results for 0°N in this study.

Those figures show that the quality of the fits is good and most of the higher data points are within the confidence intervals.

3.3.2 WIND SEA SIGNIFICANT WAVE HEIGHT

To determine the nearshore extreme wind sea significant wave height, the corresponding nearshore mean wave directions is used for the selection of data that belongs to the considered directional bin. The selected threshold values are between 0.75 and 1.5 m in order to obtain a sufficiently large number of peaks. For some directions, not enough data is available to determine reliable extreme values. This is very well explained from the sheltering effect of the coastline. The selected thresholds, the corresponding number of peaks and the numerical results for a 1/100 year return period are presented in Table 3-2. In Figure 3-5 the variation of the results for a return period of 1/100 years is presented graphically.

Nearshore direction [°N]	Threshold [m]	Nr of peaks [-]	best fit [m]	low 95% conf [m]	high 95% [m]
0	1.00	0	-	-	-
30	1.00	0	-	-	-
60	1.00	0	-	-	-
90	1.00	0	-	-	-
120	1.00	0	-	-	-
150	1.00	0	-	-	-
180	1.50	225	3.17	2.86	3.59
210	1.50	28	2.85	2.24	3.68
240	1.00	83	1.68	1.54	1.89
270	0.75	137	1.33	1.20	1.49
300	1.00	18	-	-	-
330	1.00	0	-	-	-
omni	1.50	238	3.19	2.88	3.61

Table 3-2: Applied threshold values, corresponding number of peaks and the nearshore all-year extreme wind sea significant wave heights in m for a return period of 1/100 years for various directional sectors The red number indicate directional sectors for which too few peaks are available for a reliable extreme values.

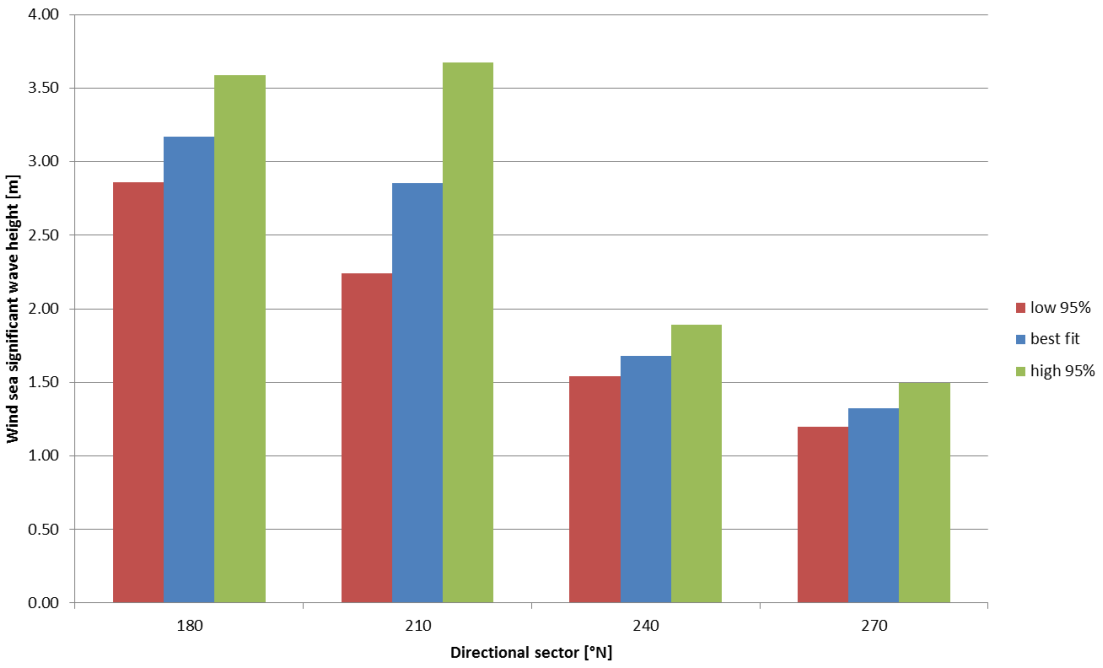

Figure 3-5: Nearshore all-year extreme wind sea significant wave heights in m and corresponding 95% confidence interval limits for various directional sectors and 1/100 year return period.

The largest extreme wind sea significant wave height occurs for directional sector 180°N, being 3.17 m for a 1/100 year return period, followed closely by 210°N. For other directional sectors, the geometry causes sheltering from penetrating waves or prohibits the generation of local waves. The confidence intervals are widest for 210°N, which is caused by the lower number of available peaks.

The extreme wind sea significant wave height conditions and their confidence intervals for all directional sectors and return periods are presented in Appendix 2.2. Figures showing the selected data, fitted Weibull functions and confidence intervals graphically are presented in the same appendix. Those show that the quality of the fits is good and all of the higher data points are within the confidence intervals.

3.3.3 SWELL SIGNIFICANT WAVE HEIGHT

The nearshore swell wave conditions are determined with SWAN and MIKE21BW wave models, as described in the wave climate study and wave penetration study reports [1] and [2]. The nearshore swell wave climate is merely the result from swell wave penetration from the Mediterranean Sea into Marsaxlokk Bay since no wind was included in the simulations.

To determine the nearshore extreme swell significant wave height, the corresponding nearshore mean wave directions is used for the selection of data that belongs to the considered directional bin. The selected threshold values are between 0.75 and 1.0 m in order to obtain a useful number of peaks. For all but two directions, not enough data is available to determine reliable extreme values. The fact that the penetration of swell waves depends more strongly on the geometry, explains that even fewer directions compared to the wind sea need to be evaluated. The selected thresholds, corresponding number of peaks and extreme swell significant wave heights for a 1/100 year return period are presented in Table 3-3. In Figure 3-6 the variation of the results for a return period of 1/100 years is presented.

Nearshore direction [°N]	Threshold [m]	Nr of peaks [-]	best fit [m]	low 95% conf [m]	high 95% [m]
0	0.75	0	-	-	-
30	0.75	0	-	-	-
60	0.75	0	-	-	-
90	0.75	0	-	-	-
120	0.75	0	-	-	-
150	0.75	0	-	-	-
180	1.00	122	2.04	1.72	2.40
210	0.75	60	1.27	1.19	1.41
240	0.75	0	-	-	-
270	0.75	0	-	-	-
300	0.75	0	-	-	-
330	0.75	0	-	-	-
omni	0.75	595	2.02	1.73	2.21

Table 3-3: Applied threshold values, corresponding number of peaks and the nearshore all-year extreme swell significant wave heights in m for a return period of 1/100 years for various directional sectors The red number indicate directional sector for which too few peaks are available for a reliable extreme values.

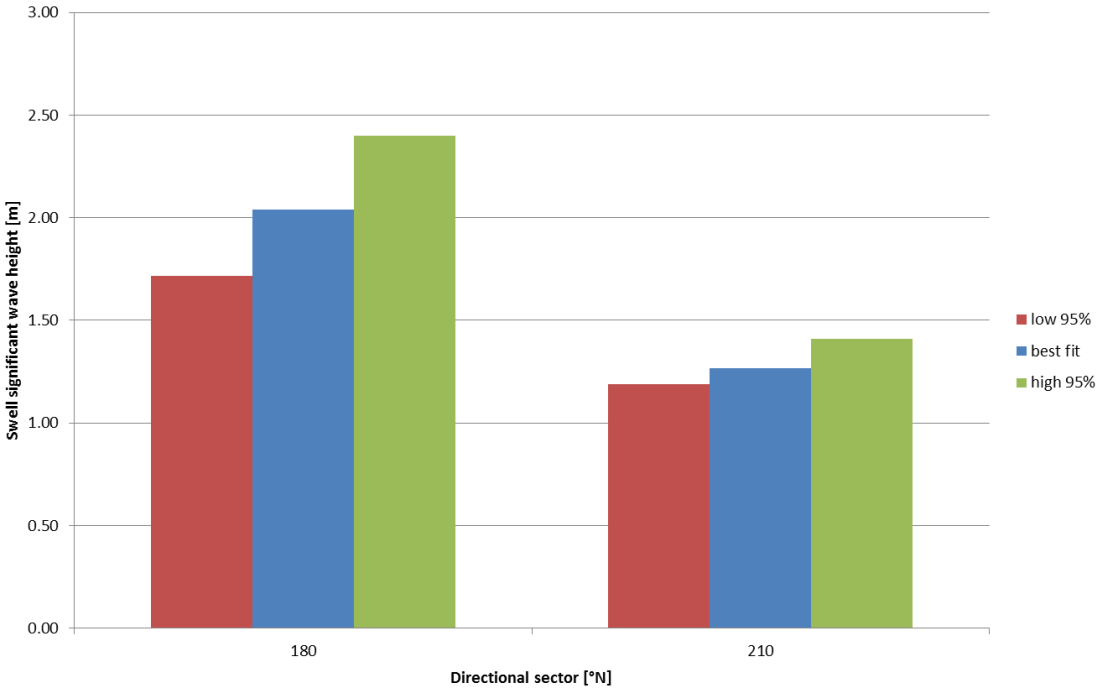

Figure 3-6: Nearshore all-year extreme swell significant wave heights in m and corresponding 95% confidence interval limits for various directional sectors and 1/100 year return period.

The extreme swell significant wave heights are largest for directional sector 180°N (2.10 m for a 1/100 year return period). It is noted that for the wind sea waves, the largest extreme significant wave height is for the same directional sector.

The extreme swell significant wave height conditions and their confidence intervals for all directional sectors and return periods are presented in Appendix 2.3. Figures showing the selected data, fitted Weibull functions and confidence intervals graphically are presented in the same appendix. Those figures confirm a good quality of the fits.

3.4 MONTHLY OMNIDIRECTIONAL EXTREMES

To investigate the seasonal variation of extreme wind and wave conditions, a second series of extreme values has been established. In this series, data has been selected per month. To restrict the number of results, this analysis has been done for omnidirectional results only. As seen in Chapter 3.3, for nearshore waves, this choice will not have a big influence on the applicability of the results since most waves directions are confined to southwest directions. The wind results should be interpreted with extra care since winds from different directions (but occurring in the same month) may have a completely different effect at the jetty.

3.4.1 WIND SPEED

A threshold value of 10 m/s is applied, consistent with the prior wave studies and Chapter 3.3. The corresponding number of peaks and the extreme wind speeds for a return period of 1/100 years are listed in Table 3-4. In Figure 3-7 the extreme wind speeds for a return period of 1/100 years are presented as well.

Period	Threshold [m/s]	Nr of peaks [-]	best fit [m/s]	low 95% conf [m/s]	high 95% conf [m/s]
Jan	10.0	222	25.8	23.6	28.3
Feb	10.0	210	25.2	23.4	27.5
Mar	10.0	217	24.0	22.1	26.2
Apr	10.0	198	20.1	19.2	21.4
May	10.0	147	20.8	19.0	23.2
Jun	10.0	105	18.2	16.9	20.1
Jul	10.0	84	19.3	18.0	21.3
Aug	10.0	70	17.2	16.4	18.7
Sep	10.0	106	17.0	16.4	18.3
Oct	10.0	148	20.5	18.8	23.0
Nov	10.0	210	21.1	19.9	22.6
Dec	10.0	233	25.1	23.3	27.3
All Year	10.0	1950	26.1	25.1	27.2

Table 3-4: Applied threshold values, corresponding number of peaks and the offshore omnidirectional extreme wind speeds in m/s for a return period of 1/100 years for various months.

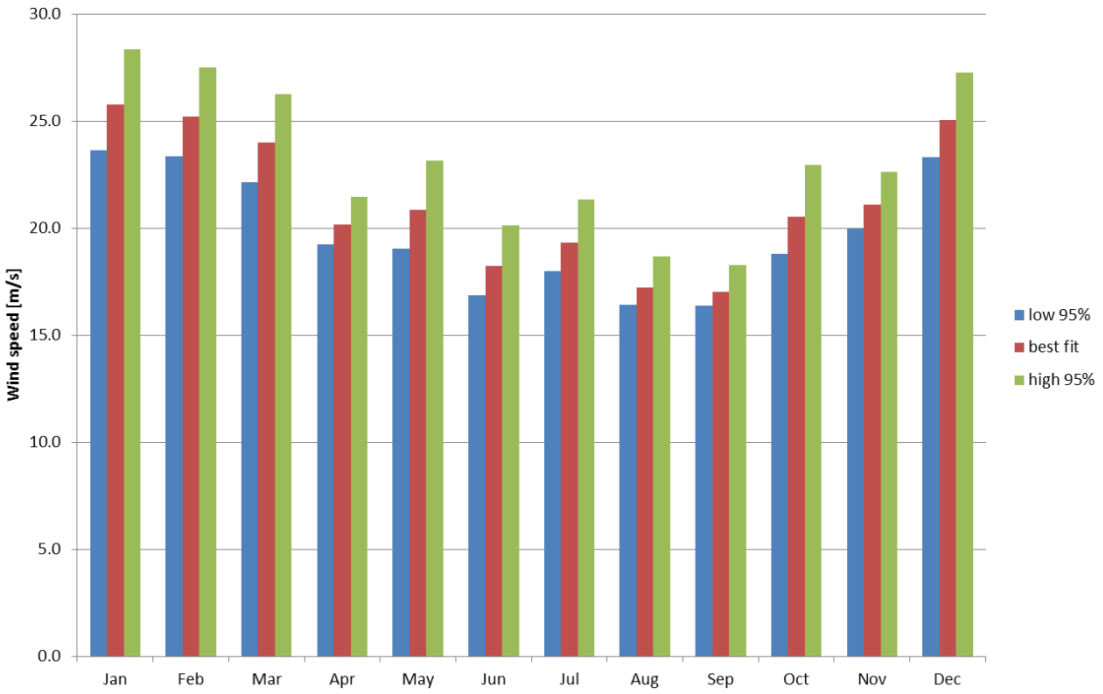

Figure 3-7: Offshore omnidirectional extreme wind speeds in m/s and corresponding 95% confidence interval limits for various months and 1/100 year return period.

The results clearly indicate that in winter, the highest extreme wind speeds are to be expected. For a 1/100 year return period, the extreme wind speed in January is 25.8 m/s, while in September it is as low as 17.0 m/s. The width of the confidence intervals varies from month to month. There does not seem to be a strong relation to the number of peaks.

The extreme wind speed conditions and their confidence intervals for all months and return periods are presented in Appendix 3.1. The figures showing the selected data, fitted Weibull functions and confidence intervals graphically are also presented in that appendix. Those figures show that the quality of the fits is good and all of the higher data points are within the confidence intervals.

3.4.2 WIND SEA SIGNIFICANT WAVE HEIGHT

The selected threshold value for wind sea significant wave heights is 1.0 m for each month. The corresponding number of peaks and the extreme wind sea significant wave heights for a return period of 1/100 years are presented in Table 3-5. For two months in summer (July and August), insufficient peaks are available. In Figure 3-7, the extreme wind sea significant wave heights for a return period of 1/100 years are presented.

Period	Threshold [m]	Nr of peaks [-]	best fit [m]	low 95% conf [m]	high 95% [m]
Jan	1.00	88	3.11	2.55	3.93
Feb	1.00	81	2.88	2.36	3.63
Mar	1.00	80	2.86	2.43	3.49
Apr	1.00	87	2.61	2.33	2.99
May	1.00	53	3.03	2.27	4.05
Jun	1.00	20	2.22	1.62	3.38
Jul	1.00	5	-	-	-
Aug	1.00	4	-	-	-
Sep	1.00	35	2.14	1.75	2.66
Oct	1.00	61	2.20	1.96	2.52
Nov	1.00	101	2.85	2.44	3.44
Dec	1.00	112	3.08	2.49	3.95
All Year	1.50	238	3.19	2.88	3.61

Table 3-5: Applied threshold values, corresponding number of peaks and the nearshore omnidirectional extreme wind sea significant wave heights in m for a return period of 1/100 years for various months The red number indicate directional sector for which too few peaks are available for a reliable extreme values.

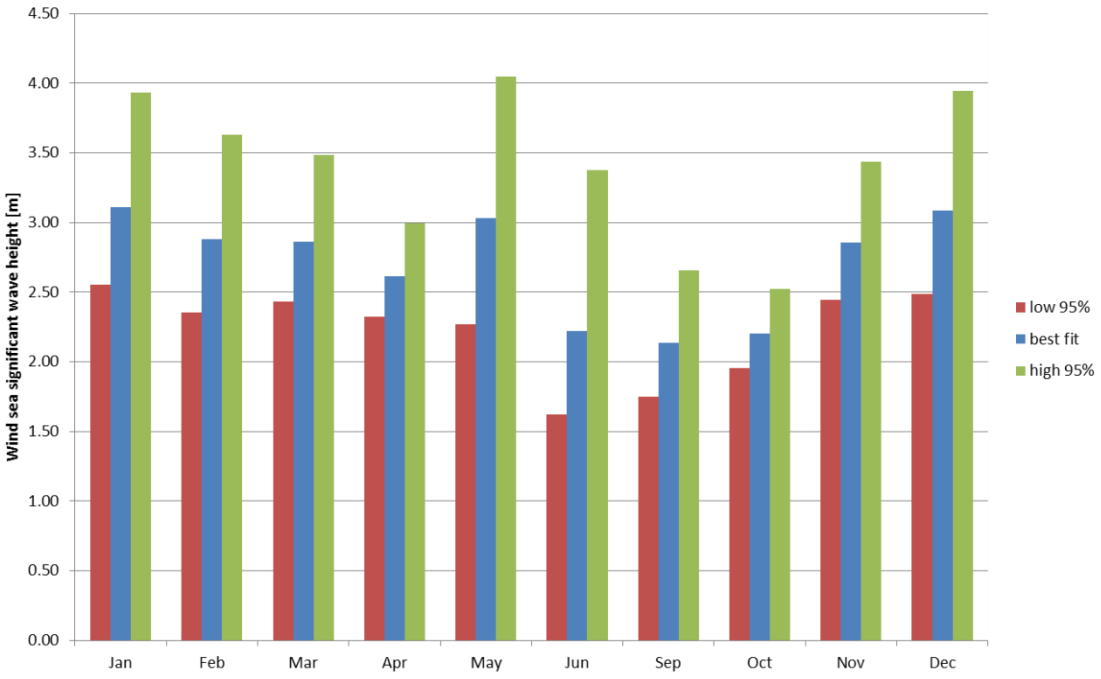

Figure 3-8: Nearshore omnidirectional extreme wind sea significant wave height in m and corresponding 95% confidence interval limits for various months and 1/100 year return period.

The results clearly indicate that in winter, the highest extreme wind sea significant wave heights are to be expected. However, the differences between months are not as clear as for the wind speeds. This may in part be due to the omission of the months July and August which are likely to experience even less extreme wind sea conditions.

The highest extreme wind sea significant wave heights occur in January and December. The results for the month May are higher than those for April and June. Although this seems surprising at first, the highest observed peak in the month May (with a corresponding probability of occurrence of approximately 1/70 years) is 2.95 m. A corresponding extreme value of 3.03 m for a 1/100 year return period seems reasonable. The figures of the selected peaks and fitted Weibull functions in Appendix 3.2 confirm that the results for May (and other months) look reliable. The extreme wind speed conditions and their confidence intervals for all months and return periods are also presented in Appendix 3.1.

3.4.3 SWELL SIGNIFICANT WAVE HEIGHT

The selected threshold value for swell significant wave heights is 0.75 m for each month. The corresponding number of peaks and extreme swell significant wave heights are presented in Table 3-6. For two months in summer (July and August), insufficient peaks are available. In Figure 3-9 the extreme swell significant wave heights for a return period of 1/100 years is presented.

Period	Threshold [m]	Nr of peaks [-]	best fit [m]	low 95% conf [m]	high 95% [m]
Jan	0.75	48	1.75	1.39	2.26
Feb	0.75	63	1.43	1.22	1.68
Mar	0.75	71	1.66	1.31	2.05
Apr	0.75	77	1.51	1.29	1.79
May	0.75	52	1.63	1.25	2.01
Jun	0.75	21	1.43	1.09	1.94
Jul	0.75	8	-	-	-
Aug	0.75	10	-	-	-
Sep	0.75	38	1.46	1.19	1.80
Oct	0.75	58	1.42	1.17	1.72
Nov	0.75	79	1.58	1.28	1.91
Dec	0.75	70	1.89	1.44	2.44
All Year	0.75	595	2.02	1.73	2.21

Table 3-6: Applied threshold values and corresponding number of peaks for the nearshore omnidirectional extreme swell significant wave height in m for various months. The red number indicate directional sector for which too few peaks are available for a reliable extreme values.

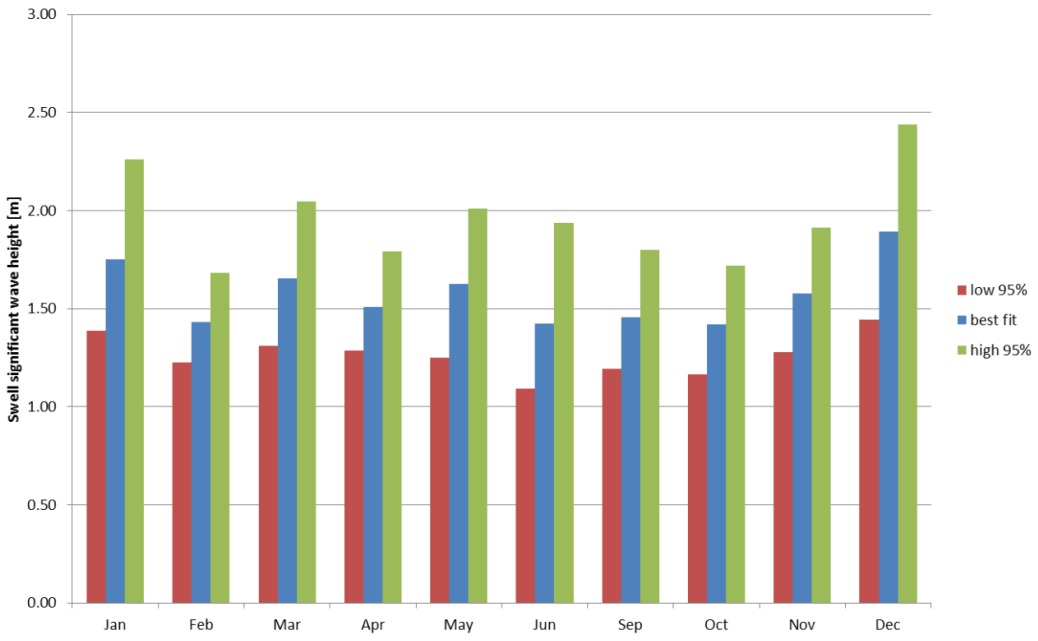

Figure 3-9: Nearshore omnidirectional extreme swell significant wave height in m and corresponding 95% confidence interval limits for various months and 1/100 year return period.

The results clearly indicate that in winter, the highest extreme swell significant wave heights occur. However, the differences between months are not very pronounced. The difference between the highest extreme 1/100 year swell significant wave heights (December 1.89 m) and the lowest (October 1.42 m) is less than 0.5 m.
In Appendix 3.3, figures showing the selected peaks, the fitted Weibull distribution function and the confidence intervals are presented. The figures of the selected peaks and fitted Weibull curve in Appendix 3.3 confirm that the results look reliable.

4 Associated conditions

4.1 INTRODUCTION

This chapter provides an outline of the method to account for joint probabilities of environmental conditions. A key notion is that we make a distinction between a primary parameter and certain associate parameters. The following primary parameters are considered: extreme wind, wind sea and swell waves. Associated values are determined for the following combinations of primary and associated parameters:

- Wind: wind speed (U10) and wind direction;
- Wind sea: significant wave height (Hm0), peak wave period (Tp) and mean wave direction;
- Swell: significant wave height (Hm0), peak wave period (Tp) and mean wave direction.

The motivation for finding associated parameters is explained in Chapter 2. The followed methodology is described in detail in Chapter 4.2. The results and important remarks regarding the interpretation of the results are presented at the end of Chapter 4.3.1, 4.3.2 and 4.3.3.

4.2 METHODOLOGY

The associated parameters values are defined as the most probable condition, given a certain primary design condition. To determine the most probable associated values, a function is fitted to the scattered data of the primary parameter (such as for instance the wind speed) against the associated parameter. Associated values are determined for the all-year directional extremes, obtained by selecting data values above a certain threshold at the nearshore location

Generally, a power function of the form

$$Y = aX^b$$

is used to determine the most probably relation for well correlated parameters. For the relation between significant wave heights and corresponding peak wave periods, typically a square root function is applied. This function is written as:

$$Y = a\sqrt{X}$$

The value for a is fitted to the scattered data using a least-squares method. For some combinations of parameters, a very poor correlation exists. The swell conditions for instance are, by definition, not well related to the local wind and wind sea wave conditions. For such cases, it is not sensible to fit a relation to the scattered data. A fitted relation will bear no meaning and will easily lead to erroneous use and conclusions. In such cases, the value for Y that is exceeded by 5% of the data, is selected as a representative associate condition. This function is expressed as:

$$Y = a$$

During the data preparation for the extreme conditions, a series of events is selected based on the considered directional sector or month and above a selected threshold of the primary parameter. The function is fitted to the data from these events only. The peak data is presented by coloured boxes that indicate how many events are present for a combination of parameter values. For reference, the data coverage of the complete time series is plotted in grey in the background. The grey boxes represent combinations of parameter values for which at least one instance is present in the complete time series.

As an example, the scattered data for the omnidirectional wind speed peaks against the wind sea significant wave height is presented in Figure 3-1. The title of the figure describes what parameters are presented and the selected directional sector. The figure shows the wind speed on the x-axis and the wind sea significant wave heights on the y-axis. The black numbers in each dotted box indicate the number of selected peaks that fall within the boundaries of that box. For instance, the number of peaks between wind speeds of 12 and 15 m/s and wind sea significant wave heights between 1.0 and 1.5 m is 105. Each box is divided into smaller boxes and the number of peaks within these smaller boxes is indicated by the colour of those boxes. The colour bar on the right side of the figure displays the relation between the colour and the number of peaks on a logarithmic scale. The grey boxes in the background of the figure display where at least one peak is present in the complete time series. This is the time series before any peaks are selected. This grey area provides some idea of the range of occurring conditions and how the selected peaks relate to the complete range. The number of occurrences of the grey boxes are not displayed and the reader is advised to be careful with the interpretation of these figures. The purple line represents the fitted function. In this case a power function is fitted and the resulting coefficients are displayed in the legend in the lower right corner.

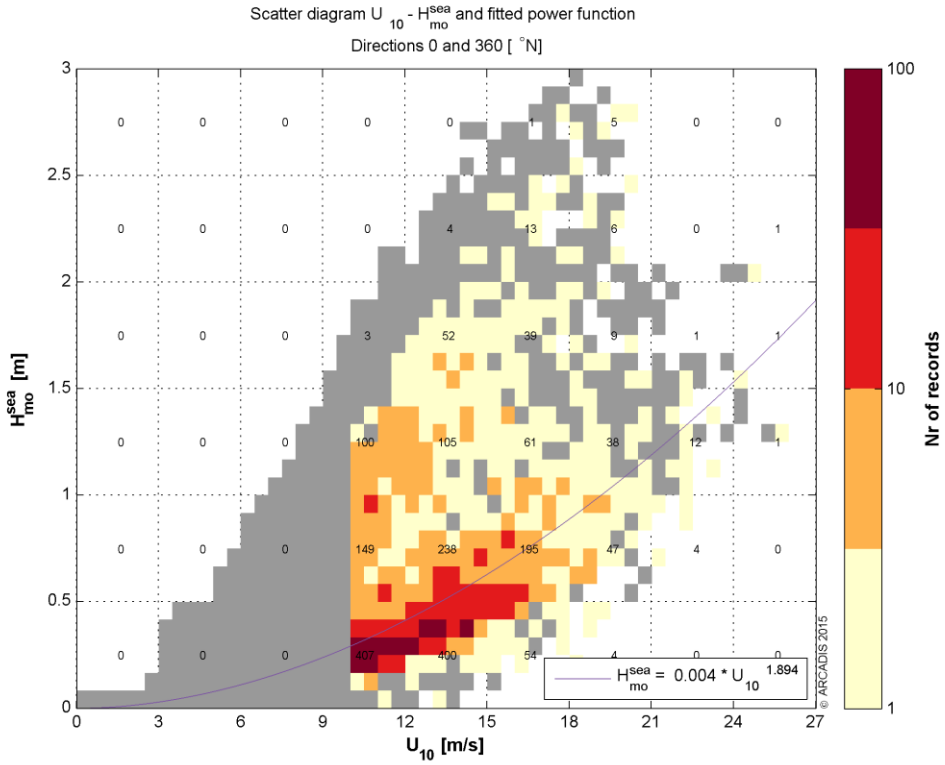

Figure 4-1: Exemplary scatter diagram of offshore all-year wind speed in m/s against nearshore all-year wind sea significant wave height in m. The box colours indicate the number of records for a combination of wind speed and wind sea significant wave height in the selected peaks. The grey boxes indicate combinations for which at least one event is present in the complete time series. The purple line represents the best fit.

4.3 RESULTS

4.3.1 WIND SPEED AND ASSOCIATED PARAMETERS

In this section, the derivation of the associated conditions for the extreme offshore all-year wind speeds is presented. The resulting associated conditions for all parameters and a 1/100 year return period are presented in Table 4-1.

Associated wind sea significant wave height

A power function is fitted to the to the scattered wind speed against wind sea significant wave height data. As an example, the scatter diagram for 180°N is presented in Figure 4-2. The figures for other directions are presented in Appendix 4.1.

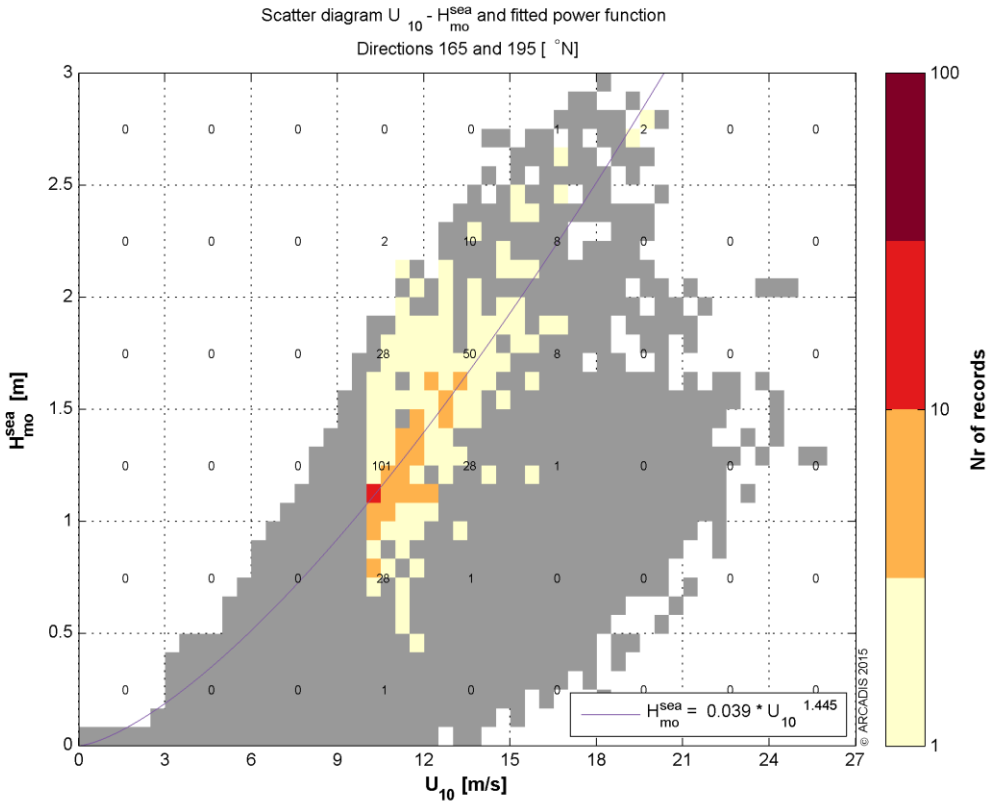

Figure 4-2: Scatter diagram of offshore all-year wind speed in m/s against nearshore all-year wind sea significant wave height in m for directional sector 180°N. The box colours indicate the number of records for a combination of wind speed and wind sea significant wave height in the selected peaks. The grey boxes indicate combinations for which at least one event is present in the complete time series. The purple line represents the best fit.

Figure 4-2 shows that for directional sector 180°N (from which most wind sea waves at the bow are coming), the highest wind speeds do not coincide with the highest wind sea significant wave heights. A possible explanation is the limited time duration of growth of the wind sea waves. Nonetheless, a trend is visible in the relation between observed wind speeds and wind sea significant wave heights.

The resulting coefficients and associated wind sea significant wave heights for a 1/100 year return period are presented in Table 4-2. The complete table of associated values is presented in Appendix 4.1.

Associated wind sea peak wave period

A power function is fitted to the scattered wind speed against wind sea peak wave period data. As an example, the scatter diagram for 180°N is presented in Figure 4-3. The figures for other directions are presented in Appendix 4.2.

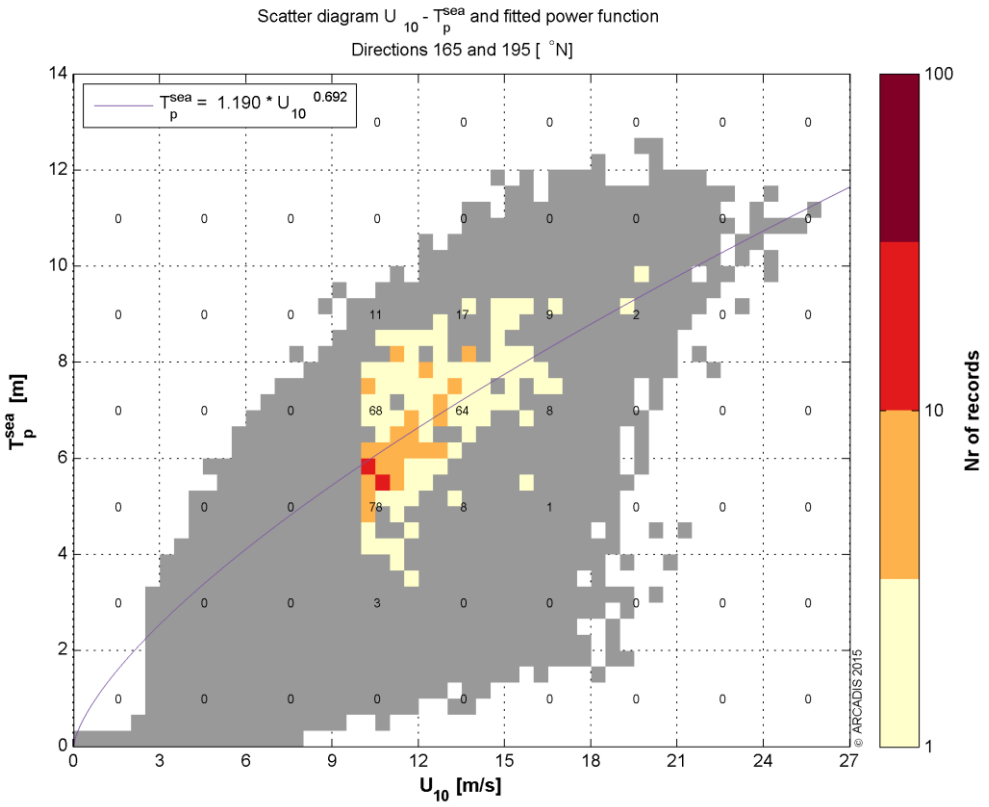

Figure 4-3: Scatter diagram of offshore all-year wind speed in m/s against nearshore all-year wind sea peak wave period in s for directional sector 180°N. The box colours indicate the number of records for a combination of wind speed and wind sea peak wave period in the selected peaks. The grey boxes indicate combinations for which at least one event is present in the complete time series. The purple line represents the best fit.

Again, the highest wind speeds do not coincide with the highest wind sea peak wave periods for directional sector 180°N.

The resulting coefficients and associated wind sea peak wave periods for a 1/100 year return period are presented in Table 4-2. The complete table of associated values is presented in Appendix 4.2. The values vary considerable between directional sectors, indicating that the results should be treated with care.

Alternatively, the relation between wind sea significant wave heights and peak wave periods can be used to select an associated wind sea peak wave period. In Chapter 8, the implications of this approach are discussed.

Associated swell significant wave height

As discussed before, the swell conditions are by definition poorly correlated to the wind conditions. Therefore it is not sensible to fit a function to the scattered data. Instead a value for the swell significant wave height is selected that is exceeded by only 5% of the selected peaks. As an example, the scatter diagram for 180°N is presented in Figure 4-4. The figures for other directions are presented in Appendix 4.3.

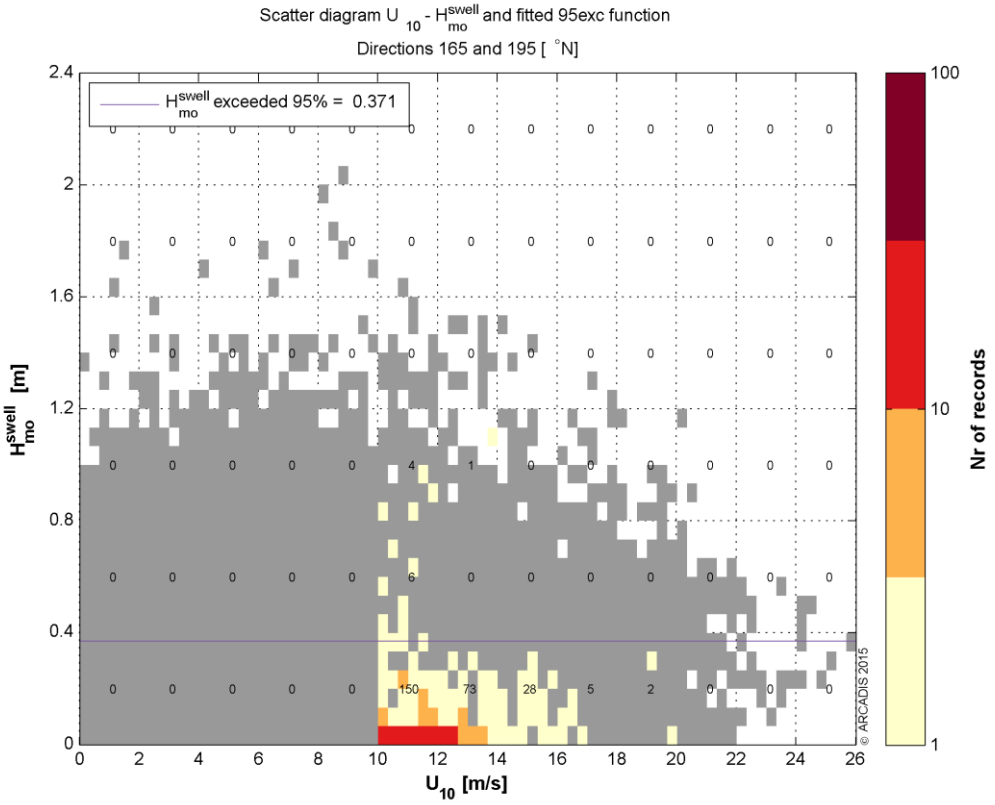

Figure 4-4: Scatter diagram of offshore all-year wind speed in m/s against nearshore all-year swell significant wave height in m for directional sector 180°N. The box colours indicate the number of records for a combination of wind speed and swell significant wave height in the selected peaks. The grey boxes indicate combinations for which at least one event is present in the complete time series. The purple line represents the best fit.

It is clearly visible that the wind speeds occur independently of the swell significant wave heights.

The resulting coefficients and associated swell significant wave heights for a 1/100 year return period are presented in Table 4-2. The complete table of associated values is presented in Appendix 4.3. The results are fairly equal for all directional sectors.

Associated swell peak wave period

Because of the poor correlation between wind speed and swell peak wave periods, a 5% exceeded value is selected as representative associate value. As an example, the scatter diagram for 180°N is presented in Figure 4-5. The figures for other directions are presented in Appendix 4.4.

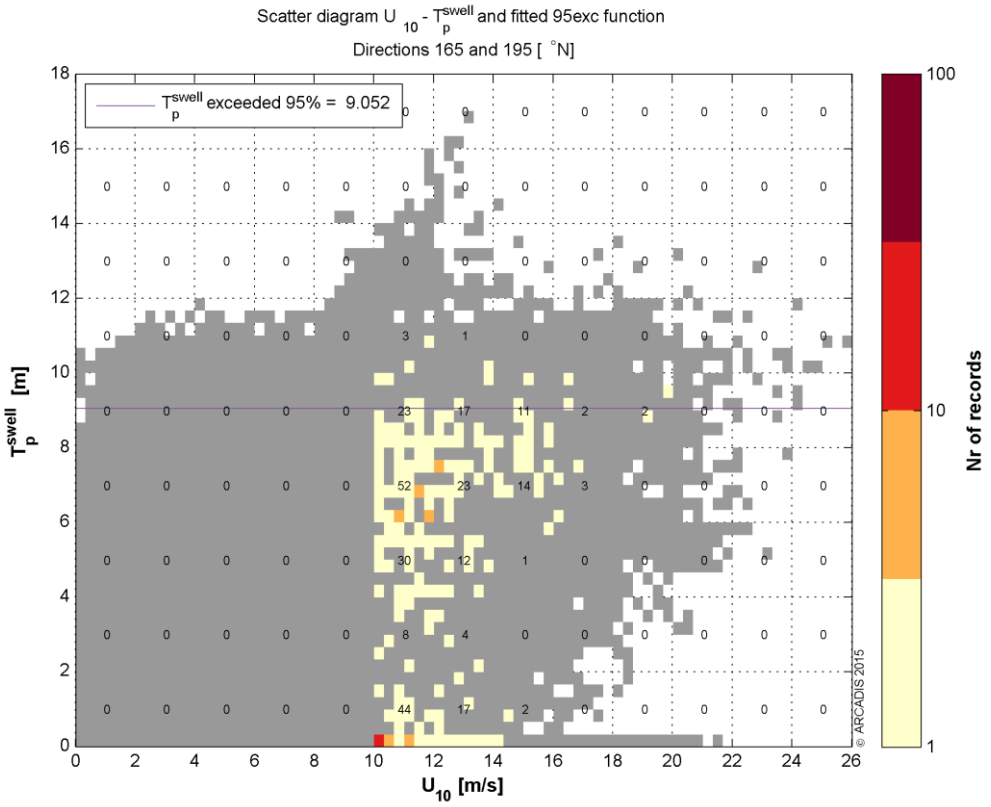

Figure 4-5: Scatter diagram of offshore all-year wind speed in m/s against swell peak wave period in s for directional sector 180°N. The box colours indicate the number of records for a combination of wind speed and swell peak wave period in the selected peaks. The grey boxes indicate combinations for which at least one event is present in the complete time series. The purple line represents the best fit.

It is clearly visible that the wind speeds occur independently of the swell peak wave periods.

The resulting coefficients and associated swell peak wave periods for a 1/100 year return period are presented in Table 4-2. The complete table of associated values is presented in Appendix 4.4. The values vary are fairly equal for all directional sectors.

Resulting associated conditions for extreme offshore all-year wind speed

The resulting associated conditions for the 1/100 year return period and various directional sectors are presented in Table 4-1. In the first two columns, the wind directional sector and the extreme wind speed are presented. In the next two columns, the components of the associated current velocities (Chapter 10) are presented. The associated wind sea conditions are presented in columns 5 – 7 and the associated swell conditions in columns 8 - 10.

A number of cells are marked by an orange colour. For those cells, the associated wind sea wave conditions corresponding to wind directional sectors 270°N – 30°N, a distinction should be made between penetrating wind sea waves and locally generated wind sea waves. This is further explained in Chapter 5. The green cells indicate associated directions which were not part of the scope of this chapter. Determining associated directions is part of the collinearity analysis, which is presented in Chapter 7. Representative values for the associated mean wave directions of wind sea and swell are presented there.

Governing wind		Associated current		Associated wind sea			Associated swell		
Udir	U10	U	V	Dir	Hm0 sea	Tp sea	Dir	Hm0 swell	Tp swell
[°N]	[m/s]	[m/s]	[m/s]	[°N]	[m]	[s]	[°N]	[m]	[s]
0	25.9	0.02	0.12		1.51	11.7		0.58	10.5
30	25.2	0.02	0.11		1.30	13.6		0.59	10.6
60	23.1	0.05	0.04		1.53	11.8		0.59	10.5
90	21.1	0.02	0.08		2.07	11.0		0.54	10.0
120	20.4	-0.03	0.15		2.53	10.3		0.49	8.8
150	21.9	0.01	0.09		3.09	11.0		0.34	9.3
180	20.0	-0.01	0.08		2.96	9.5		0.37	9.1
210	20.7	-0.05	-0.20		2.61	10.3		0.53	9.2
240	21.4	-0.02	-0.21		2.07	10.3		0.59	9.9
270	25.4	0.04	-0.22		1.87	12.8		0.62	9.7
300	25.0	0.08	-0.16		1.91	15.9		0.56	9.2
330	24.4	0.15	0.08		1.40	10.6		0.62	9.4

Table 4-1: Associated condition results for the extreme offshore all-year wind speeds for a return period of 1/100 years and various wind directional sectors. Green marked cells are presented in Chapter 7. Orange cells are discussed in Chapter 5.

For each associated function, the type of the function and the fitted parameter values are presented in Table 4-2. The various fitted functions and the meaning of the parameters are described in Chapter 4.2. The associated conditions for other return periods can be derived from the function values and the extreme wind speed conditions in Table A-1.

Hm0 sea	power		Tp sea	power		Hm0 swell	exc	Tp swell	exc
[m]	a	b	[s]	a	b	[m]	a	[s]	a
1.51	0.004	1.823	11.72	0.016	2.027	0.58	0.580	10.48	10.475
1.30	0.007	1.620	13.61	0.420	1.078	0.59	0.594	10.60	10.596
1.53	0.007	1.716	11.84	0.706	0.898	0.59	0.591	10.49	10.489
2.07	0.003	2.144	11.00	0.512	1.006	0.54	0.542	9.96	9.964
2.53	0.015	1.700	10.31	0.651	0.916	0.49	0.485	8.76	8.764
3.09	0.032	1.481	10.98	0.717	0.884	0.34	0.337	9.34	9.336
2.96	0.039	1.445	9.46	1.190	0.692	0.37	0.371	9.05	9.052
2.61	0.040	1.379	10.33	0.756	0.863	0.53	0.526	9.23	9.228
2.07	0.036	1.322	10.31	0.782	0.842	0.59	0.585	9.86	9.861
1.87	0.009	1.649	12.82	0.298	1.163	0.62	0.620	9.66	9.663
1.91	0.002	2.132	15.89	0.003	2.664	0.56	0.558	9.17	9.172
1.40	0.004	1.833	10.59	0.008	2.250	0.62	0.621	9.37	9.365

Table 4-2: Associated condition fitted function results for various wind directional sectors.

4.3.2 WIND SEA SIGNIFICANT WAVE HEIGHT AND ASSOCIATED PARAMETERS

In this section, the derivation of the associated conditions for the extreme nearshore all-year wind sea significant wave heights is presented. The resulting associated conditions for all parameters and a 1/100 year return period are presented in Table 4-3.

Associated wind speed

A power function is fitted to the to the scattered wind sea significant wave height against wind speed data. Results are provided for the directional sectors for which extreme wind sea significant wave heights are determined (180°N – 270°N). Because the number of peaks for directions 210°N and 240°N is limited (see Table 3-2), those results need to be interpreted with care. As an example, the scatter diagram for 180°N is presented in Figure 4-6. The figures for other directions are presented in Appendix 5.1.

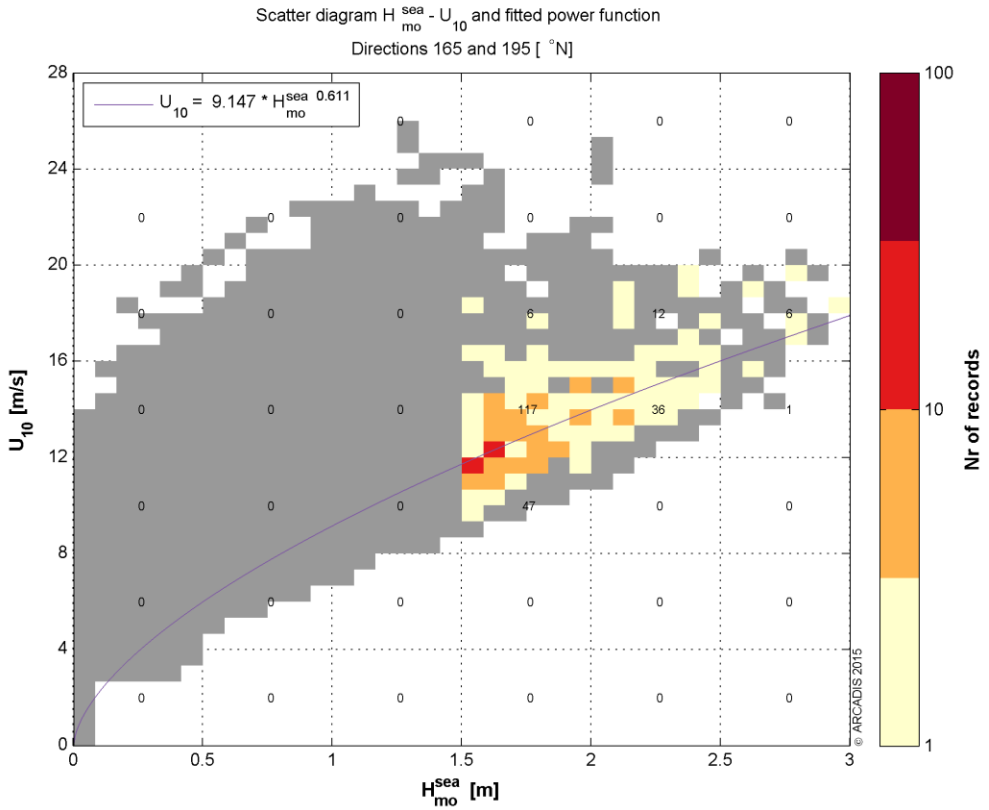

Figure 4-6: Scatter diagram of nearshore all-year wind sea significant wave height in m against offshore all-year wind speed in m/s for directional sector 180°N. The box colours indicate the number of records for a combination of wind sea significant wave height and wind speed in the selected peaks. The grey boxes indicate combinations for which at least one event is present in the complete time series. The purple line represents the best fit.

Figure 4-6 shows that for directional sector 180°N, the highest wind sea significant wave heights do not coincide with the highest wind speeds. From the fact that the wind sea is generated by the wind, it is not surprising that a clear relation between the two parameters is present.

The resulting coefficients and associated wind speeds for a 1/100 year return period are presented in Table 4-4. The complete table of associated values is presented in Appendix 5.1. The fitted coefficients of the power functions vary quite a bit for the various directional sectors due to the variation in the number of selected peaks.

Associated wind sea peak wave period

A square root function is fitted to the scattered wind sea significant wave height against wind sea peak wave period data. As an example, the scatter diagram for 180°N is presented in Figure 4-7. The figures for other directions are presented in Appendix 5.2.

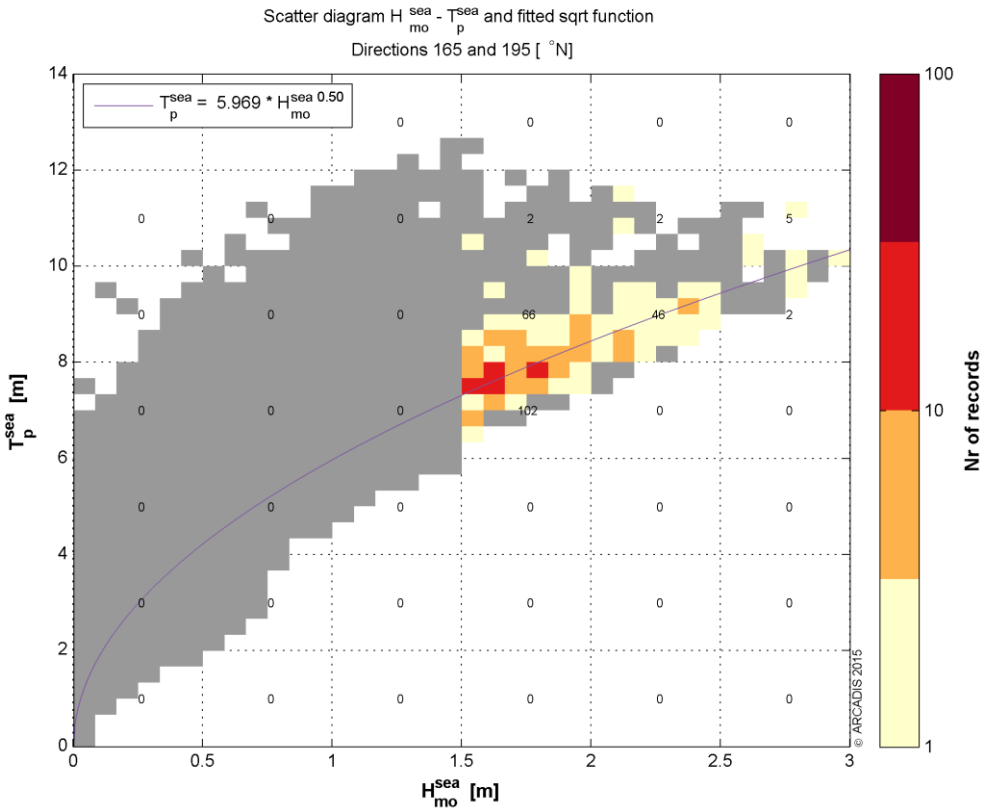

Figure 4-7: Scatter diagram of nearshore all-year wind sea significant wave height in m against nearshore all-year wind sea peak wave period in s for directional sector 180°N. The box colours indicate the number of records for a combination of wind sea significant wave height and peak wave period in the selected peaks. The grey boxes indicate combinations for which at least one event is present in the complete time series. The purple line represents the best fit.

A very clear relation between the wind sea significant wave heights and peak wave periods is visible in both the selected peak data and the complete time series (grey). This is the result of a natural balance between those parameters that is observed very often in nature. The square root relationship describes this balance well.

The resulting coefficients and associated wind sea peak wave periods for a 1/100 year return period are presented in Table 4-4. The complete table of associated values is presented in Appendix 5.2. The values vary considerable between directional sectors, indicating that the results should be treated with care.

Alternatively, the relation between wind sea significant wave heights and peak wave periods can be used to select an associated wind sea peak wave period. In Chapter 8, the implications of this approach are discussed.

Associated swell significant wave height

The swell conditions are by definition poorly correlated to the wind sea conditions. Therefore it is not sensible to fit a function to the scattered data. Instead a value for the swell significant wave height is selected that is exceeded by only 5% of the selected peaks. As an example, the scatter diagram for 180°N is presented in Figure 4-8. The figures for other directions are presented in Appendix 5.3.

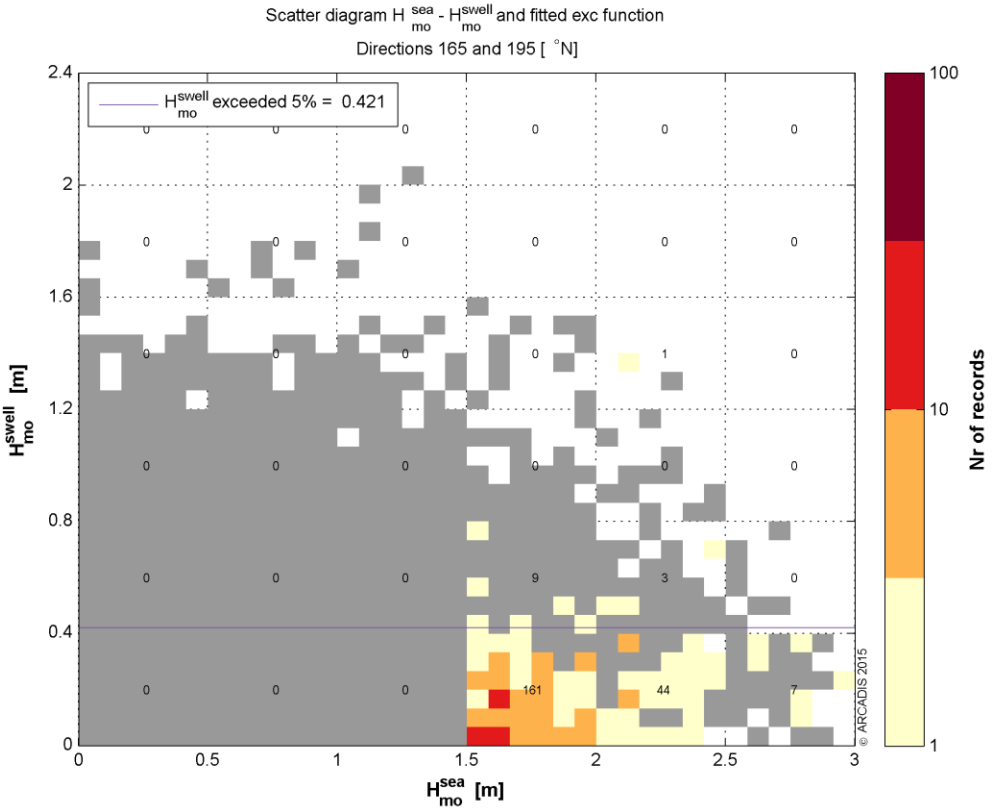

Figure 4-8: Scatter diagram of nearshore all-year wind sea significant wave height in m against nearshore all-year swell significant wave height in m for directional sector 180°N. The box colours indicate the number of records for a combination of wind sea significant wave height and swell significant wave height in the selected peaks. The grey boxes indicate combinations for which at least one event is present in the complete time series. The purple line represents the best fit.

The wind sea significant wave heights occur independently of the swell significant wave heights. The results should be treated with care when selecting a swell significant wave height for the loading of the mooring system.

The resulting coefficients and associated swell significant wave heights for a 1/100 year return period are presented in Table 4-4. The complete table of associated values is presented in Appendix 5.3. The results vary quite a bit from one directional sector to another due to the limited number of peaks for some sectors.

Associated swell peak wave period

Because of the poor correlation between wind sea significant wave height and swell peak wave periods, a 5% exceeded value is selected as representative associate value. As an example, the scatter diagram for 180°N is presented in Figure 4-9. The figures for other directions are presented in Appendix 5.4.

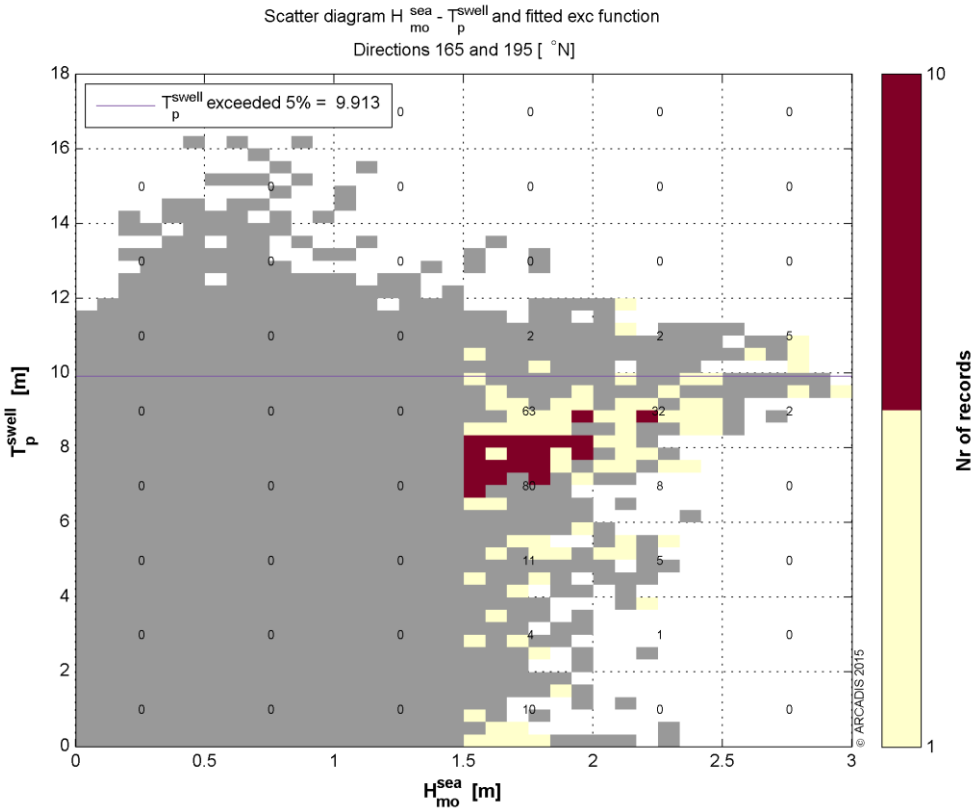

Figure 4-9: Scatter diagram of nearshore all-year wind sea significant wave height in m against nearshore all-year swell peak wave period in s for directional sector 180°N. The box colours indicate the number of records for a combination of wind sea significant wave height and swell peak wave period in the selected peaks. The grey boxes indicate combinations for which at least one event is present in the complete time series. The purple line represents the best fit.

Both the selected peak data and the complete time series indicate that the wind sea significant wave height and swell peak wave period are not related.

The resulting coefficients and associated swell peak wave periods for a 1/100 year return period are presented in Table 4-4. The complete table of associated values is presented in Appendix 5.4. The values vary are fairly equal for all directional sectors.

Resulting associated conditions for extreme nearshore all-year wind sea significant wave height

The resulting associated conditions for the 1/100 year return period and various directional sectors are presented in Table 4-3. In columns 5 - 7, the governing extreme wind sea conditions are presented. In the first two columns, the associated wind conditions are presented. In the next two columns, the components of the associated current velocities are presented. The associated swell conditions are presented in columns 8 - 10.

A number of cells are marked by an orange colour. For those cells, the wind sea wave conditions should be split into two components, i.e. penetrating wind sea waves and locally generated wind sea waves. This is further explained in Chapter 5. A number of cells are marked by a green colour. For those cells, the associated conditions cannot be determined straightforward. The collinearity between the wind and wave mean wave directions is presented in Chapter 7. It is advised to use those results to select appropriate wind directions and swell mean wave directions for the presented wind sea mean wave directions. This is also discussed in Chapter 11.

Since a detailed flow study was beyond the scope of this analysis no associated current conditions were determined for the governing wind sea. It is advised to select appropriate conservative estimates for the current conditions based on the results presented in Table 4-1 and Chapter 9.

Associated wind		Associated current		Governing wind sea			Associated swell		
Udir	U10	U	V	Dir	Hm0 sea	Tp sea	Dir	Hm0 swell	Tp swell
[°N]	[m/s]	[m/s]	[m/s]	[°N]	[m]	[s]	[°N]	[m]	[s]
	18.5			180	3.17	10.4		0.42	9.9
	18.5			210	2.85	10.4		0.63	11.7
	21.7			240	1.68	12.1		0.68	10.8
	22.7			270	1.33	13.3		0.53	10.3

Table 4-3: Associated condition results for the extreme nearshore all-year wind sea significant wave heights for a return period of 1/100 years and various wind sea directional sectors. Green marked cells are presented in Chapter 7. Orange cells are discussed in Chapter 5.

For each associated function, the type of the function and the fitted parameter values are presented in Table 4-4. The various fitted functions and the meaning of the parameters are described in Section 4.2. The associated conditions for other return periods can be derived from the function values and the extreme wind speed conditions in Table A-2.

U10	power		Tp sea	power		Hm0 swell	exc	Tp swell	exc
[m/s]	a	b	[s]	a	b	[m]	a	[s]	a
18.5	9.147	0.611	10.35	6.230	0.440	0.42	0.421	9.91	9.913
18.5	16.128	0.132	10.44	8.740	0.170	0.63	0.626	11.66	11.664
21.7	15.990	0.588	12.14	9.320	0.510	0.68	0.684	10.79	10.793
22.7	18.149	0.778	13.30	10.170	0.940	0.53	0.531	10.32	10.321

Table 4-4: Associated condition fitted function results for various wind sea directional sectors.

4.3.3 SWELL SIGNIFICANT WAVE HEIGHT AND ASSOCIATED PARAMETERS

In this section, the derivation of the associated conditions for the extreme nearshore all-year swell significant wave heights is presented. The resulting associated conditions for all parameters and a 1/100 year return period are presented in Table 4-5. As discussed in Chapter 2.3 and confirmed in Chapter 4.3.2, swell characteristics are poorly correlated with wind and wind generated waves. This lack of correlation is also found in this section where swell waves are considered as the primary parameter.

Associated wind speed

Associated conditions are provided for directional sectors 180°N and 210°N. For all other directional sector, insufficient peaks are available (see Table 3-3). Because of the poor correlation between swell peak wave periods and wind speed, a 5% exceeded value is selected as representative condition. As an example, the scatter diagram for 180°N is presented in Figure 4-10. The figure confirms that no correlation exists between the swell significant wave height and wind speed. The figures for the other directional sectors are presented in Appendix 6.1.

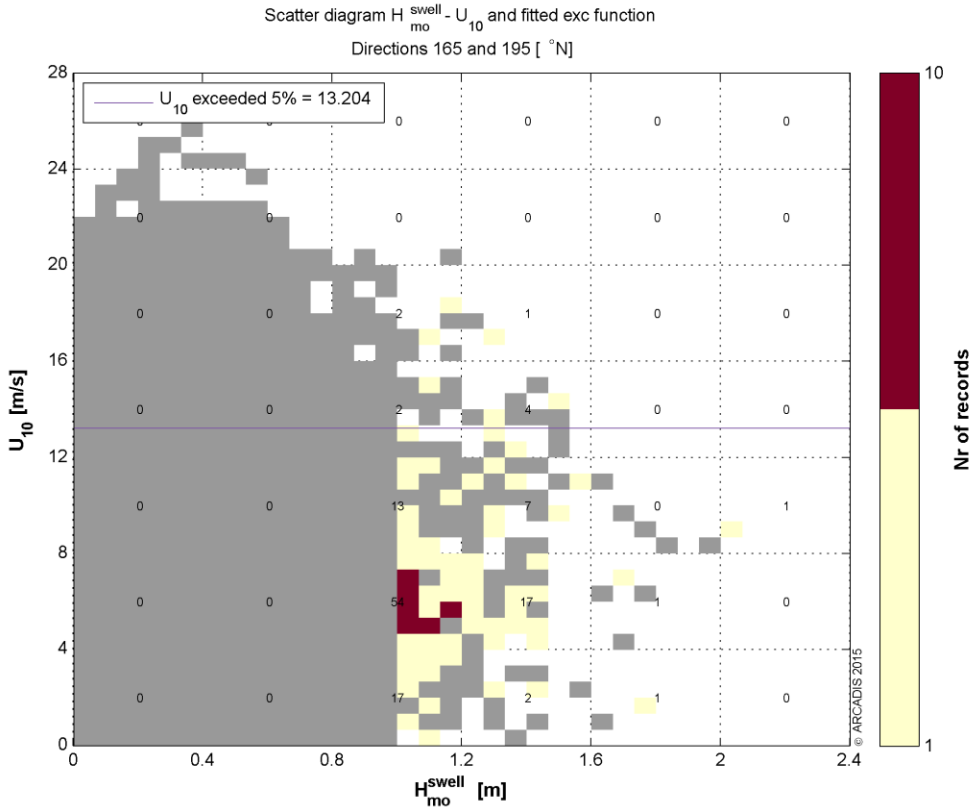

Figure 4-10: Scatter diagram of nearshore all-year swell significant wave height in m against offshore all-year wind speed in m/s for directional sector 180°N. The box colours indicate the number of records for a combination of swell significant wave height and wind speed in the selected peaks. The grey boxes indicate combinations for which at least one event is present in the complete time series. The purple line represents the best fit.

The resulting coefficients and associated wind speeds for a 1/100 year return period are presented in Table 4-6. The complete table of associated values is presented in Appendix 6.1. The fitted coefficients of the power functions vary quite a bit for both directional sectors.

Associated wind sea significant wave height

The wind sea and swell wave conditions are by definition not correlated. Therefore, a 5% exceeded value is selected as representative associated condition. As an example, the scatter diagram for 180°N is presented in Figure 4-11. The figure shows that no correlation exists between the swell significant wave height and wind sea significant wave height. The figures for the other directional sectors are presented in Appendix 6.2.

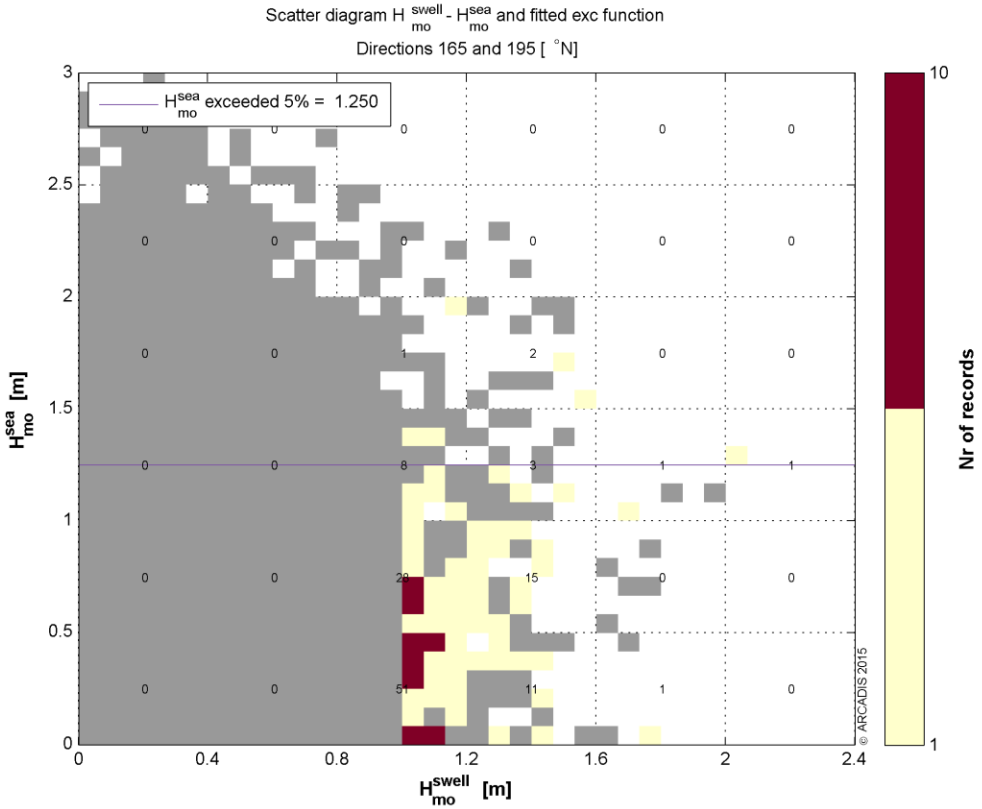

Figure 4-11: Scatter diagram of nearshore all-year swell significant wave height in m against nearshore all-year wind sea significant wave height in m for directional sector 180°N. The box colours indicate the number of records for a combination of swell significant wave height and wind sea significant wave height in the selected peaks. The grey boxes indicate combinations for which at least one event is present in the complete time series. The purple line represents the best fit.

The resulting coefficients and associated wind sea significant wave heights for a 1/100 year return period are presented in Table 4-6. The complete table of associated values is presented in Appendix 6.2. The fitted coefficients of the power functions vary a bit between both directional sectors.

Associated wind sea peak wave period

The swell significant wave heights and wind sea peak wave periods have not physical connection. Consequently, the associated wind sea peak wave period is represented by a 5% exceeded value. As an example, the scatter diagram for 180°N is presented in Figure 4-12. The figure shows that no correlation exists between the swell significant wave height and wind sea peak wave period. The figures for the other directional sectors are presented in Appendix 6.3.

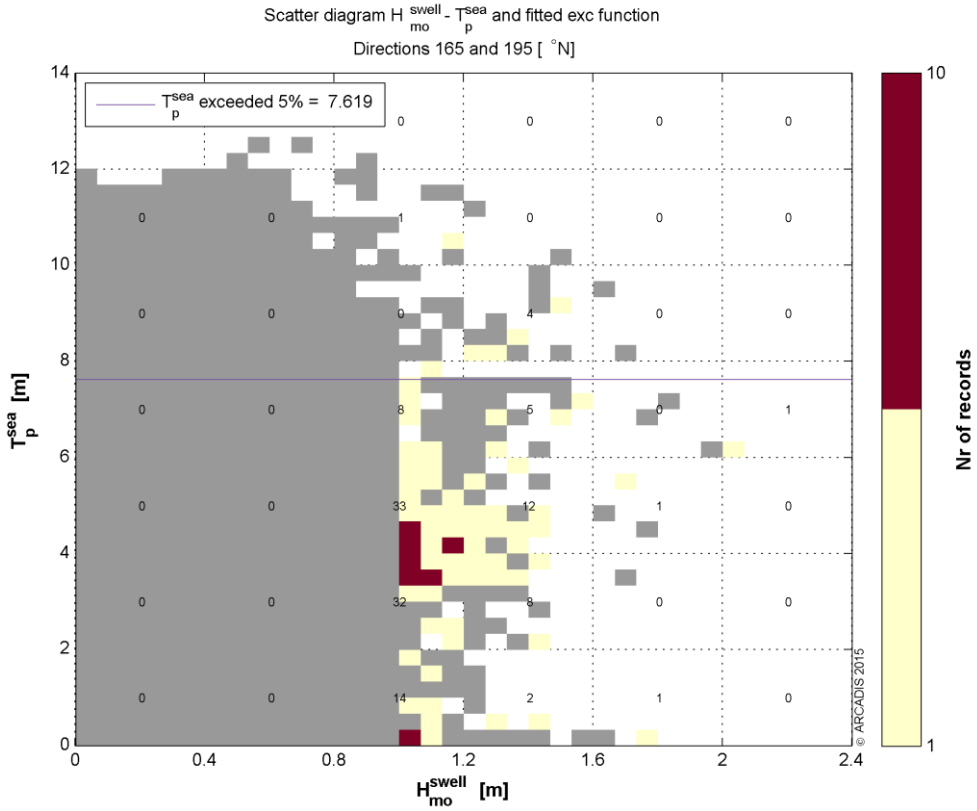

Figure 4-12: Scatter diagram of nearshore all-year swell significant wave height in m against nearshore all-year wind sea peak wave period in s for directional sector 180°N. The box colours indicate the number of records for a combination of swell significant wave height and wind sea peak wave periods in the selected peaks. The grey boxes indicate combinations for which at least one event is present in the complete time series. The purple line represents the best fit.

The resulting coefficients and associated wind sea peak wave periods for a 1/100 year return period are presented in Table 4-6. The complete table of associated values is presented in Appendix 6.3. The fitted coefficients of the power functions vary much between both directional sectors.

Associated swell peak wave period

A square root function is fitted to the scattered swell significant wave height against swell peak wave period data. As an example, the scatter diagram for 180°N is presented in Figure 4-13. The figures for the other directional sector are presented in Appendix 6.4.

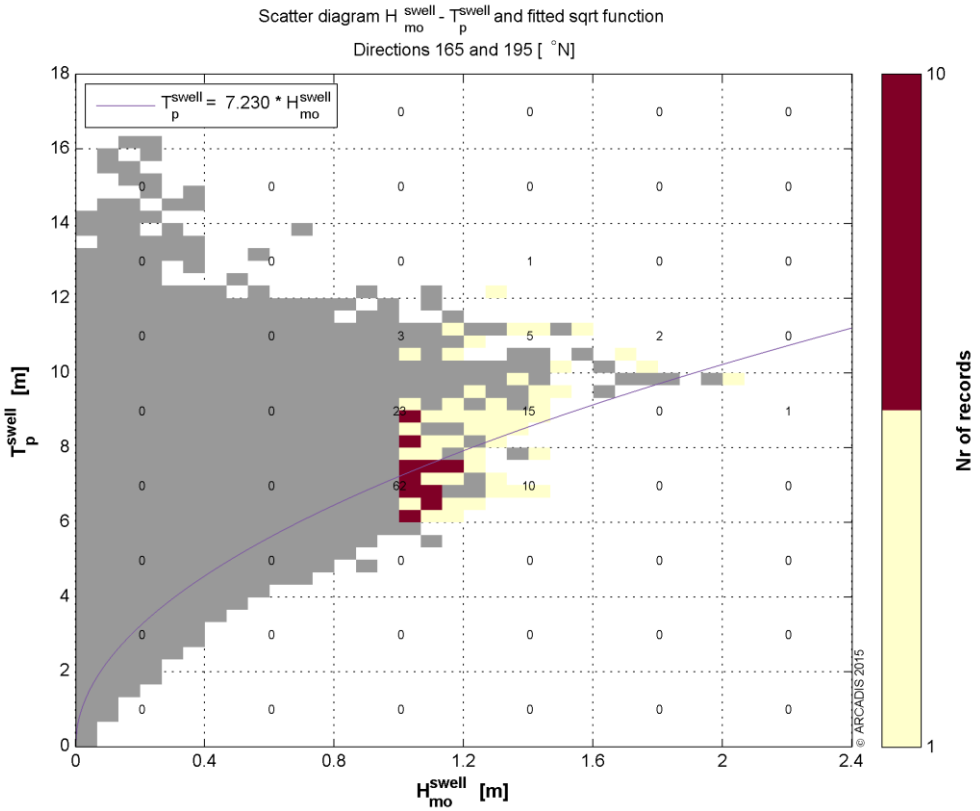

Figure 4-13: Scatter diagram of nearshore all-year swell significant wave height in m against nearshore all-year swell peak wave period in s for directional sector 180°N. The box colours indicate the number of records for a combination of swell significant wave height and swell period in the selected peaks. The grey boxes indicate combinations for which at least one event is present in the complete time series. The purple line represents the best fit.

A very clear relation between the swell significant wave heights and peak wave periods is visible in both the selected peak data and the complete time series (grey). This is the results of a natural balance between those parameters that is observed frequently. The data of the entire time series shows a large variation in peak wave periods for lower significant wave heights. This is often observed for swell waves.

The resulting coefficients and associated swell peak wave periods for a 1/100 year return period are presented in Table 4-6. The complete table of associated values is presented in Appendix 6.4. The values vary considerable between directional sectors for high significant wave heights, indicating that the results should be treated with care.

Alternatively, the relation between swell significant wave heights and peak wave periods can be used to select an associated swell peak wave period. In Chapter 8, the implications of this approach are discussed.

Resulting associated conditions for extreme nearshore all-year swell significant wave height

The resulting associated conditions for the 1/100 year return period and various directional sectors are presented in Table 4-5. In columns 8 - 10, the governing extreme swell conditions are presented. In the first two columns, the associated wind conditions are presented. In the next two columns, the components of the associated current velocities are presented. The associated wind sea conditions are presented in columns 5 - 7.

A number of cells are marked by a green colour. For those cells, the associated conditions cannot be determined straightforward. The collinearity between the wind and wave mean wave directions is presented in Chapter 7. It is advised to use those results to select appropriate wind directions and wind sea mean wave directions for the presented swell mean wave directions. No current velocities were determined corresponding to the extreme wind sea conditions. It is advised to select appropriate conservative estimates for the current conditions based on the results presented in Chapter 9.

Associated wind		Associated current		Associated wind sea			Governing swell		
Udir [°N]	U10 [m/s]	U [m/s]	V [m/s]	Dir [°N]	Hm0 sea [m]	Tp sea [s]	Dir [°N]	Hm0 swell [m]	Tp swell [s]
	13.2				1.25	7.6	180	2.04	10.3
	17.5				1.41	10.8	210	1.27	11.2

Table 4-5: Associated condition results for the extreme nearshore all-year swell significant wave heights for a return period of 1/100 years and various swell directional sectors. Green marked cells are presented in Chapter 7.

For each associated function, the type of the function and the fitted parameter values are presented in Table 4-6. The various fitted functions and the meaning of the parameters are described in Chapter 4.2. The associated conditions for other return periods can be derived from the function values and the extreme wind speed conditions in Table A-3.

U10 [m/s]	exc a	Hm0 sea [m]	exc a	Tp sea [s]	exc a	Tp swell [s]	sqrt a
13.2	13.200	1.25	1.250	7.62	7.619	10.33	7.230
17.5	17.535	1.41	1.406	10.81	10.809	11.20	9.943

Table 4-6: Associated condition fitted function results for various swell directional sectors.

5 Locally generated wind sea waves

5.1 INTRODUCTION

As discussed in Chapter 2.3, the wave conditions at the project site consist of three components:

- Wind sea waves which are penetrating from the Mediterranean Sea into Marsaxlokk Bay;
- Wind sea waves which are generated inside Marsaxlokk Bay by the wind;
- Swell waves which are penetrating from the Mediterranean Sea into Marsaxlokk Bay.

Because of the differences between swell, locally generated and penetrating wind sea waves, it is useful to make a distinction between the three types for the design of the mooring system. In this chapter, the characteristics of the various components are investigated and the consequences of the differences are discussed (Chapter 5.2). Thereafter (Chapter 5.3), a refinement of the associated wind sea wave conditions from Chapter 4.3.1 is presented. The results of this refinement is a description of the nearshore wave conditions such that the various components can be evaluated separately.

It is noted that all components should be considered for a proper evaluation of the mooring system design.

5.2 CHARACTERISTICS OF THE VARIOUS WAVE COMPONENTS

5.2.1 SWELL WAVES

Swell waves are those waves that are generated in distant storms instead of local wind. They are characterised by relatively long periods and a narrow directional distribution. For this project, the nearshore swell wave conditions are determined with SWAN and MIKE21BW wave models, as described in the wave climate study and wave penetration study reports [1] and [2]. Because the swell wave conditions at the project site are well described, they are not evaluated in more detail in this chapter.

5.2.2 WIND SEA WAVES

Wind sea waves are generated by local wind conditions and characterised by relatively short wave periods, large directional spreading and a strong relation with local wind conditions. The nearshore wind sea wave conditions are determined with the SWAN wave model, as described in the wave climate study and wave penetration study reports [1] and [2].

The nearshore wind sea wave climate is the result from two contributing components:

- Wind sea waves which are penetrating from the Mediterranean Sea into Marsaxlokk Bay;
- Wind sea waves which are locally generated inside Marsaxlokk Bay.

Additional SWAN simulations have been performed to evaluate the differences between locally generated wind waves and wind waves penetrating via the entrance of Marsaxlokk Bay. In these simulations, the extreme wind and wind sea wave conditions for a return period of 1/100 years and directions 270, 300, 330, 0 and 30 °N have been applied as boundary conditions. Simulations were performed for the following conditions:

- offshore (penetrating) wind sea wave boundary conditions (taken from the prior wave propagation study [1]) without wind in the most detailed grid (which only covers Marsaxlokk Bay);
- wind without offshore wind sea wave boundary conditions (representing local wave growth inside Marsaxlokk Bay).

The first simulation is representative for penetrating wind sea wave conditions and the second for locally generated conditions. It is noted that the wind sea wave boundary conditions were determined with wind on in the SWAN simulations. Despite the fact that in reality both wave systems will weakly interact with each other, we deem that these simulations give a good indication of the differences between locally generated and penetrating wind sea waves.

Wind direction 270°N is presented in this chapter since for this direction the fetch length at the bow is largest and therefore it is expected that for this direction the contribution of locally generated wind waves is most important. For wind directions from the South, the locally generated waves are assimilated by the penetrated wind sea waves and it is not possible to discriminate between the two components. For northerly and easterly wind directions, the fetch and water depth are too small to sustain significant wave growth. Only for winds from the West, the effect of locally generated wind waves is significant. To aid the interpretation of the results, the reflections of the coastline was not included in the simulations, whereas it was in the prior wave studies [1], [2].

Figure 5-1 shows the spatial distribution of the significant wave height and mean wave direction for a SWAN simulation with the extreme offshore (penetrating) wind sea wave boundary conditions without wind. Clearly visible is that the waves outside are penetrating into the bay along approximately northward trajectories. In the western part of the bay, hardly any waves are penetrating from outside the bay and no waves are generated. At the jetty, the significant wave height is 1.4 m and the mean wave direction is 190°N.

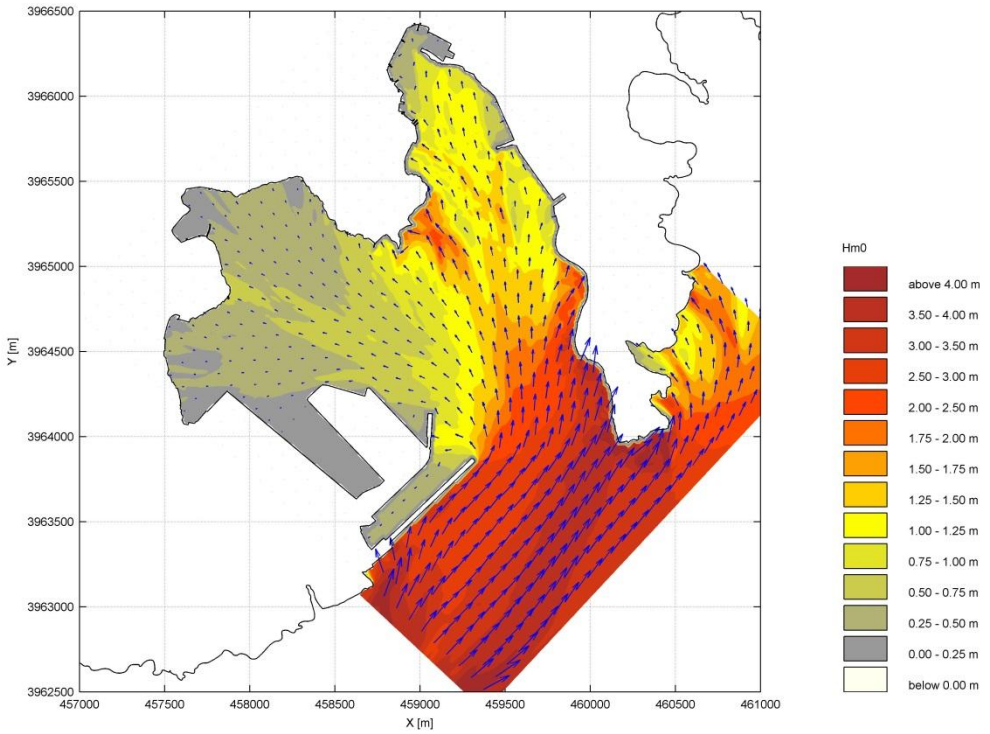

Figure 5-1: Spatial distribution of the significant wave height in SWAN grid C01 for extreme offshore (penetrating) wind sea wave boundary conditions without wind with return period 1/100 years and direction 270°N. The blue arrows indicate the mean wave direction, scaled with the significant wave height.

The SWAN simulation with the extreme offshore wind without boundary wave conditions shows a significantly different pattern of wind sea wave conditions (Figure 5-2). The significant wave heights are lower with maximum values less than 1.25 m close to the jetty. The significant wave height increases from west to east due to available fetch length. The mean wave direction is approximately equal to the wind direction (270°N) but is rotated towards the coastline by refraction, directional spreading and upwind fetch restrictions. At the jetty, the significant wave height is 1.0 m and the mean wave direction is 266°N.

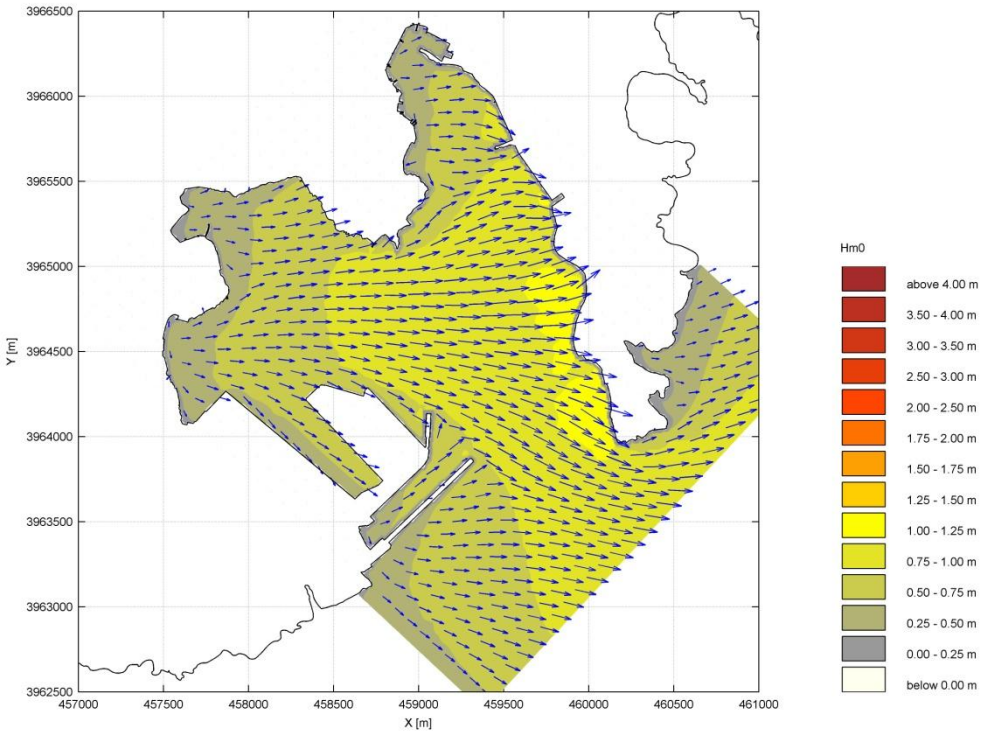

Figure 5-2: Spatial distribution of the significant wave height in SWAN grid C01 for extreme wind without offshore wind sea wave boundary conditions with return period 1/100 years and direction 270°N. The blue arrows indicate the mean wave direction, scaled with the significant wave height.

Based on the above results, as expected, it is concluded that the locally generated wind sea waves are lower and shorter than offshore generated wind sea waves. The locally generated waves have mean wave directions which are generally aligned with the wind direction, although locally their mean wave directions can be rotated due to refraction and upwind fetch restrictions. Due to the geometry and bathymetry of Marsaxlokk Bay, the wind sea waves penetrating from offshore have mean wave directions close to 190°N at the jetty (this is described in Chapter 7.2).

In Figure 5-3 and Figure 5-4, the spectra at the location of the bow are plotted for both simulations. In the top panel, the one-dimensional frequency spectrum is plotted. In the bottom left panel the one-dimensional directional spectrum is presented. The bottom right panel shows a contour plot of the two-dimensional spectrum.

It is apparent that the spectra for locally generated wind sea conditions are broader and less peaked than those for penetrating wind sea wave conditions. Also the directional spectrum is broader for the locally generated waves. In the two-dimensional contour plot, the effect of reflection can be seen as blobs of wave energy propagating westwards. These results clearly demonstrate the differences between locally generated and penetrating wind sea waves.

The observation that the peak frequencies of the spectra computed for both conditions are well separated in frequency-direction space implies that the non-linear interaction between both wave systems is very weak. This notion supports our choice to handle both wave systems separately.

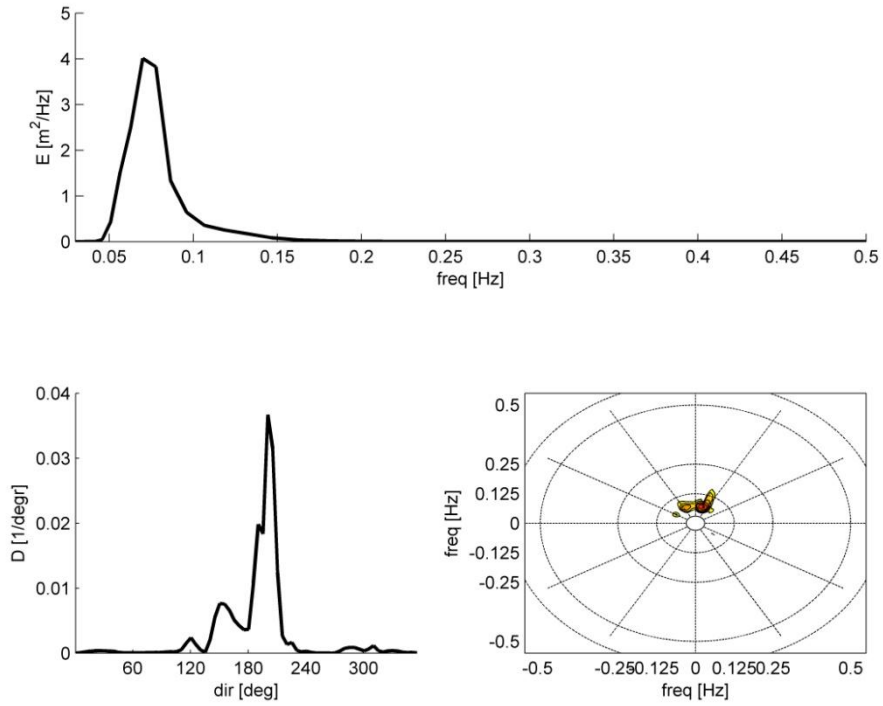

Figure 5-3: Spectra at the bow for extreme offshore (penetrating) wind sea wave boundary conditions without wind with return period 1/100 years and direction 270°N. Top panel: one-dimensional frequency spectrum. Bottom left panel: one-dimensional direction spectrum. Bottom right panel: polar representation of the two-dimensional spectrum.

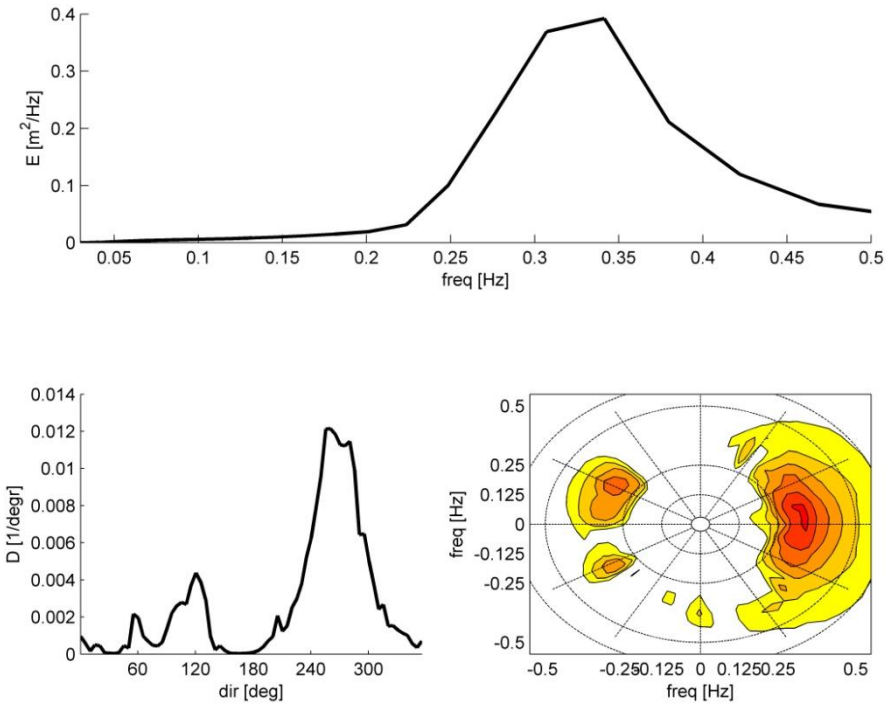

Figure 5-4: Spectra at the bow for extreme wind without offshore wind sea wave boundary conditions with return period 1/100 years and direction 270°N. Top panel: one-dimensional frequency spectrum. Bottom left panel: one-dimensional direction spectrum. Bottom right panel: polar representation of the two-dimensional spectrum.

5.3 REFINEMENT OF THE EXTREME WIND SEA WAVE CONDITIONS

Methodology

In the prior wave studies ([1], [2]), the locally generated waves were implicitly added to the penetrating wind sea waves through applying the local wind conditions in the SWAN model. In other words: the resulting nearshore time series of wind sea waves, that was created and presented in the prior wave studies, included both the penetrating wind sea and the locally generated wind sea component, represented by one significant wave height, peak wave period and mean wave direction. That way of presenting results could not distinguish between the two types of wind sea systems. The mean wave direction of locally generated waves is usually parallel to the wind direction but the mean wave direction of the penetrating waves depends on the geometry of the bay. As a result the mean wave direction of both components is more or less the energy weighted average of both directions.

The extreme wind sea wave conditions that were evaluated in Chapter 3 were based on the time series from the prior wave studies and consequently represent the combination of penetrated and locally generated waves. A proper separation of the wind sea wave conditions would be based on an evaluation of the nearshore wind sea wave spectra and a modelling study on the interaction between the two components. Due to time constraints, it is not possible to redo the wave penetration study in such a manner that this can be done. Therefore, a pragmatic methodology is applied to split the wind sea waves into locally generated and penetrating wind sea wave components.

To estimate the separate contributions of the locally generated wind sea waves and the penetrating wind sea waves, additional SWAN simulations have been done similar to the simulation with wind only, described in the above section (Chapter 5.2.2). The resulting wind sea wave conditions from these simulations are then subtracted from the total wind sea waves. As no wave spectra are available, this subtraction is performed in terms of the moments of the spectra, which can be determined from the significant wave height Hm0. The difference between the two is then presented as the penetrating wind sea wave component. The following relation holds true for the relation between the significant wave heights of the wind sea wave components:

$$H_{m0}^{pen} = \sqrt{H_{m0}^{pen2} - H_{m0}^{pen2}}$$

The superscripts tot, loc and pen refer to the total, locally generated and penetrating wind sea components. The spectral moments m_n are defined as:

$$m_n = \iint \omega^n E(\omega, \theta) d\omega d\theta$$

It is noted that the results of the separation should be used with care. The extreme nearshore wind sea wave conditions were derived from an extrapolation of a fitted extreme value probability distribution function to the nearshore time series. The presented results for the locally generated wind sea waves however are from model results. The different nature of the origin of the results for these two components may lead to slight difference inherent to modelling uncertainties. The results are intended as a first-order estimate of the separate contributions of penetrating and locally generated wind sea waves.

By applying the above relation, it is assumed that there is no interaction between the locally generated and penetrating wind sea waves. The validity of this assumption is supported by the analysis in the previous section that the peak frequencies of both components are well separated in frequency-direction space, implying that the interactions are weak. Also, it is assumed that wave reflection is not an important

process affecting the nearshore wave conditions as this is not accounted for in the proposed methodology. This assumption is supported from the prior wave studies, where it is concluded that the reflected components are of minor importance on the total wind sea wave conditions.

The additional simulations and refinement of the wind sea conditions are done for two types of wind sea wave conditions:

- Associated wind sea waves for governing extreme wind speeds (from Chapter 4.3.1
- (Governing) extreme wind sea waves (from Chapter 4.3.2).

It is expected that for northern and eastern wind directions, the contribution of locally generated waves is insignificant due to the short fetch lengths and small water depths inside Marsaxlokk Bay. For southern wind directions, the locally generated waves are propagating more or less parallel with the penetrating waves. For western wind directions, the locally generated wind waves approach the vessel beam-on and the available fetch length is relatively long. For this case differentiation must be made between wind waves penetrating into the bay from the South (these waves will approach the vessel head-on) and locally generated wind waves from the west (beam-on). The locally generated wind sea waves, which approach the FSU perpendicularly, primarily consist of short period waves.

For the extreme wind sea conditions, simulations have been performed for directions 180°N through 270°N. These directions have been selected because for those directions, the locally generated wind sea wave is more than 20% of the total wave energy. The associated wind speeds from Chapter 4.3.2 have been applied in the SWAN simulations. For the associated wind sea conditions for governing extreme wind speeds, simulations have been performed for directions 300°N through 60°N and the governing extreme wind speeds from Chapter 3.3.1 have been applied.

The peak wave periods of the penetrating wind sea waves are determined using engineering judgement. For the penetrating wind sea waves, the peak wave periods of the total wind sea wave conditions are assumed to be equal to the penetrating wind sea waves. Although it is likely that the periods of both contributions are different, this is deemed a reasonable choice compared to the nearshore extreme peak wave period results from the prior wave penetration study [2] and a closer inspection of the available time series from this and the previous wave studies. To account for the uncertainty in the presented peak wave periods, it is recommended to investigate the resulting loads on the mooring system within a band width of +/-10% of the presented peak wave periods.

The directions of the penetrating wind sea waves are taken to be approximately 190°N. The geometry of the bay acts as a filter on waves with angles not approximately perpendicular to the mouth of the bay. This is clearly demonstrated for penetrating swell waves in Chapter 7.2, but is also applicable to penetrating wind sea waves. Due to the larger directional spreading of wind sea waves, it is expected that the range of nearshore wind sea waves is larger. It is therefore recommended to investigate the resulting loads on the mooring system within a band width of +/-10° of the presented mean wave direction.

Results

The resulting nearshore extreme wind sea wave conditions are presented in Table 5-2. The wind sea wave conditions corresponding to governing extreme wind conditions are presented in Table 5-1. The first two columns represent the extreme wind speeds and directions and columns 3-5 the total wind sea conditions. In columns 6 – 8, the locally generated component of the associated nearshore wind sea conditions is presented and in columns 9 – 11 the penetrating component. From the table, it can be seen that the locally generated wind waves have lower significant wave heights and much shorter peak wave periods than the penetrating wind sea waves.

The recommended bandwidths for the penetrating wind sea peak wave periods and mean wave directions are indicated in the results.

Governing wind		Associated total wind sea			Associated locally generated wind sea			Associated penetrating wind sea		
Udir	U10	Dir	Hm0	Tp	Dir	Hm0	Tp	Dir	Hm0	Tp
[°N]	[m/s]	[°N]	[m]	[s]	[°N]	[m]	[s]	[°N]	[m]	[s]
0	25.9	298	1.51	11.7	341	0.75	2.6	190 +/- 10	1.31	11.7 +/- 10%
30	25.2	243	1.30	13.6	4	0.59	2.4	190 +/- 10	1.16	13.6 +/- 10%
270	25.4	214	1.87	12.8	269	0.91	2.9	190 +/- 10	1.63	12.8 +/- 10%
300	25.0	255	1.91	15.9	292	0.89	2.9	190 +/- 10	1.69	15.9 +/- 10%
330	24.4	290	1.40	10.6	320	0.79	2.6	190 +/- 10	1.15	10.6 +/- 10%

Table 5-1: Associated nearshore wind sea condition results, divided into locally generated and penetrating components, for the extreme offshore all-year wind speeds for a return period of 1/100 years and various wind sea directional sectors.

Associated wind		Governing total wind sea			Locally generated wind sea			Penetrating wind sea		
Udir	U10	Dir	Hm0 sea	Tp sea	Dir	Hm0	Tp	Dir	Hm0	Tp
[°N]	[m/s]	[°N]	[m]	[s]	[°N]	[m]	[s]	[°N]	[m]	[s]
180	18.5	190	3.17	10.4	184	0.62	2.6	190 +/- 10	3.11	10.4 +/- 10%
210	18.5	191	2.85	10.4	204	0.62	2.6	190 +/- 10	2.78	10.4 +/- 10%
240	21.7	200	1.68	12.1	242	0.76	2.6	190 +/- 10	1.50	12.1 +/- 10%
270	22.7	216	1.33	13.3	270	0.79	2.9	190 +/- 10	1.07	13.3 +/- 10%

Table 5-2: Nearshore extreme wind sea condition results, divided into locally generated and penetrating components, for a return period of 1/100 years and various wind sea directional sectors.

6 Spectral shape for nearshore extreme wave conditions

To obtain estimates for the spectral shape under extreme conditions, the computed wave spectra at the bow are analysed. For this analysis, the results from the extreme simulations from the previous wave studies [1, 2] are used. It is noted that these conditions are based on a propagation of offshore extreme boundary conditions towards the project site[2]. The motivation for using the results from the previous wave penetration study is that it is less time consuming compared to analysing all the spectra that were used to create the nearshore time series. The analysis will provide information about the spectral shape of conditions which are representative of wind sea waves. Estimates for the swell waves will be provided, based on literature.

The wave spectra that are used in this chapter are obtained from MIKE21BW simulations. Figures of the spectra for a return period of 1/100 years and offshore directions 60°N – 240°N are presented in Appendix 8. As an example, the results for offshore direction 180°N are reproduced here. The figure shows the wave spectrum as calculated with MIKE21BW in the wave penetration study [2] at the location of the bow for a return period of 1/100 years and an offshore direction 180°N.

In the top panel, the one-dimensional frequency spectrum is plotted. A JONSWAP spectrum is fitted to the frequency spectrum to obtain an estimate for a representative value for the spectral peakedness (γ). In this case, the value for γ is found to be 3.3. In the bottom left panel the one-dimensional directional spectrum is presented. To the directional spectrum, a $\cos^m((\theta-\theta_0)/2)$ directional distribution is fitted. Details of this function can be found in Appendix 1. For 180°N the optimum value form is 5.0 which is equivalent to a one-sided directional spreading of 22.9°. The bottom right panel shows a polar contour plot of the two-dimensional spectrum. In this contour plot, it can be seen that most of the wave energy comes from directions around 200°N. A smaller constituent of reflected waves from the north of the bay (330°N) is also visible.

[2] As a note: the reader is referred to Chapter 3.1 in this report, to understand the differences between the extreme conditions in this study (based on local time series) and the previous (based on a propagation of offshore extreme conditions towards the project site).

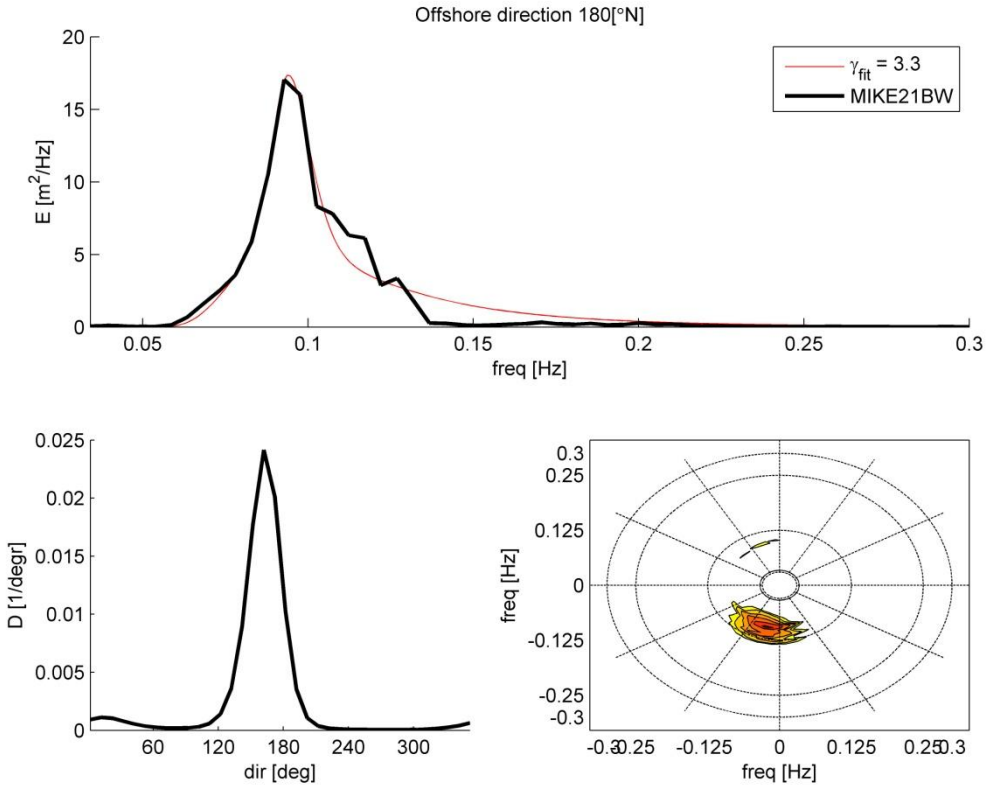

Figure 6-1: Spectra at the bow for extreme conditions with return period 1/100 years and direction 180°N as calculated with MIKE21BW in the wave penetration study in [2]. Top panel: one-dimensional frequency spectrum. Bottom left panel: one-dimensional direction spectrum. Bottom right panel: polar representation of the two-dimensional spectrum.

A summary of all fitted values for the spectral peakedness (γ), the directional spreading power (m) and the corresponding one-sided directional spreading for the extreme conditions with a return period of 1/100 year and all evaluated offshore directions, is presented in Table 6-1. The table shows that the spectral peakedness factor γ varies between 2.9 and 4.9. The directional spreading factor varies between 5.0° for an offshore wind direction of 60°N and 27.4° for an offshore wind direction of 240°N. These ranges are representative for the nearshore extreme wind sea wave conditions.

As the values for both γ and m vary considerably, they should be interpreted and applied with care. It is recommended to investigate the effect of the proposed range of values for γ on the mooring system. A bandwidth of approximately 5° is proposed for the directional spreading.

Offshore [°N]	γ [-]	m [-]	dspr [°N]
60	3.2	5.0	22.9 +/- 2°
90	3.5	5.1	22.7 +/- 2°
120	4.9	5.8	21.5 +/- 2°
150	3.9	10.9	16.4 +/- 2°
180	3.3	11.9	15.8 +/- 2°
210	3.6	23.1	11.6 +/- 2°
240	2.9	27.4	10.7 +/- 2°

Table 6-1:.Spectral peakedness, directional power and one-sided directional spreading representative for wind sea wave conditions, obtained from fitting to the extreme wave conditions at the bow for return period 1/100 years and various offshore directions.

Swell wave are characterised by very peaked spectra with narrower directional distributions than for wind seas. For swell waves, a common value for the spectral peakedness (γ) is approximately 10. In literature, a

value of 5 is also reported for swell in the Mediterranean Sea (see Saulnier, 2013). Given the uncertainty in the presented values, it is recommended to investigate a range of values between 5 and 10. The directional spreading of swell at the berth will be less than at the entrance of Marsaxlokk Bay (due to sheltering effects some side wave components are filtered out). As no model results or measured data is available, a typical value for the directional spreading of swell waves of 10° is proposed for the design of the mooring system. To account for the uncertainty of this value, a range of width from 10° to 15° is proposed for the directional spreading. Smaller values than 10° are considered to be unrealistic.

7 Collinearity analysis

7.1 WIND DIRECTION AND WIND SEA MEAN WAVE DIRECTION

To investigate the relation between wind and wind sea wave directions, the omnidirectional all-year scattered offshore wind directions are plotted against the nearshore wind sea mean wave directions (Figure 7-1). In grey the complete range of occurring directions is presented, and in colours the directions for a wind sea significant wave height above 0.5 m are shown. Please note that the figure does not indicate the strength of the wind speed or the significant wave heights, but merely the number of occurring conditions.

The figure indicates that for wind sea mean wave directions around 180°N, the corresponding wind directions vary between roughly 60°N and 270°N. This is attributed to the directional steering of penetrated wind sea waves from offshore into Marsaxlokk Bay. Due to the geometry of the bay, these waves approach the jetty always from approximately 180°N.

For wind directions between 240°N and 360°N, the mean wave direction of wind sea is approximately the same as the wind direction. This is a well know feature of locally generated waves inside the bay. For wind directions between 0°N and 90°N, the wind sea mean wave direction pattern is more complex. The combined effect of refraction on the penetrating waves and the effect of local wave generation lead to results which need careful interpretation. In Figure 7-2, an example of the wind sea waves is presented for offshore wind and wind sea wave boundary conditions from 60°N. The mean wave direction at the jetty is approximately 235°N which demonstrates that penetrating wind sea waves have mean wave directions which are not collinear to the wind direction.

To further aid the interpretation of the collinearity of wind directions and nearshore wind sea mean wave directions, the joint probabilities of occurrence are presented in Table 7-1. The colours indicate the misalignment with dark green being 0° and dark red 180°. The table shows the same data as Figure 7-1, albeit in a different format and with the vertical axis is reversed.

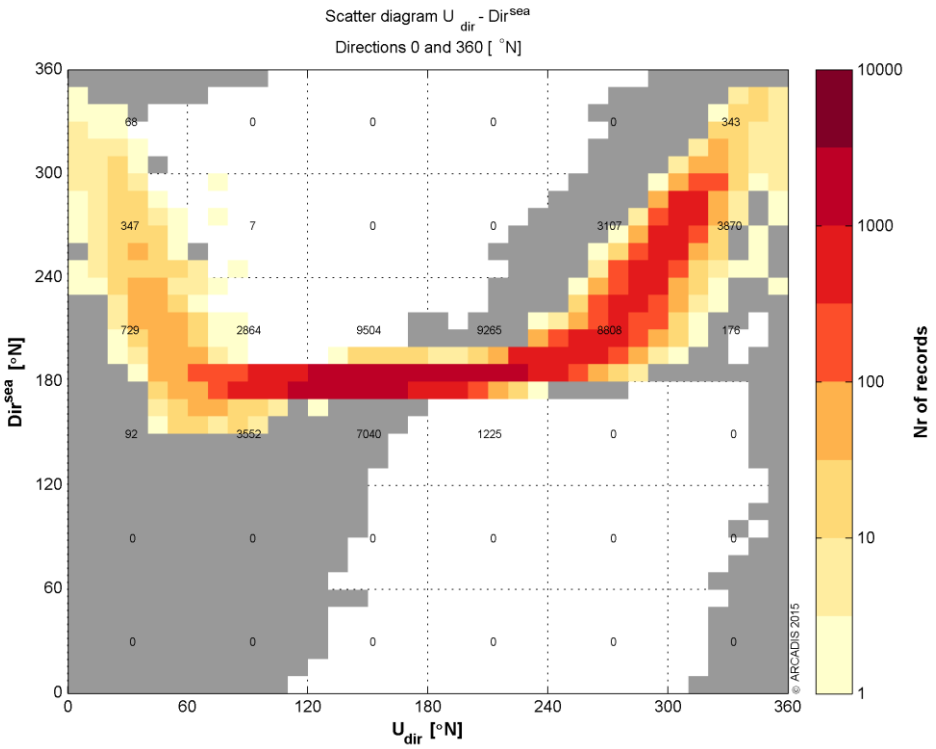

Figure 7-1: Scatter diagram of omnidirectional nearshore all-year wind directions in °N against omnidirectional nearshore all-year wind sea mean wave directions in °N. The box colours indicate the number of records for a combination of wind directions and wind sea mean wave directions in the complete nearshore time series. The purple line represents the best fit.

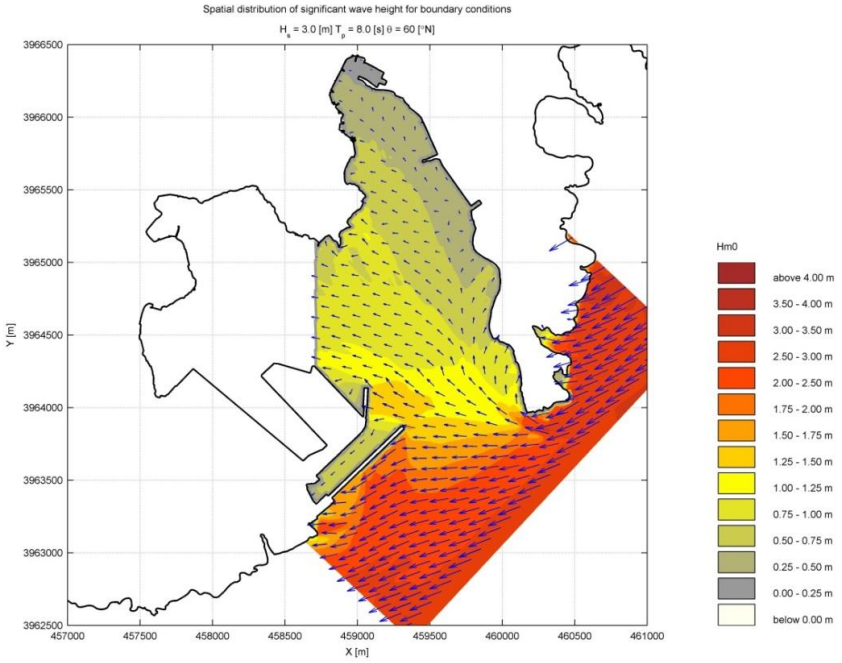

Figure 7-2: Spatial distribution of the significant wave height in SWAN grid C01 for normal offshore wind sea wave with boundary conditions Hs = 3.0 m, Tp = 8.0 s, Dir = 60°N. The blue arrows indicate the mean wave direction, scaled with the significant wave height.

wave direction degrees		wind direction degrees												
		-15 to	15 to	45 to	75 to	105 to	135 to	165 to	195 to	225 to	255 to	285 to	315 to	Total
Lower	Upper	15	45	75	105	135	165	195	225	255	285	315	345	
-15	15	2.58	1.86	.23	.03	.00	.	.	.	.	.00	.03	.47	5.19
15	45	.13	1.20	1.49	.19	.01	.	.	.	.	.	.	.02	3.03
45	75	.04	.20	1.17	.36	.02	.00	.	.	.	.	.	.01	1.79
75	105	.03	.11	.87	.66	.05	.00	.	.	.	.	.	.00	1.73
105	135	.02	.10	.58	1.06	.12	.00	.	.	.	.	.	.00	1.88
135	165	.02	.09	.48	2.01	.94	.05	.00	.	.	.	.	.00	3.59
165	195	.32	.35	.69	2.56	6.66	7.62	6.63	5.63	3.90	.86	.43	.34	36.00
195	225	.01	.10	.10	.00	.	.	.00	.14	2.71	3.98	.70	.03	7.77
225	255	.02	.09	.03	.00	.	.	.	.00	.19	4.08	2.42	.08	6.91
255	285	.02	.06	.01	.	.	.	.	.00	.02	1.93	7.38	.44	9.85
285	315	.06	.03	.00	.00	.	.	.	.	.00	.24	10.22	3.63	14.18
315	345	1.24	.03	.00	.	.	.	.	.	.	.01	.93	5.87	8.08
Total		4.47	4.20	5.65	6.87	7.80	7.68	6.63	5.77	6.81	11.09	22.11	10.90	100.00

Table 7-1:.Joint probability of occurrence of omnidirectional nearshore all-year wind directions in °N against omnidirectional nearshore all-year wind sea mean wave directions in °N. The dark green colour indicates a misalignment of 0° and the dark red 180°.

7.2 WIND DIRECTION AND SWELL MEAN WAVE DIRECTION

To investigate the relations between wind and wind sea wave directions, the omnidirectional all-year scattered offshore wind directions are plotted against the nearshore swell mean wave directions (Figure 7-3). In grey the complete range of occurring directions is presented, and in colours the directions for a swell significant wave height above 0.25 m are shown. The figure does not show any information regarding the severity of wind and wave conditions, but merely the number of occurring conditions. The figure shows that the swell waves have mean wave directions around 190°N for all wind directions. This is precisely as expected and consistent with the results in the wave penetration study [2]. It is recommended to investigate the resulting loads on the mooring system within a band width of +/-10° of the presented mean wave direction.

In Table 7-2, the numerical values for the joint probabilities of occurrence are presented. The colours indicate the misalignment with dark green being 0° and dark red 180°. The table corresponds with Figure 7-3, albeit in a different format and with the vertical axis is reversed.

It is noted that for any wind direction, a swell mean wave direction around 190°N is an appropriate choice. Inversely, for a swell mean wave direction of about 190°N, any wind direction may occur. It is not possible to select an associated swell mean wave direction from the investigated data. It is recommended to select an associated wind direction that represents a conservative load on the mooring system. The same is applicable to the associated wind sea mean wave direction.

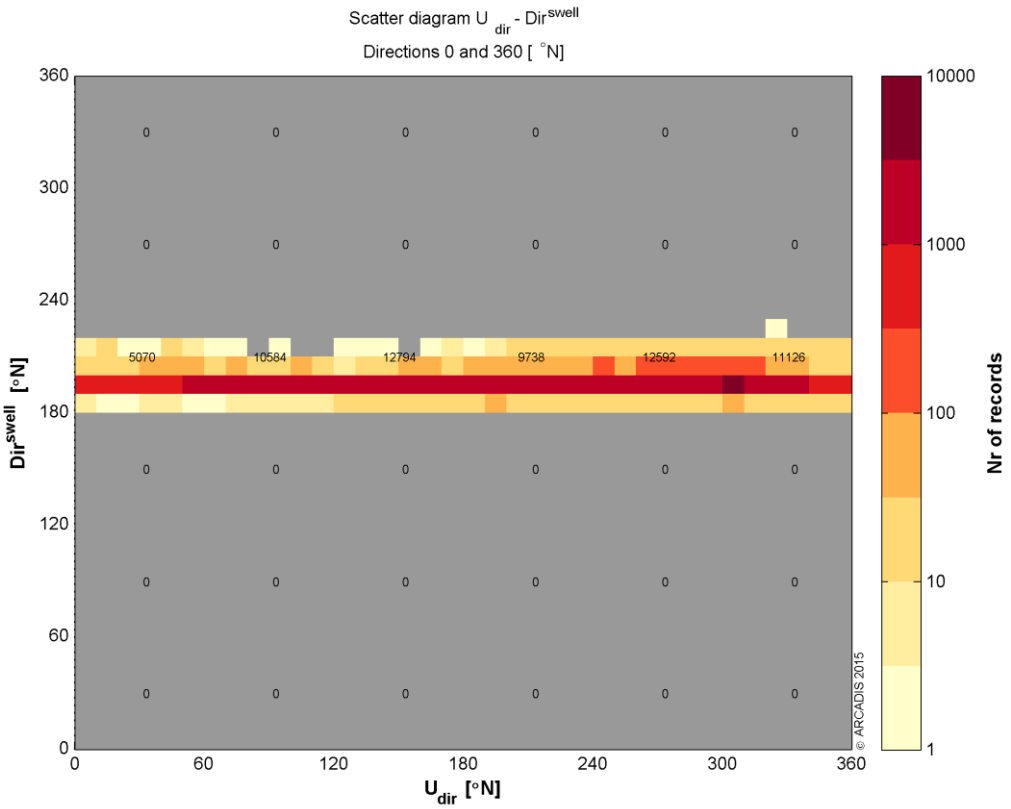

Figure 7-3: Scatter diagram of omnidirectional nearshore all-year wind directions in °N against omnidirectional nearshore all-year swell mean wave directions in °N. The box colours indicate the number of records for a combination of wind directions and swell mean wave directions in the complete nearshore time series. The purple line represents the best fit.

wave direction degrees		wind direction degrees												
		-15 to	15 to	45 to	75 to	105 to	135 to	165 to	195 to	225 to	255 to	285 to	315 to	Total
Lower	Upper	15	45	75	105	135	165	195	225	255	285	315	345	
-15	15	.21	.14	.15	.20	.17	.15	.14	.14	.28	.56	.50	.34	3.00
15	45	.11	.08	.09	.14	.13	.09	.08	.09	.14	.35	.28	.19	1.76
45	75	.04	.03	.04	.06	.05	.03	.03	.03	.05	.11	.12	.07	.65
75	105	.05	.04	.05	.08	.06	.04	.03	.04	.05	.12	.14	.08	.77
105	135	.09	.07	.09	.19	.20	.10	.07	.08	.1	.23	.32	.15	1.70
135	165	.14	.11	.17	.30	.36	.27	.15	.16	.18	.41	.67	.28	3.19
165	195	1.34	1.43	2.28	3.30	4.35	3.79	3.02	2.37	2.42	3.78	9.88	3.93	41.89
195	225	1.05	1.33	1.76	1.74	1.84	2.32	2.01	1.52	1.73	2.67	6.30	2.76	27.02
225	255	.93	.62	.63	.40	.3	.52	.76	.78	.87	1.30	2.15	2.13	11.41
255	285	.18	.14	.16	.16	.13	.14	.14	.26	.36	.55	.76	.40	3.39
285	315	.15	.10	.11	.12	.08	.07	.09	.14	.32	.47	.47	.26	2.39
315	345	.18	.12	.14	.17	.12	.14	.11	.15	.33	.55	.52	.31	2.84
Total		4.47	4.20	5.65	6.87	7.80	7.68	6.63	5.77	6.81	11.09	22.11	10.90	100.00

Table 7-2:.Joint probability of occurrence of omnidirectional nearshore all-year wind directions in °N against omnidirectional nearshore all-year swell mean wave directions in °N. The dark green colour indicates a misalignment of 0° and the dark red 180°.

8 Significant wave height – peak wave period relations

For the fatigue analysis of the mooring system, tables with the joint probability of significant wave height and peak wave period are required. In Table 8-1, the joint probability of occurrence of nearshore wind sea significant wave height and peak wave period at the bow is presented. In Table 8-2, the same is presented for swell waves.

In the wave penetration study report [2], tables for the joint probability with nearshore mean wave periods (Tm-10) were presented. A close relation between the mean wave period and peak wave period exists. As a result, the tables show the same relations of peak and mean wave periods with significant wave heights albeit with slightly different values. For fatigue analyses the period measures should be based on the estimated zero-crossing period which can be estimated by the mean period T_{m02}. The above tables provided the necessary input information.

Hs		spectral peak wave period seconds														
meters		<	2.0	3.0	4.0	5.0	6.0	7.0	8.0	9.0	10.0	11.0	12.0	13.0	14.0	
		to	to	to	to	to	to	to	to	to	to	to	to	to	to	Total
Lower	Upper	2.0	3.0	4.0	5.0	6.0	7.0	8.0	9.0	10.0	11.0	12.0	13.0	14.0	>	
<	.25	48.55	6.76	3.82	.75	.29	.05	.00		.00						60.22
.25	.50	3.08	3.57	8.68	4.20	1.78	.60	.17	.02	.00	.00					22.10
.50	.75		.07	.55	3.79	2.49	1.18	.55	.28	.03	.00	.00				8.93
.75	1.00			.00	.68	1.84	.80	.57	.37	.21	.05	.00				4.52
1.00	1.25				.00	.64	.85	.34	.21	.14	.11	.02				2.30
1.25	1.50					.01	.49	.35	.14	.05	.04	.01	.00			1.10
1.50	1.75						.02	.30	.12	.03	.02	.00	.00			.48
1.75	2.00							.06	.11	.03	.01	.00				.21
2.00	2.25							.00	.06	.01	.01	.00				.08
2.25	2.50								.01	.02	.01					.03
2.50	2.75									.00	.01	.00				.01
2.75	3.00									.00	.00	.00				.01
3.00	3.25															.
3.25	3.50															.
3.50	>															.
Total		51.62	10.40	13.05	9.42	7.05	3.99	2.33	1.32	.54	.25	.04	.00	.	.	100.00

Table 8-1: Joint probability of occurrence of omnidirectional nearshore all-year wind sea significant wave height in m against peak wave periods in s. The red colour indicates conditions with a high probability of occurrence and the green colours low.

Hs		spectral peak wave period seconds														
meters		<	2.0	3.0	4.0	5.0	6.0	7.0	8.0	9.0	10.0	11.0	12.0	13.0	14.0	
		to	to	to	to	to	to	to	to	to	to	to	to	to	to	Total
Lower	Upper	2.0	3.0	4.0	5.0	6.0	7.0	8.0	9.0	10.0	11.0	12.0	13.0	14.0	>	
<	.25	26.49	3.82	5.86	9.00	10.71	9.40	6.96	4.17	1.59	.39	.07	.03	.01	.01	78.51
.25	.50		.00	.55	2.30	4.39	3.46	2.20	.98	.75	.57	.02	.00	.00	.00	15.22
.50	.75				.05	1.16	1.90	1.01	.40	.14	.23	.03	.00	.00		4.91
.75	1.00				.00	.08	.50	.36	.13	.06	.05	.01	.00			1.18
1.00	1.25					.00	.03	.04	.03	.02	.01	.01	.00			.14
1.25	1.50						.00	.00	.01	.01	.00	.00	.00			.03
1.50	1.75									.00	.00	.00				.00
1.75	2.00									.00	.00					.00
2.00	2.25									.00						.00
2.25	2.50															.
2.50	2.75															.
2.75	3.00															.
3.00	3.25															.
3.25	3.50															.
3.50	>															.
Total		26.49	3.82	6.41	11.35	16.34	15.29	10.56	5.72	2.56	1.25	.14	.04	.02	.01	100.00

Table 8-2: Joint probability of occurrence of omnidirectional nearshore all-year swell significant wave height in m against peak wave periods in s. The red colour indicates conditions with a high probability of occurrence and the green colours low.

9 Current conditions

This chapter describes the results of the assessment of current effects on the hydraulic conditions in the Bay of Marsaxlokk. As a full-blown modelling study to these effects is unfeasible within the scope of this project, we performed a literature survey and simplified computations to provide an estimate of the current conditions. Based on the information from [3] it turned out to be very difficult to provide (even a rough estimate of) current conditions under extreme conditions at the location where the ship will be anchored, the main reasons being:

- It is very difficult to accurately determine the velocities from the figures;
- the numerical simulations have been carried out for wind speeds of 1.5 m/s.

Since the flow is not a linear function of the wind speed, it is impossible to use rules of thumb. Instead we have set up our own flow simulations using the open source Delft3D software, as developed by Deltares, to provide a first guess of the flow conditions. The model setup has been based on the most detailed SWAN wave model schematisation that has been used in the previous studies [1] and [2]. However, the results show that the domain is too small and some instabilities from the open boundary are influencing the flow patterns in the harbour entrance.

Simulations have been carried out for the all-year extreme wind conditions with a return period of 1/100 years and all 12 direction sectors (see Table 2-2 in [1]). Table 9-1 presents for all simulations the current velocities and direction at the stern, mid ship and at the bow of the anchored ship (70 m west of the jetty).

Since the model is run in 2DH mode, the presented values are depth-average values. The results provide no information on current profile. It is estimated that a power law current profile can be applied (see ISO 19901-1 Part 1: Metocean design and operating considerations) to get an indication of the current profile. If more detailed information on the current conditions inside the bay and at the location of the FSU is needed then a more extended flow study is required.

The results show that the highest velocity at the bow is 0.29 m/s. It has a direction of 300°N. This current condition is found for a wind from the west (270 °N). It is noted that the current velocities can vary significantly with position along the ship.

Governing wind		Associated current - stern		Associated current - mid		Associated current - bow	
Udir [°N]	U10 [m/s]	U [m/s]	Dir [°N]	U [m/s]	Dir [°N]	U [m/s]	Dir [°N]
0	25.9	0.09	198	0.10	196	0.12	188
30	25.2	0.08	201	0.09	197	0.11	191
60	23.1	0.09	201	0.08	217	0.06	230
90	21.1	0.09	169	0.09	180	0.08	196
120	20.4	0.13	152	0.14	160	0.16	167
150	21.9	0.08	156	0.08	171	0.09	183
180	20.0	0.06	132	0.06	158	0.08	171
210	20.7	0.19	353	0.22	359	0.20	375
240	21.4	0.22	312	0.19	340	0.21	365
270	25.4	0.29	303	0.21	329	0.23	351
300	25.0	0.22	281	0.20	307	0.18	332
330	24.4	0.15	147	0.13	193	0.17	242

Table 9-1: Current velocity and direction at the stern, midway and bow of the ship for 1/100 year wind conditions and all directional wind sectors.

The current directions are not well aligned with the wind direction. The reason is illustrated with Figure 9-1 that shows the current pattern for the 1/100 year wind condition from the west. The positions of the locations at the bow, stern and midship have been indicated with the white dots, west of the jetty. The flow conditions near the ship are the result of the clockwise eddy in the centre of the port. This explains the large variation of flow conditions along the ship. A counter clockwise eddy in the port entrance is the result of the strong current in front of the port. Since in reality the currents near the southeast point of Malta are a result of the large scale wind driven circulation in the Mediterranean Sea, and as this is not included in the flow model, it is uncertain whether these results are representative. From these results, it is also not clear to what extent the eddy in the port entrance is also driving the eddy in the port itself. For this reason it's hard to give an accuracy bandwidth of the results. For a proper analysis of the flow conditions near the jetty, a more detailed flow study is recommended.

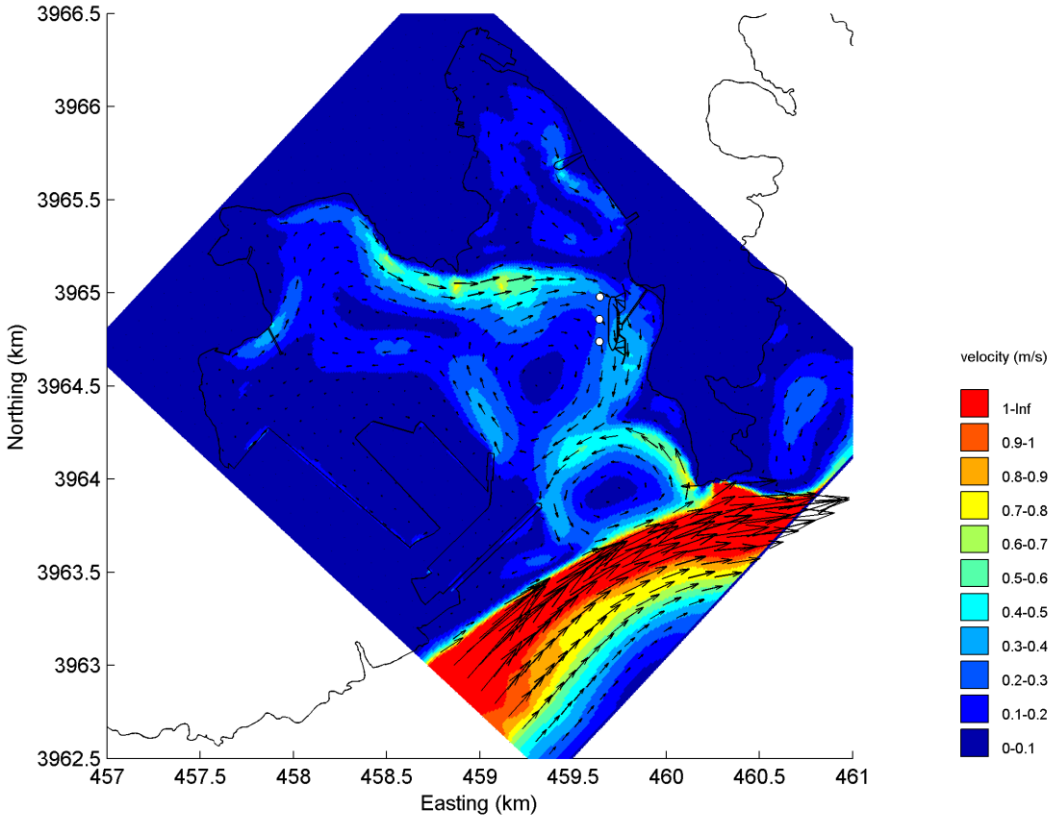

Figure 9-1: Current pattern for wind 25.4 m/s, 270 °N. The blue arrows indicate the current direction, scaled with the current velocity.

The significance of large scale current effects can be judged by comparing the computed flow velocities with the highest expected orbital velocities at the crest of the incident waves. In view of the limited amount of information available only a crude estimate is made. Based on the results in Table 9-1, the highest current velocity is about 0.25 m/s, for a wind direction of 270°. This number can be compared with the orbital velocity at the crest of an associated wind sea wave (see Table 4-3). Using linear wave theory this leads to a maximum crest velocity of about 12 m/s.

As the estimates, both for the current velocity and the orbital velocities are crude estimates, it can be concluded that the current velocities are about 5% to 10% of the orbital velocities. In practise, it should be realized that the wave induced orbital velocities have a cyclic character whereas the large current is more or less stationary in time.

10 Qualitative analysis of wave conditions at more westward locations

Under extreme conditions the FSU won't be kept at the jetty but will be moored approximately 70 m further west in a spread mooring system. This shift will result in slightly different wave conditions found earlier for the location at the jetty. Unfortunately no output point is located at the shifted position so no full quantitative analysis could be performed. Therefore, we are only able to present indicative results. Our analysis is based on inspection of figures showing the spatial variation of the significant wave height that are calculated in the wave penetration study [2]. The results for extreme conditions with a return period of 1/100 years are discussed in this chapter.

Because the nature of the spread mooring system being more vulnerable to beam waves, it is important to consider a longitudinal and lateral component for the wave conditions. The most severe wave conditions are coming from the southern offshore conditions (120°N - 240°N) and result in a mostly longitudinal component. The largest lateral component will be obtained from local fetch in the harbour basin due to extreme winds from western directions (240°N - 300°N). Below, we consider the relevant direction sectors to estimate the variation in wave conditions when the FSU is located 70 m more to the west.

Offshore directions 60°N - 240°N

In Appendix 9, figures are presented with the spatial variation of significant wave height centred on the original and 70 m westward shifted FSU positions. As an example, the spatial variation of the significant wave height for the 1/100 conditions with an offshore 180°N direction is shown in Figure 10-1. Because of the combined effect of refraction and energy dissipation at the shallow bathymetry near the eastern land boundary, the significant wave height will increase the further west the ship is moored. The differences in significant wave height are largest at the stern (an increase of approximately 0.5 m at the 70 m westward shifted position), while they are almost equal at the bow. For other directional sectors similar trends in the variation of significant wave height are observed, although the differences in significant wave height are altered.

Offshore direction 270°N – 300°N

For other directions larger than 240°N, no extreme computations were done and consequently figures cannot be presented for these directions. The westward shift reduces slightly the fetch length of locally generated waves, but this reduction of 70 m is relatively small compared to the entire fetch-length which is approximately 2.5 km. It is expected that the effect of the shift on the wave conditions is small.

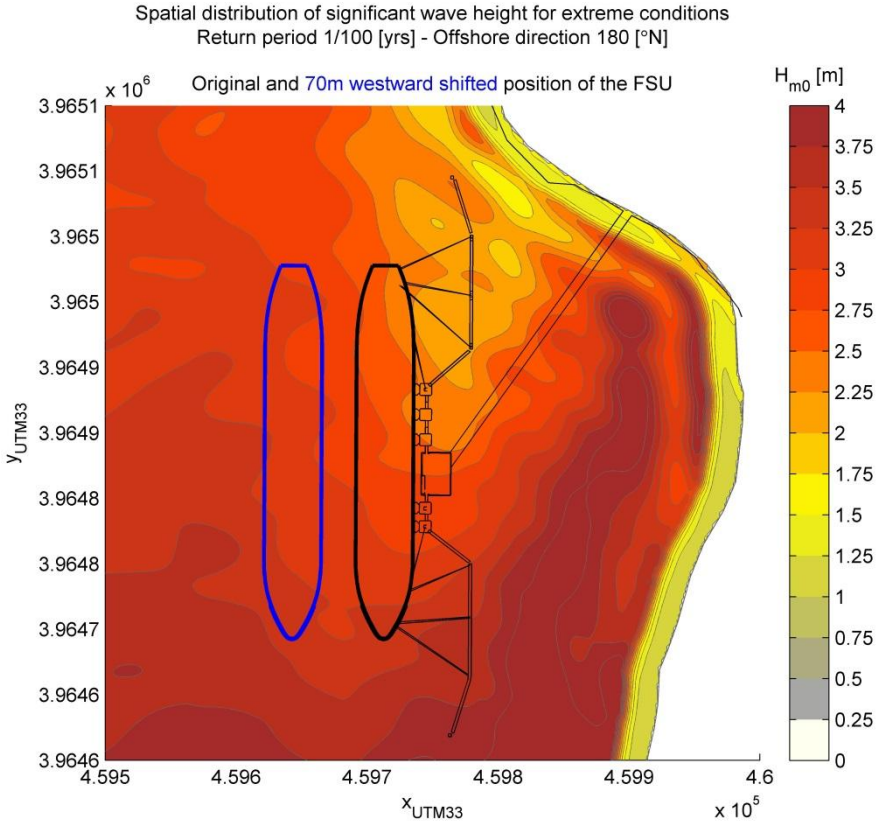

Figure 10-1: Spatial distribution of the significant wave height in SWAN grid C01, centred around the FSU, for extreme wind sea wave conditions with return period 1/100 years and offshore direction 180°N.

11 Conclusions and recommendations

A detailed analysis of the nearshore time series has been performed to provide design metocean data for the mooring system. Firstly, the directional extremes of offshore all-year wind speed, wind sea and swell significant wave height were determined (Chapter 3). Secondly, for each of these parameters, the most likely values of a series of associated parameters are subsequently determined in Chapter 4. In this chapter a general methodology was followed which involved making scatter plots of combinations of parameters and fitting a suitable function to the scattered data. In the subsequent chapters (Chapters 5 - 8) various relations between parameters were investigated in more detail.

Associated wind, wave and current conditions for 1/100 year conditions

In Table 11-1 - Table 11-3, an overview of the results are presented for wind, wind sea and swell governed conditions. In the second row of the tables, the chapter is indicated in which the derivation of the results in that column is presented. The reader is referred to Chapters 2.2 for an outline of the followed methodology and to the chapters mentioned in the header for more details and the applicability of the results.

For swell governed conditions, no associated wind directions and wind sea mean wave directions are presented. This was not possible since for swell directions, no associated wind directions and wind sea mean wave directions can be defined. This is explained in Chapter 7. It is recommended to investigate the range of occurring wind directions and wind sea mean wave directions and select conservative conditions, based on the characteristics of the designed mooring system. It is noted that swell waves at the location of the bow of the FSU are always coming from about 190^{0}N.

Governing wind		Associated current		Associated wind sea			Associated swell		
3.3.1	3.3.1	10	10	7.1	4.3.1	4.3.1	7.2	4.3.1	4.3.1
Udir	U10	U	V	Dir	Hm0 sea	Tp sea	Dir	Hm0 swell	Tp swell
[°N]	[m/s]	[m/s]	[m/s]	[°N]	[m]	[s]	[°N]	[m]	[s]
0	25.9	0.02	0.12				193	0.58	10.5
30	25.2	0.02	0.11				194	0.59	10.6
60	23.1	0.05	0.04	191	1.53	11.8	194	0.59	10.5
90	21.1	0.02	0.08	179	2.07	11.0	192	0.54	10.0
120	20.4	-0.03	0.15	180	2.53	10.3	192	0.49	8.8
150	21.9	0.01	0.09	181	3.09	11.0	192	0.34	9.3
180	20.0	-0.01	0.08	181	2.96	9.5	192	0.37	9.1
210	20.7	-0.05	-0.20	184	2.61	10.3	192	0.53	9.2
240	21.4	-0.02	-0.21	192	2.07	10.3	193	0.59	9.9
270	25.4	0.04	-0.22				193	0.62	9.7
300	25.0	0.08	-0.16				193	0.56	9.2
330	24.4	0.15	0.08				193	0.62	9.4

Table 11-1: Extreme and associated condition results for wind governed conditions for a return period of 1/100 years and various wind directional sectors. For the orange marked cells the wind sea conditions are split into a local and a penetrating wind sea component, see Table 11-4.

Associated wind		Governing wind sea			Associated swell		
7.1	4.3.2	3.3.2	3.3.2	4.3.2	7.2	4.3.2	4.3.2
Udir	U10	Dir	Hm0 sea	Tp sea	Dir	Hm0 swell	Tp swell
[°N]	[m/s]	[°N]	[m]	[s]	[°N]	[m]	[s]
180	18.5				190 +/- 10	0.42	9.9
210	18.5				190 +/- 10	0.63	11.7
240	21.7				190 +/- 10	0.68	10.8
270	22.7				190 +/- 10	0.53	10.3

Table 11-2: Extreme and associated condition results for wind sea governed conditions for a return period of 1/100 years and various wind sea directional sectors. For the orange marked cells the wind sea conditions are split into a local and a penetrating wind sea component, see Table 11-5.

Associated wind		Associated wind sea			Governing swell		
	4.3.3		4.3.3	4.3.3	3.3.3	3.3.3	4.3.3
Udir	U10	Dir	Hm0 sea	Tp sea	Dir	Hm0 swell	Tp swell
[°N]	[m/s]	[°N]	[m]	[s]	[°N]	[m]	[s]
	13.2		1.25	7.6	180	2.04	10.3
	17.5		1.41	10.8	210	1.27	11.2

Table 11-3: Extreme and associated condition results for swell governed conditions for a return period of 1/100 years and various swell directional sectors.

A number of cells in Table 11-1 and Table 11-2 are marked by an orange colour. For these directions, the wave conditions are comprised of three significant contributions:

- Wind sea waves which are penetrating from the Mediterranean Sea into Marsaxlokk Bay;
- Wind sea waves which are generated inside Marsaxlokk Bay by the wind;
- Swell wave which are penetrating from the Mediterranean Sea into Marsaxlokk Bay.

It is advised to evaluate the combined effect of all three wave components for the evaluation of the mooring system.

The two wind sea wave components were evaluated in Chapter 5. In Table 11-4 and Table 11-5, the results are presented. The results for the locally generated wind sea waves were obtained from additional SWAN simulations in which wind was included, but no wave boundary conditions. The significant wave heights of the penetrating wind sea waves are obtained by subtracting the locally generated significant wave heights from the total. The peak wave periods and directions were based on engineering judgement. The table shows that the locally generated wind waves have lower significant wave heights, shorter peak wave periods than the penetrating wind sea waves. The mean wave directions of the locally generated waves are more or less parallel to the wind direction, in contrast to the penetrating waves which come from approximately 190°N. Given, the uncertainties of the results, recommendations for a bandwidth of the presented results are made.

For the mooring analysis it is recommended to use the separated wind sea components since the total wind sea has a mean wave direction which is not representative for the actual situation.

Governing wind		Associated total wind sea			Associated locally generated wind sea			Associated penetrating wind sea		
Udir	U10	Dir	Hm0	Tp	Dir	Hm0	Tp	Dir	Hm0	Tp
[°N]	[m/s]	[°N]	[m]	[s]	[°N]	[m]	[s]	[°N]	[m]	[s]
0	25.9	298	1.51	11.7	341	0.75	2.6	190 +/- 10	1.31	11.7 +/- 10%
30	25.2	243	1.30	13.6	4	0.59	2.4	190 +/- 10	1.16	13.6 +/- 10%
270	25.4	214	1.87	12.8	269	0.91	2.9	190 +/- 10	1.63	12.8 +/- 10%
300	25.0	255	1.91	15.9	292	0.89	2.9	190 +/- 10	1.69	15.9 +/- 10%
330	24.4	290	1.40	10.6	320	0.79	2.6	190 +/- 10	1.15	10.6 +/- 10%

Table 11-4: Associated nearshore wind sea conditions, divided into locally generated and penetrating components, for the extreme offshore all-year wind speeds for a return period of 1/100 years and various wind sea directional sectors.

Associated wind		Governing total wind sea			Locally generated wind sea			Penetrating wind sea		
Udir	U10	Dir	Hm0 sea	Tp sea	Dir	Hm0	Tp	Dir	Hm0	Tp
[°N]	[m/s]	[°N]	[m]	[s]	[°N]	[m]	[s]	[°N]	[m]	[s]
180	18.5	190	3.17	10.4	184	0.62	2.6	190 +/- 10	3.11	10.4 +/- 10%
210	18.5	191	2.85	10.4	204	0.62	2.6	190 +/- 10	2.78	10.4 +/- 10%
240	21.7	200	1.68	12.1	242	0.76	2.6	190 +/- 10	1.50	12.1 +/- 10%
270	22.7	216	1.33	13.3	270	0.79	2.9	190 +/- 10	1.07	13.3 +/- 10%

Table 11-5: Nearshore extreme wind sea condition results, divided into locally generated and penetrating components, for a return period of 1/100 years and various wind sea directional sectors.

Spectral shape of wind sea and swell

The following recommendations are made for the spectral peakedness (γ) and directional spreading of swell and wind sea wave conditions

- Wind sea wave conditions.
  Based on the modelling results from the wave penetration study for extreme wave conditions A range for γ between 2.9 and 4.9 is recommended and the directional spreading factor varies between 5 and 27, or in terms of the directional spreading between 10.7° and 22.9°.
- Swell wave conditions.
  Based on engineering judgement representative values of γ between 5 and 10 are proposed for swell wave conditions. A directional spreading of penetrating swell waves of 10° is proposed for the design of the mooring system.

As the values for both γ and m vary considerably, they should be interpreted and applied with care. It is recommended to investigate the effect of the proposed ranges of γ on the mooring system. A bandwidth of approximately 5° is proposed for the directional spreading for both wind sea and swell waves, with a minimum value of 10° for swell waves. The presented values are based on a JONSWAP spectral shape.

Current conditions

Current conditions have been investigated using a review of available literature. Additionally, 2DH-simulations have been performed with the flow model Delft3D for extreme wind speeds of all directional sectors. The resulting current conditions from Delft3D at the stern, midship and bow location of the ship are presented in Table 11-6. It is noted that the simulations were intended to get a first estimate of the current conditions at the locations of the jetty. For a proper analysis of the flow conditions near the jetty, a more detailed flow study is recommended.

For wind sea and swell governed conditions, no associated current conditions are presented because a detailed flow study was beyond the scope of this study (see Chapter 9). It is recommended to investigate the range of occurring current conditions and select conservative conditions, based on the characteristics of the designed mooring system.

Governing wind		Associated current - stern		Associated current - mid		Associated current - bow	
Udir [°N]	U10 [m/s]	U [m/s]	Dir [°N]	U [m/s]	Dir [°N]	U [m/s]	Dir [°N]
0	25.9	0.09	198	0.10	196	0.12	188
30	25.2	0.08	201	0.09	197	0.11	191
60	23.1	0.09	201	0.08	217	0.06	230
90	21.1	0.09	169	0.09	180	0.08	196
120	20.4	0.13	152	0.14	160	0.16	167
150	21.9	0.08	156	0.08	171	0.09	183
180	20.0	0.06	132	0.06	158	0.08	171
210	20.7	0.19	353	0.22	359	0.20	375
240	21.4	0.22	312	0.19	340	0.21	365
270	25.4	0.29	303	0.21	329	0.23	351
300	25.0	0.22	281	0.20	307	0.18	332
330	24.4	0.15	147	0.13	193	0.17	242

Table 11-6: Current velocity and direction at the stern, midway and bow of the FSU for 1/100 year wind conditions and all directional wind sectors.

Wave condition 70 m westward of jetty

A qualitative evaluation of the spatial variation of the significant wave height for extreme conditions with a return period of 1/100 years was carried out to investigate the effect of moving the FSU 70 m westward on the applicable extreme wave conditions. It was found that for offshore directions 60°N - 240°N, the significant wave height will increase the further west the ship is moored. The differences in significant wave height are largest at the stern (an increase of approximately 0.5 m at the 70 m westward shifted position), while they are almost equal at the bow. For offshore direction 270°N – 300°N, no extreme computations were done and consequently figures cannot be presented for these directions. It is expected that the effect of the shift on the wave conditions is small.

12 References

[1] ARCADIS 2015, Nautical and risk studies for the Delimara LNG Terminal in Marsaxlokk Port, Malta. Item 1: Wave climate study. Final report, 10 March 2015.

[2] ARCADIS 2015, Nautical and risk studies for the Delimara LNG Terminal in Marsaxlokk Port, Malta. Item 2: Wave penetration study. Final report, 10 March 2015 .

[3] SVASEK, 2013, Current and Wave Study Marsaxlokk Bay, Enemalta - LNG jetty at Delimara, Final report, August 20th 2013, Reference 1720/U13238/B/BvL

[4] Goda, Y., 2000: "Random Seas and Design of Maritime Structures". Advanced Series on Ocean Engineering **15** (2 ed.).

Appendix 1 Definitions of wind and wave parameters

The definition of the wind speed is according to the project description of the Global Reanalysis of Ocean Waves Fine Mediterranean (GROW-FINE MED), provided by Oceanweather. The definition of wave parameters is according to the description in SWAN manual [3].

Wind speed
One-hour average of the effective neutral wind at a height of 10 meters.

Wind direction
The direction from which wind is coming in degrees, measured clockwise with respect to the North (nautical convention).

Significant wave height

$$H_{m0} = 4m_0 = 4\sqrt{\iint E(\omega,\theta)d\omega d\theta}$$

Peak wave period

$$T_p = \frac{1}{f_p}$$
$$f_p = f(E_p)$$
$$E_p = max(E_p)$$

Mean wave period

$$T_{m-1,0} = 2\pi\frac{m_{-1}}{m_0} = 2\pi\frac{\iint \omega^{-1}E(\omega,\theta)d\omega d\theta}{\iint E(\omega,\theta)d\omega d\theta}$$

Mean wave direction
The direction from which wave are coming in degrees, measured clockwise with respect to the North (nautical convention).

$$dir = \arctan\left[\frac{\int \sin\theta\, E(\omega,\theta)d\omega d\theta}{\int \cos\theta\, E(\omega,\theta)d\omega d\theta}\right]$$

Peak wave direction
The direction corresponding to the maximum energy in the two dimensional spectrum.

$$\theta_p = \theta(E_p)$$

Directional spreading
The directional spreading is the one-sided width, or standard deviation, of the spectrum, as defined by Kuik et al [6].

$$dspr = \frac{\pi}{180}\sqrt{2\left(1-\sqrt{\left[\left(\int \sin\theta \frac{\int E(\omega,\theta)d\omega}{\int E(\omega)d\omega}d\theta\right)^2+\left(\int \cos\theta \frac{\int E(\omega,\theta)d\omega}{\int E(\omega)d\omega}d\theta\right)^2\right]}\right)}$$

Directional distribution

The following directional distribution is applied in this study:

$$D(\theta) = \begin{cases} \cos^m(\theta-\theta_0) & for\ |\theta-\theta_0| < 90° \\ 0 & for\ |\theta-\theta_0| \geq 90° \end{cases}$$

The parameter m is referred to a directional distribution power. A fixed relationship exists between the value of m and the directional spreading.

Deep water wave steepness

The wave steepness is defined as wave height divided by wave length. In deep water, the wave length is equal to:

$$L_{deep} = \frac{gT^2}{2\pi}$$

The deep water steepness then expressed as:

$$s_{deep} = \frac{H_s}{L_{deep}} = \frac{2\pi H_s}{gT_p^2} \approx \frac{H_s}{1.56T_p^2}$$

With:

E	variance density spectrum [m²]
θ	wave direction [°N]
ω	radian frequency [Hz]
f	angular frequency [Hz]
m_n	n-th order moment of the spectrum, defined as $\iint \omega^n E(\omega,\theta)d\omega d\theta$

Appendix 2 Results all-year directional extremes

Appendix 2.1 Wind speed

Offshore direction [°N]	0			30			60		
Return period [yr]	best fit	low 95% conf	high 95% conf	best fit	low 95% conf	high 95% conf	best fit	low 95% conf	high 95% conf
1	13.5	13.0	14.2	14.9	14.3	15.6	15.0	14.5	15.6
5	17.6	16.1	19.3	18.8	17.5	20.2	18.3	17.2	19.4
10	19.5	17.3	21.8	20.4	18.6	22.4	19.5	18.1	21.0
25	22.0	18.7	25.4	22.4	19.9	25.4	21.0	19.2	23.2
50	23.9	19.7	28.2	23.8	20.8	27.8	22.1	19.9	24.8
100	25.9	20.7	31.2	25.2	21.7	30.2	23.1	20.6	26.5
Offshore direction [°N]	**90**			**120**			**150**		
Return period [yr]	**best fit**	**low 95% conf**	**high 95% conf**	**best fit**	**low 95% conf**	**high 95% conf**	**best fit**	**low 95% conf**	**high 95% conf**
1	14.8	14.4	15.4	15.1	14.6	15.4	15.4	15.0	15.9
5	17.5	16.7	18.4	17.3	16.6	18.1	18.0	17.2	19.0
10	18.4	17.4	19.6	18.1	17.2	19.1	19.0	18.0	20.2
25	19.6	18.3	21.2	19.1	18.0	20.4	20.2	18.9	21.8
50	20.4	18.9	22.3	19.8	18.5	21.3	21.1	19.5	23.0
100	21.1	19.4	23.5	20.4	19.0	22.2	21.9	20.1	24.2
Offshore direction [°N]	**180**			**210**			**240**		
Return period [yr]	**best fit**	**low 95% conf**	**high 95% conf**	**best fit**	**low 95% conf**	**high 95% conf**	**best fit**	**low 95% conf**	**high 95% conf**
1	14.1	13.6	14.5	13.3	12.8	13.6	15.3	14.8	15.7
5	16.4	15.6	17.2	16.0	14.9	16.8	17.8	16.9	18.6
10	17.3	16.3	18.4	17.1	15.7	18.3	18.8	17.7	19.9
25	18.4	17.1	20.0	18.5	16.6	20.3	19.9	18.5	21.4
50	19.2	17.6	21.1	19.6	17.2	21.9	20.7	19.1	22.5
100	20.0	18.1	22.3	20.7	17.8	23.5	21.4	19.7	23.6
Offshore direction [°N]	**270**			**300**			**330**		
Return period [yr]	**best fit**	**low 95% conf**	**high 95% conf**	**best fit**	**low 95% conf**	**high 95% conf**	**best fit**	**low 95% conf**	**high 95% conf**
1	18.5	18.0	19.0	19.4	19.0	19.8	17.6	17.1	18.1
5	21.3	20.5	22.3	21.7	21.0	22.4	20.3	19.4	21.2
10	22.4	21.3	23.5	22.5	21.8	23.3	21.4	20.3	22.5
25	23.6	22.4	25.1	23.6	22.7	24.5	22.6	21.3	24.1
50	24.5	23.1	26.2	24.3	23.3	25.4	23.6	22.1	25.3
100	25.4	23.8	27.3	25.0	23.9	26.2	24.4	22.8	26.4

Table A-1: Offshore all-year extreme wind speeds in m/s for all return periods and directional sectors.

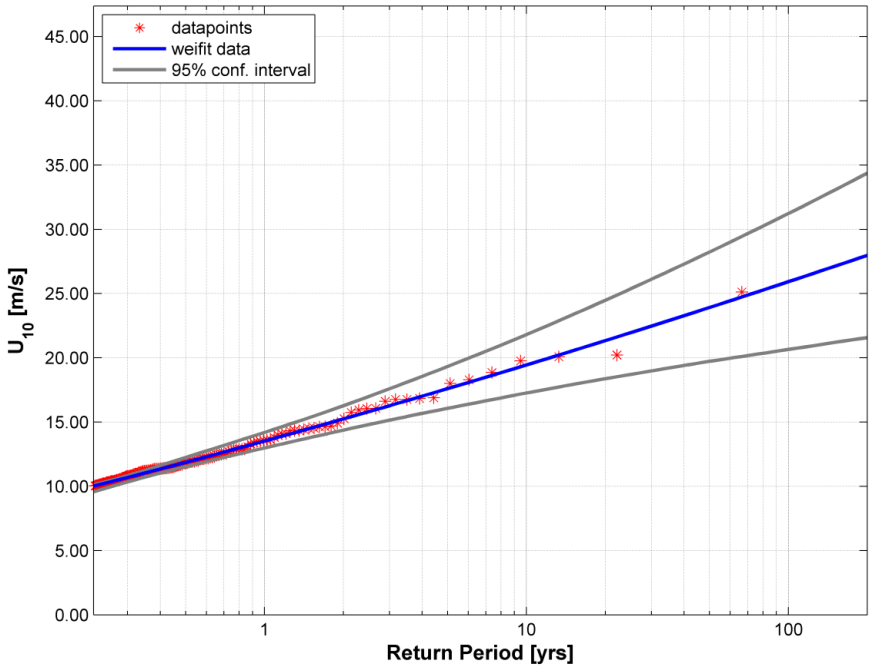

Figure A-1: Selected offshore all-year extreme wind speed peaks, fitted Weibull distribution function and bootstrap 95% confidence interval limits for directional sectors 0°N.

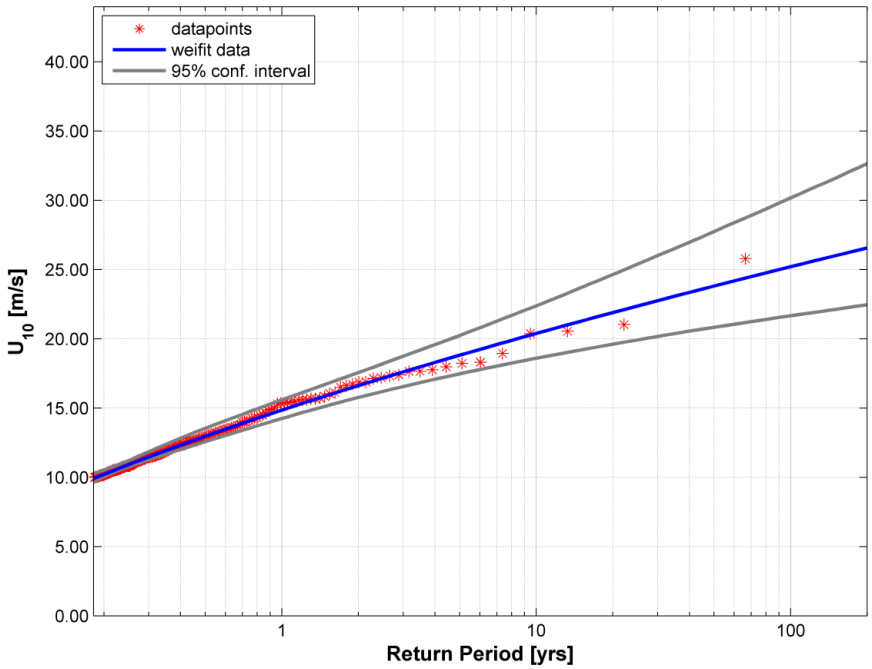

Figure A-2: Selected offshore all-year extreme wind speed peaks, fitted Weibull distribution function and bootstrap 95% confidence interval limits for directional sectors 30°N.

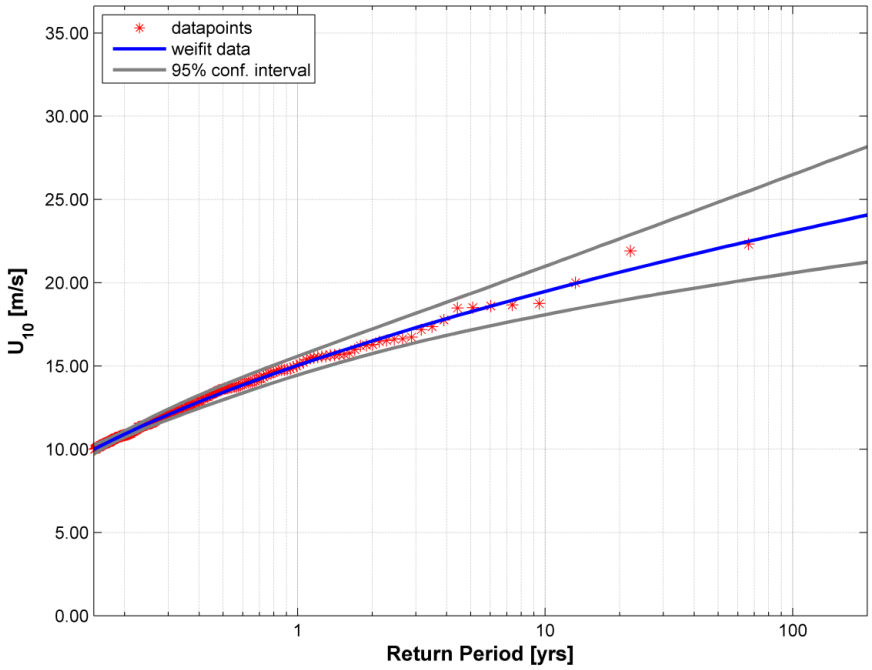

Figure A-3: Selected offshore all-year extreme wind speed peaks, fitted Weibull distribution function and bootstrap 95% confidence interval limits for directional sectors 60°N.

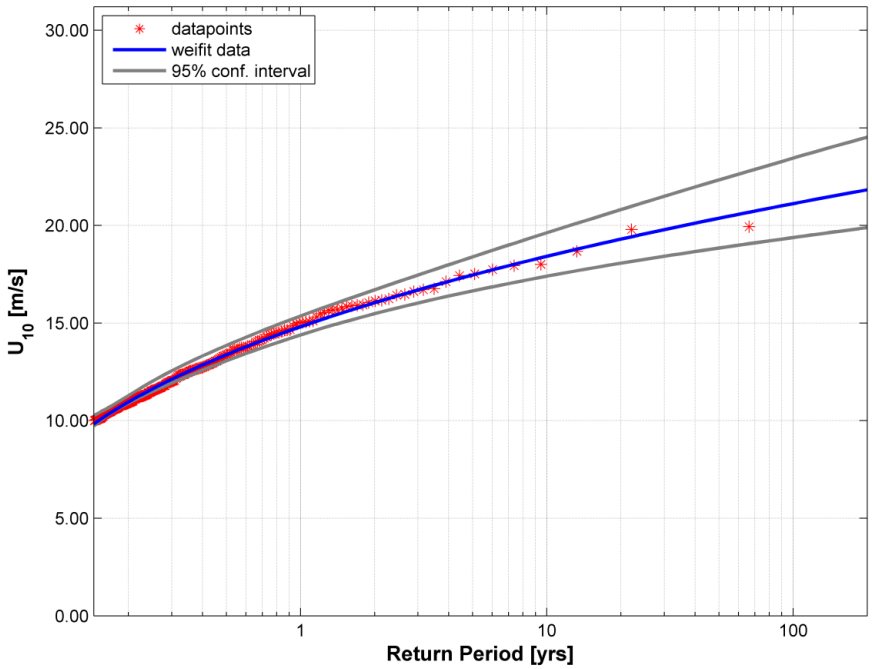

Figure A-4: Selected offshore all-year extreme wind speed peaks, fitted Weibull distribution function and bootstrap 95% confidence interval limits for directional sectors 90°N.

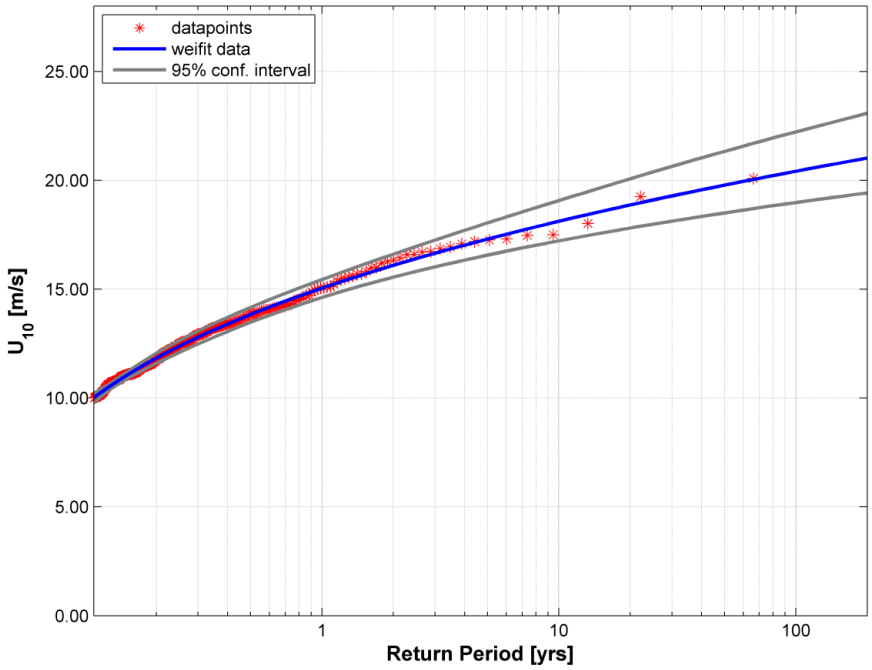

Figure A-5: Selected offshore all-year extreme wind speed peaks, fitted Weibull distribution function and bootstrap 95% confidence interval limits for directional sectors 120°N.

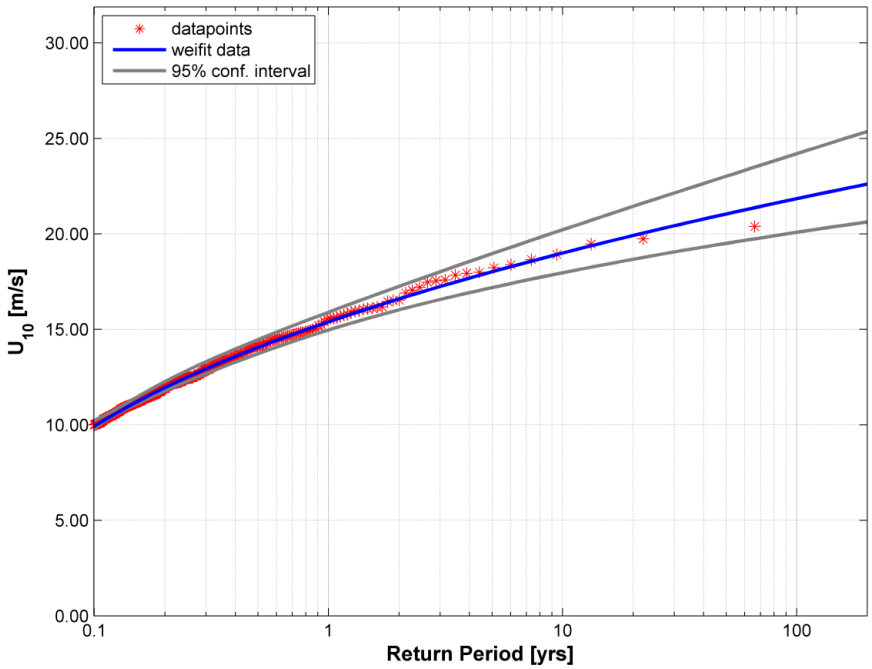

Figure A-6: Selected offshore all-year extreme wind speed peaks, fitted Weibull distribution function and bootstrap 95% confidence interval limits for directional sectors 150°N.

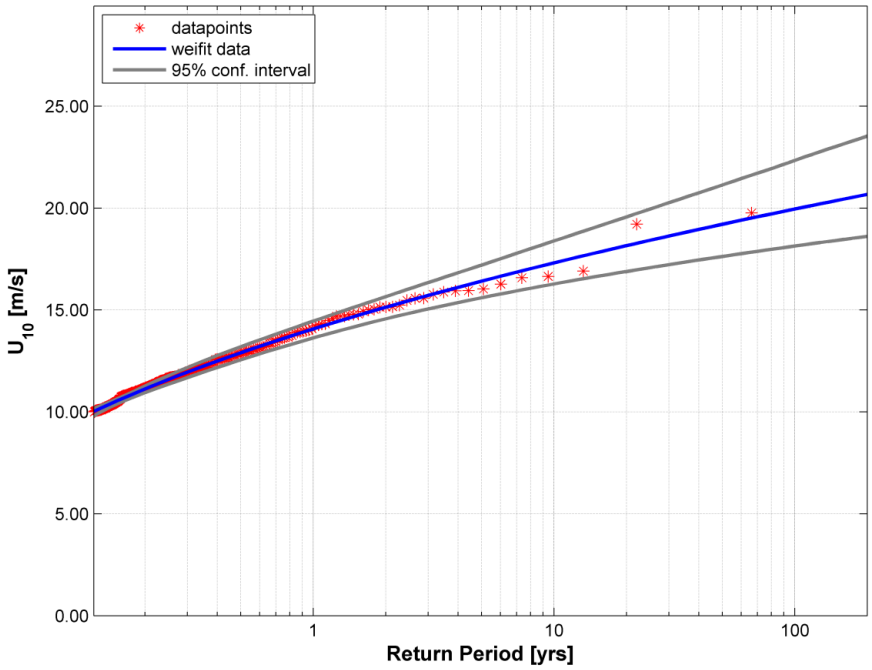

Figure A-7: Selected offshore all-year extreme wind speed peaks, fitted Weibull distribution function and bootstrap 95% confidence interval limits for directional sectors 180°N.

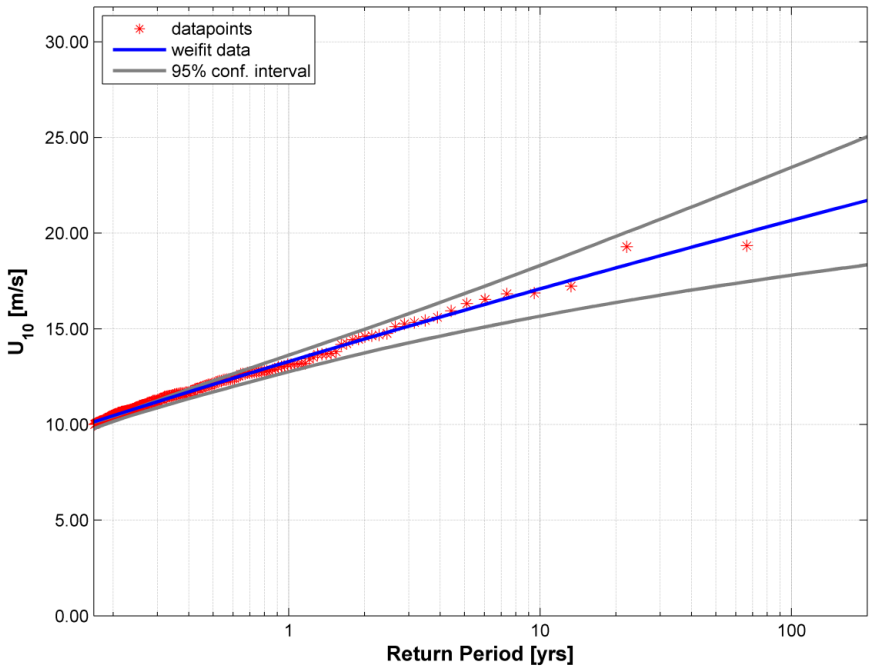

Figure A-8: Selected offshore all-year extreme wind speed peaks, fitted Weibull distribution function and bootstrap 95% confidence interval limits for directional sectors 210°N.

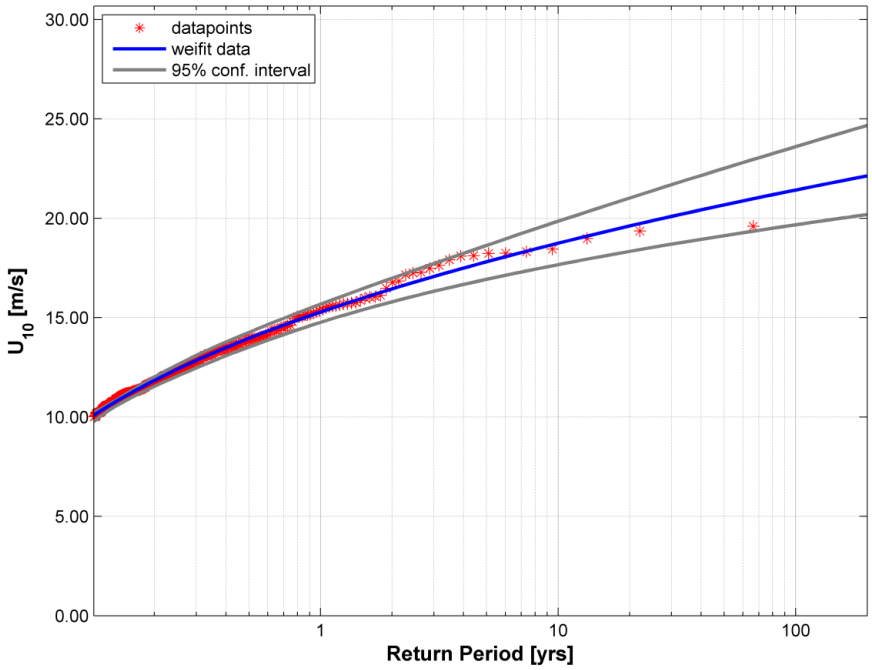

Figure A-9: Selected offshore all-year extreme wind speed peaks, fitted Weibull distribution function and bootstrap 95% confidence interval limits for directional sectors 240°N.

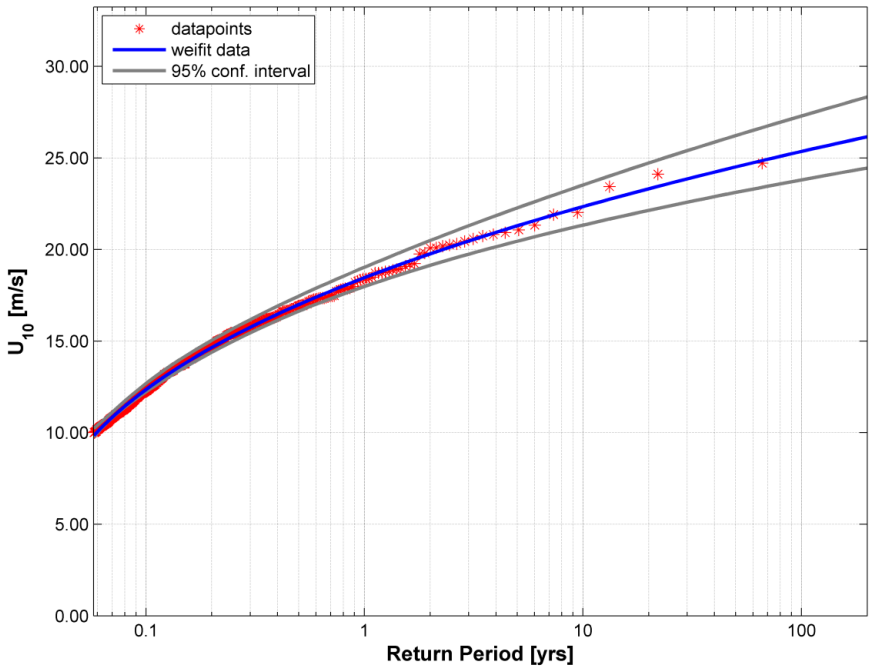

Figure A-10: Selected offshore all-year extreme wind speed peaks, fitted Weibull distribution function and bootstrap 95% confidence interval limits for directional sectors 270°N.

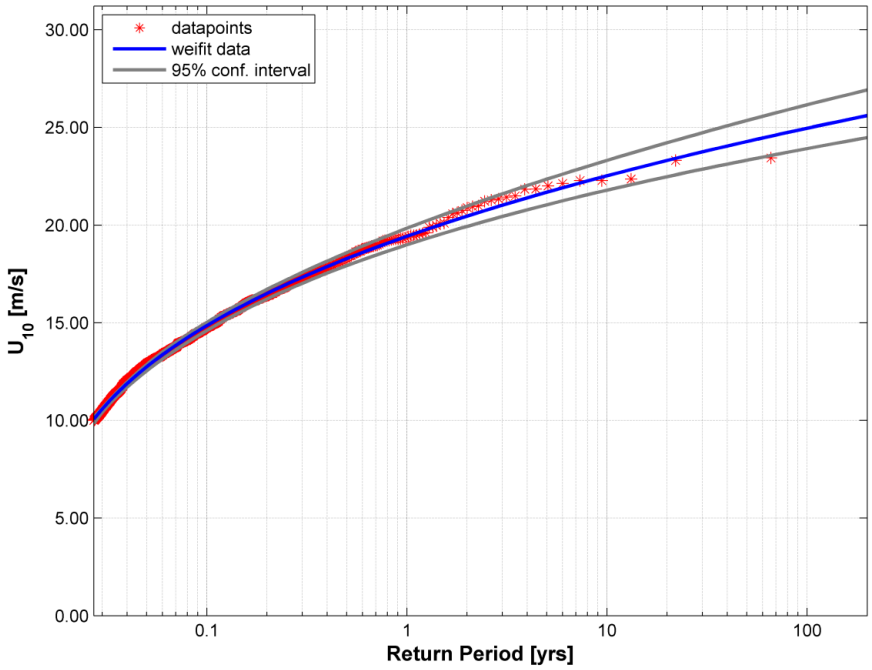

Figure A-11: Selected offshore all-year extreme wind speed peaks, fitted Weibull distribution function and bootstrap 95% confidence interval limits for directional sectors 300°N.

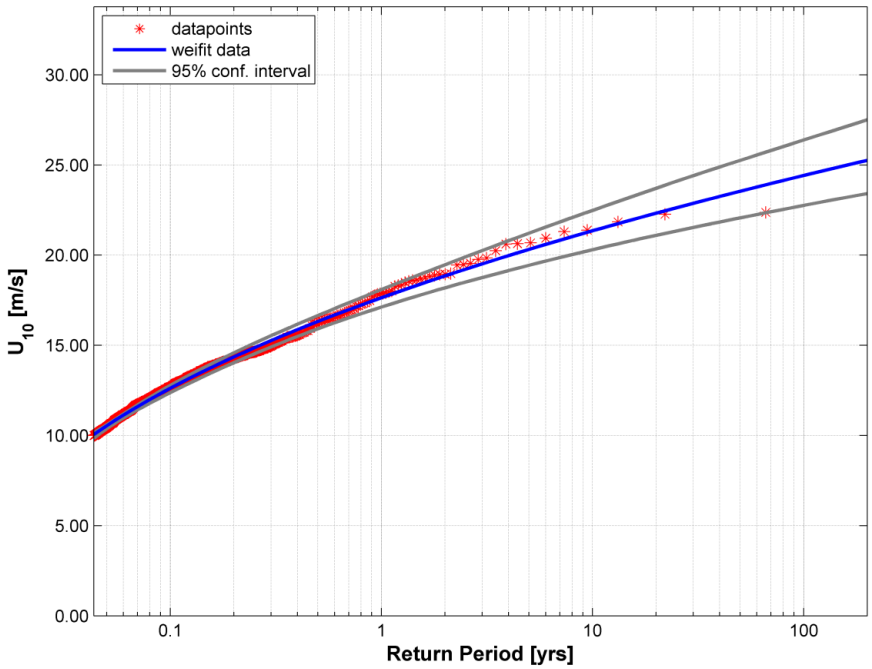

Figure A-12: Selected offshore all-year extreme wind speed peaks, fitted Weibull distribution function and bootstrap 95% confidence interval limits for directional sectors 330°N.

Appendix 2.2 Wind sea significant wave height

Nearshore direction [°N]	180			210		
Return period [yr]	best fit	low 95% conf	high 95% conf	best fit	low 95% conf	high 95% conf
1	2.17	2.09	2.24	1.43	1.19	1.49
5	2.58	2.44	2.71	1.94	1.81	2.14
10	2.73	2.55	2.92	2.15	1.94	2.44
25	2.91	2.69	3.19	2.43	2.08	2.89
50	3.05	2.78	3.39	2.64	2.17	3.27
100	3.17	2.86	3.59	2.85	2.24	3.68
Nearshore direction [°N]	**240**			**270**		
Return period [yr]	**best fit**	**low 95% conf**	**high 95% conf**	**best fit**	**low 95% conf**	**high 95% conf**
1	1.17	1.15	1.23	0.95	0.91	0.97
5	1.40	1.34	1.48	1.10	1.05	1.15
10	1.48	1.40	1.57	1.16	1.09	1.23
25	1.56	1.46	1.70	1.23	1.14	1.33
50	1.62	1.51	1.79	1.28	1.17	1.41
100	1.68	1.54	1.89	1.33	1.20	1.49

Table A-2: Nearshore all-year extreme wind sea significant wave heights in m for all return periods and directional sectors.

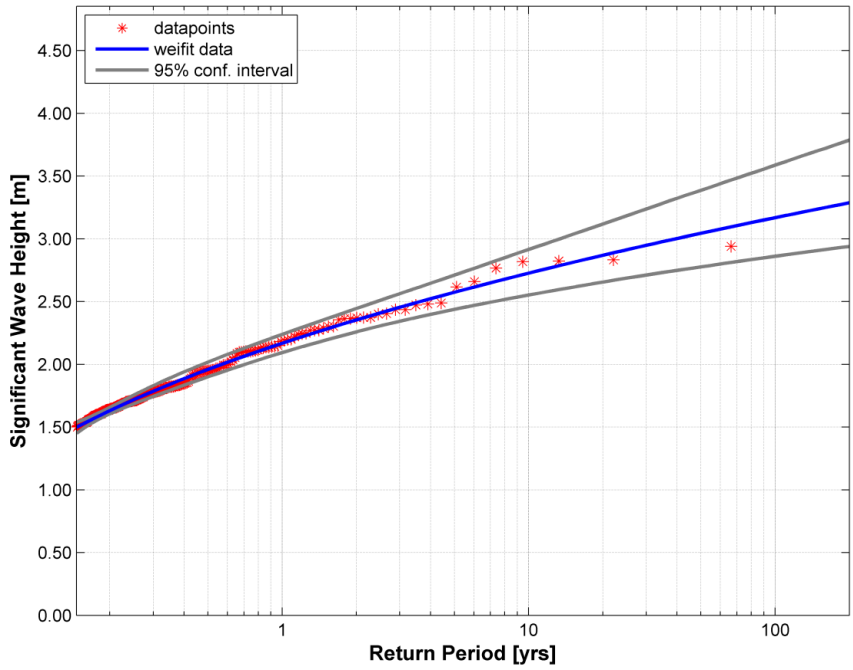

Figure A-13: Selected nearshore all-year extreme wind sea significant wave height peaks, fitted Weibull distribution function and bootstrap 95% confidence interval limits for directional sectors 180°N.

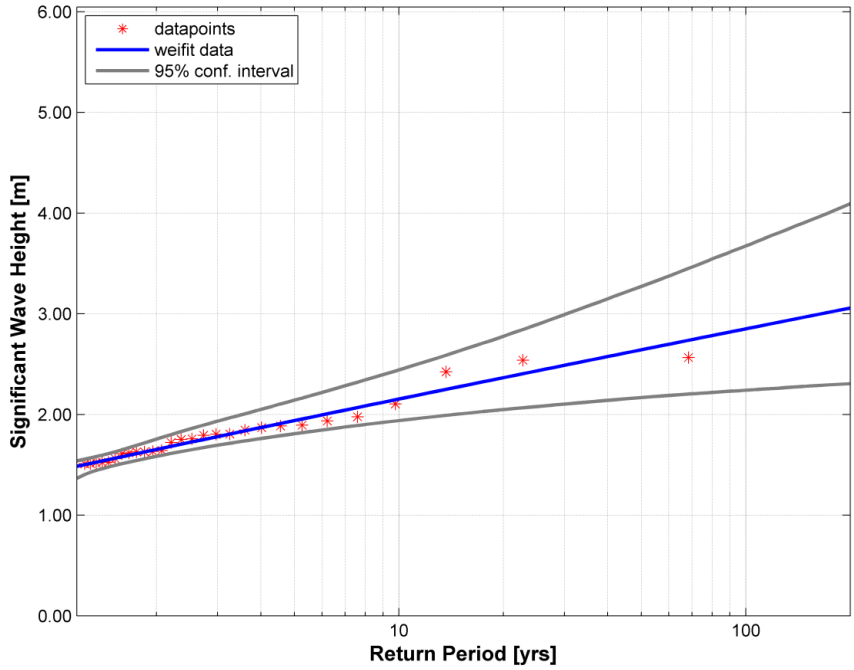

Figure A-14: Selected nearshore all-year extreme wind sea significant wave height peaks, fitted Weibull distribution function and bootstrap 95% confidence interval limits for directional sectors 210°N.

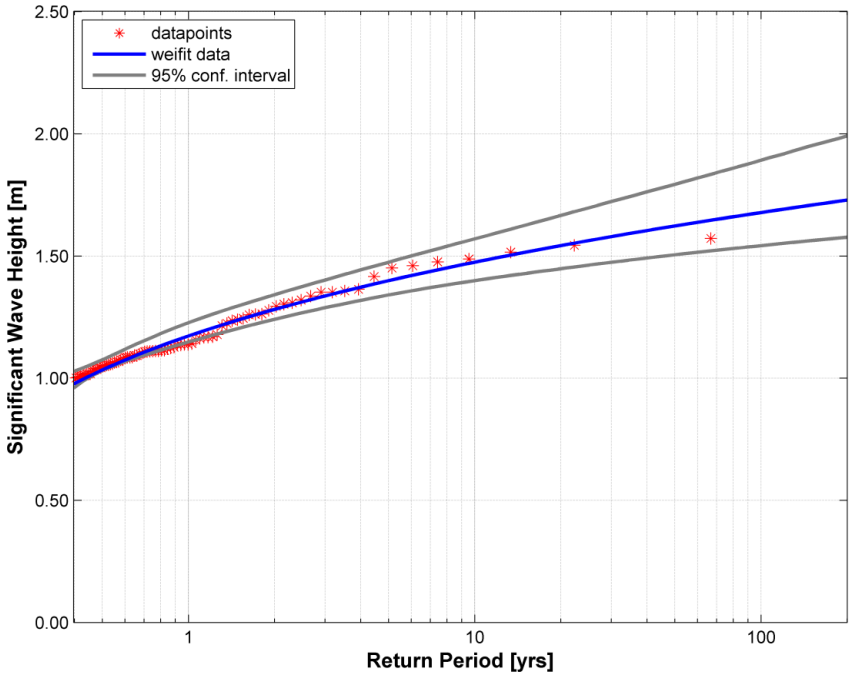

Figure A-15: Selected nearshore all-year extreme wind sea significant wave height peaks, fitted Weibull distribution function and bootstrap 95% confidence interval limits for directional sectors 240°N.

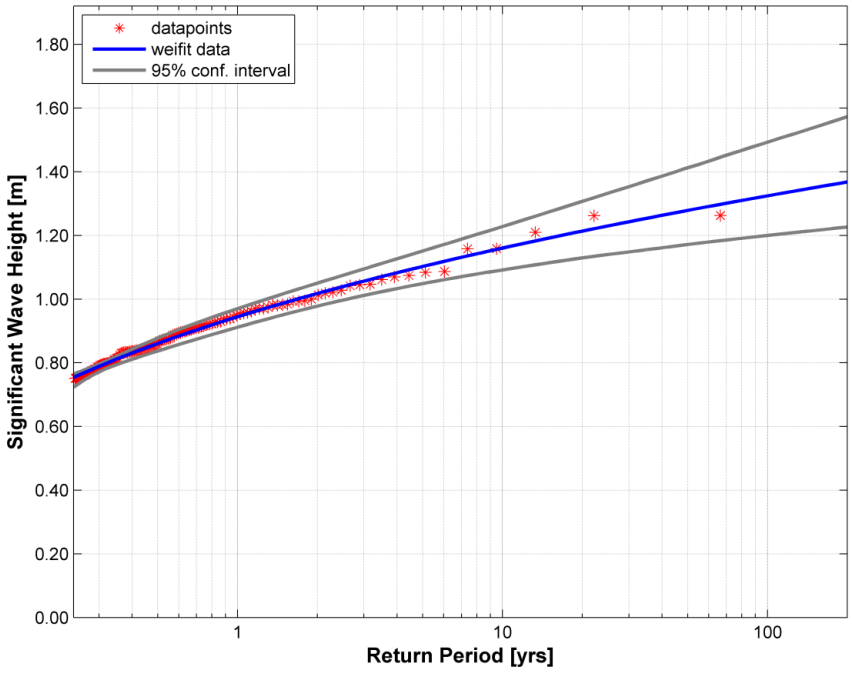

Figure A-16: Selected nearshore all-year extreme wind sea significant wave height peaks, fitted Weibull distribution function and bootstrap 95% confidence interval limits for directional sectors 270°N.

Appendix 2.3 Swell significant wave height

Nearshore direction [°N]	180			210		
Return period [yr]	best fit	low 95% conf	high 95% conf	best fit	low 95% conf	high 95% conf
1	1.21	1.19	1.27	0.86	0.85	0.91
5	1.49	1.41	1.63	1.07	1.02	1.13
10	1.61	1.49	1.80	1.13	1.07	1.20
25	1.78	1.59	2.03	1.19	1.12	1.29
50	1.91	1.66	2.21	1.23	1.16	1.35
100	2.04	1.72	2.40	1.27	1.19	1.41

Table A-3: Nearshore all-year extreme swell significant wave heights in m for all return periods and directional sectors.

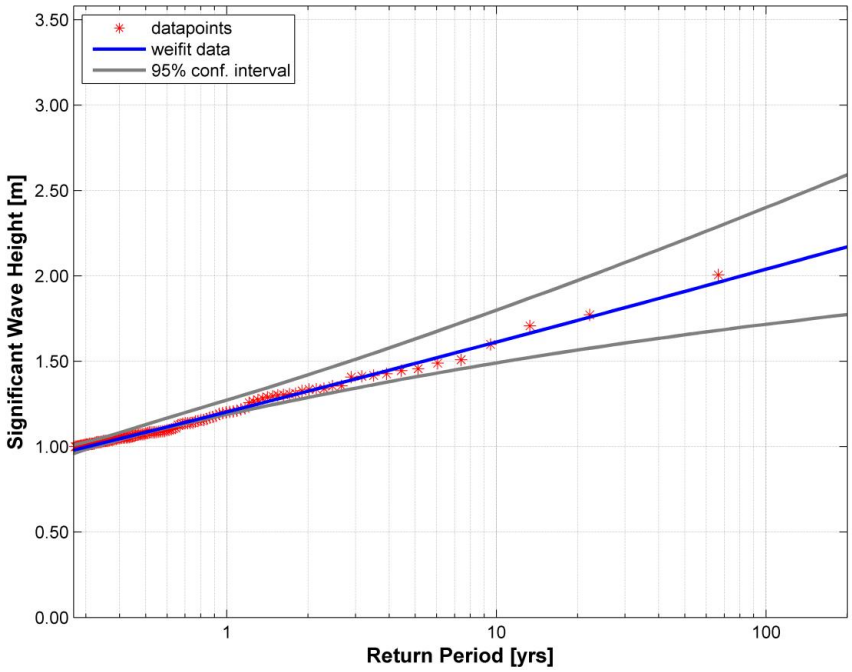

Figure A-17: Selected nearshore all-year extreme swell significant wave height peaks, fitted Weibull distribution function and bootstrap 95% confidence interval limits for directional sectors 180°N.

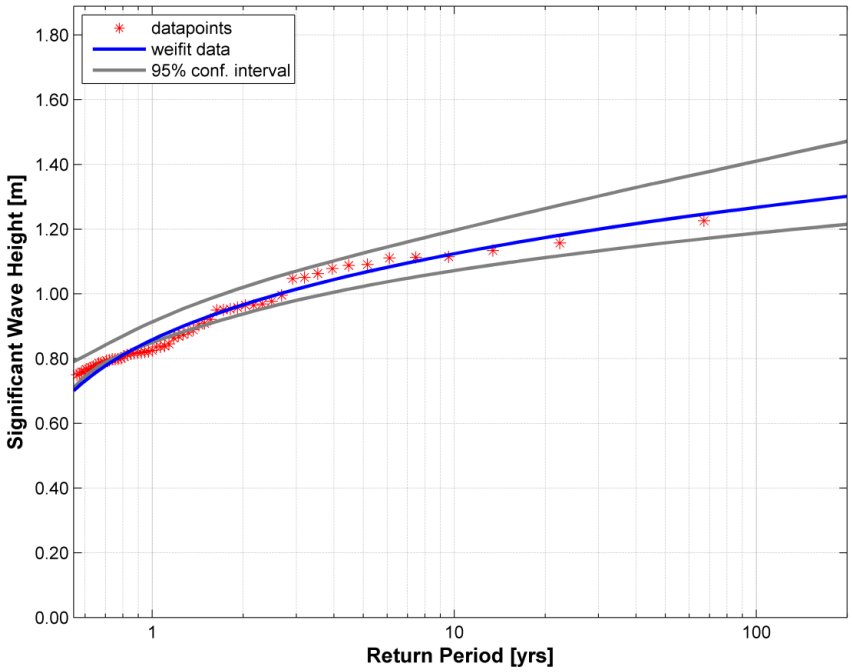

Figure A-18: Selected nearshore all-year extreme swell significant wave height peaks, fitted Weibull distribution function and bootstrap 95% confidence interval limits for directional sectors 210°N.

Appendix 3 Results monthly directional extremes

Appendix 3.1 Wind speed

Month	Jan			Feb			Mar		
Return period [yr]	best fit	low 95% conf	high 95% conf	best fit	low 95% conf	high 95% conf	best fit	low 95% conf	high 95% conf
1	17.7	16.9	18.2	17.6	17.0	18.3	16.8	16.2	17.4
5	21.2	20.0	22.2	21.0	20.0	22.1	19.9	19.0	20.9
10	22.4	21.0	23.8	22.1	20.9	23.5	21.0	19.8	22.3
25	23.8	22.1	25.7	23.4	22.0	25.2	22.3	20.8	23.9
50	24.9	22.9	27.0	24.4	22.7	26.4	23.2	21.5	25.1
100	25.8	23.6	28.3	25.2	23.4	27.5	24.0	22.1	26.2
Month	**Apr**			**May**			**Jun**		
Return period [yr]	**best fit**	**low 95% conf**	**high 95% conf**	**best fit**	**low 95% conf**	**high 95% conf**	**best fit**	**low 95% conf**	**high 95% conf**
1	15.5	15.1	15.9	14.4	13.9	14.9	13.0	12.5	13.4
5	17.6	17.0	18.3	17.2	16.3	18.1	15.4	14.7	16.1
10	18.3	17.7	19.1	18.2	17.1	19.3	16.2	15.3	17.1
25	19.1	18.3	20.1	19.3	18.0	20.9	17.1	16.0	18.3
50	19.7	18.8	20.8	20.1	18.5	22.0	17.7	16.5	19.2
100	20.1	19.2	21.4	20.8	19.0	23.2	18.2	16.9	20.1
Month	**Jul**			**Aug**			**Sep**		
Return period [yr]	**best fit**	**low 95% conf**	**high 95% conf**	**best fit**	**low 95% conf**	**high 95% conf**	**best fit**	**low 95% conf**	**high 95% conf**
1	13.2	12.8	13.9	12.5	11.9	12.8	13.0	12.5	13.3
5	16.2	15.5	17.0	14.9	14.2	15.4	15.0	14.4	15.4
10	17.1	16.2	18.2	15.6	14.8	16.3	15.5	14.9	16.2
25	18.1	17.0	19.5	16.3	15.5	17.3	16.2	15.6	17.1
50	18.7	17.5	20.4	16.8	16.0	18.0	16.6	16.0	17.7
100	19.3	18.0	21.3	17.2	16.4	18.7	17.0	16.4	18.3
Month	**Oct**			**Nov**			**Dec**		
Return period [yr]	**best fit**	**low 95% conf**	**high 95% conf**	**best fit**	**low 95% conf**	**high 95% conf**	**best fit**	**low 95% conf**	**high 95% conf**
1	14.2	13.7	14.7	15.9	15.5	16.4	17.7	17.2	18.4
5	16.9	16.1	17.9	18.2	17.6	19.0	20.9	20.0	22.0
10	17.9	16.9	19.1	19.0	18.3	20.0	22.0	20.9	23.4
25	19.0	17.7	20.7	19.9	19.0	21.1	23.3	22.0	25.0
50	19.8	18.3	21.9	20.5	19.5	21.9	24.2	22.7	26.2
100	20.5	18.8	23.0	21.1	19.9	22.6	25.1	23.3	27.3

Table A-4: Offshore all-omnidirectional wind speeds in m/s for all return periods and directional sectors.

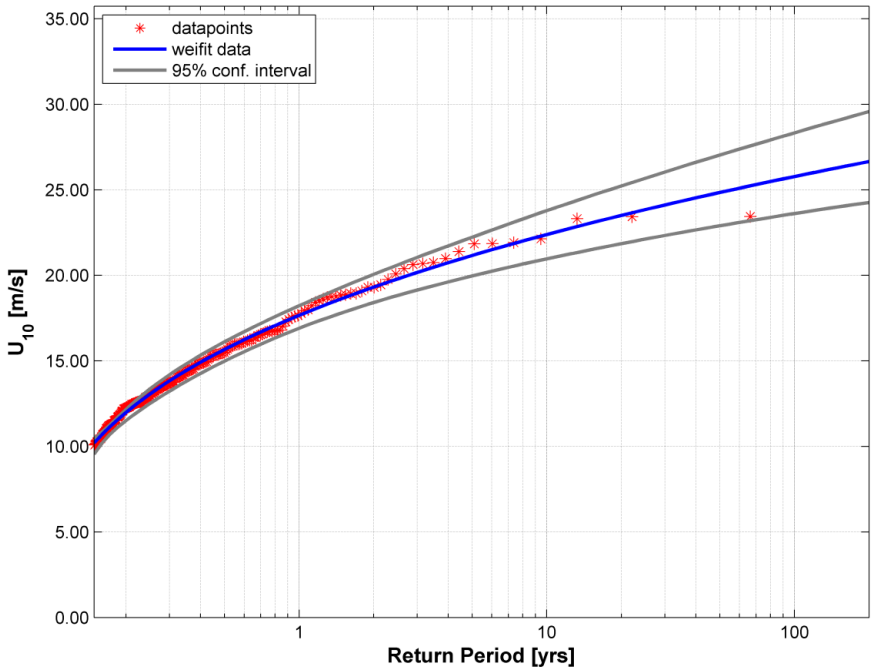

Figure A-19: Selected offshore omnidirectional extreme wind speed peaks, fitted Weibull distribution function and bootstrap 95% confidence interval limits for January.

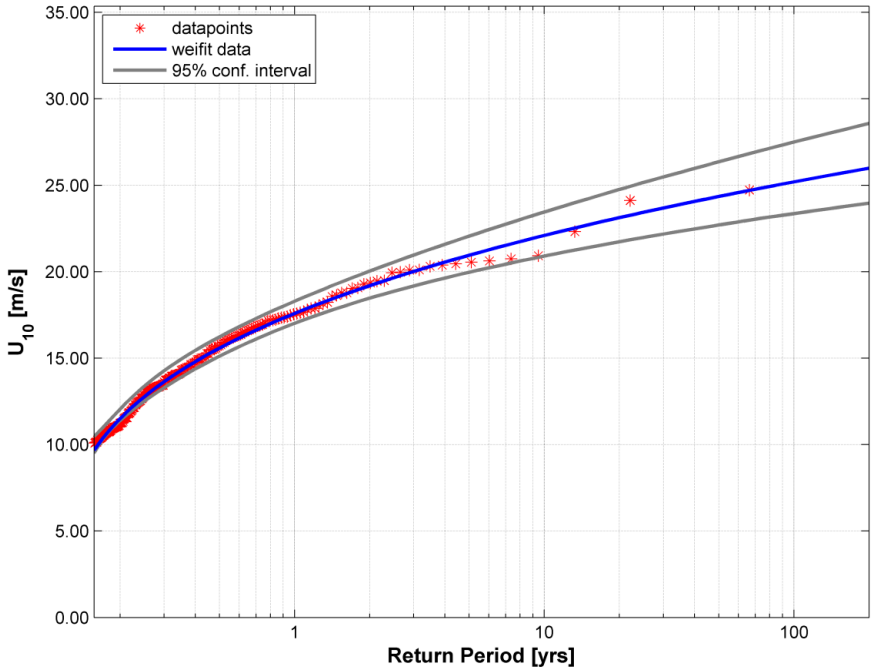

Figure A-20: Selected offshore omnidirectional extreme wind speed peaks, fitted Weibull distribution function and bootstrap 95% confidence interval limits for February.

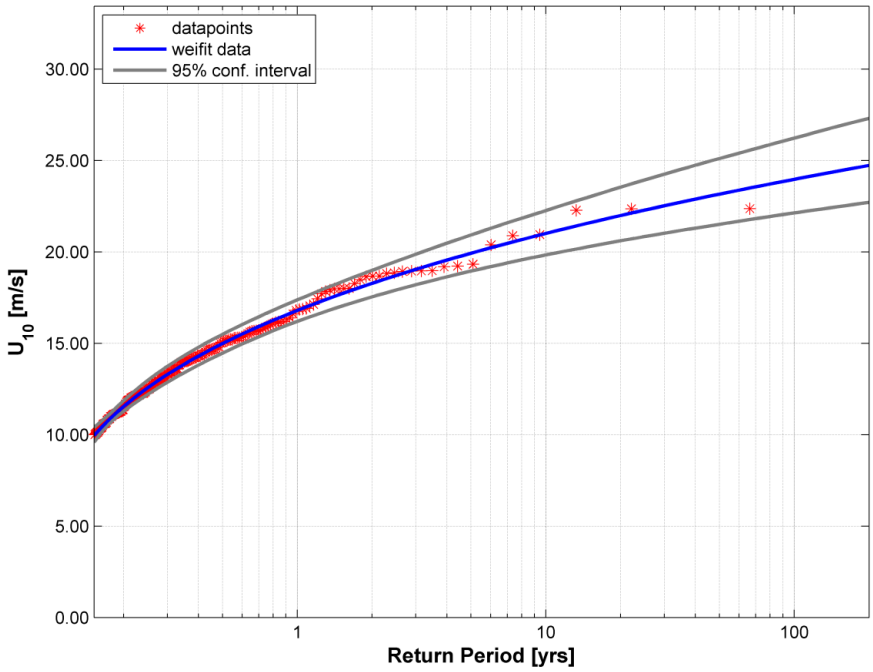

Figure A-21: Selected offshore omnidirectional extreme wind speed peaks, fitted Weibull distribution function and bootstrap 95% confidence interval limits for March.

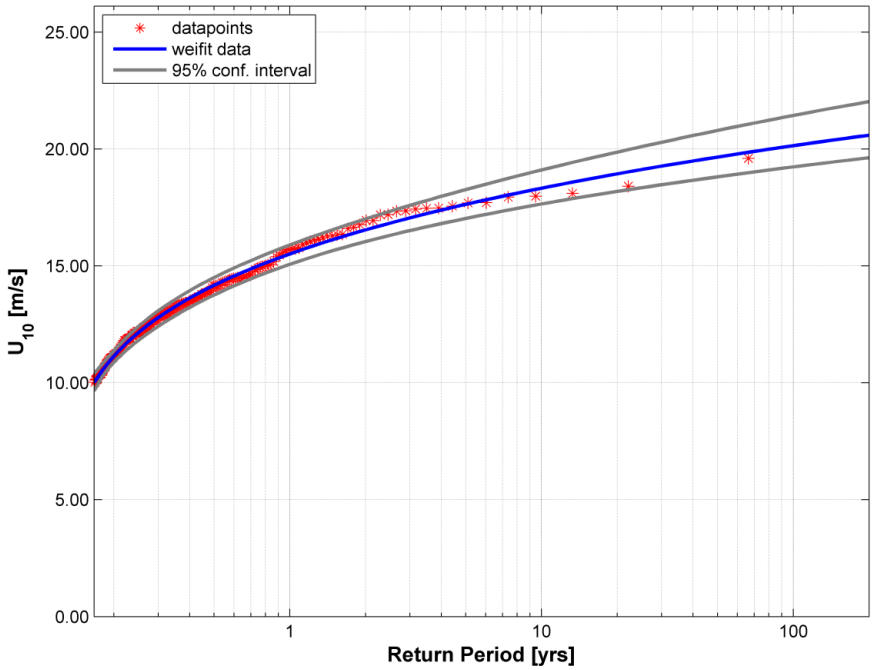

Figure A-22: Selected offshore omnidirectional extreme wind speed peaks, fitted Weibull distribution function and bootstrap 95% confidence interval limits for April.

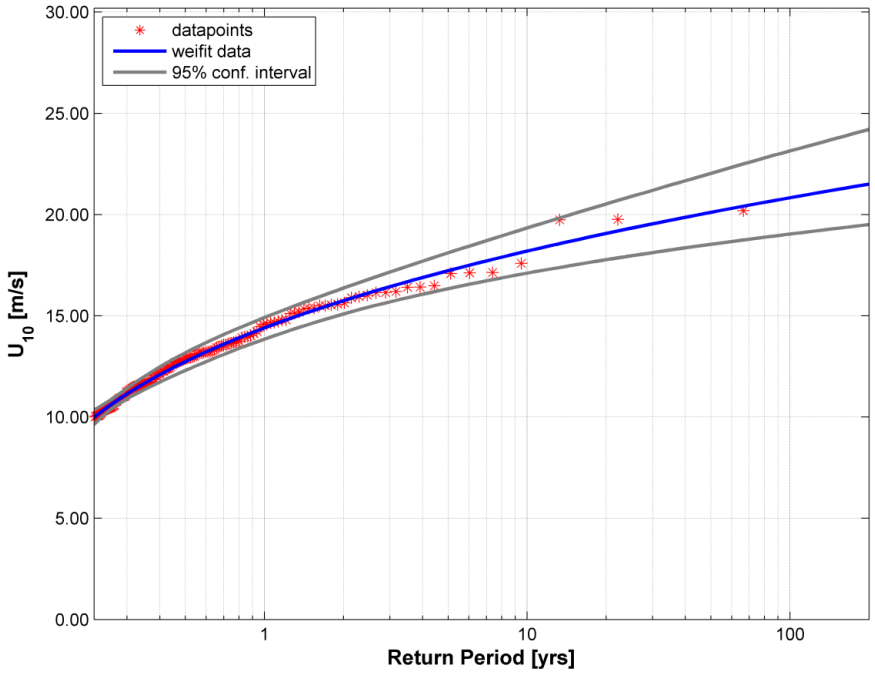

Figure A-23: Selected offshore omnidirectional extreme wind speed peaks, fitted Weibull distribution function and bootstrap 95% confidence interval limits for May.

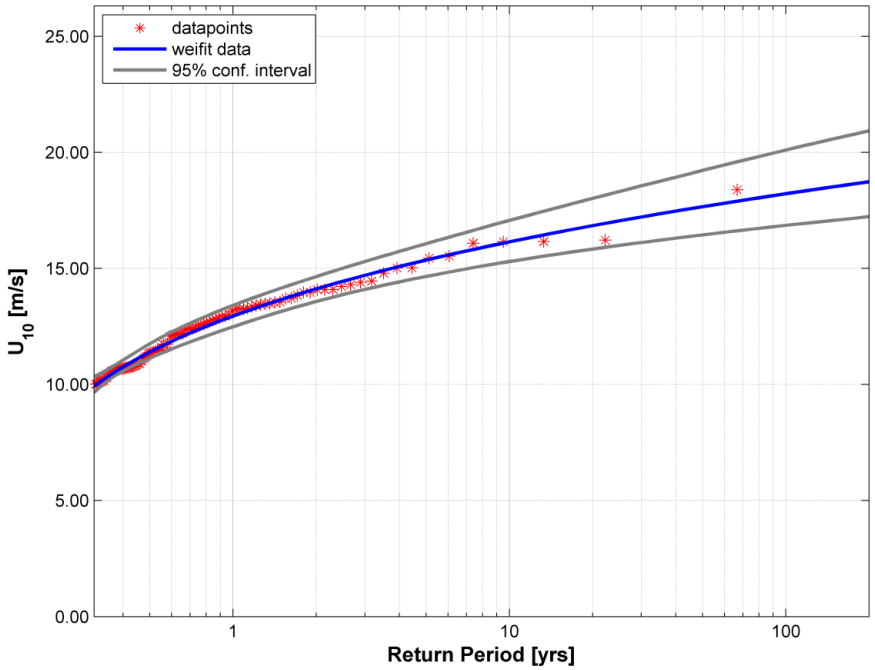

Figure A-24: Selected offshore omnidirectional extreme wind speed peaks, fitted Weibull distribution function and bootstrap 95% confidence interval limits for June.

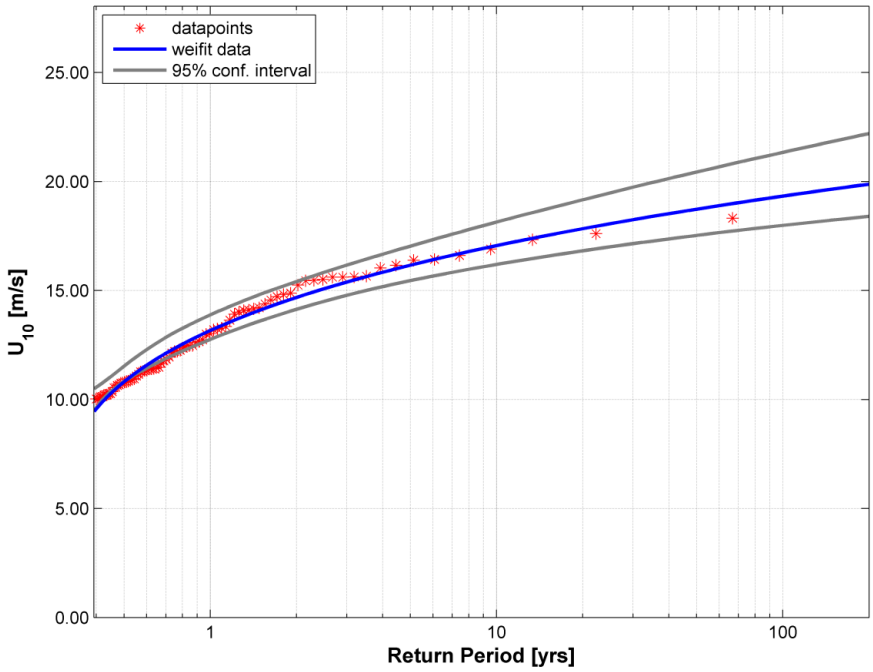

Figure A-25: Selected offshore omnidirectional extreme wind speed peaks, fitted Weibull distribution function and bootstrap 95% confidence interval limits for July.

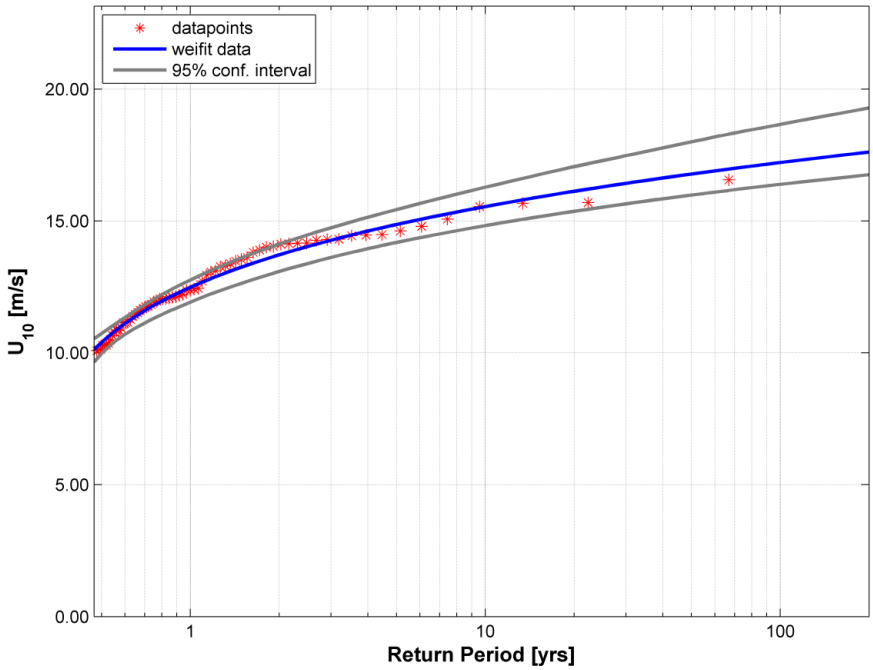

Figure A-26: Selected offshore omnidirectional extreme wind speed peaks, fitted Weibull distribution function and bootstrap 95% confidence interval limits for August.

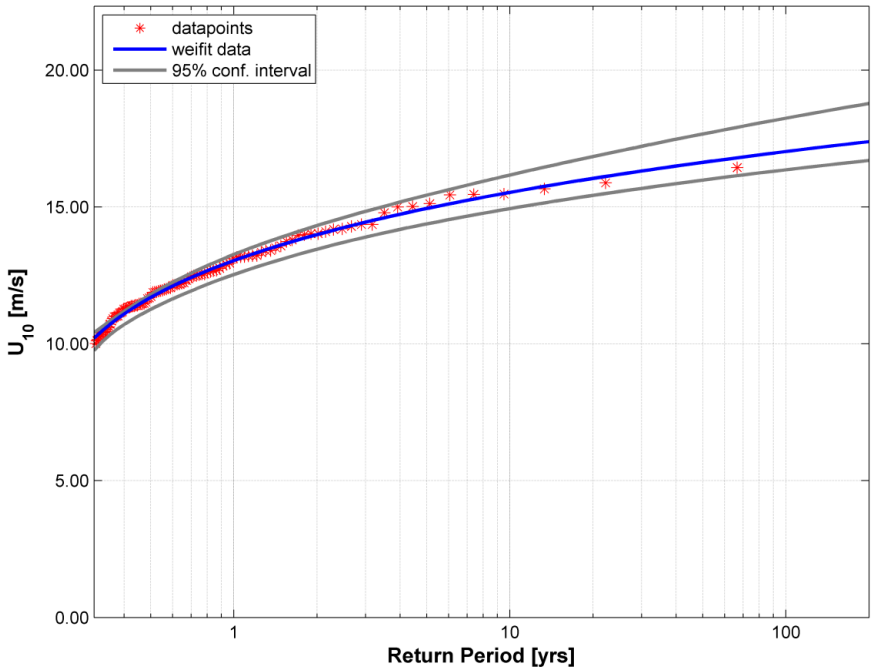

Figure A-27: Selected offshore omnidirectional extreme wind speed peaks, fitted Weibull distribution function and bootstrap 95% confidence interval limits for September.

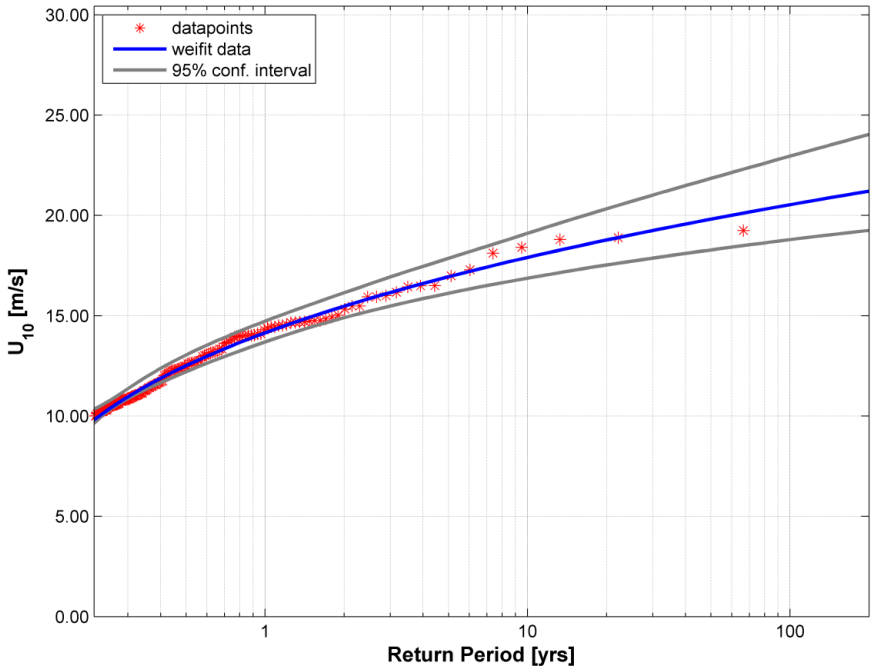

Figure A-28: Selected offshore omnidirectional extreme wind speed peaks, fitted Weibull distribution function and bootstrap 95% confidence interval limits for October.

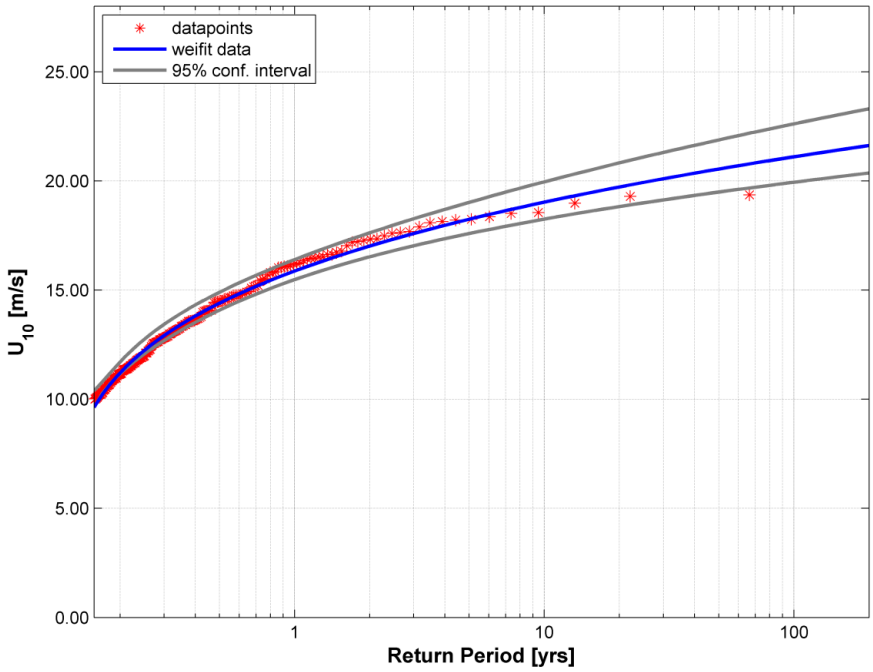

Figure A-29: Selected offshore omnidirectional extreme wind speed peaks, fitted Weibull distribution function and bootstrap 95% confidence interval limits for November.

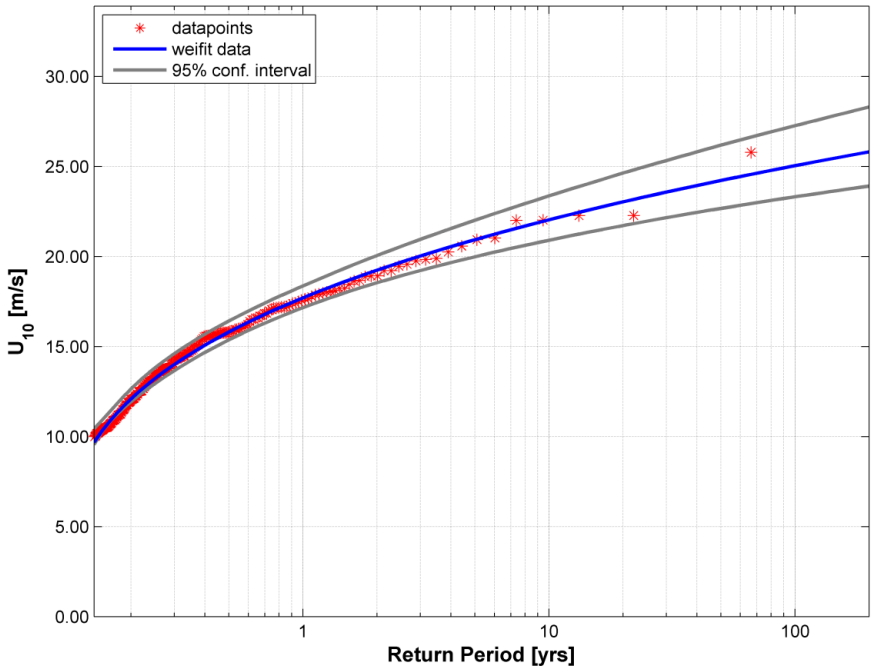

Figure A-30: Selected offshore omnidirectional extreme wind speed peaks, fitted Weibull distribution function and bootstrap 95% confidence interval limits for December.

Appendix 3.2 Wind sea significant wave height

Month	Jan			Feb			Mar		
Return period [yr]	best fit	low 95% conf	high 95% conf	best fit	low 95% conf	high 95% conf	best fit	low 95% conf	high 95% conf
1	1.49	1.39	1.62	1.40	1.32	1.51	1.47	1.38	1.59
5	2.14	1.94	2.36	1.99	1.80	2.19	2.07	1.90	2.26
10	2.39	2.12	2.69	2.22	1.96	2.49	2.28	2.05	2.54
25	2.69	2.31	3.16	2.49	2.14	2.91	2.53	2.22	2.91
50	2.91	2.44	3.54	2.69	2.25	3.26	2.70	2.33	3.20
100	3.11	2.55	3.93	2.88	2.36	3.63	2.86	2.43	3.49
Month	**Apr**			**May**			**Jun**		
Return period [yr]	**best fit**	**low 95% conf**	**high 95% conf**	**best fit**	**low 95% conf**	**high 95% conf**	**best fit**	**low 95% conf**	**high 95% conf**
1	1.56	1.47	1.67	1.20	1.13	1.28	0.83	0.46	0.79
5	2.06	1.92	2.20	1.87	1.65	2.10	1.25	1.18	1.48
10	2.21	2.04	2.40	2.14	1.83	2.48	1.45	1.30	1.83
25	2.39	2.17	2.64	2.50	2.02	3.06	1.74	1.44	2.37
50	2.51	2.25	2.82	2.77	2.15	3.53	1.97	1.53	2.85
100	2.61	2.33	2.99	3.03	2.27	4.05	2.22	1.62	3.38
Month	**Jul**			**Aug**			**Sep**		
Return period [yr]	**best fit**	**low 95% conf**	**high 95% conf**	**best fit**	**low 95% conf**	**high 95% conf**	**best fit**	**low 95% conf**	**high 95% conf**
1							1.01	0.94	1.08
5							1.52	1.38	1.66
10							1.68	1.50	1.87
25							1.88	1.62	2.16
50							2.01	1.69	2.40
100							2.14	1.75	2.66
Month	**Oct**			**Nov**			**Dec**		
Return period [yr]	**best fit**	**low 95% conf**	**high 95% conf**	**best fit**	**low 95% conf**	**high 95% conf**	**best fit**	**low 95% conf**	**high 95% conf**
1	1.32	1.24	1.39	1.54	1.46	1.67	1.49	1.40	1.60
5	1.75	1.62	1.86	2.10	1.95	2.29	2.08	1.88	2.30
10	1.88	1.73	2.02	2.30	2.09	2.55	2.32	2.05	2.63
25	2.02	1.83	2.22	2.54	2.25	2.91	2.63	2.24	3.12
50	2.12	1.90	2.37	2.70	2.35	3.17	2.86	2.37	3.52
100	2.20	1.96	2.52	2.85	2.44	3.44	3.08	2.49	3.95

Table A-5: Nearshore all-omnidirectional wind sea significant wave heights in m for all return periods and directional sectors.

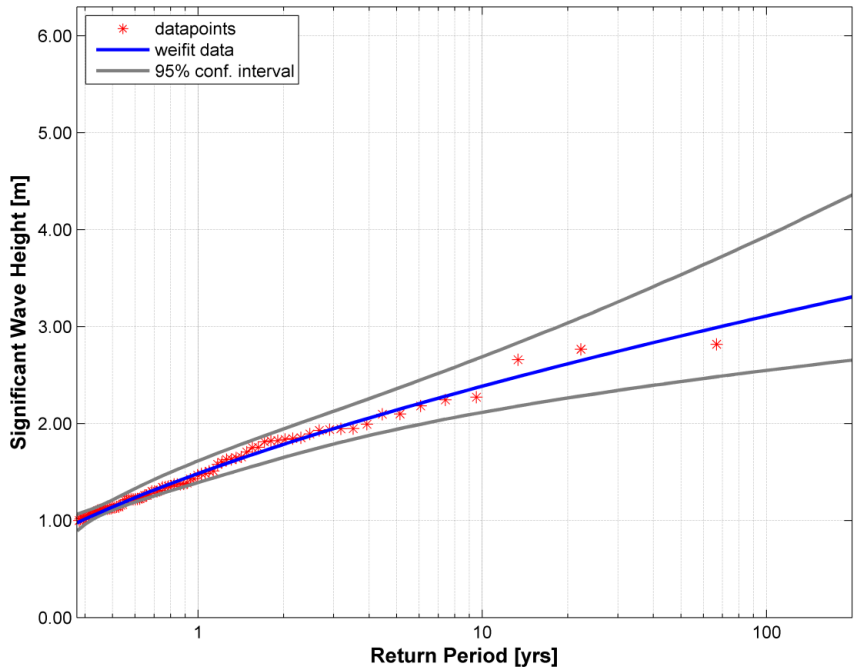

Figure A-31: Selected nearshore omnidirectional extreme wind sea significant wave height peaks, fitted Weibull distribution function and bootstrap 95% confidence interval limits for January.

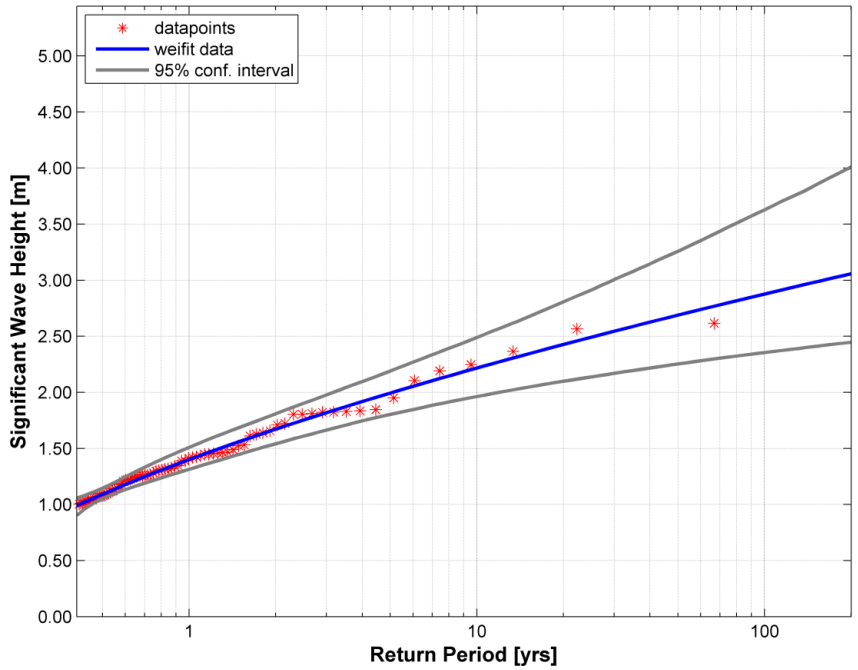

Figure A-32: Selected nearshore omnidirectional extreme wind sea significant wave height peaks, fitted Weibull distribution function and bootstrap 95% confidence interval limits for February.

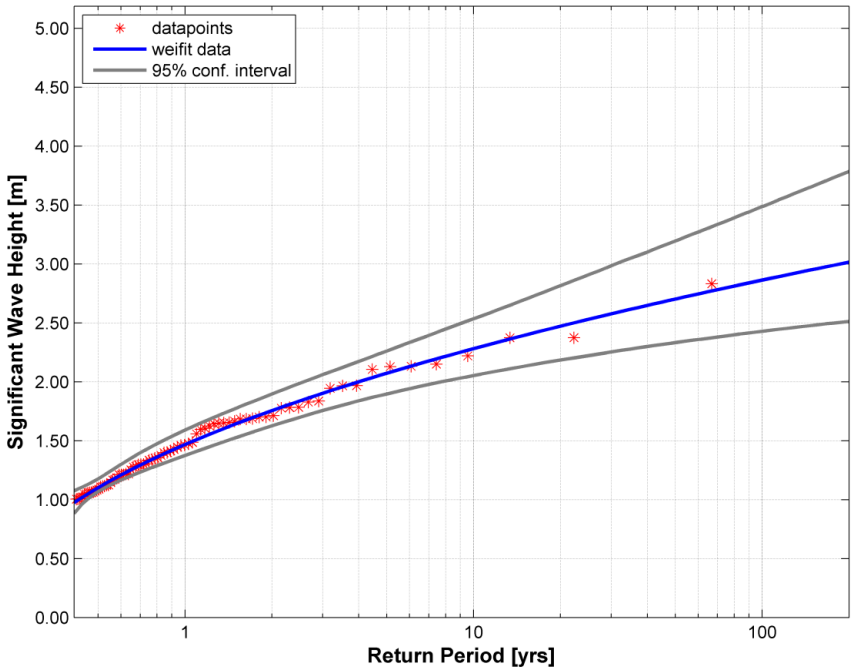

Figure A-33: Selected nearshore omnidirectional extreme wind sea significant wave height peaks, fitted Weibull distribution function and bootstrap 95% confidence interval limits for March.

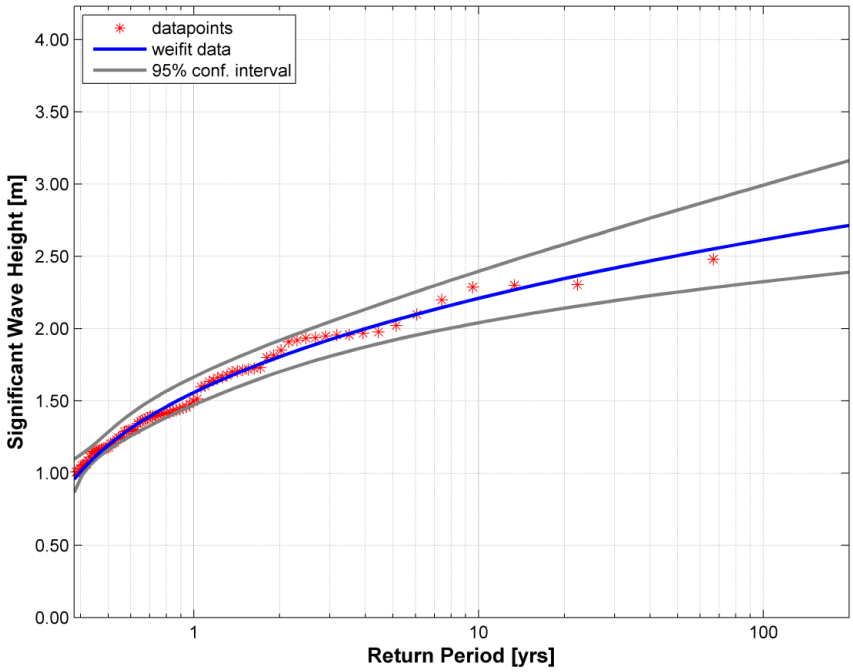

Figure A-34: Selected nearshore omnidirectional extreme wind sea significant wave height peaks, fitted Weibull distribution function and bootstrap 95% confidence interval limits for April.

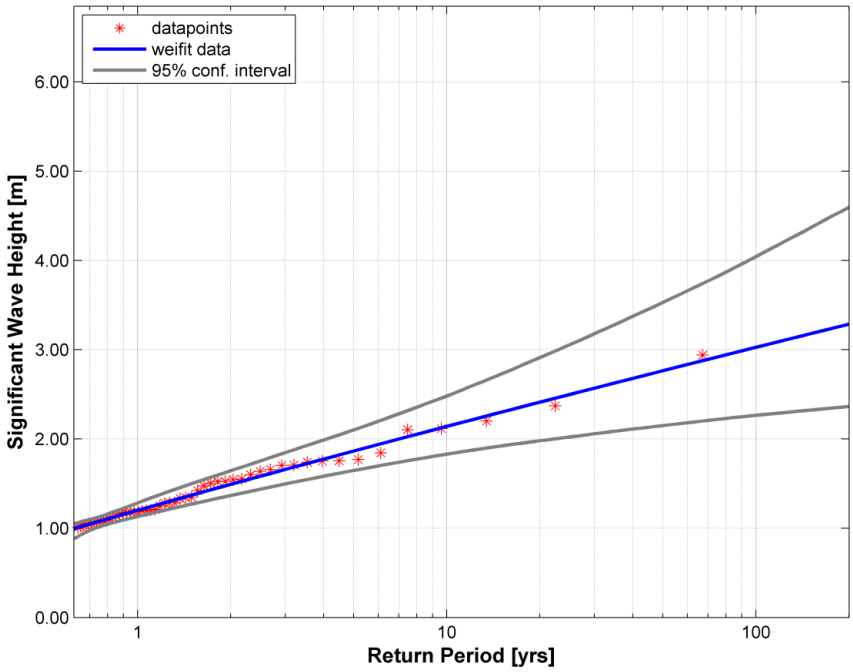

Figure A-35: Selected nearshore omnidirectional extreme wind sea significant wave height peaks, fitted Weibull distribution function and bootstrap 95% confidence interval limits for May.

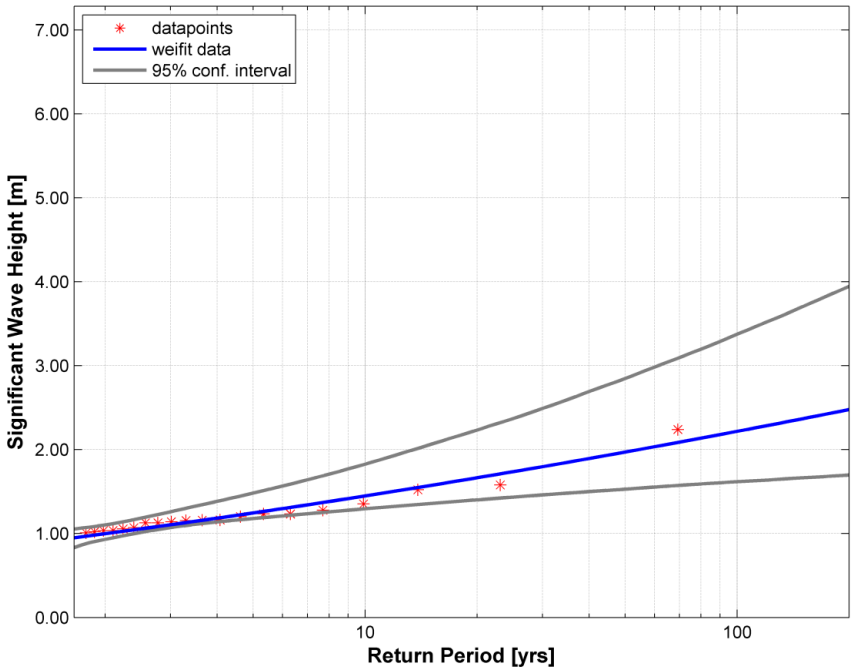

Figure A-36: Selected nearshore omnidirectional extreme wind sea significant wave height peaks, fitted Weibull distribution function and bootstrap 95% confidence interval limits for June.

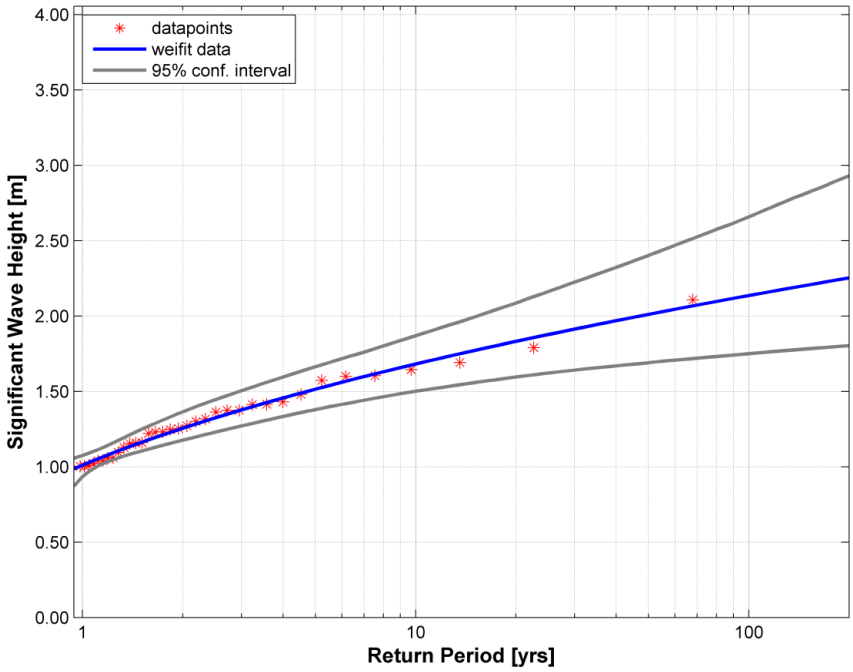

Figure A-37: Selected nearshore omnidirectional extreme wind sea significant wave height peaks, fitted Weibull distribution function and bootstrap 95% confidence interval limits for September.

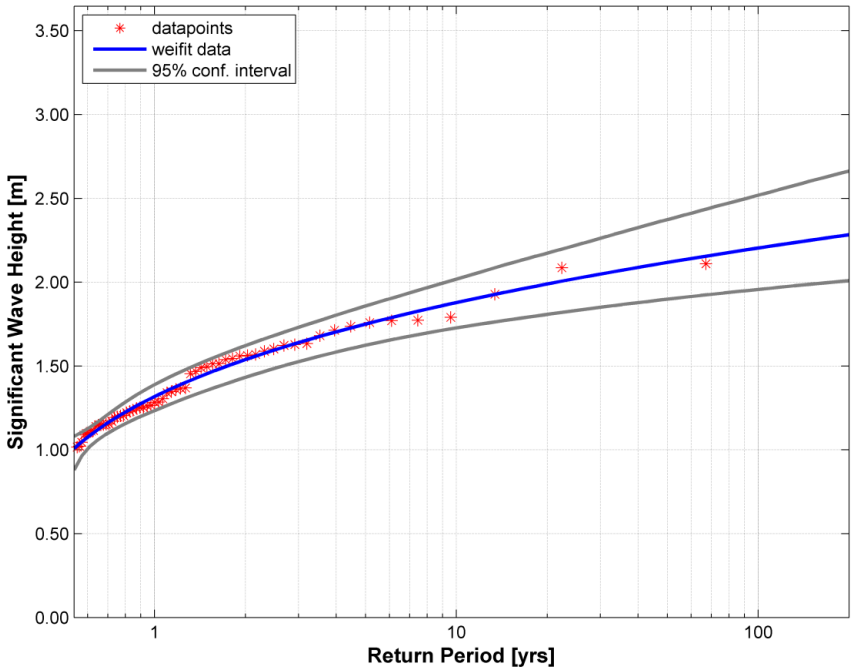

Figure A-38: Selected nearshore omnidirectional extreme wind sea significant wave height peaks, fitted Weibull distribution function and bootstrap 95% confidence interval limits for October.

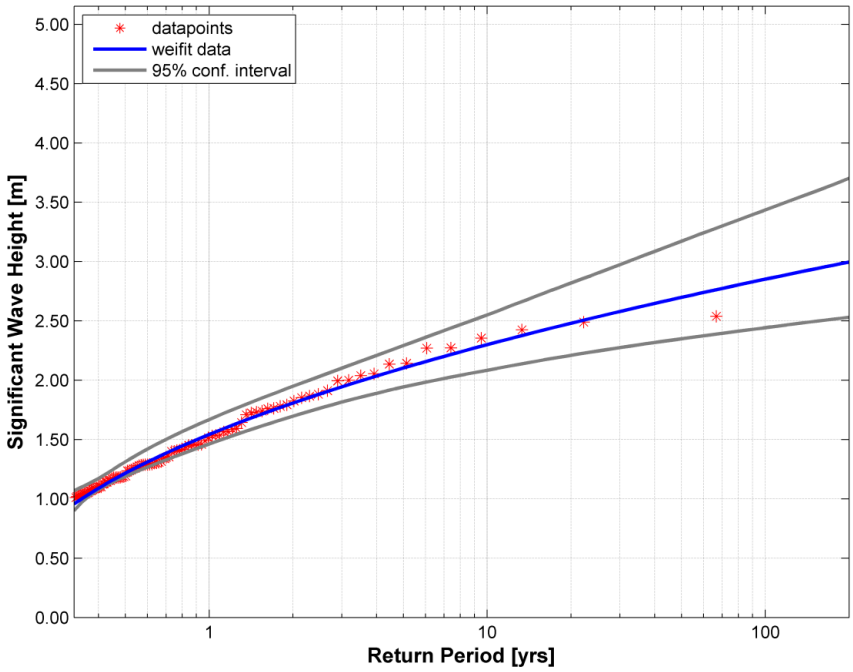

Figure A-39: Selected nearshore omnidirectional extreme wind sea significant wave height peaks, fitted Weibull distribution function and bootstrap 95% confidence interval limits for November.

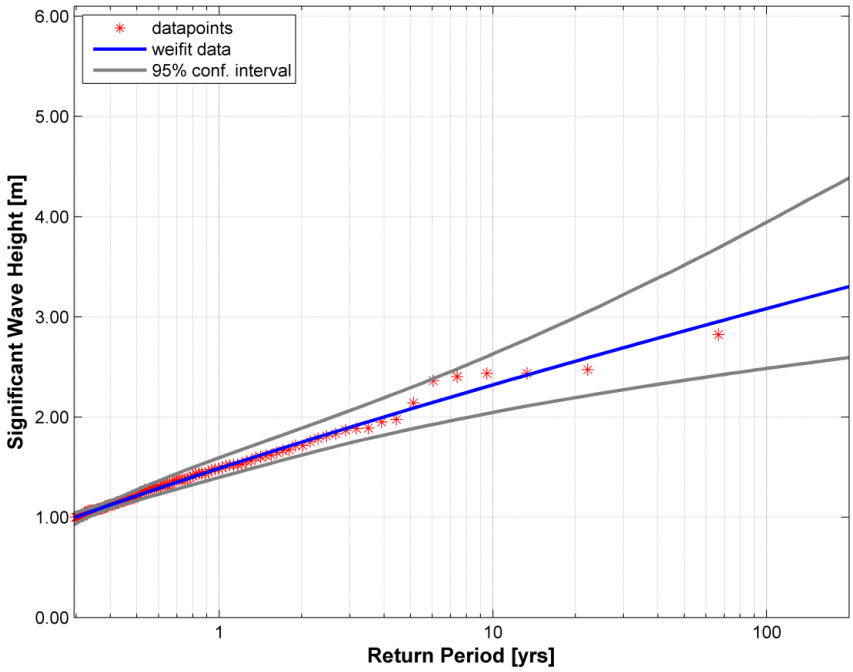

Figure A-40: Selected nearshore omnidirectional extreme wind sea significant wave height peaks, fitted Weibull distribution function and bootstrap 95% confidence interval limits for December.

Appendix 3.3 Swell significant wave height

Month	Jan			Feb			Mar		
Return period [yr]	best fit	low 95% conf	high 95% conf	best fit	low 95% conf	high 95% conf	best fit	low 95% conf	high 95% conf
1	0.81	0.80	0.87	0.88	0.83	0.90	0.87	0.84	0.90
5	1.17	1.08	1.31	1.11	1.02	1.17	1.13	1.04	1.24
10	1.31	1.17	1.50	1.19	1.08	1.28	1.25	1.11	1.41
25	1.49	1.27	1.78	1.29	1.15	1.43	1.40	1.20	1.65
50	1.62	1.33	2.02	1.36	1.19	1.56	1.53	1.26	1.85
100	1.75	1.39	2.26	1.43	1.22	1.68	1.66	1.31	2.05
Month	**Apr**			**May**			**Jun**		
Return period [yr]	**best fit**	**low 95% conf**	**high 95% conf**	**best fit**	**low 95% conf**	**high 95% conf**	**best fit**	**low 95% conf**	**high 95% conf**
1	0.91	0.87	0.95	0.84	0.79	0.85	0.68	0.33	0.72
5	1.15	1.07	1.22	1.10	0.99	1.19	0.92	0.86	1.03
10	1.24	1.13	1.35	1.22	1.07	1.36	1.03	0.93	1.20
25	1.36	1.20	1.52	1.38	1.15	1.60	1.19	1.00	1.46
50	1.44	1.25	1.65	1.50	1.20	1.80	1.30	1.05	1.69
100	1.51	1.29	1.79	1.63	1.25	2.01	1.43	1.09	1.94
Month	**Jul**			**Aug**			**Sep**		
Return period [yr]	**best fit**	**low 95% conf**	**high 95% conf**	**best fit**	**low 95% conf**	**high 95% conf**	**best fit**	**low 95% conf**	**high 95% conf**
1							0.77	0.74	0.80
5							1.05	0.97	1.14
10							1.15	1.04	1.28
25							1.28	1.11	1.47
50							1.37	1.16	1.63
100							1.46	1.19	1.80
Month	**Oct**			**Nov**			**Dec**		
Return period [yr]	**best fit**	**low 95% conf**	**high 95% conf**	**best fit**	**low 95% conf**	**high 95% conf**	**best fit**	**low 95% conf**	**high 95% conf**
1	0.82	0.80	0.85	0.87	0.85	0.91	0.88	0.85	0.93
5	1.02	0.96	1.11	1.11	1.03	1.21	1.20	1.10	1.36
10	1.11	1.01	1.24	1.21	1.10	1.36	1.35	1.19	1.58
25	1.23	1.08	1.43	1.36	1.18	1.57	1.56	1.30	1.90
50	1.33	1.13	1.57	1.47	1.23	1.74	1.72	1.38	2.16
100	1.42	1.17	1.72	1.58	1.28	1.91	1.89	1.44	2.44

Table A-6: Nearshore all-omnidirectional swell significant wave heights in m for all return periods and directional sectors.

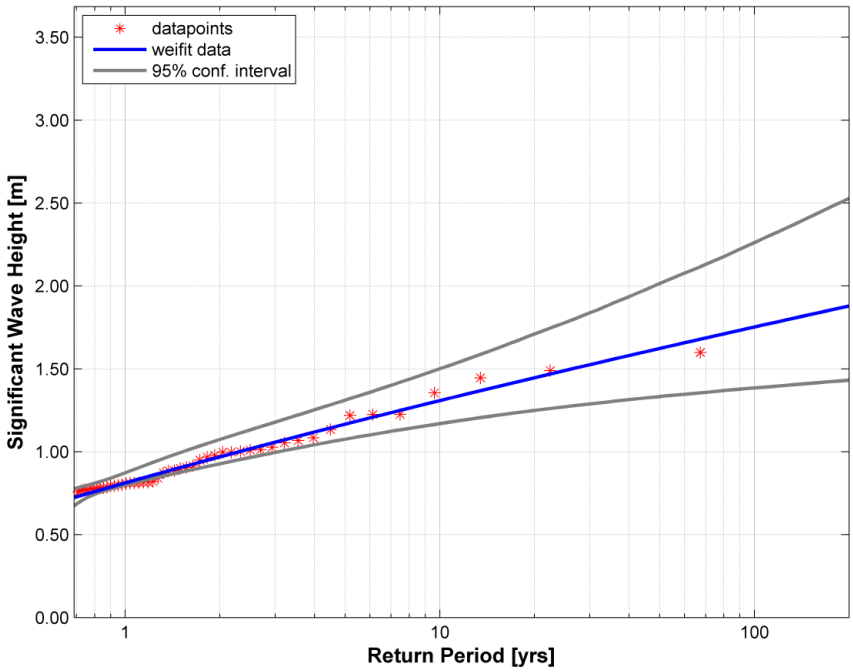

Figure A-41: Selected nearshore omnidirectional extreme swell significant wave height peaks, fitted Weibull distribution function and bootstrap 95% confidence interval limits for January.

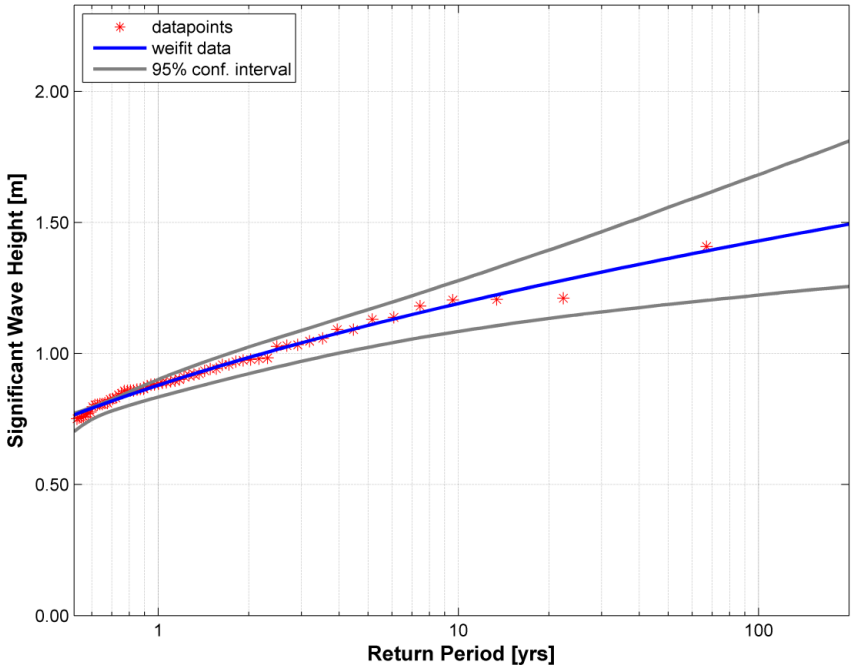

Figure A-42: Selected nearshore omnidirectional extreme swell significant wave height peaks, fitted Weibull distribution function and bootstrap 95% confidence interval limits for February.

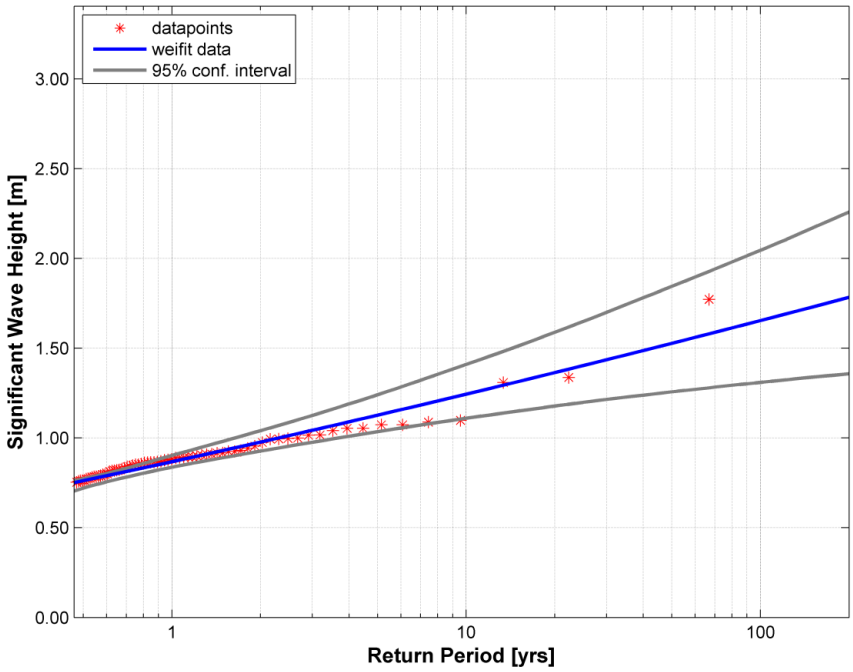

Figure A-43: Selected nearshore omnidirectional extreme swell significant wave height peaks, fitted Weibull distribution function and bootstrap 95% confidence interval limits for March.

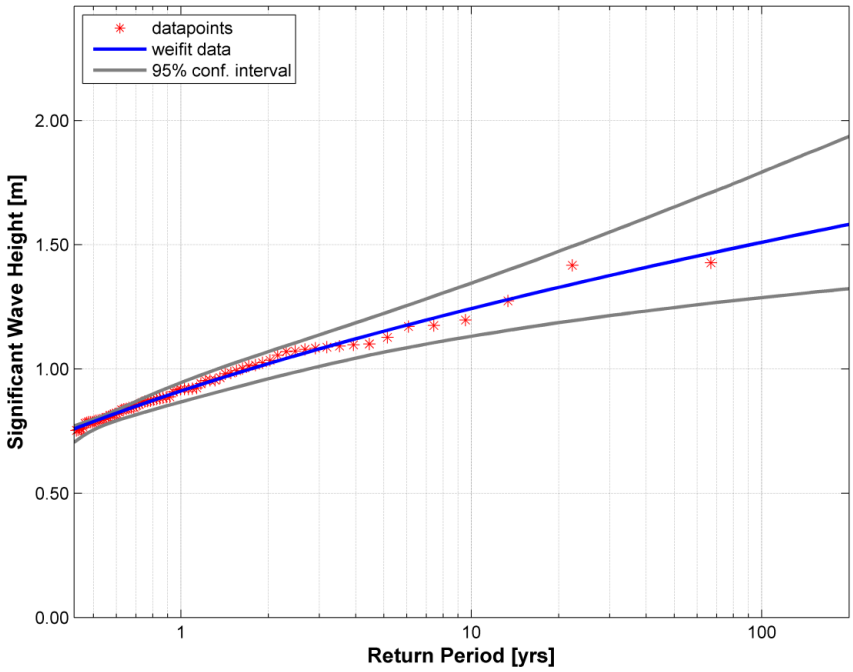

Figure A-44: Selected nearshore omnidirectional extreme swell significant wave height peaks, fitted Weibull distribution function and bootstrap 95% confidence interval limits for April.

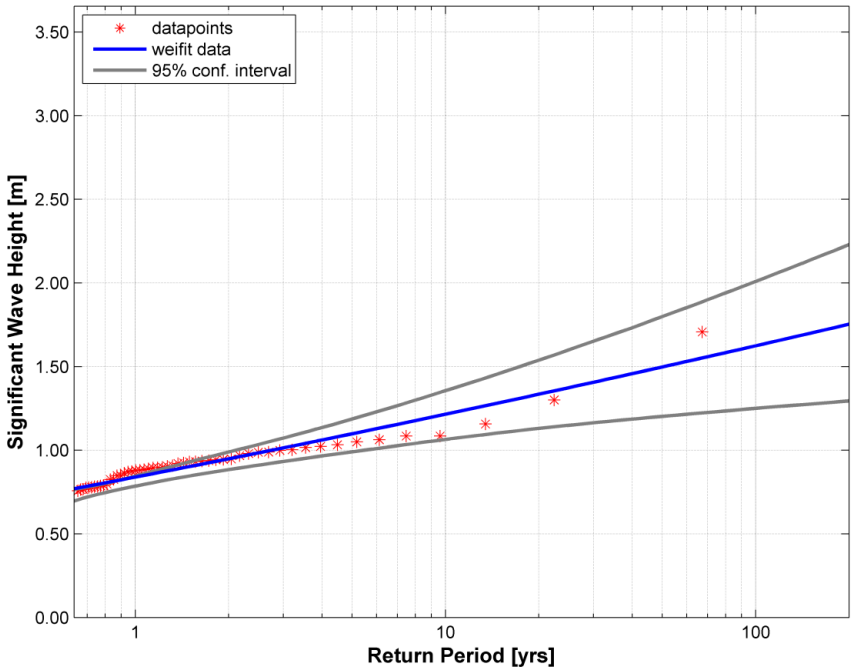

Figure A-45: Selected nearshore omnidirectional extreme swell significant wave height peaks, fitted Weibull distribution function and bootstrap 95% confidence interval limits for May.

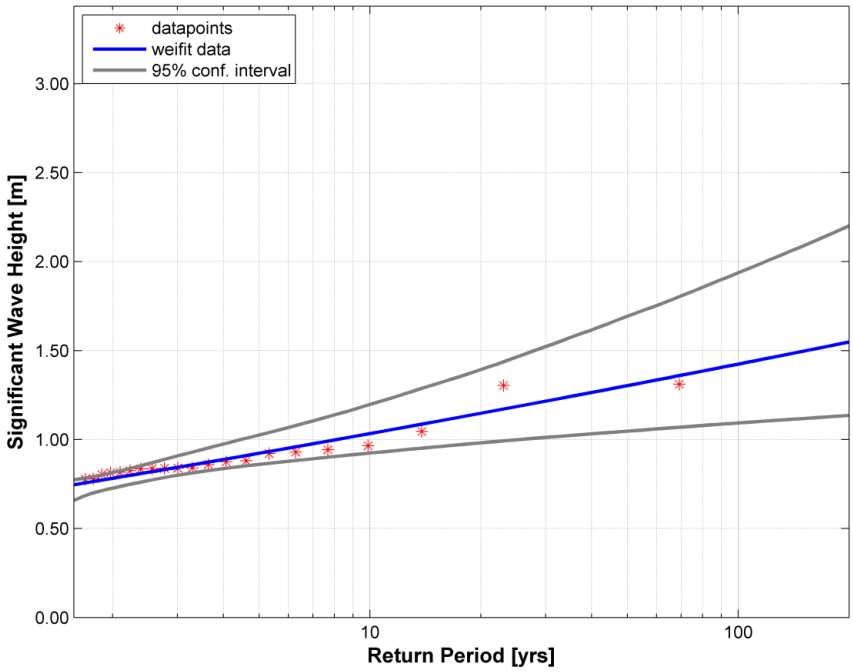

Figure A-46: Selected nearshore omnidirectional extreme swell significant wave height peaks, fitted Weibull distribution function and bootstrap 95% confidence interval limits for June.

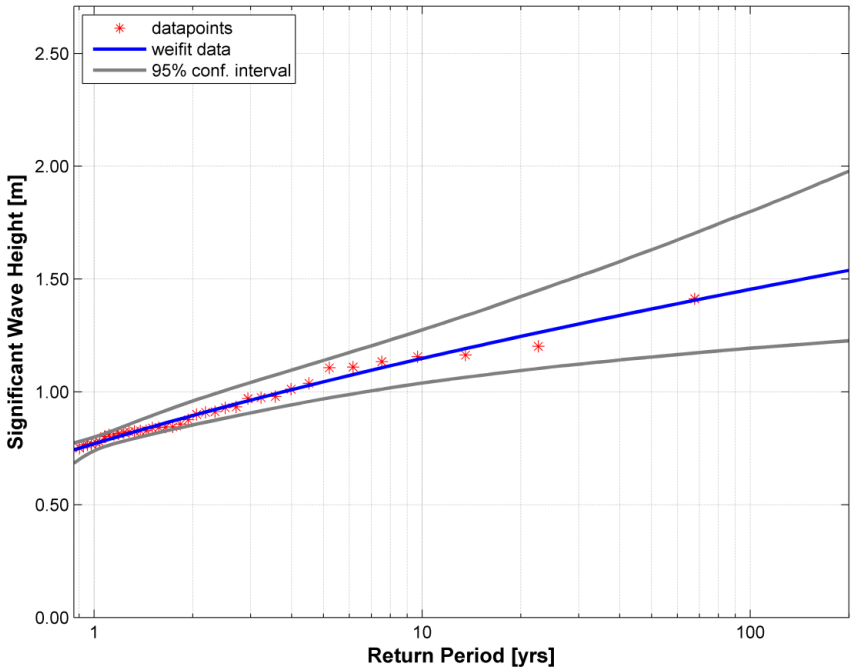

Figure A-47: Selected nearshore omnidirectional extreme swell significant wave height peaks, fitted Weibull distribution function and bootstrap 95% confidence interval limits for September.

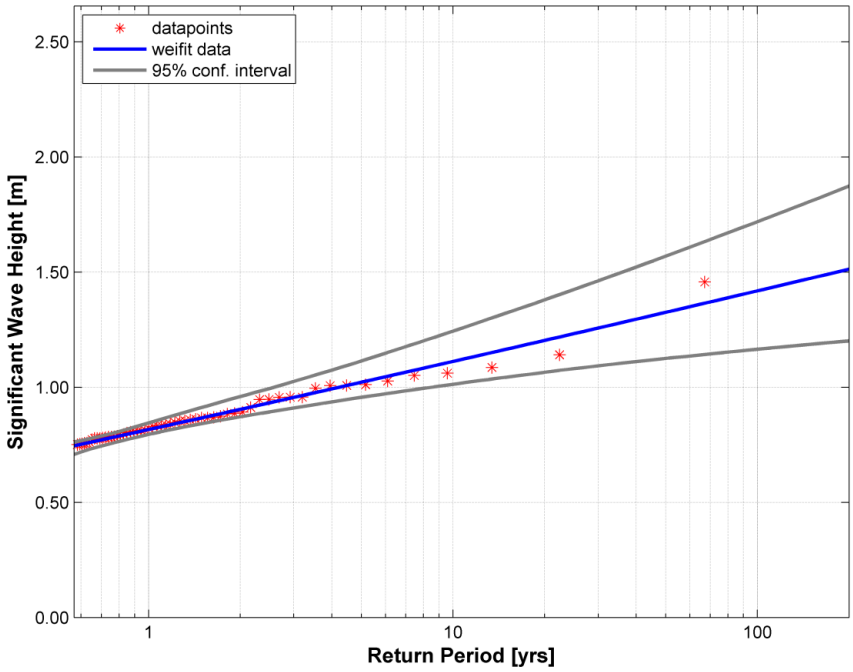

Figure A-48: Selected nearshore omnidirectional extreme swell significant wave height peaks, fitted Weibull distribution function and bootstrap 95% confidence interval limits for October.

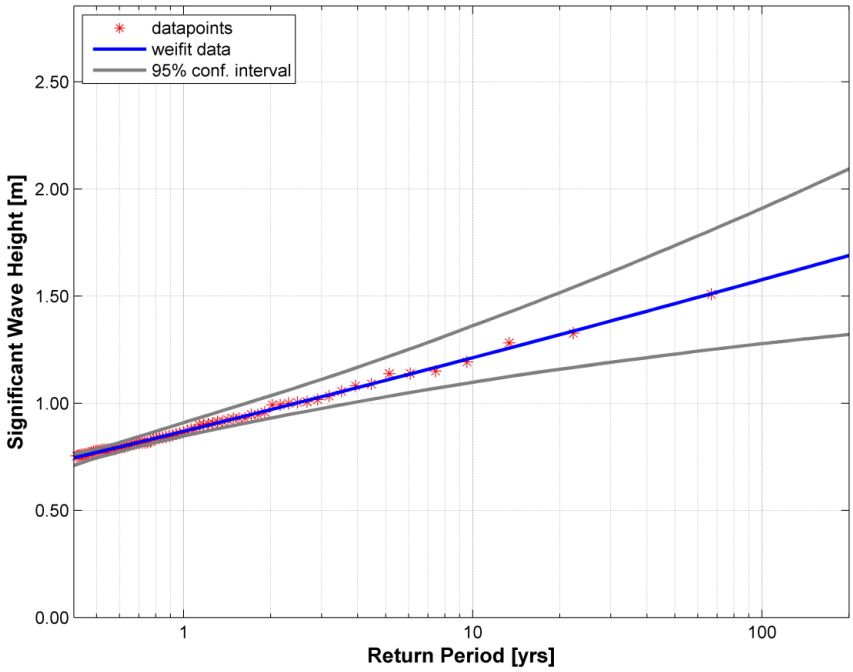

Figure A-49: Selected nearshore omnidirectional extreme swell significant wave height peaks, fitted Weibull distribution function and bootstrap 95% confidence interval limits for November.

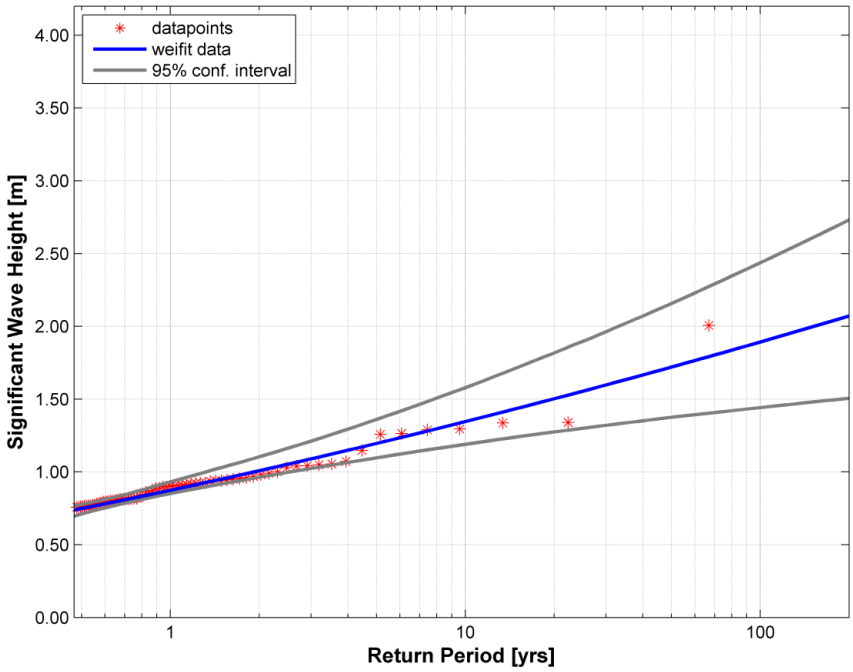

Figure A-50: Selected nearshore omnidirectional extreme swell significant wave height peaks, fitted Weibull distribution function and bootstrap 95% confidence interval limits for December.

Appendix 4 Figures of conditions associated to U_{10} extremes

Appendix 4.1 U_{10} vs H_{m0} wind sea

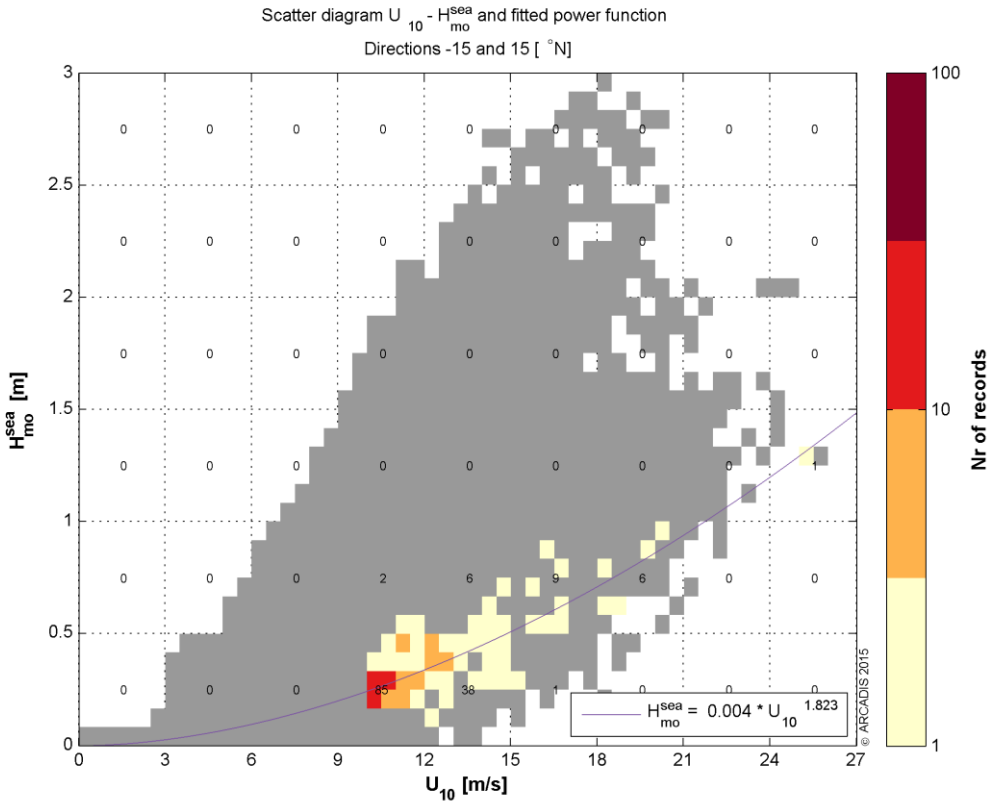

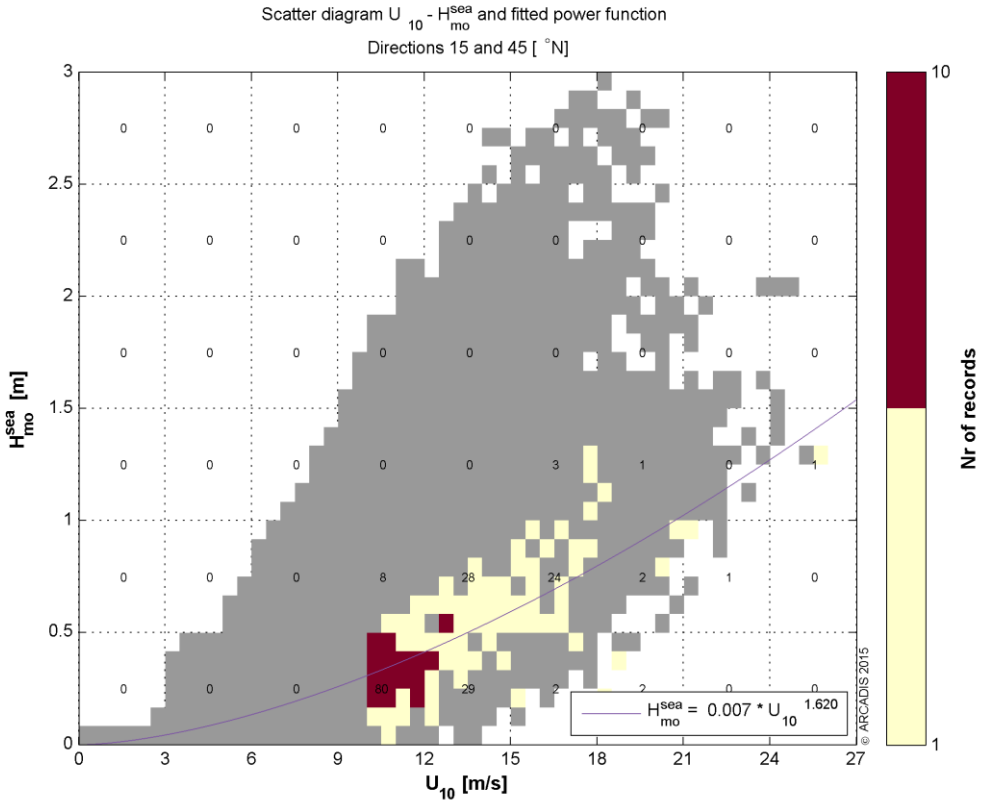

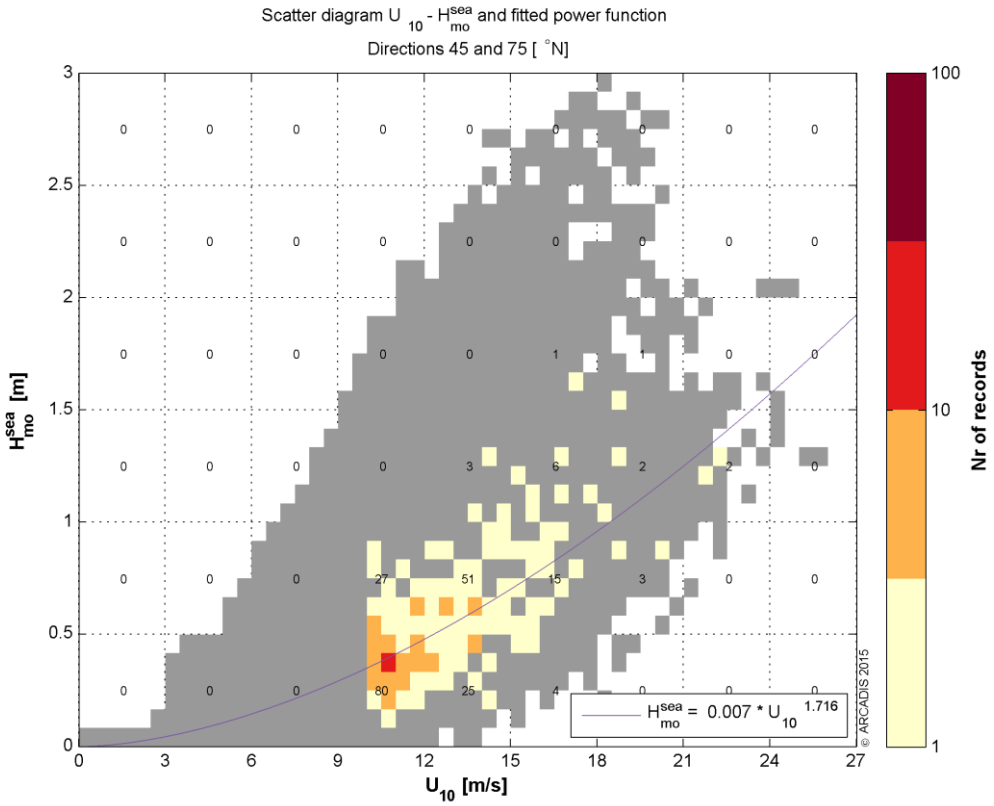
Scatter diagram U 10 - Hmosea and fitted power function
Directions 45 and 75 [°N]
Hmosea [m]
U10 [m/s]
Nr of records
Hmosea = 0.007 * U10 1.716
© ARCADIS 2015

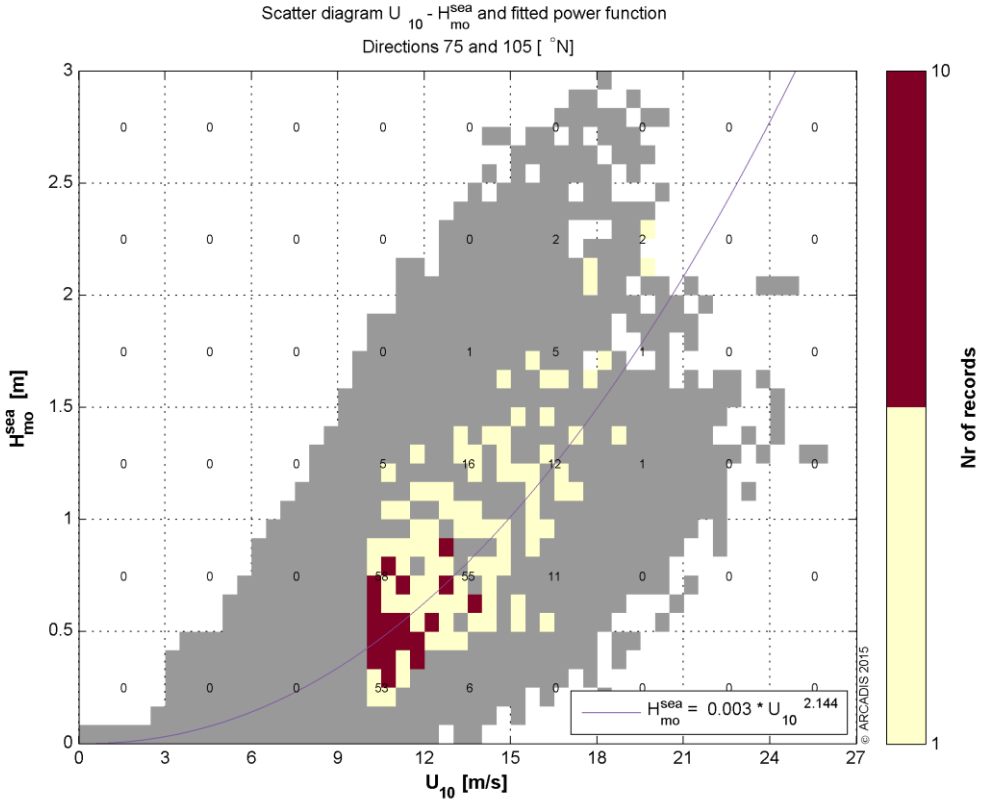
Scatter diagram U 10 - Hmosea and fitted power function
Directions 75 and 105 [°N]
Hmosea [m]
U10 [m/s]
Nr of records
Hmosea = 0.003 * U10 2.144
© ARCADIS 2015

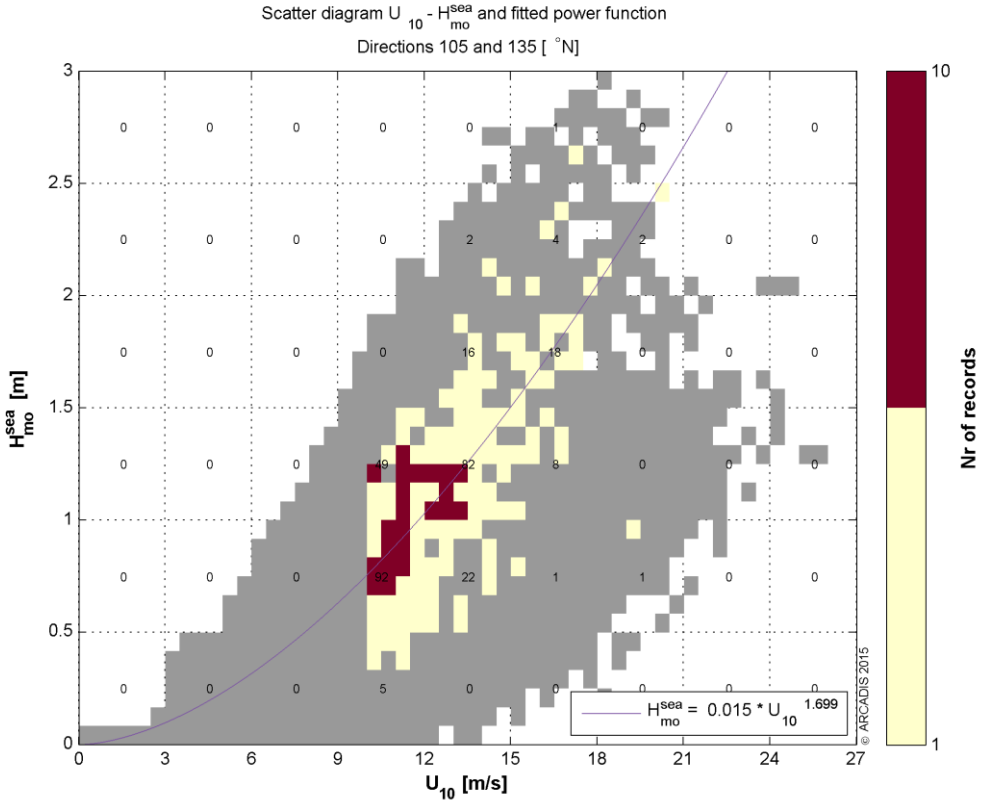
Scatter diagram U 10 - Hmosea and fitted power function
Directions 105 and 135 [°N]
Hmosea [m]
U10 [m/s]
Hmosea = 0.015 * U10 1.699
© ARCADIS 2015
Nr of records

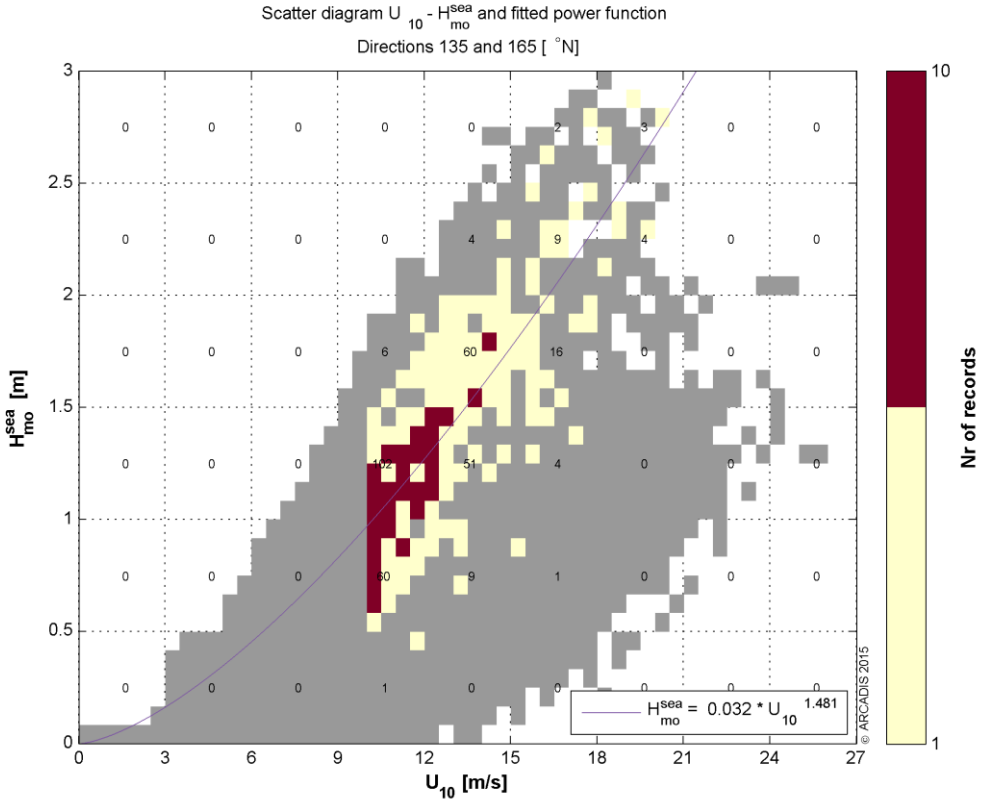
Scatter diagram U 10 - Hmosea and fitted power function
Directions 135 and 165 [°N]
Hmosea [m]
U10 [m/s]
Hmosea = 0.032 * U10 1.481
© ARCADIS 2015
Nr of records

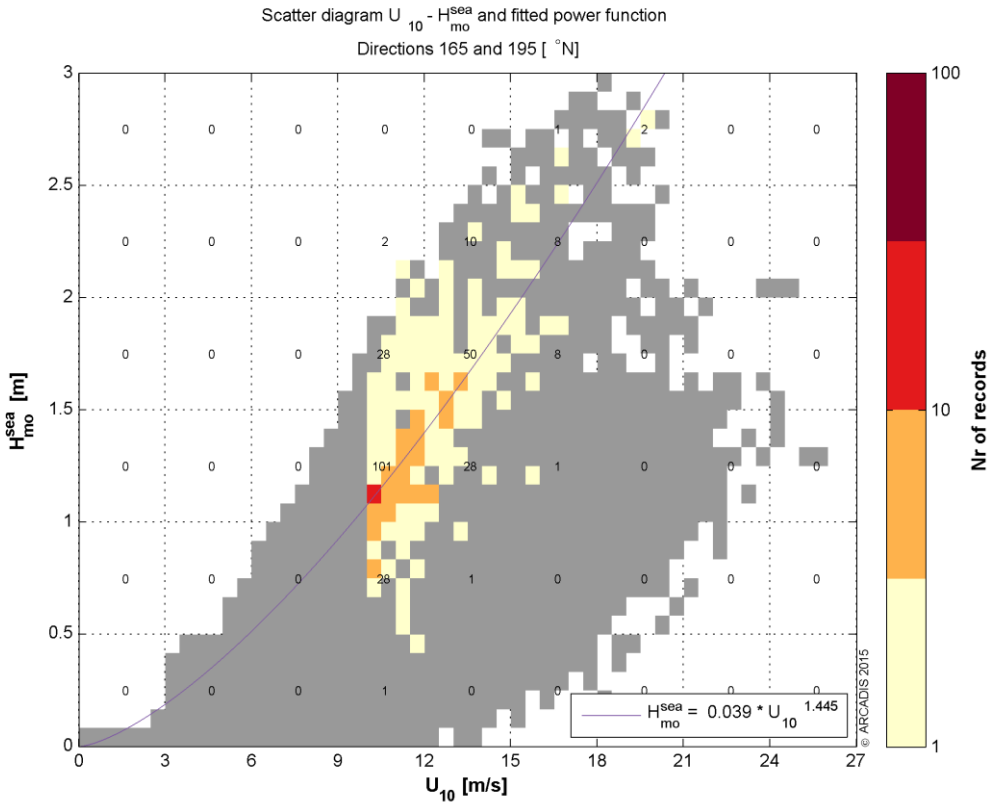
Scatter diagram U 10 - Hmosea and fitted power function
Directions 165 and 195 [°N]
Hmosea [m]
U10 [m/s]
Hmosea = 0.039 * U10 1.445
© ARCADIS 2015
Nr of records
100
10
1

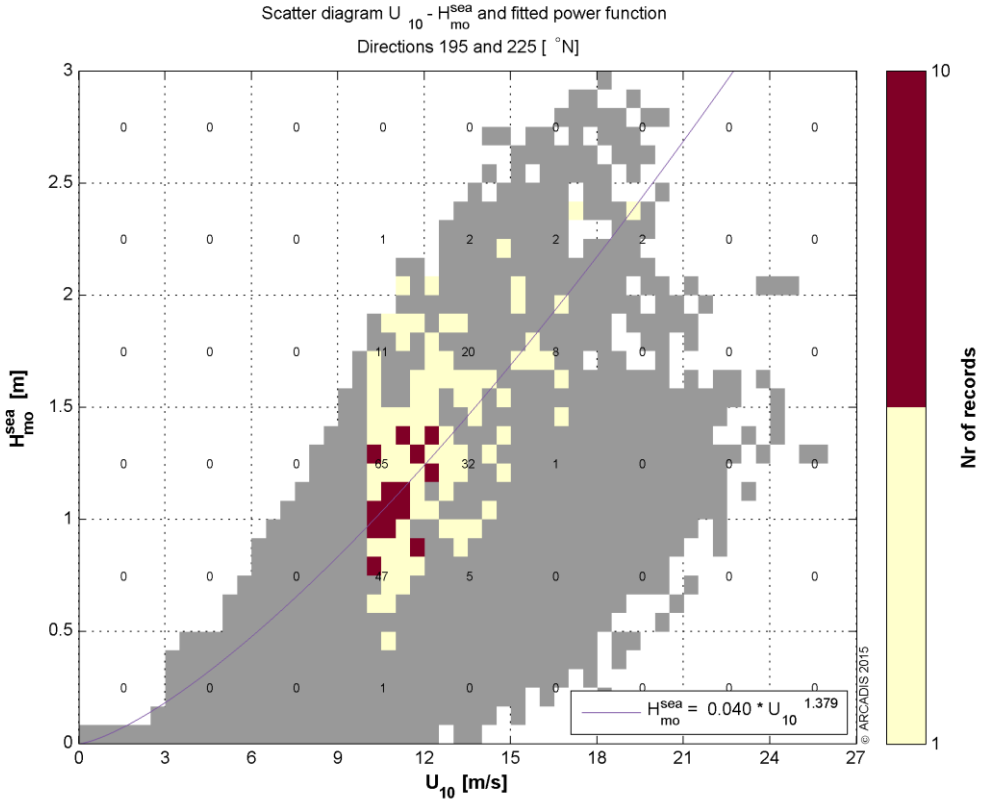
Scatter diagram U 10 - Hmosea and fitted power function
Directions 195 and 225 [°N]
Hmosea [m]
U10 [m/s]
Hmosea = 0.040 * U10 1.379
© ARCADIS 2015
Nr of records
10
1

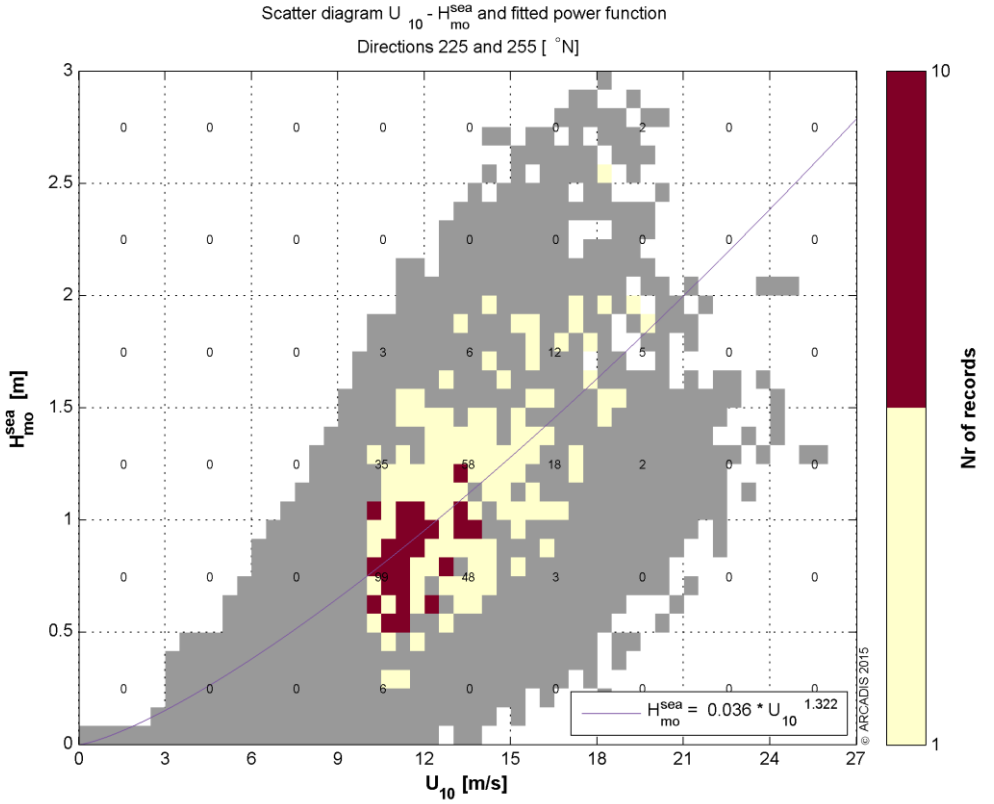
Scatter diagram U 10 - Hmosea and fitted power function
Directions 225 and 255 [°N]
Hmosea [m]
U10 [m/s]
Hmosea = 0.036 * U10 1.322
© ARCADIS 2015
Nr of records

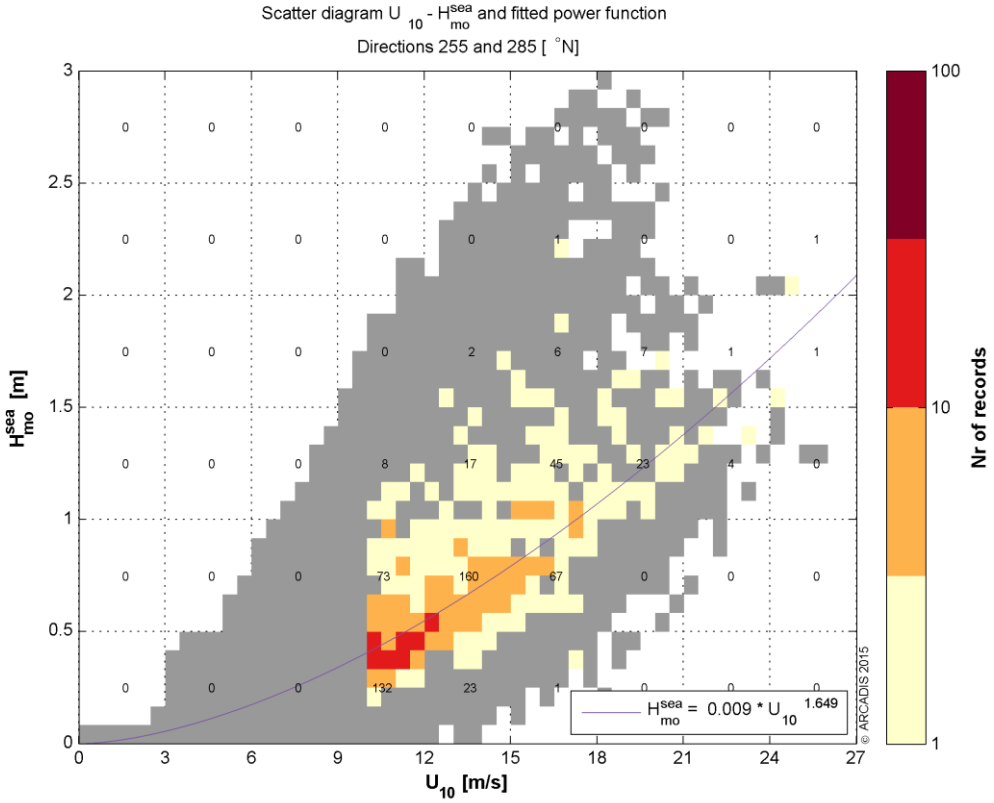
Scatter diagram U 10 - Hmosea and fitted power function
Directions 255 and 285 [°N]
Hmosea [m]
U10 [m/s]
Hmosea = 0.009 * U10 1.649
© ARCADIS 2015
Nr of records

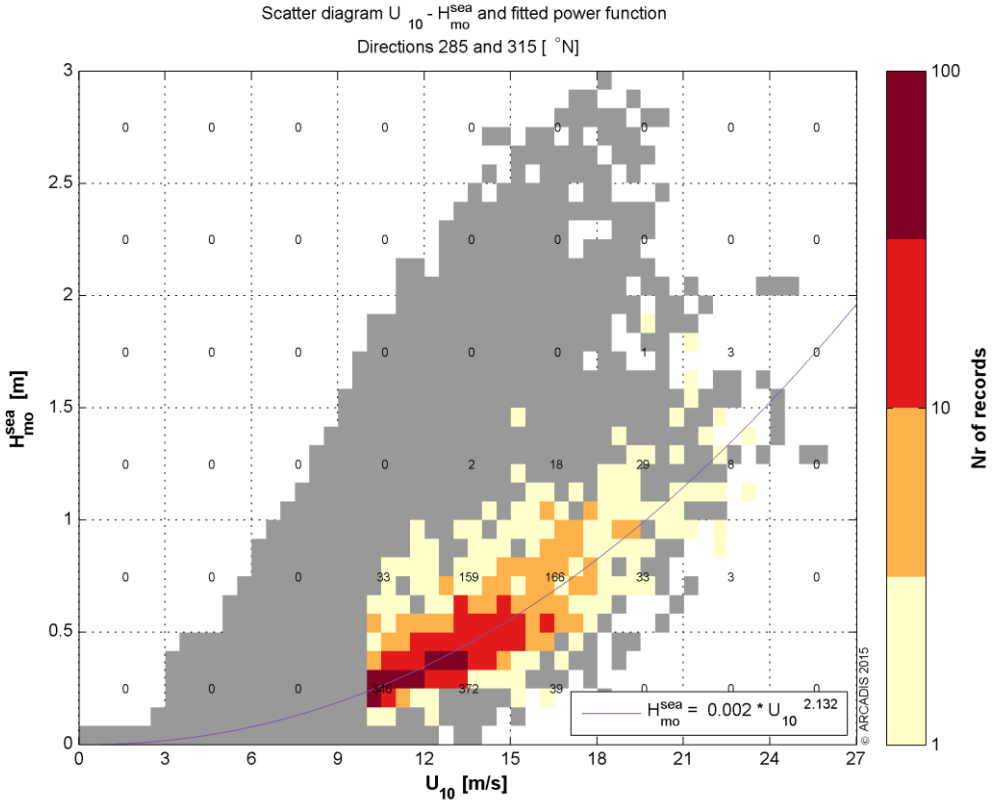
Scatter diagram U 10 - Hmosea and fitted power function
Directions 285 and 315 [°N]
Hmosea [m]
U10 [m/s]
Nr of records
Hmosea = 0.002 * U10 2.132
© ARCADIS 2015

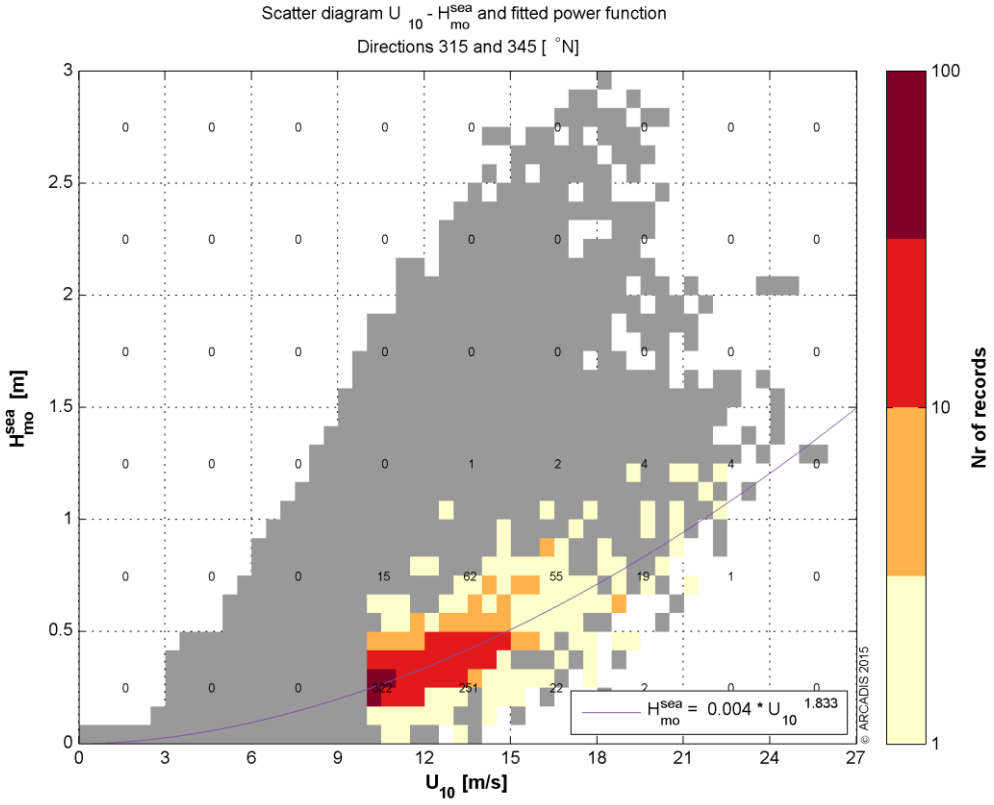
Scatter diagram U 10 - Hmosea and fitted power function
Directions 315 and 345 [°N]
Hmosea [m]
U10 [m/s]
Nr of records
Hmosea = 0.004 * U10 1.833
© ARCADIS 2015

Appendix 4.2 U_{10} vs T_p wind sea

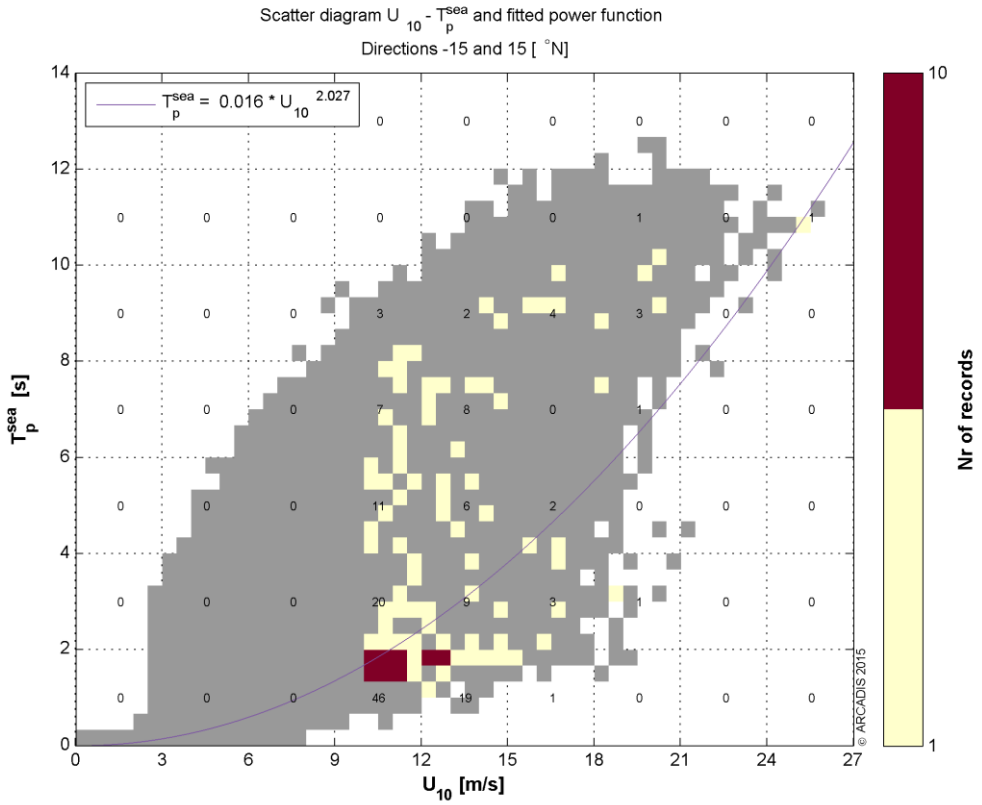

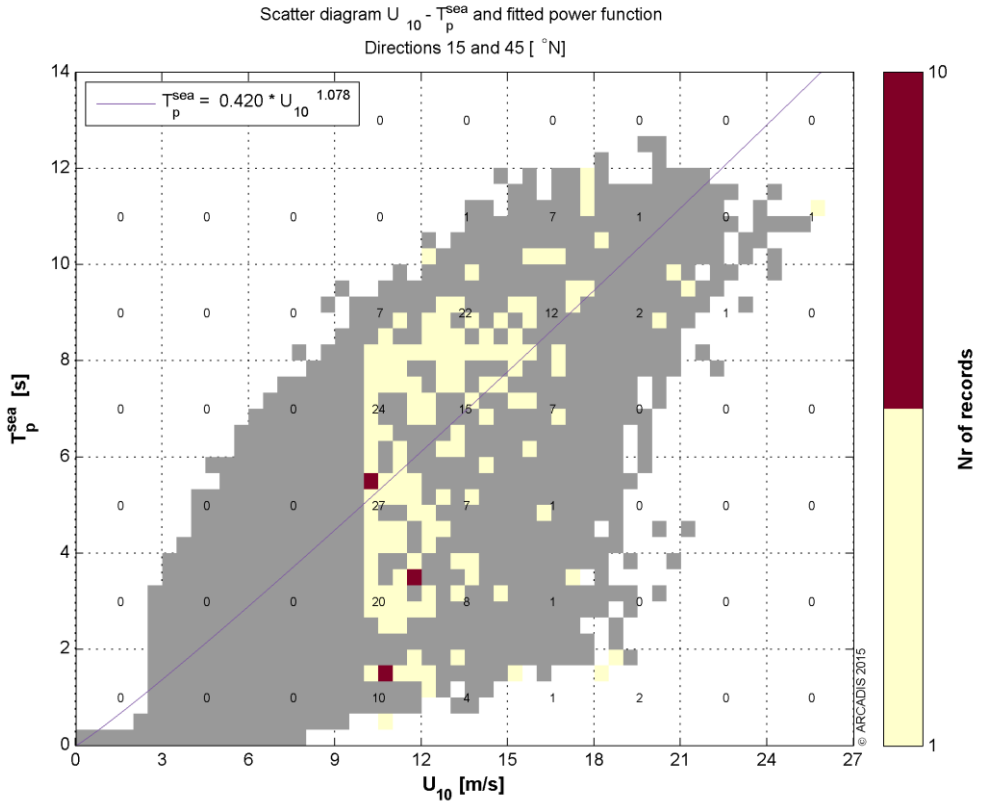

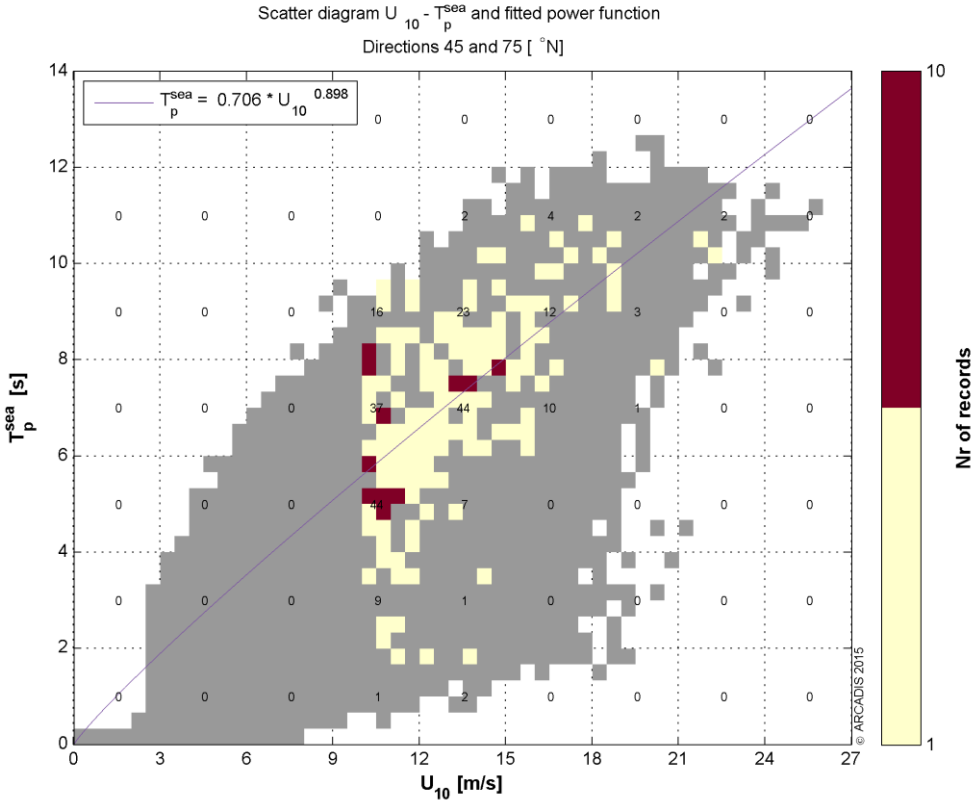
Scatter diagram U 10 - T p sea and fitted power function
Directions 45 and 75 [°N]
T p sea = 0.706 * U 10 0.898
T p sea [s]
U 10 [m/s]
Nr of records
© ARCADIS 2015

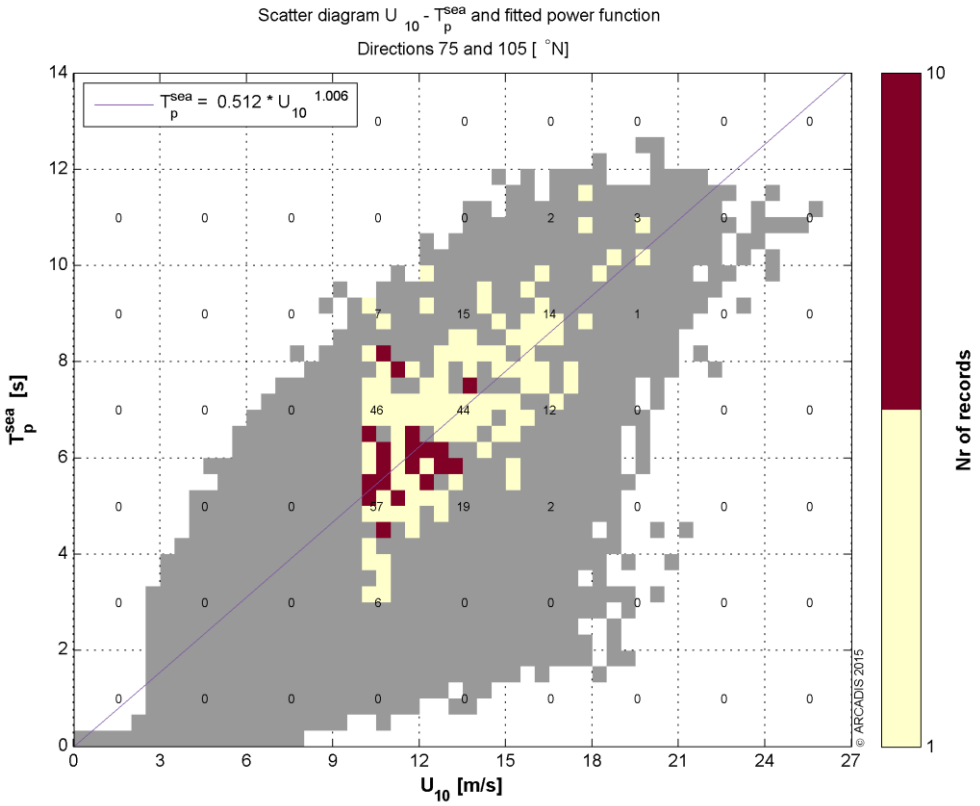
Scatter diagram U 10 - T p sea and fitted power function
Directions 75 and 105 [°N]
T p sea = 0.512 * U 10 1.006
T p sea [s]
U 10 [m/s]
Nr of records
© ARCADIS 2015

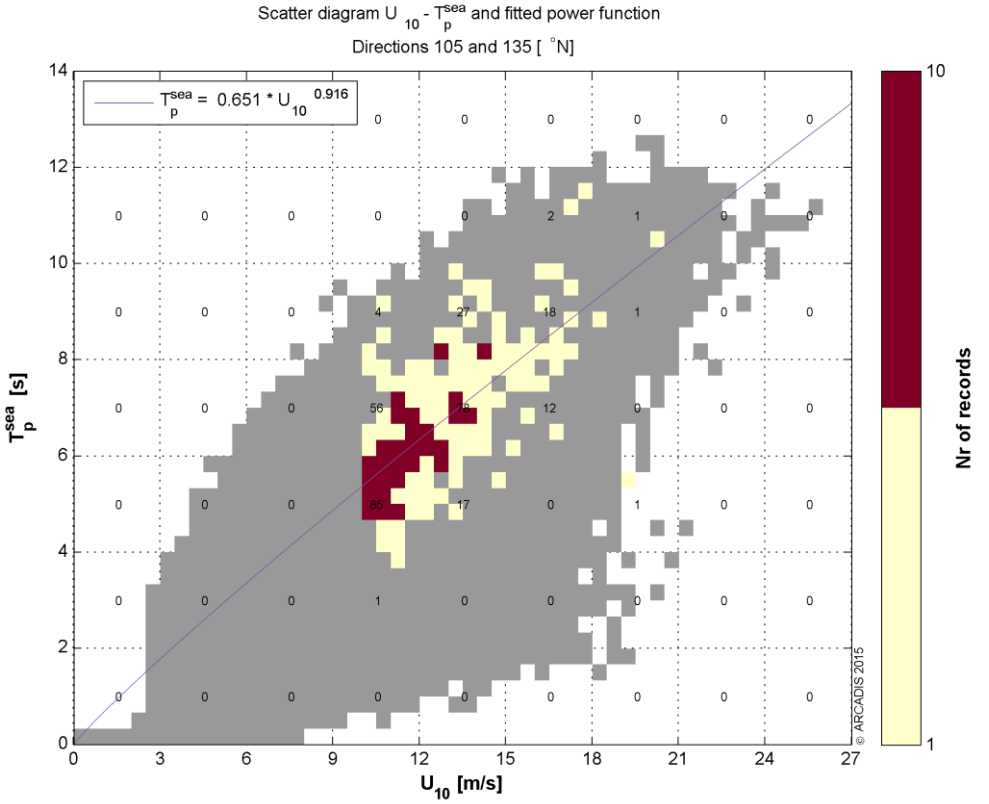
Scatter diagram U 10 - T p sea and fitted power function
Directions 105 and 135 [°N]
T p sea = 0.651 * U 10 0.916
T p sea [s]
U 10 [m/s]
Nr of records
© ARCADIS 2015

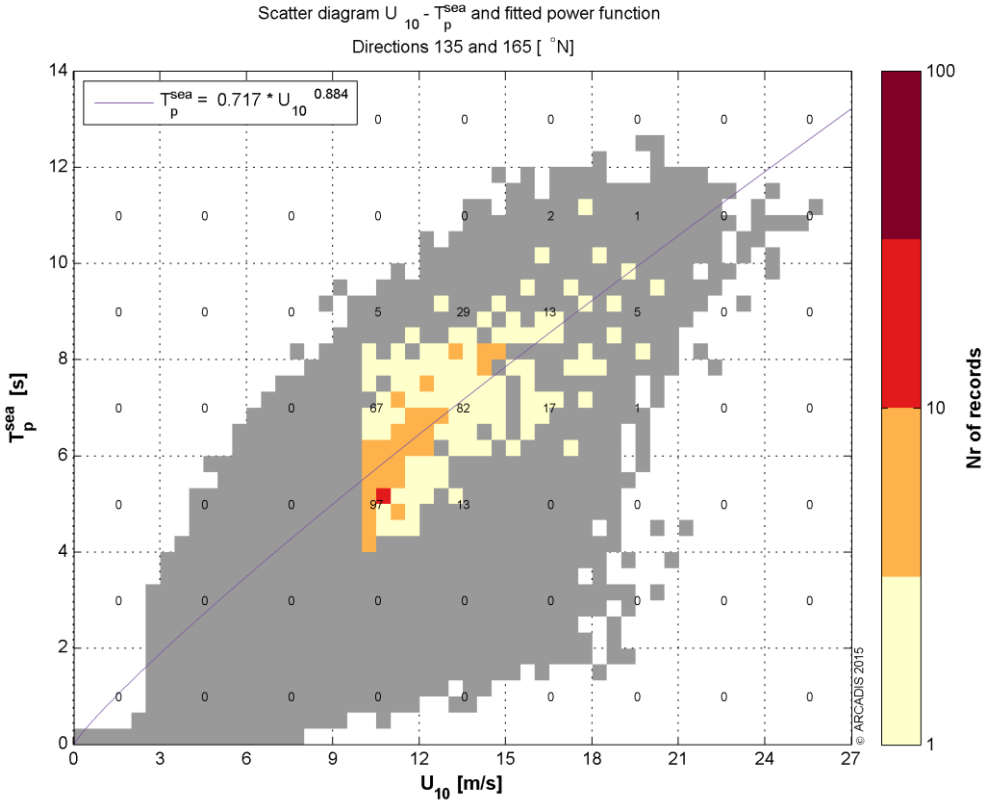
Scatter diagram U 10 - T p sea and fitted power function
Directions 135 and 165 [°N]
T p sea = 0.717 * U 10 0.884
T p sea [s]
U 10 [m/s]
Nr of records
© ARCADIS 2015

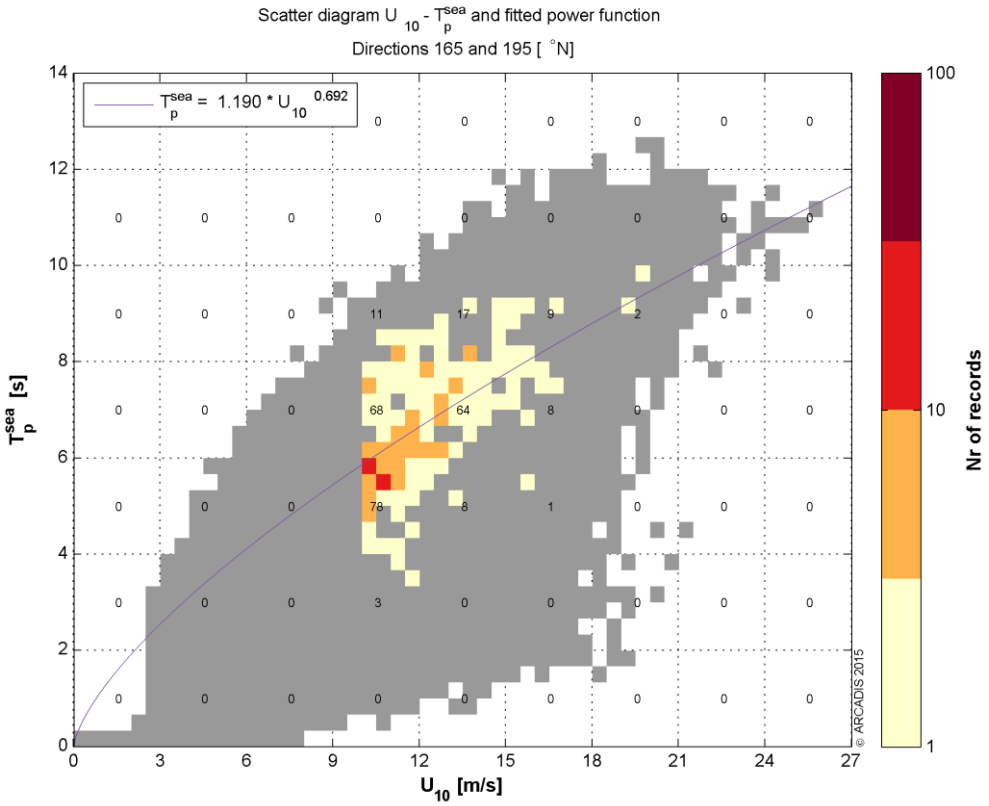
Scatter diagram U 10 - T p sea and fitted power function
Directions 165 and 195 [°N]
T p sea = 1.190 * U 10 0.692
T p sea [s]
U 10 [m/s]
Nr of records
© ARCADIS 2015

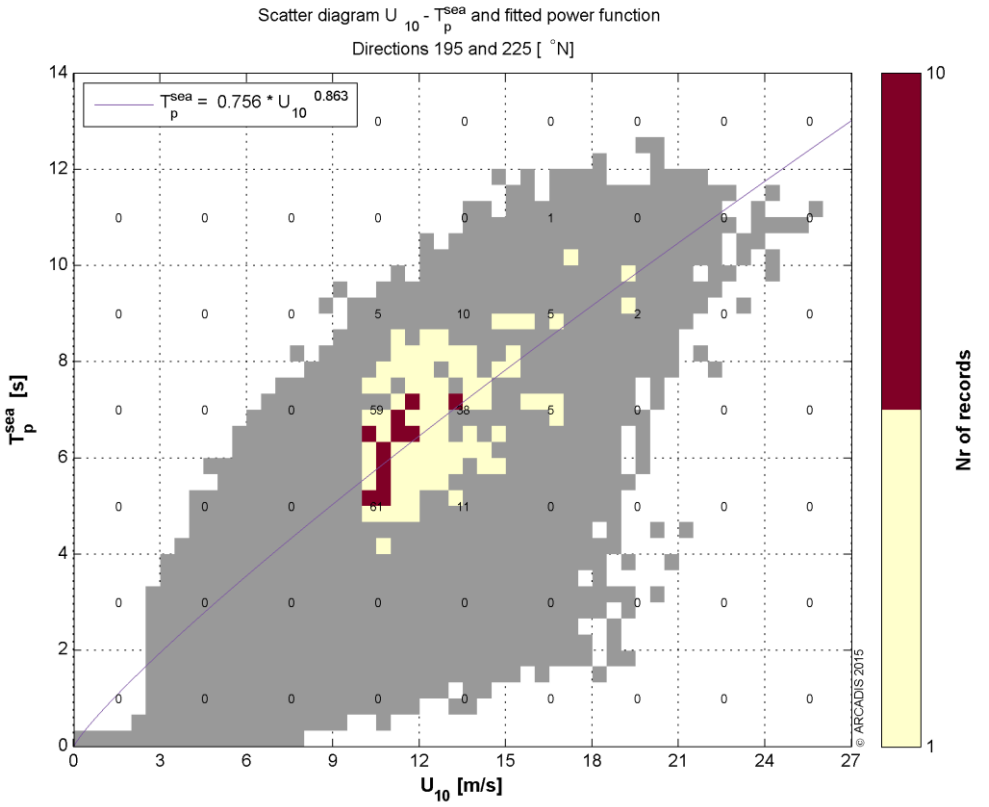
Scatter diagram U 10 - T p sea and fitted power function
Directions 195 and 225 [°N]
T p sea = 0.756 * U 10 0.863
T p sea [s]
U 10 [m/s]
Nr of records
© ARCADIS 2015

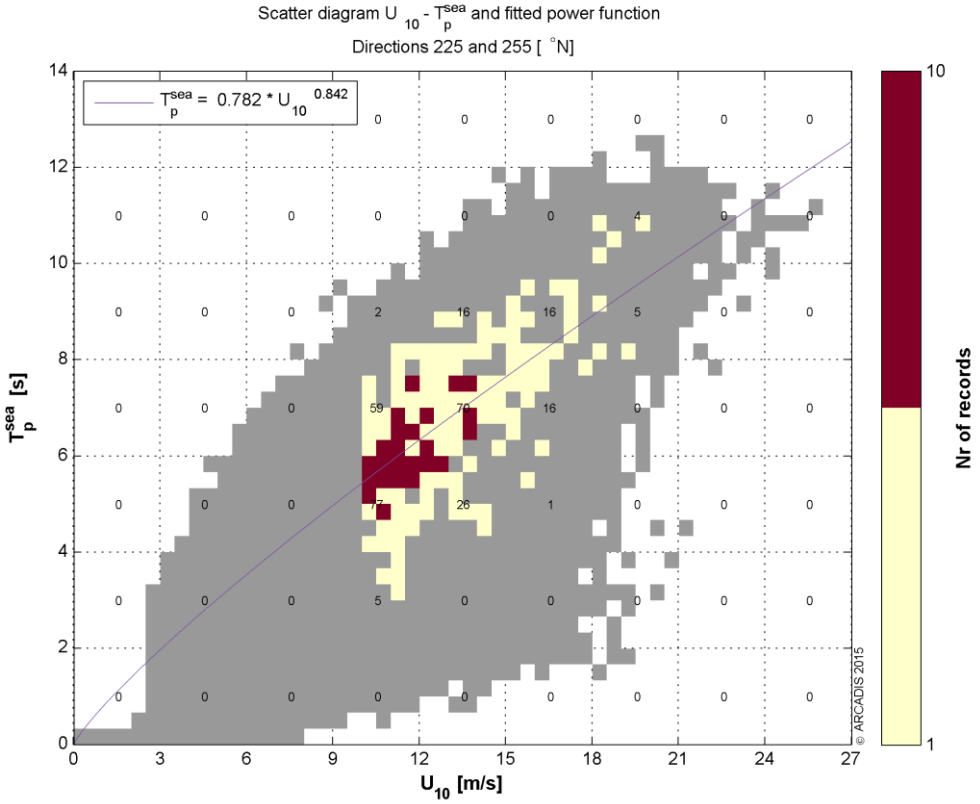
Scatter diagram U 10 - T p sea and fitted power function
Directions 225 and 255 [°N]
T p sea = 0.782 * U 10 0.842
T p sea [s]
U 10 [m/s]
Nr of records
© ARCADIS 2015

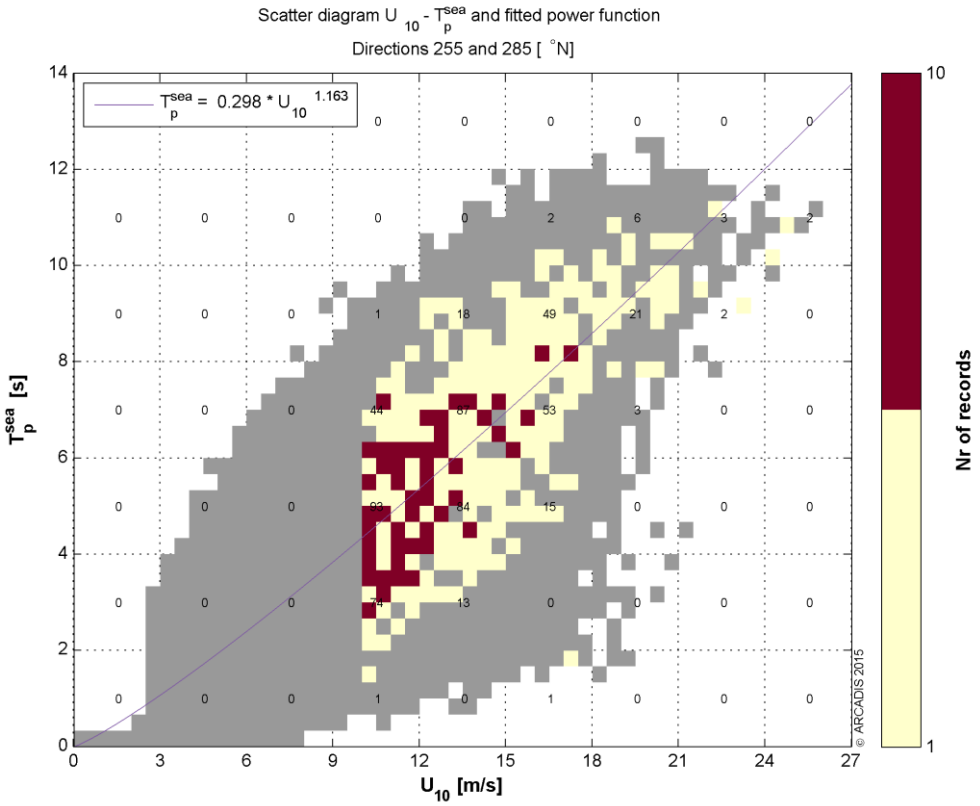
Scatter diagram U 10 - T p sea and fitted power function
Directions 255 and 285 [°N]
T p sea = 0.298 * U 10 1.163
T p sea [s]
U 10 [m/s]
Nr of records
© ARCADIS 2015

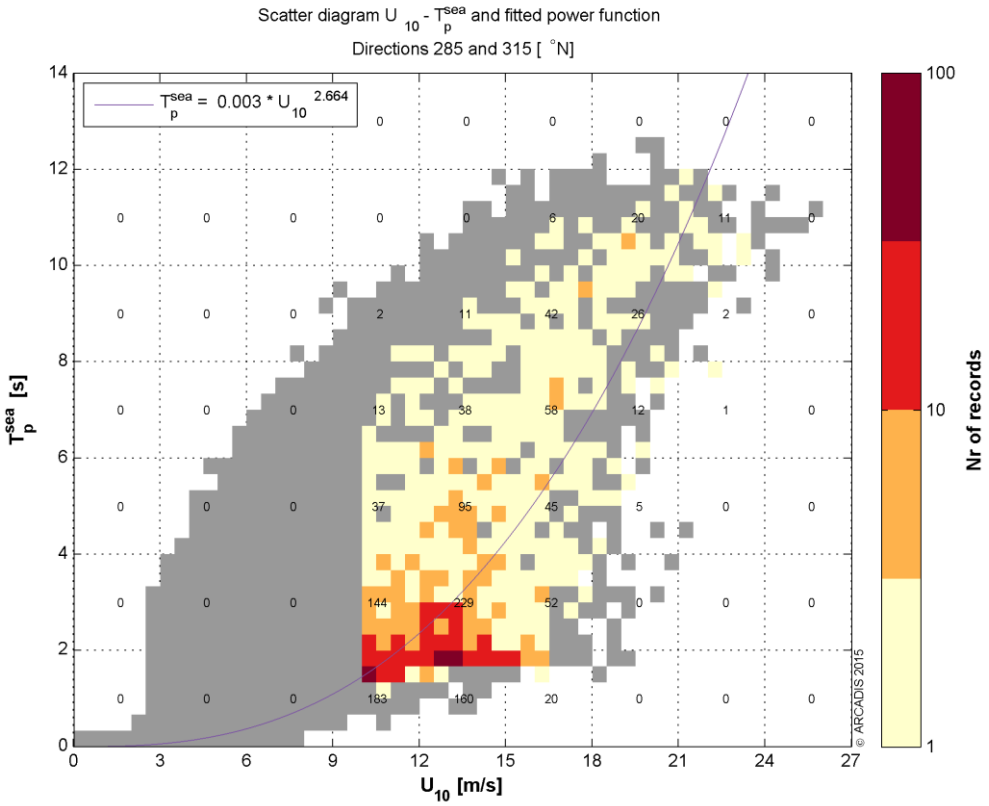
Scatter diagram U 10 - T p sea and fitted power function
Directions 285 and 315 [°N]
T p sea = 0.003 * U 10 2.664
T p sea [s]
U 10 [m/s]
Nr of records
© ARCADIS 2015

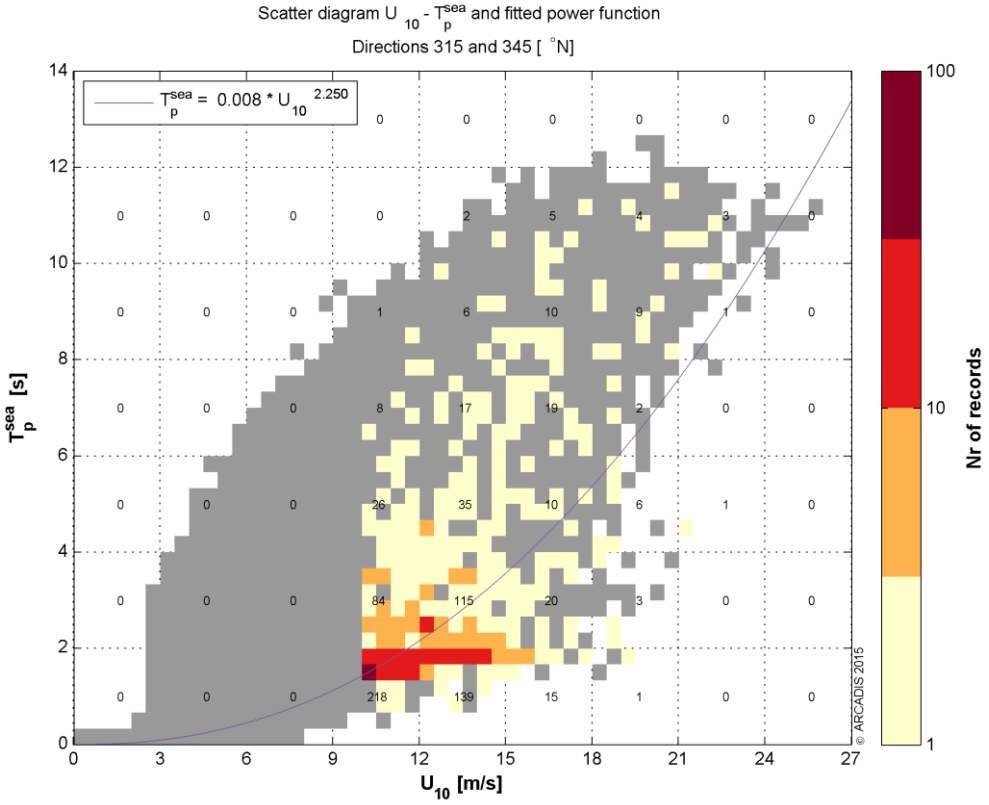
Scatter diagram U 10 - T p sea and fitted power function
Directions 315 and 345 [°N]
T p sea = 0.008 * U 10 2.250
T p sea [s]
U 10 [m/s]
Nr of records
© ARCADIS 2015

Appendix 4.3 U_{10} vs H_{m0} swell

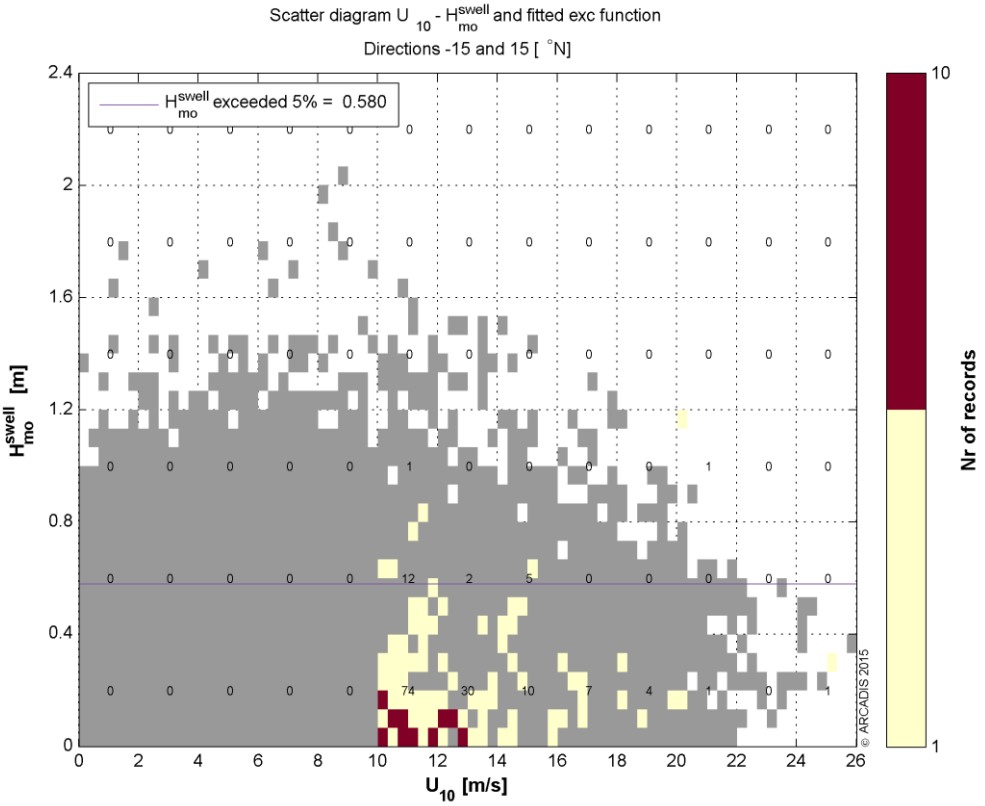

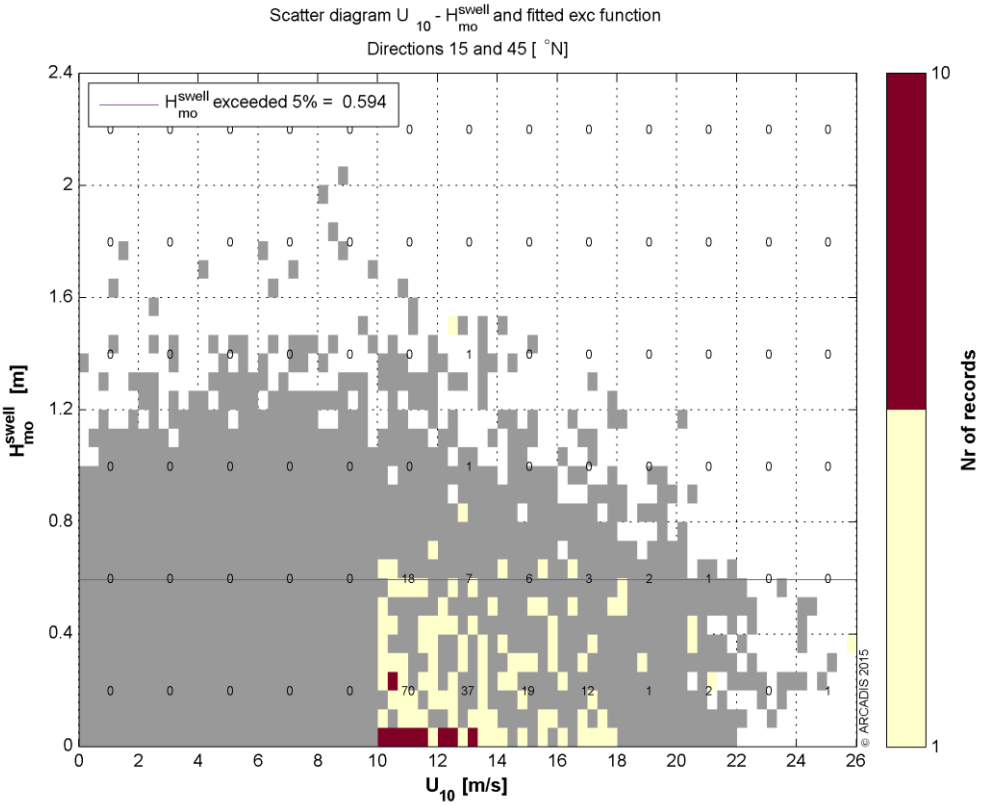

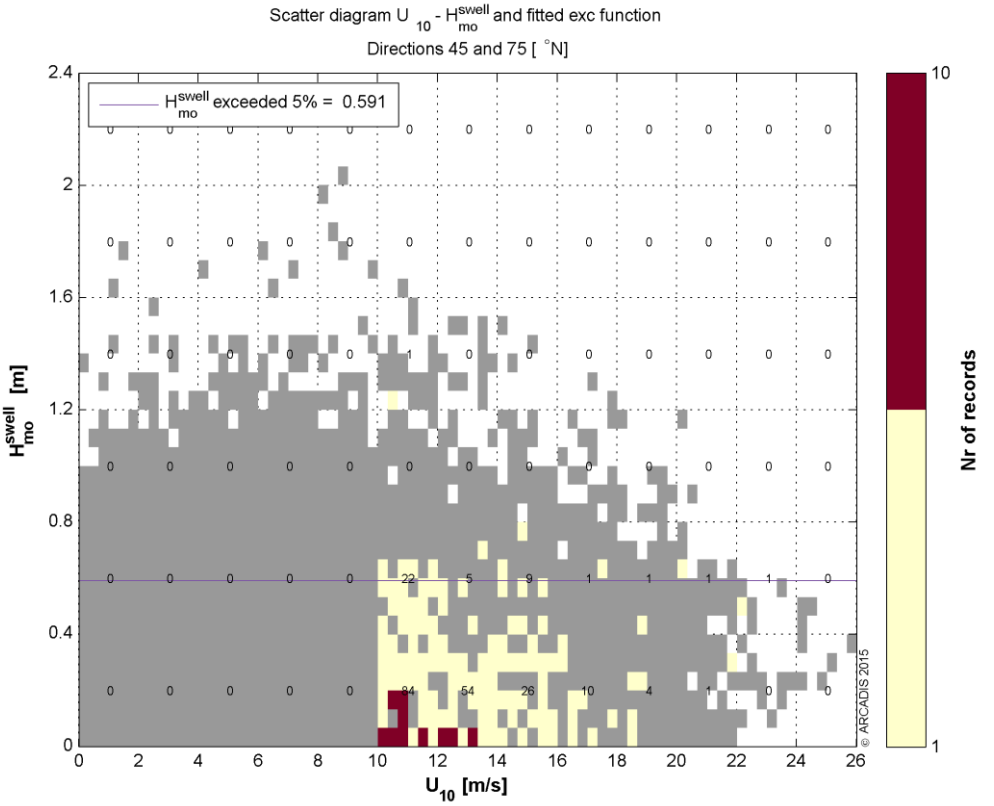
Scatter diagram U 10 - H mo swell and fitted exc function
Directions 45 and 75 [°N]
H mo swell exceeded 5% = 0.591
H mo swell [m]
U 10 [m/s]
Nr of records
© ARCADIS 2015

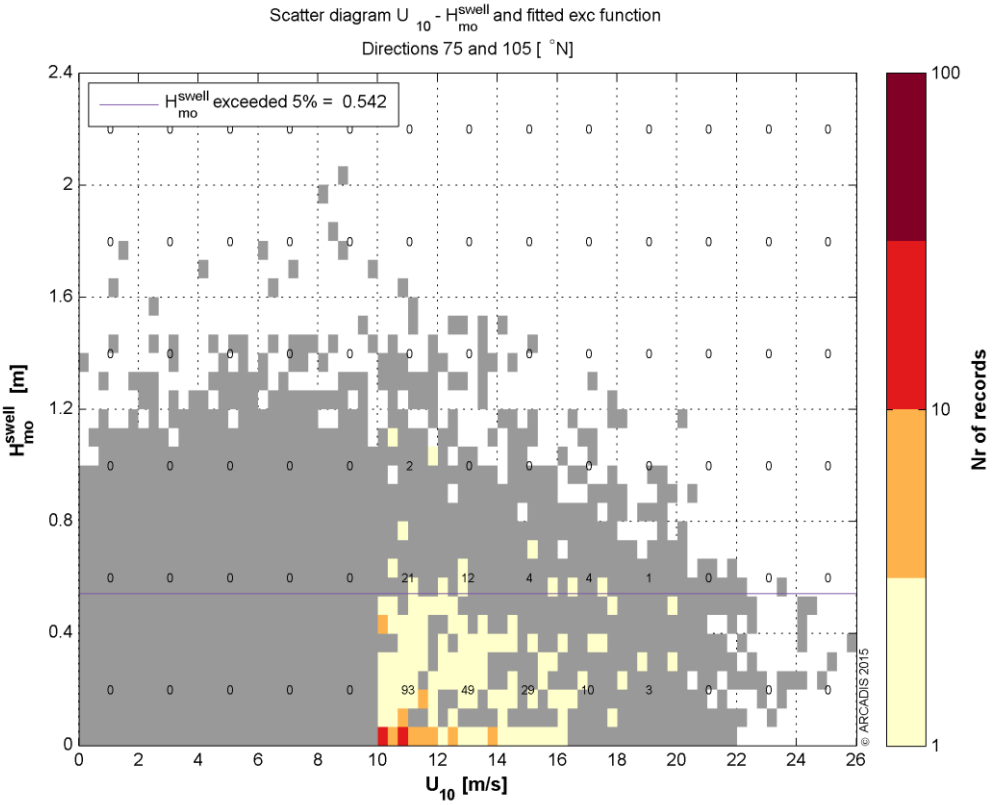
Scatter diagram U 10 - H mo swell and fitted exc function
Directions 75 and 105 [°N]
H mo swell exceeded 5% = 0.542
H mo swell [m]
U 10 [m/s]
Nr of records
© ARCADIS 2015

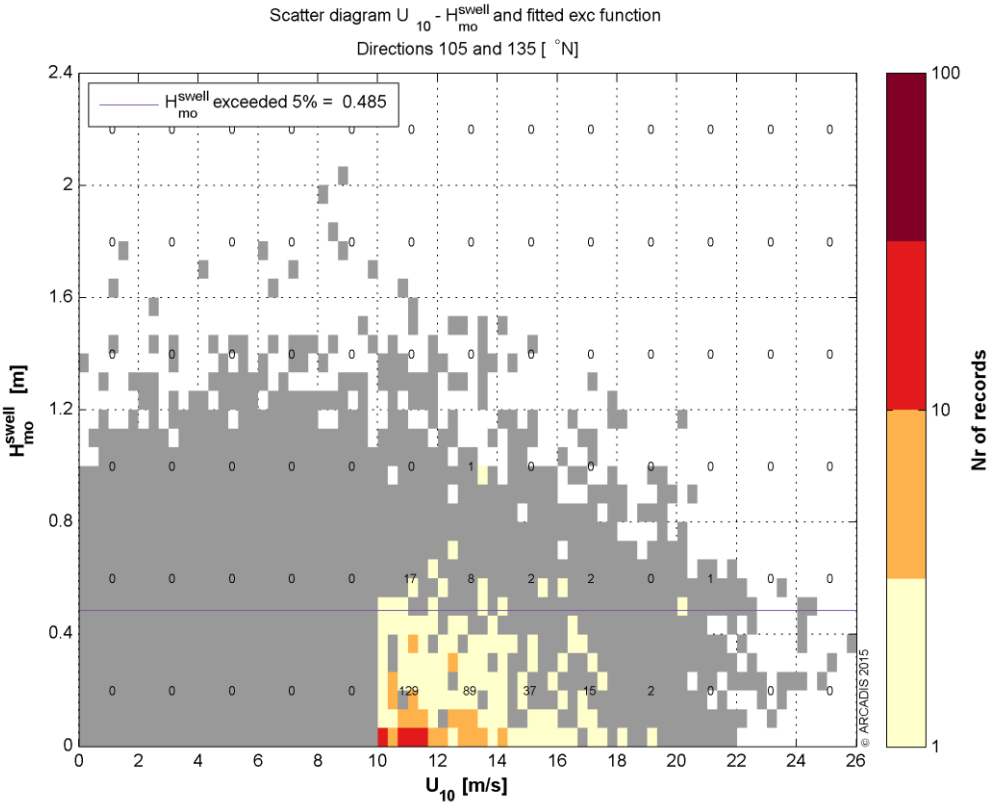
Scatter diagram U 10 - Hmo swell and fitted exc function
Directions 105 and 135 [°N]
Hmo swell exceeded 5% = 0.485
Hmo swell [m]
U10 [m/s]
Nr of records
© ARCADIS 2015

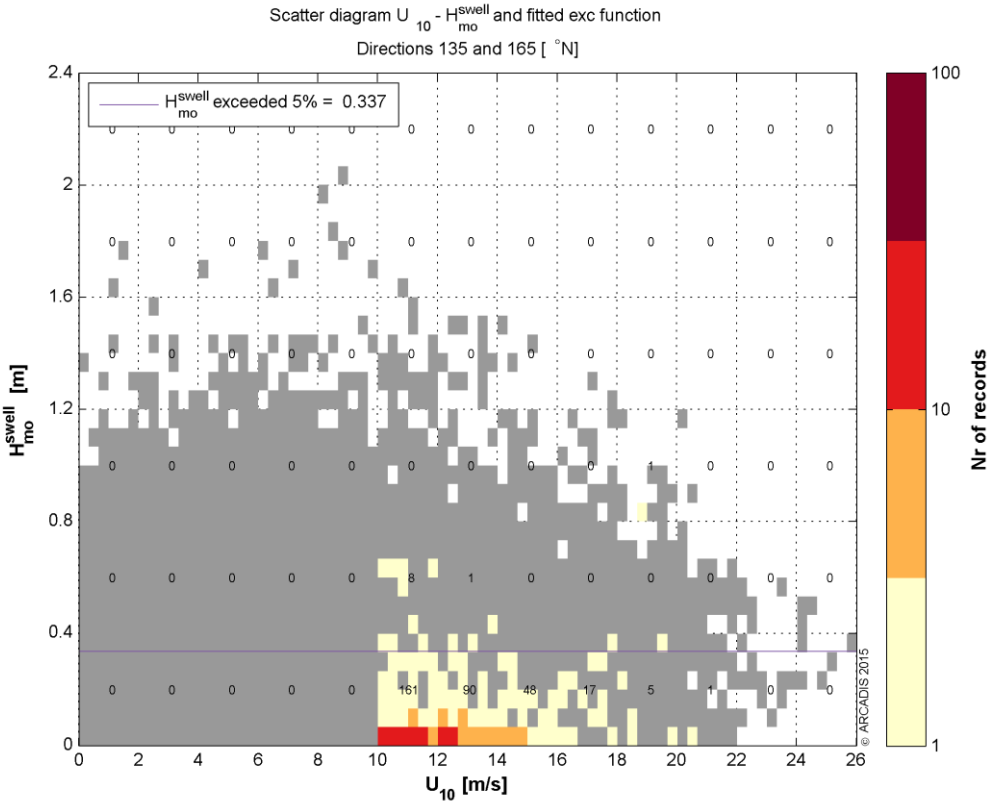
Scatter diagram U 10 - Hmo swell and fitted exc function
Directions 135 and 165 [°N]
Hmo swell exceeded 5% = 0.337
Hmo swell [m]
U10 [m/s]
Nr of records
© ARCADIS 2015

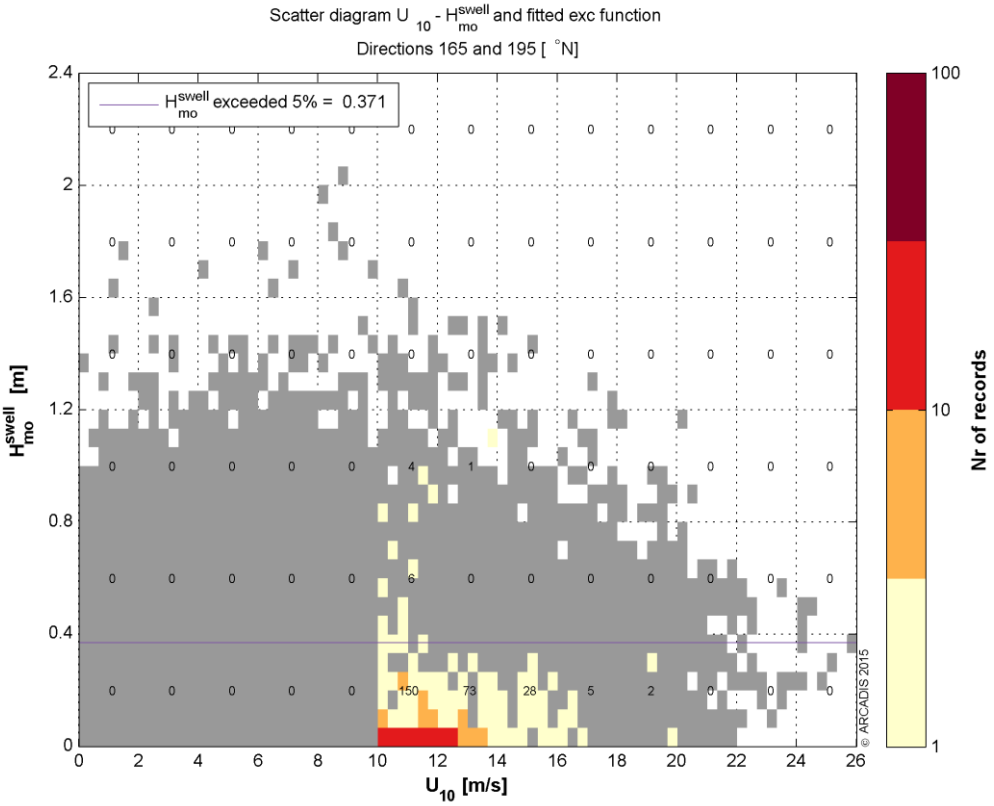
Scatter diagram U 10 - H mo swell and fitted exc function
Directions 165 and 195 [°N]
H mo swell exceeded 5% = 0.371
H mo swell [m]
U 10 [m/s]
Nr of records
© ARCADIS 2015

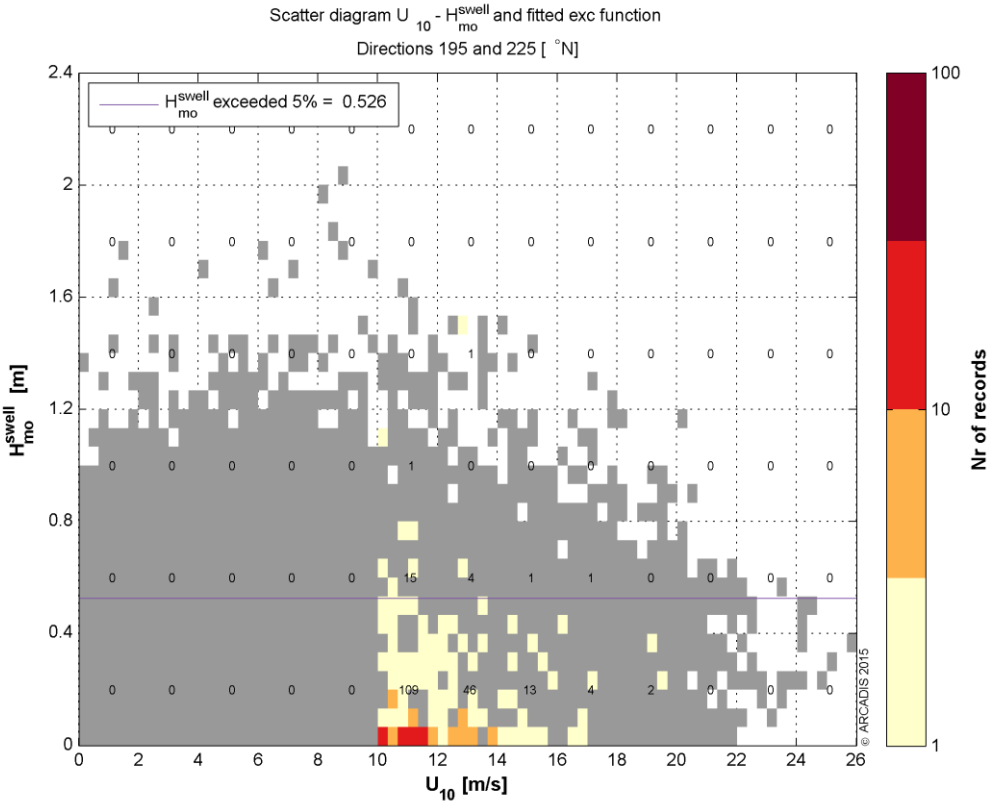
Scatter diagram U 10 - H mo swell and fitted exc function
Directions 195 and 225 [°N]
H mo swell exceeded 5% = 0.526
H mo swell [m]
U 10 [m/s]
Nr of records
© ARCADIS 2015

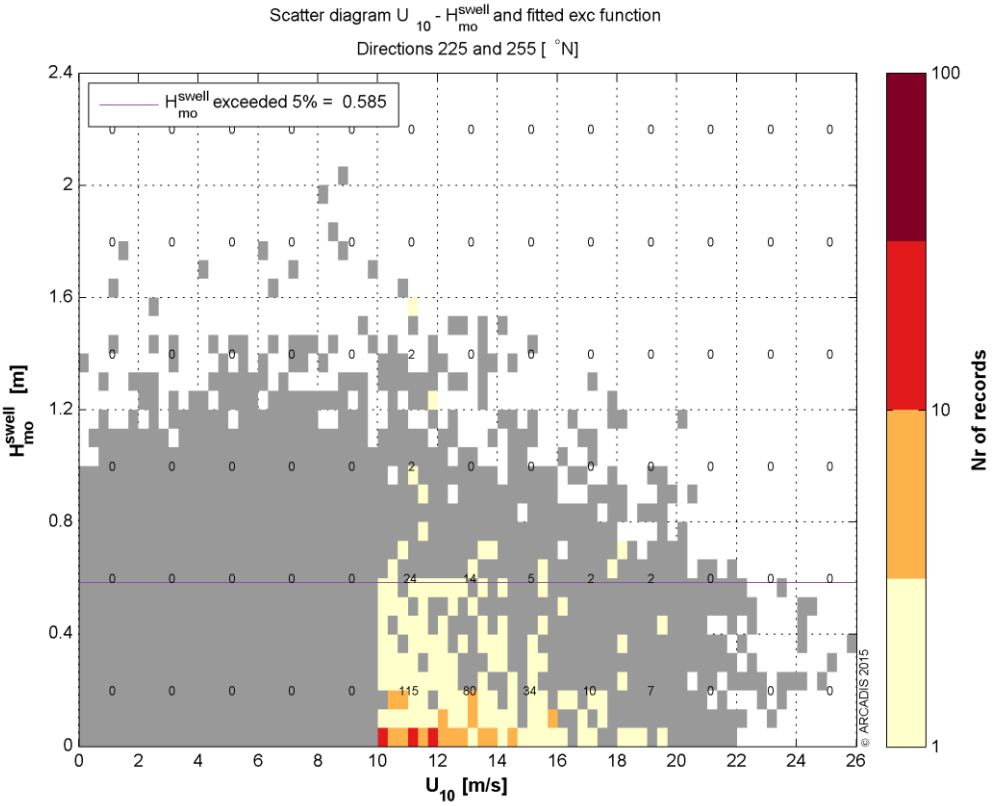
Scatter diagram U 10 - H mo swell and fitted exc function
Directions 225 and 255 [°N]
H mo swell exceeded 5% = 0.585
H mo swell [m]
U 10 [m/s]
Nr of records
© ARCADIS 2015

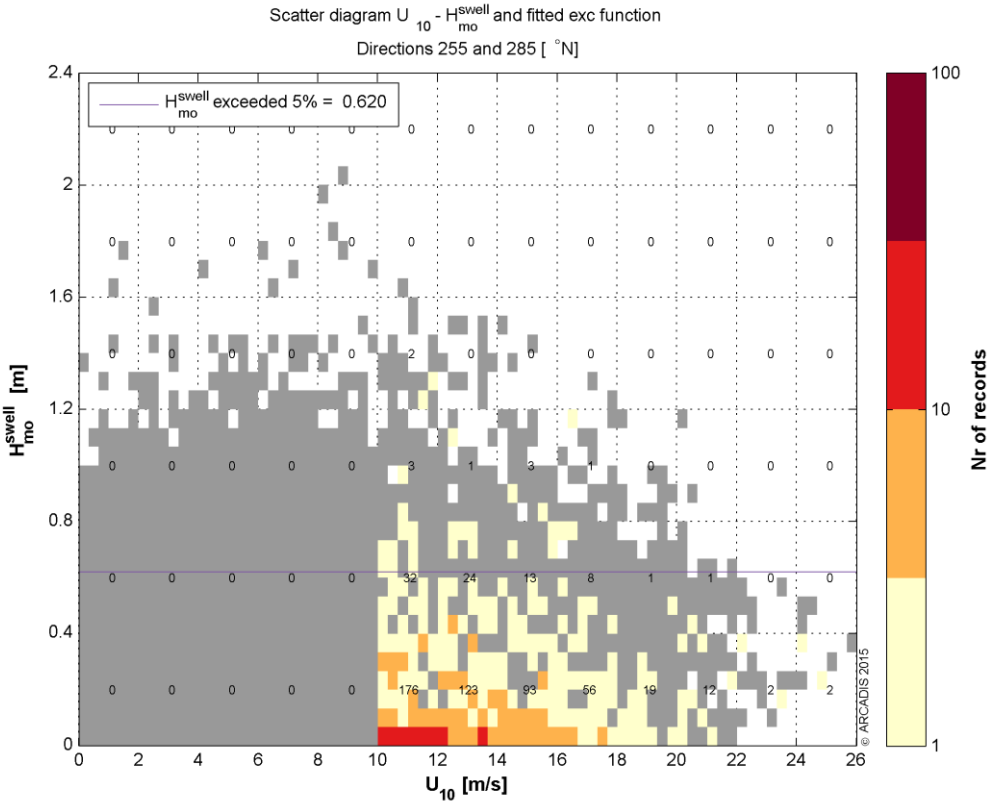
Scatter diagram U 10 - H mo swell and fitted exc function
Directions 255 and 285 [°N]
H mo swell exceeded 5% = 0.620
H mo swell [m]
U 10 [m/s]
Nr of records
© ARCADIS 2015

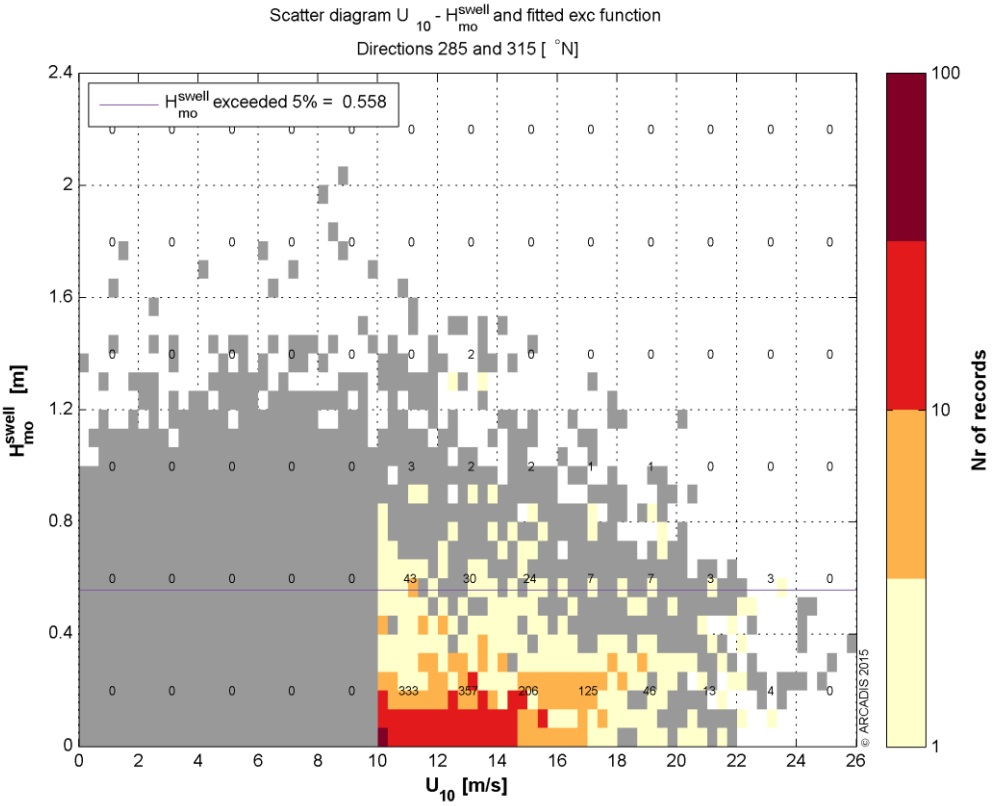
Scatter diagram U 10 - Hmo swell and fitted exc function
Directions 285 and 315 [°N]
Hmo swell exceeded 5% = 0.558
Hmo swell [m]
U10 [m/s]
Nr of records
© ARCADIS 2015

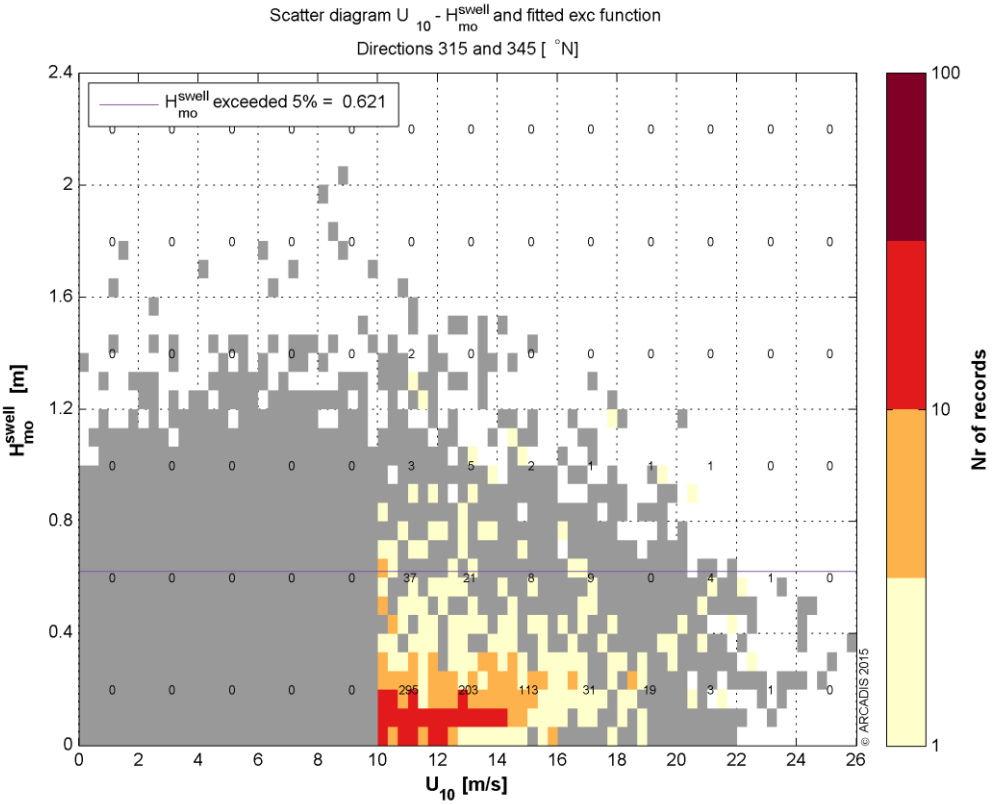
Scatter diagram U 10 - Hmo swell and fitted exc function
Directions 315 and 345 [°N]
Hmo swell exceeded 5% = 0.621
Hmo swell [m]
U10 [m/s]
Nr of records
© ARCADIS 2015

Appendix 4.4 U_{10} vs T_p swell

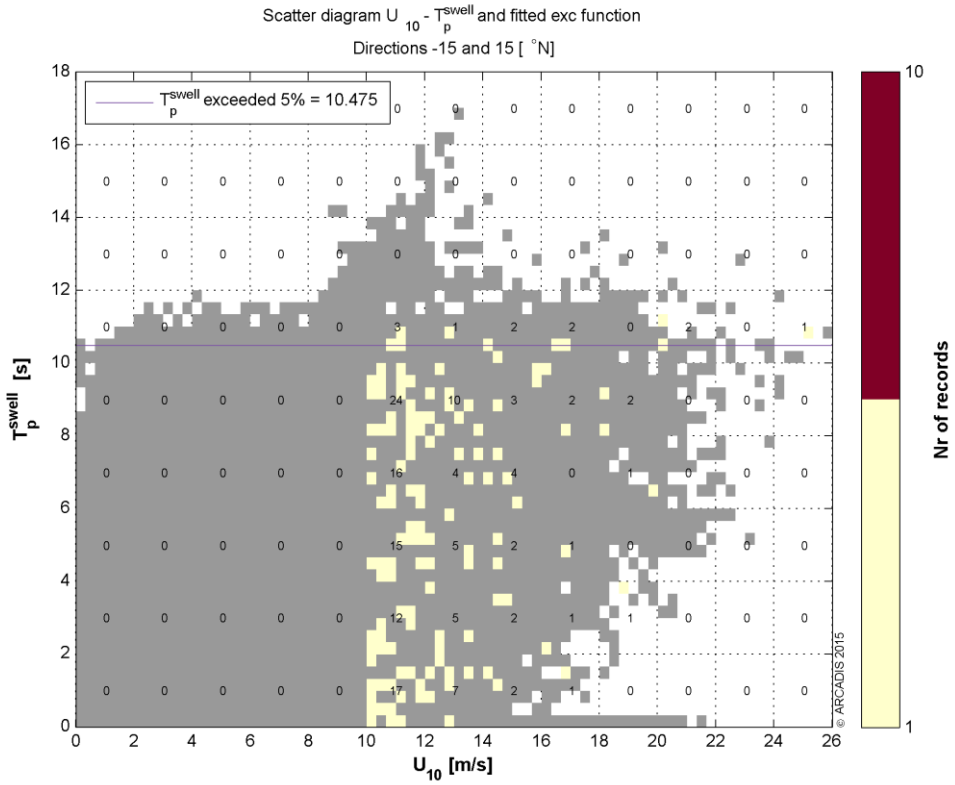

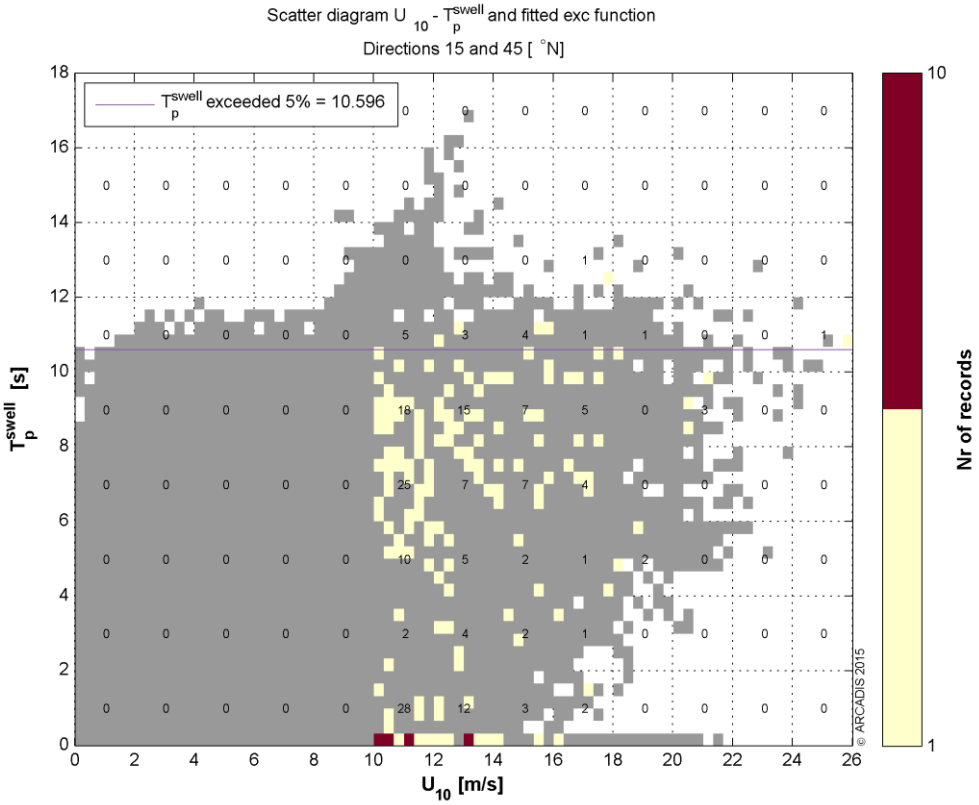

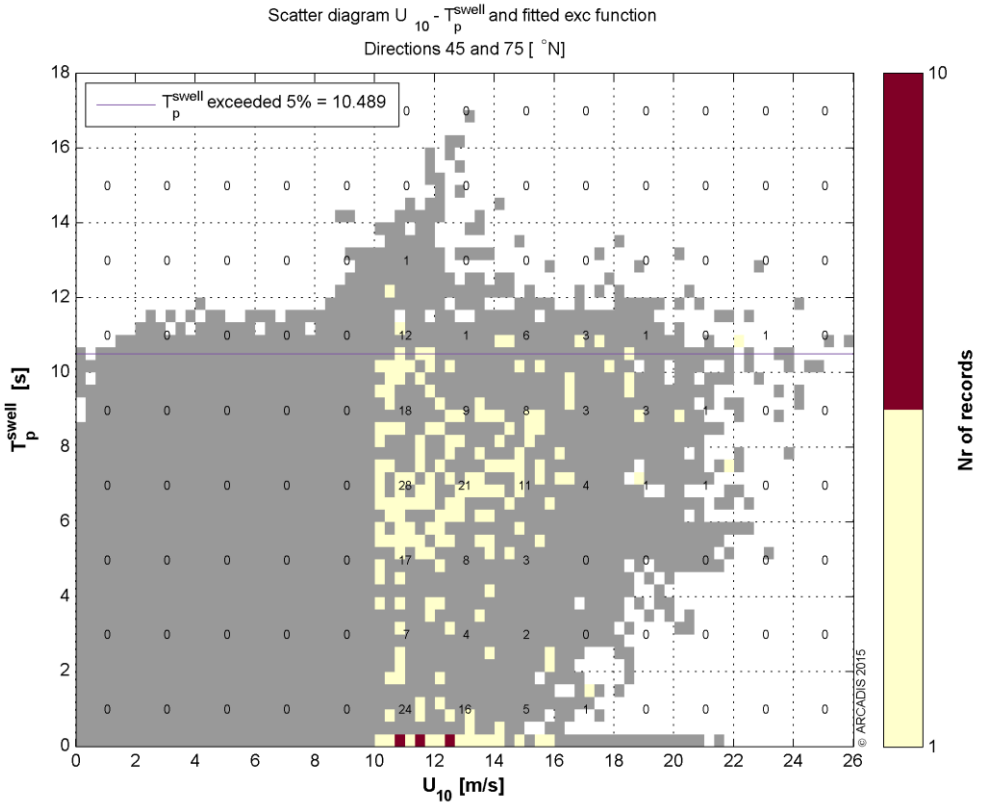
Scatter diagram U 10 - T p swell and fitted exc function
Directions 45 and 75 [°N]
T p swell exceeded 5% = 10.489
T p swell [s]
U 10 [m/s]
Nr of records
© ARCADIS 2015

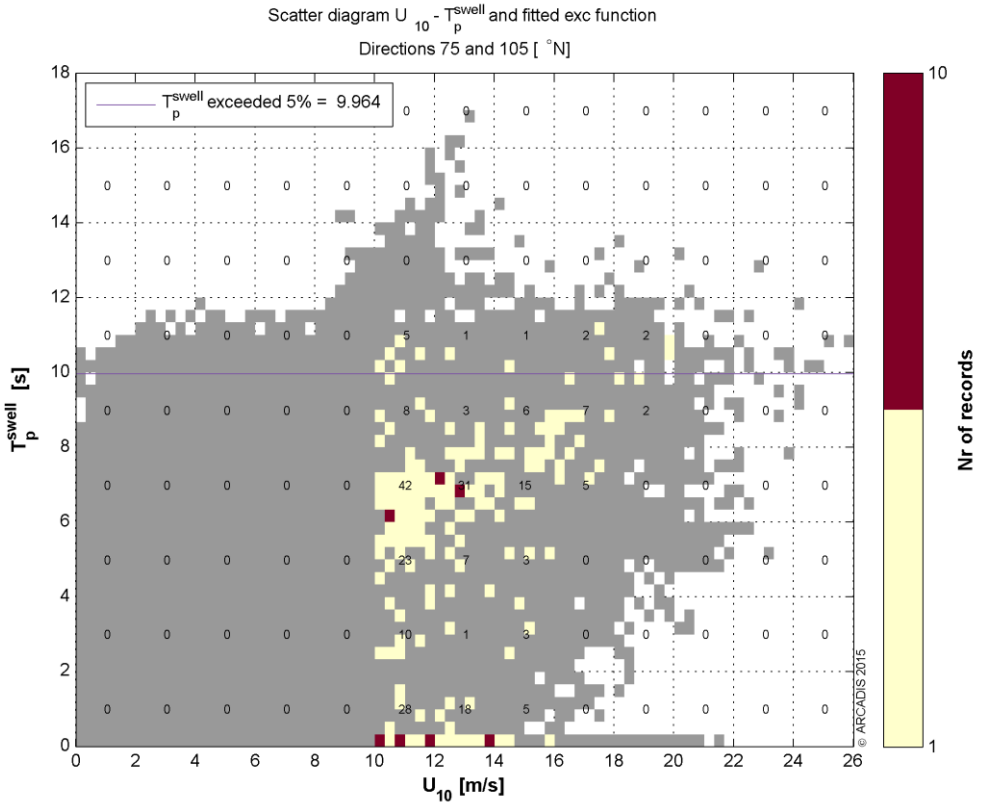
Scatter diagram U 10 - T p swell and fitted exc function
Directions 75 and 105 [°N]
T p swell exceeded 5% = 9.964
T p swell [s]
U 10 [m/s]
Nr of records
© ARCADIS 2015

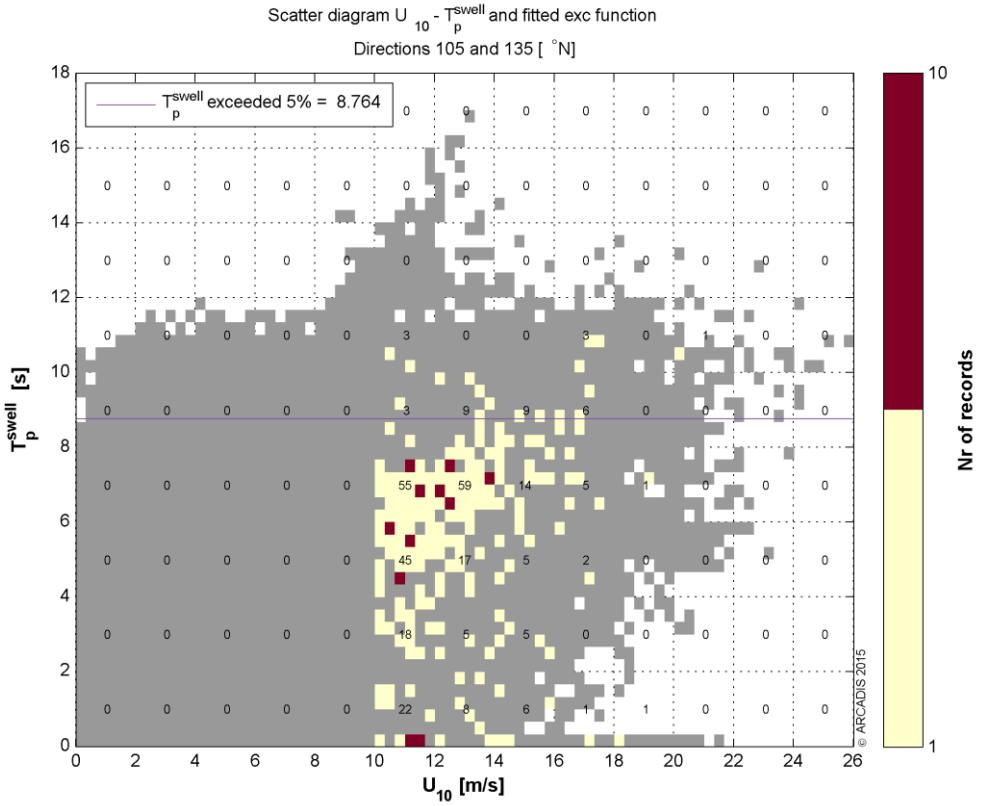
Scatter diagram U 10 - T p swell and fitted exc function
Directions 105 and 135 [°N]
T p swell exceeded 5% = 8.764
T p swell [s]
U 10 [m/s]
Nr of records
© ARCADIS 2015

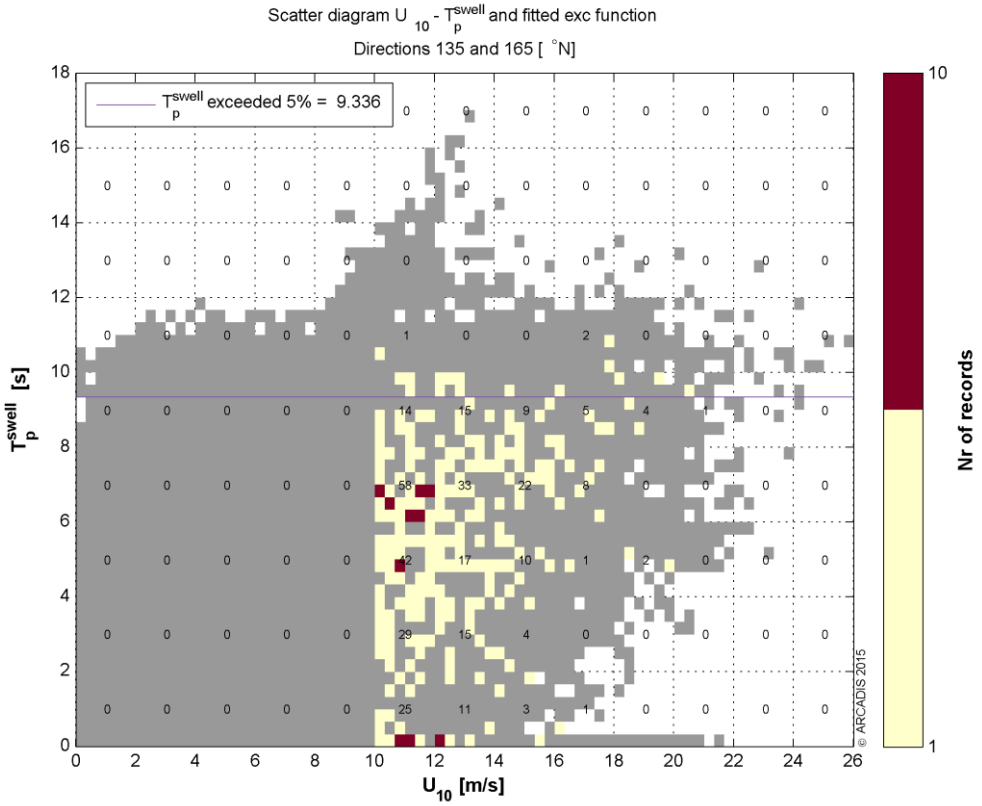
Scatter diagram U 10 - T p swell and fitted exc function
Directions 135 and 165 [°N]
T p swell exceeded 5% = 9.336
T p swell [s]
U 10 [m/s]
Nr of records
© ARCADIS 2015

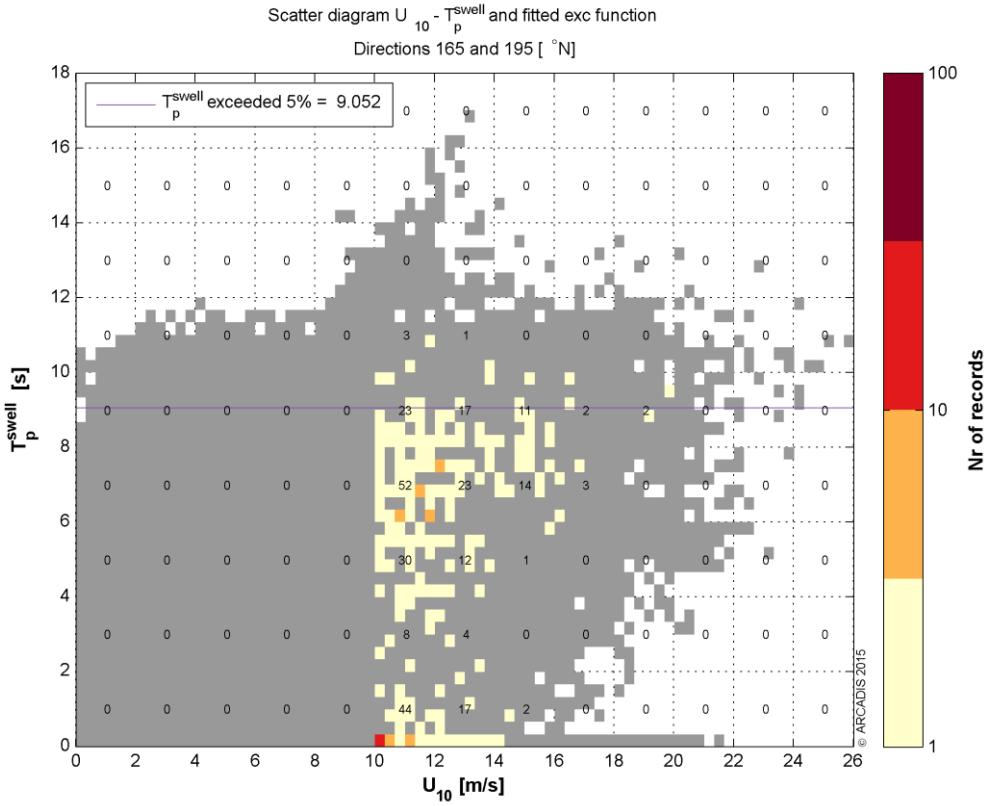
Scatter diagram U 10 - T p swell and fitted exc function
Directions 165 and 195 [°N]
T p swell exceeded 5% = 9.052
T p swell [s]
U 10 [m/s]
Nr of records
© ARCADIS 2015

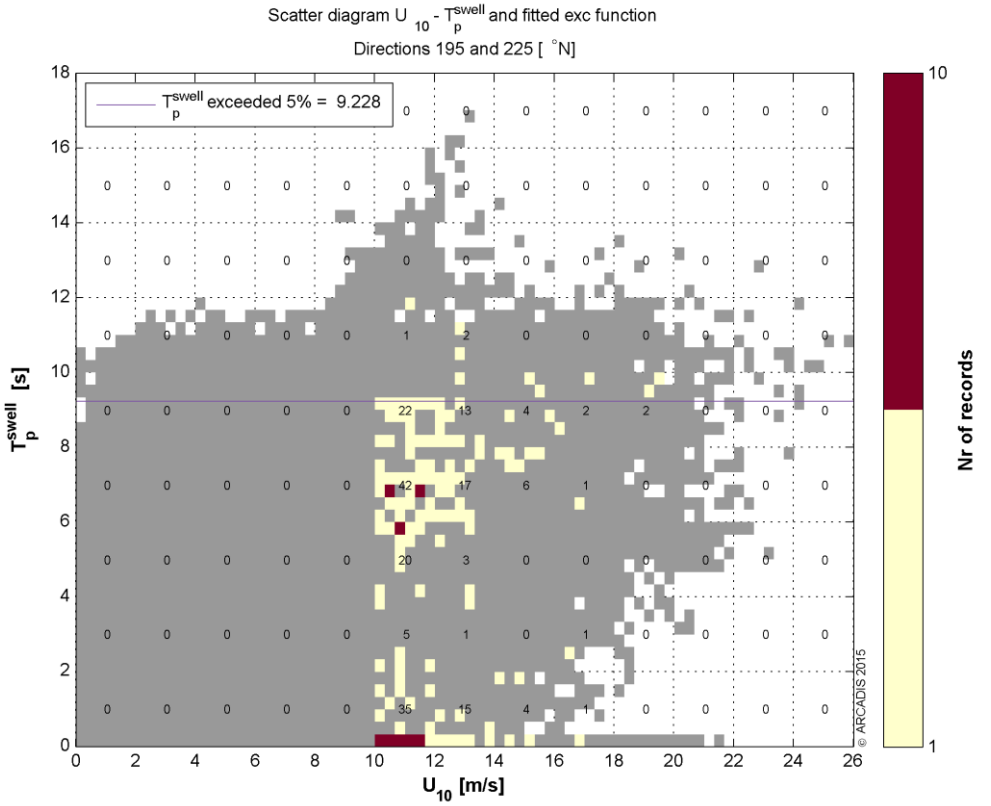
Scatter diagram U 10 - T p swell and fitted exc function
Directions 195 and 225 [°N]
T p swell exceeded 5% = 9.228
T p swell [s]
U 10 [m/s]
Nr of records
© ARCADIS 2015

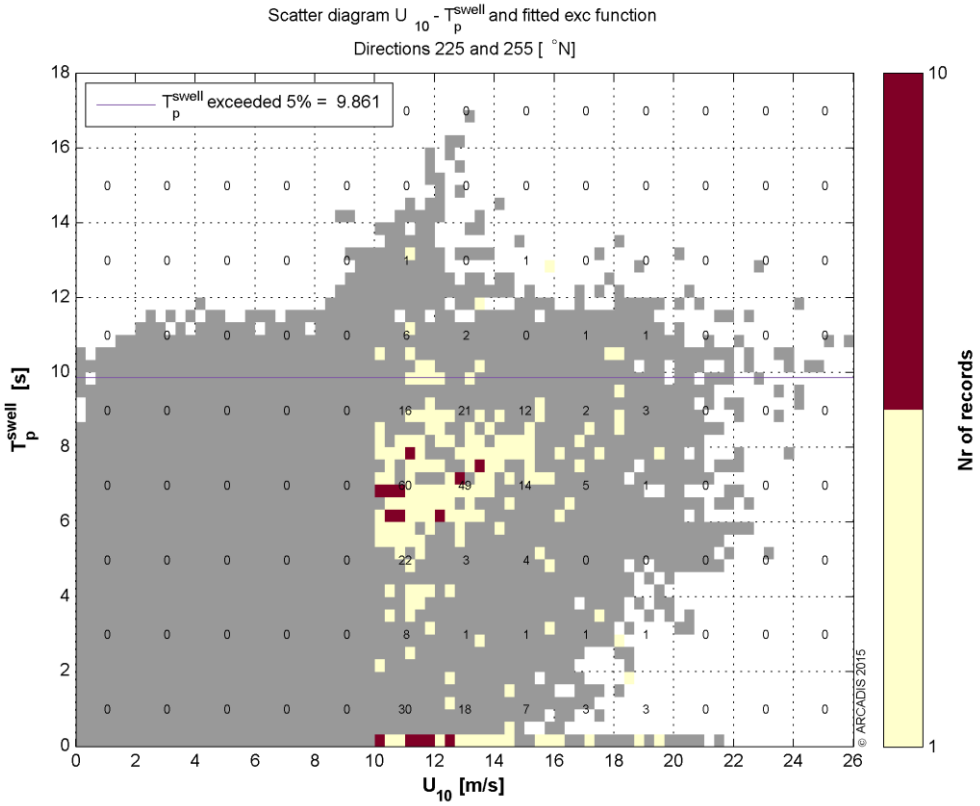
Scatter diagram U 10 - T p swell and fitted exc function
Directions 225 and 255 [°N]
T p swell exceeded 5% = 9.861
T p swell [s]
U 10 [m/s]
Nr of records
© ARCADIS 2015

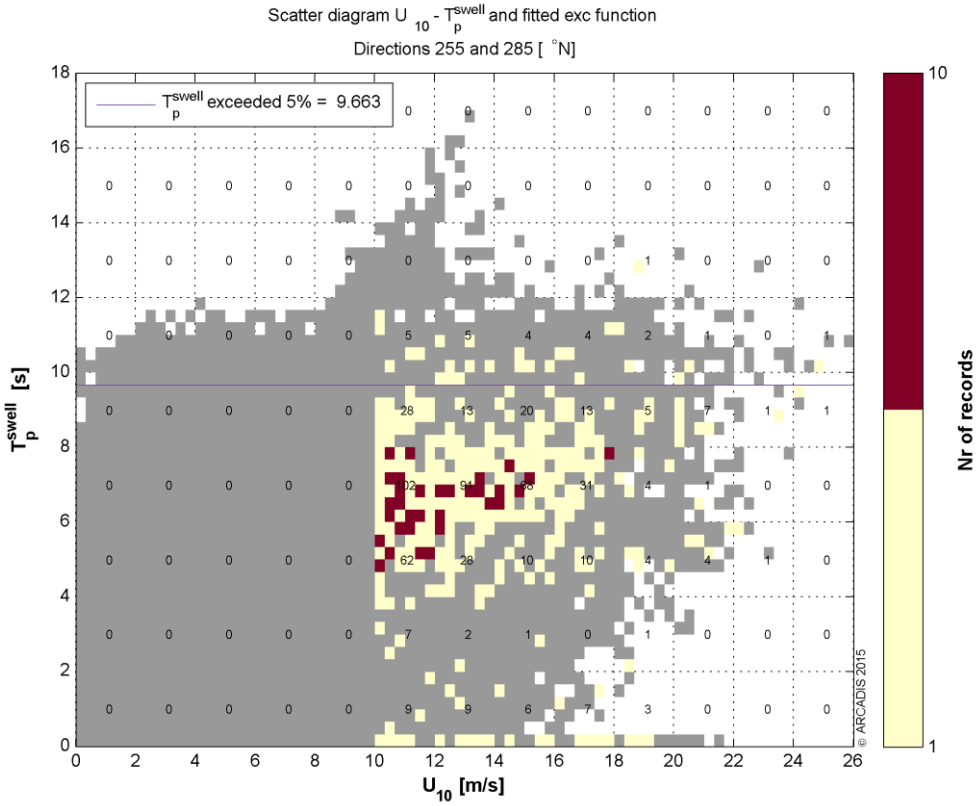
Scatter diagram U 10 - T p swell and fitted exc function
Directions 255 and 285 [°N]
T p swell exceeded 5% = 9.663
T p swell [s]
U 10 [m/s]
Nr of records
© ARCADIS 2015

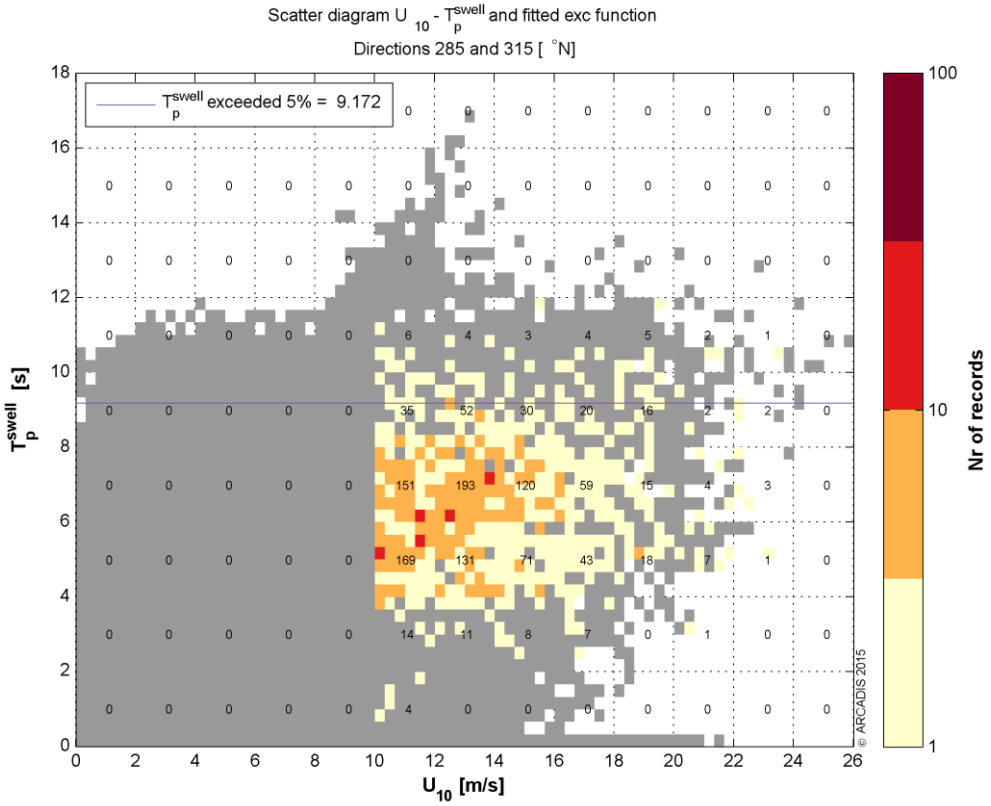
Scatter diagram U 10 - T p swell and fitted exc function
Directions 285 and 315 [°N]
T p swell exceeded 5% = 9.172
T p swell [s]
U 10 [m/s]
Nr of records
© ARCADIS 2015

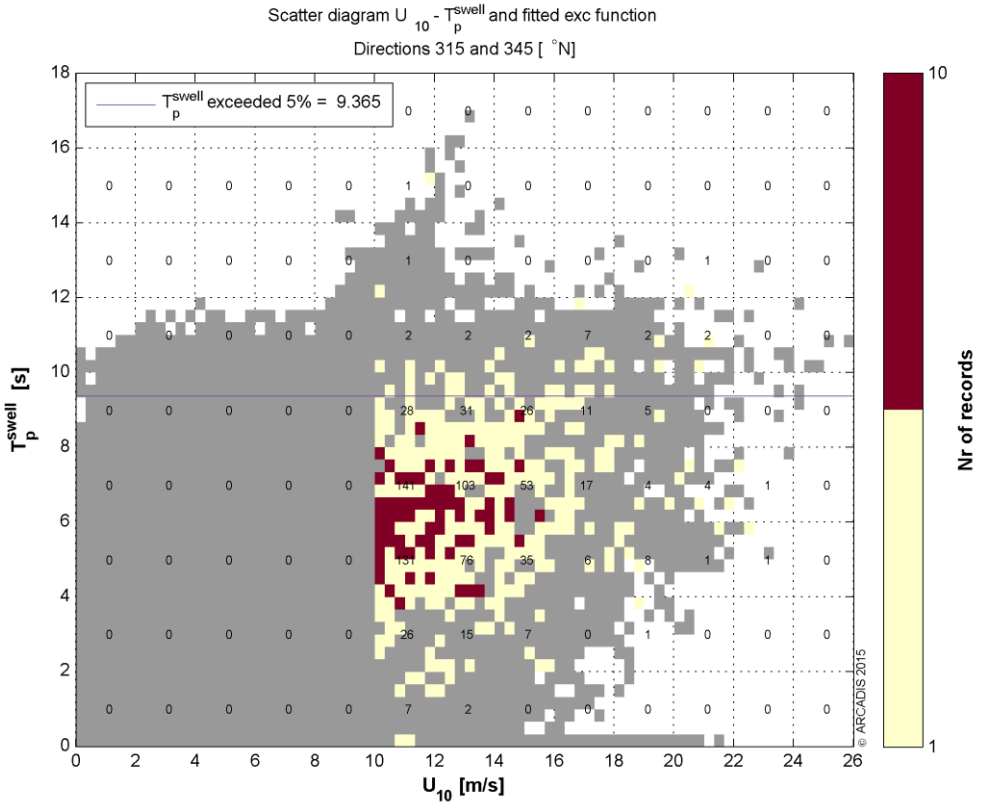
Scatter diagram U 10 - T p swell and fitted exc function
Directions 315 and 345 [°N]
T p swell exceeded 5% = 9.365
T p swell [s]
U 10 [m/s]
Nr of records
© ARCADIS 2015

Appendix 5 Figures of conditions associated to H_{m0} sea extremes

Appendix 5.1 H_{m0} sea vs U_{10}

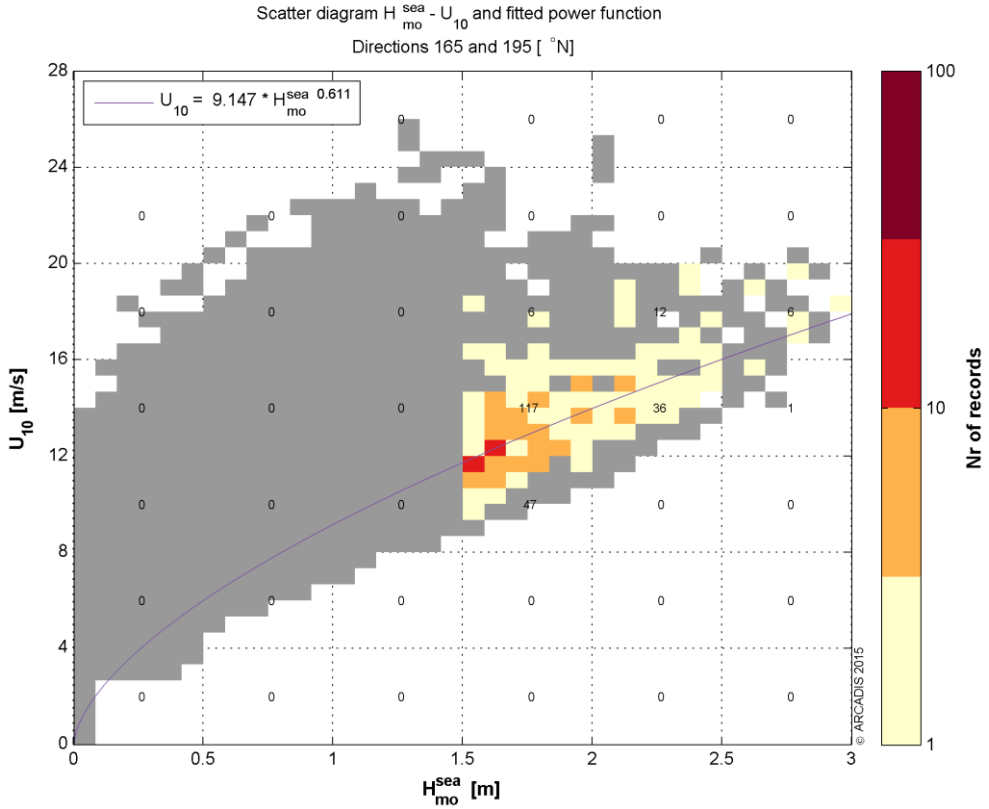

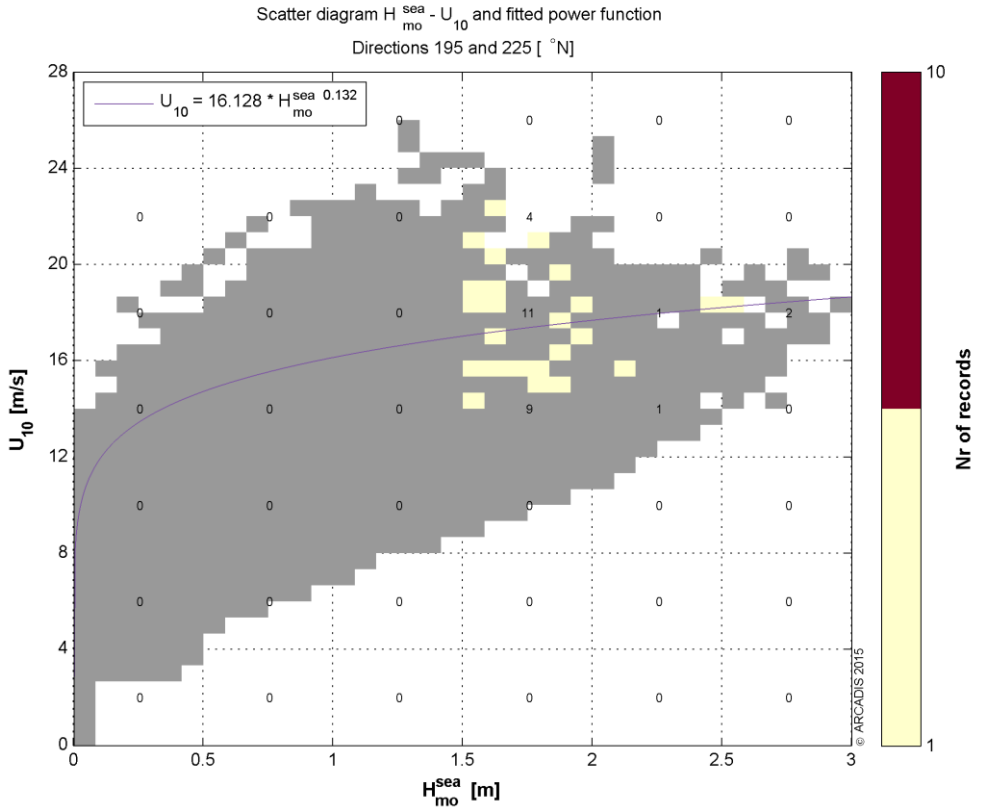

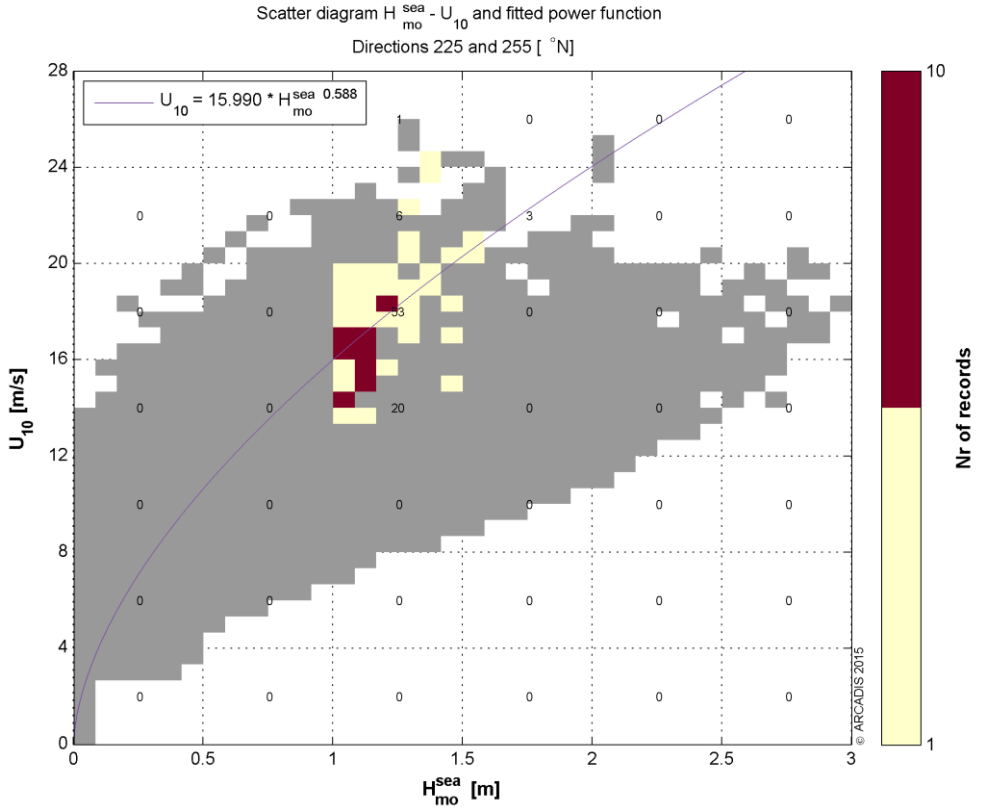
Scatter diagram H sea mo - U10 and fitted power function
Directions 225 and 255 [°N]
U10 = 15.990 * H sea mo 0.588
U10 [m/s]
Hsea mo [m]
Nr of records
© ARCADIS 2015

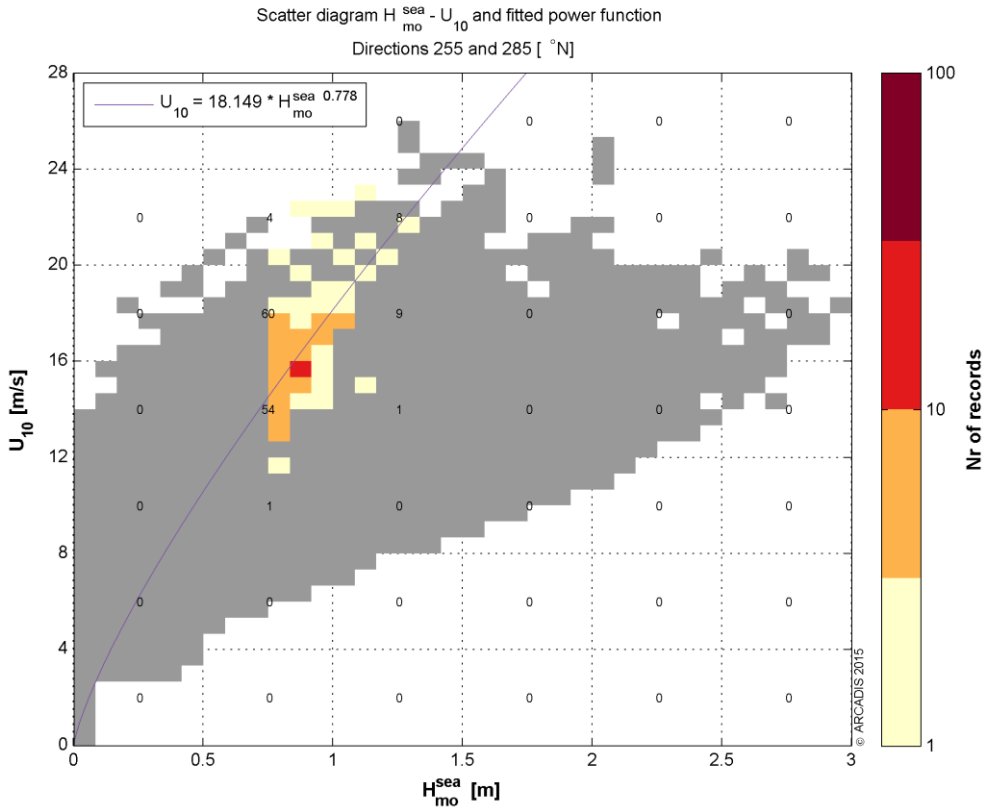
Scatter diagram H sea mo - U10 and fitted power function
Directions 255 and 285 [°N]
U10 = 18.149 * H sea mo 0.778
U10 [m/s]
Hsea mo [m]
Nr of records
© ARCADIS 2015

Appendix 5.2 H_{m0} sea vs T_p wind sea

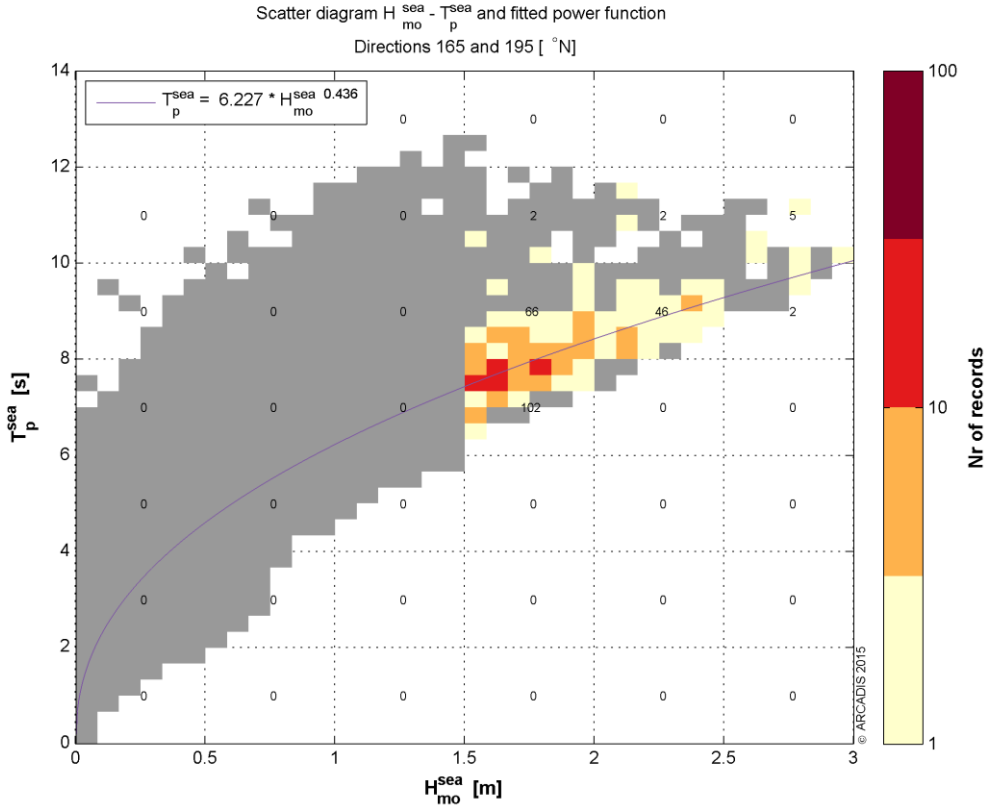

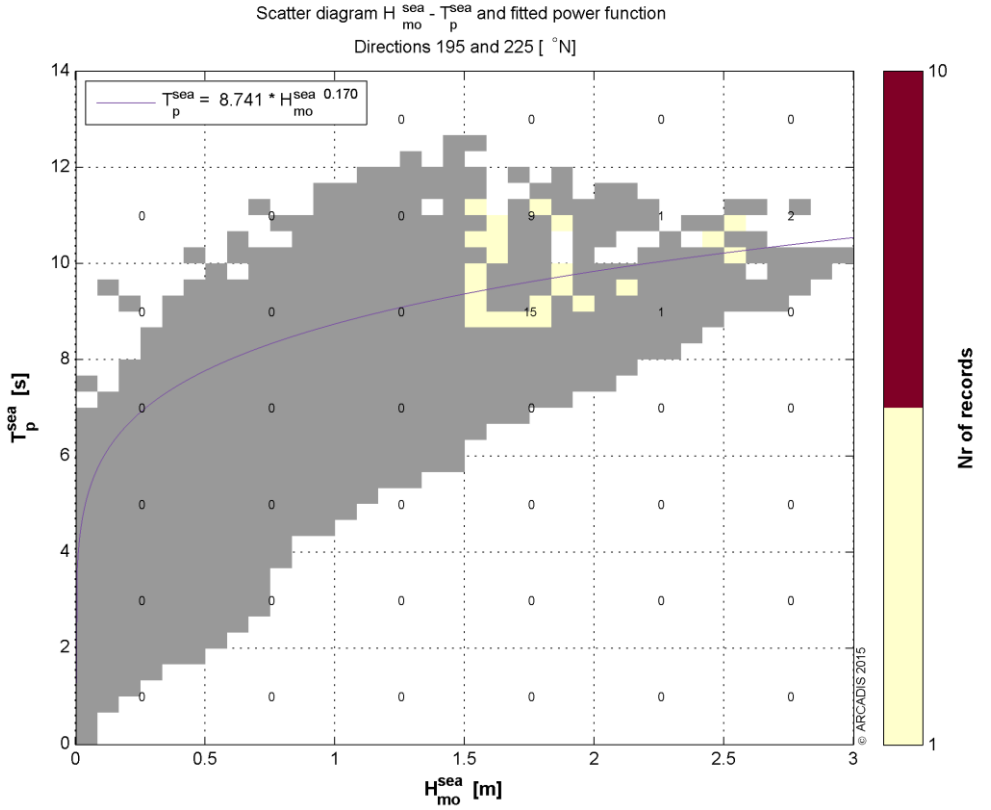

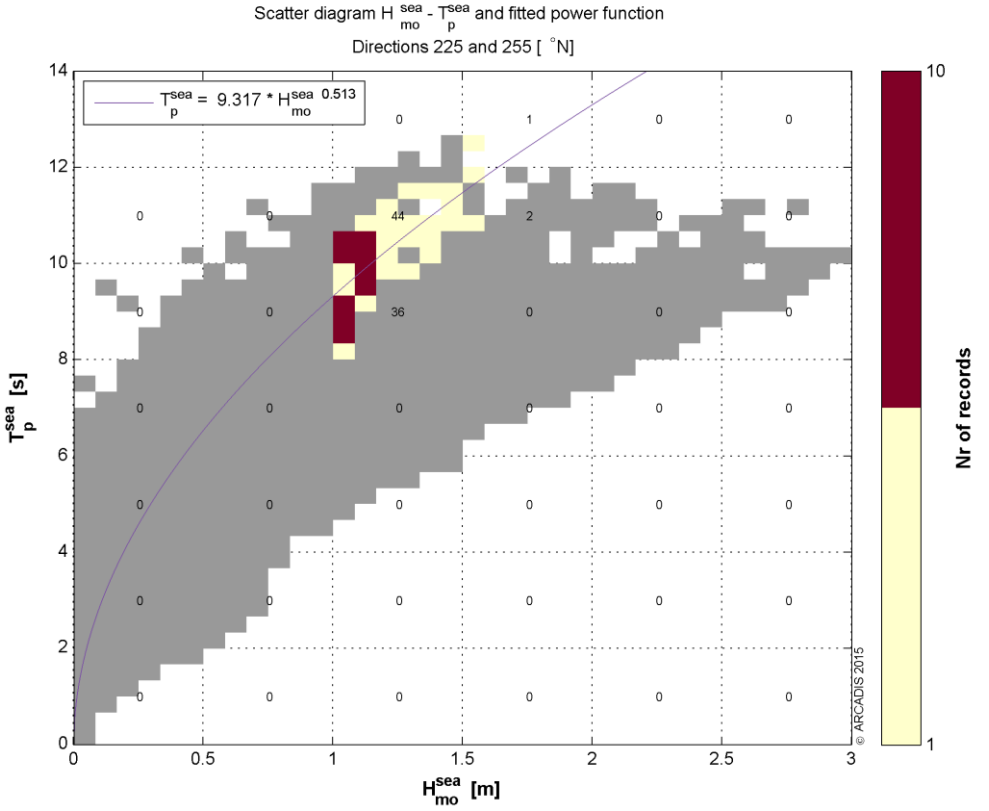
Scatter diagram H sea mo - T sea p and fitted power function
Directions 225 and 255 [°N]
T sea p = 9.317 * H sea mo 0.513
T sea p [s]
H sea mo [m]
Nr of records
© ARCADIS 2015

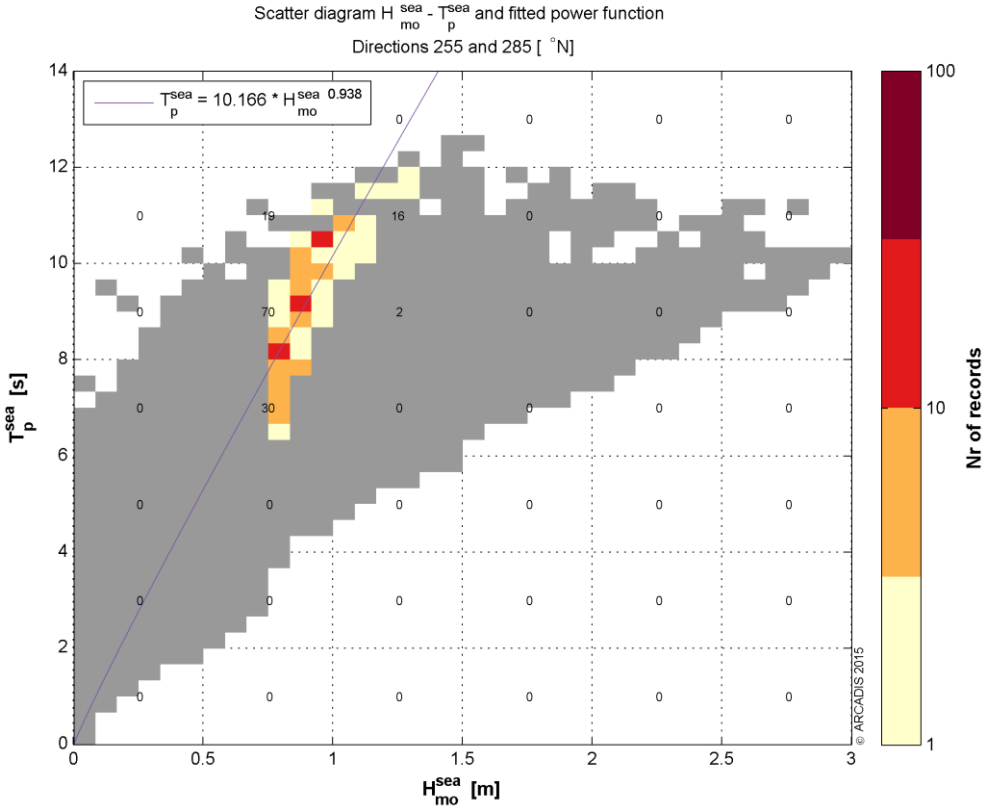
Scatter diagram H sea mo - T sea p and fitted power function
Directions 255 and 285 [°N]
T sea p = 10.166 * H sea mo 0.938
T sea p [s]
H sea mo [m]
Nr of records
© ARCADIS 2015

Appendix 5.3 H_{m0} sea vs H_{m0} swell

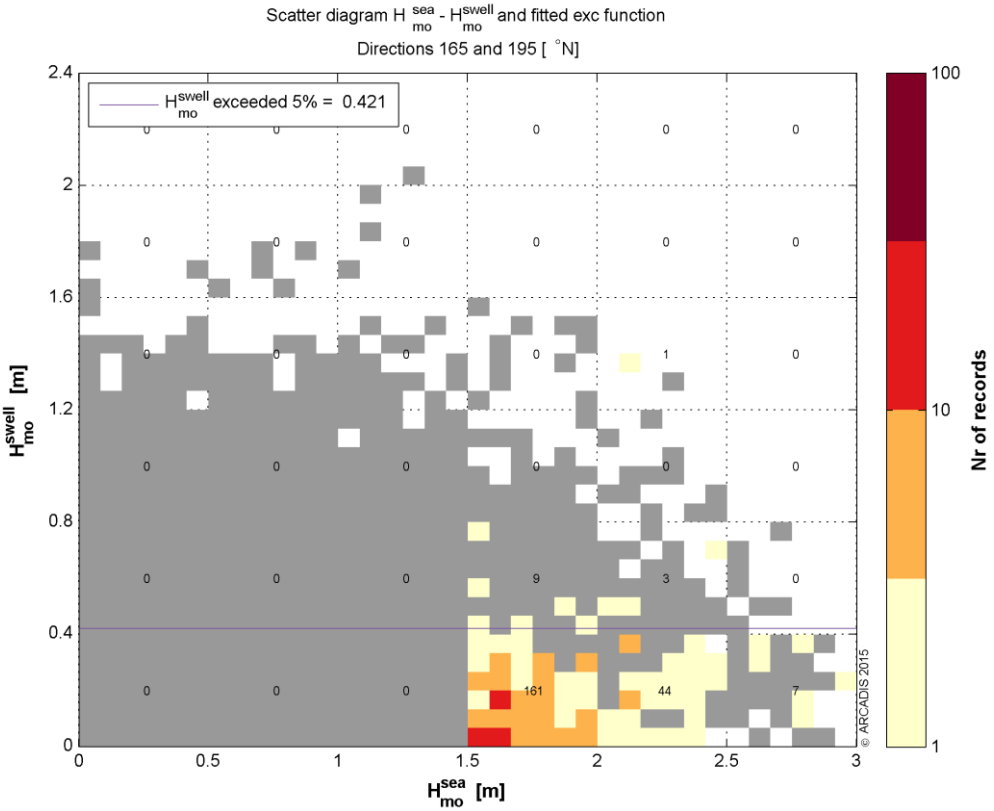

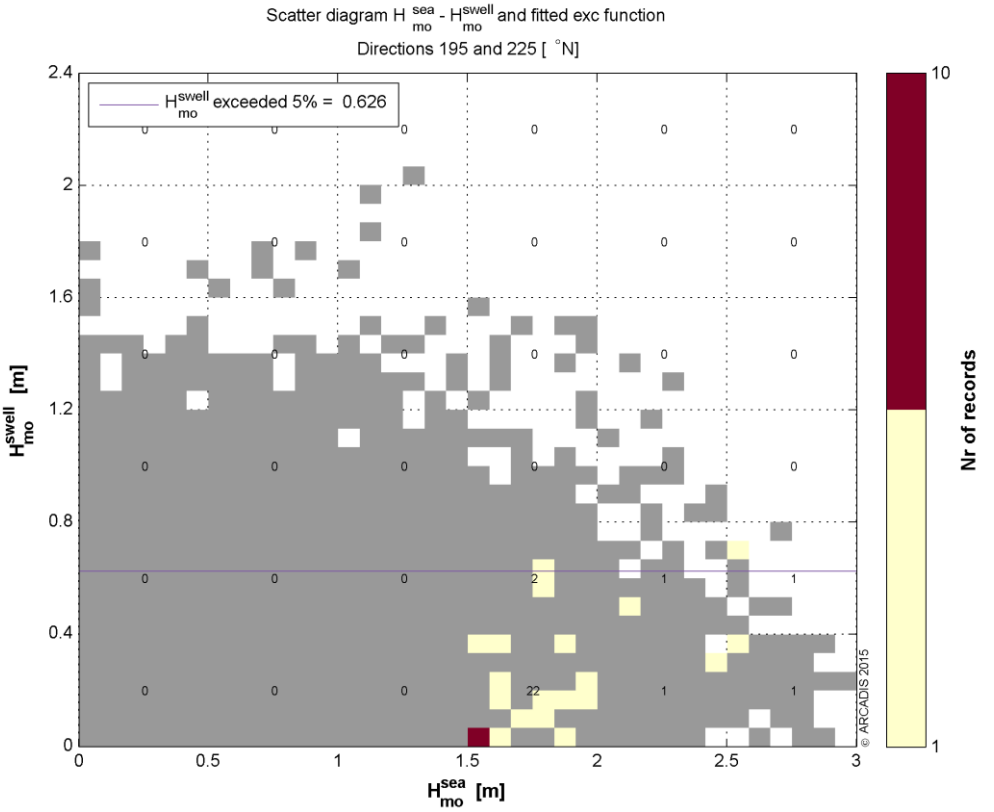

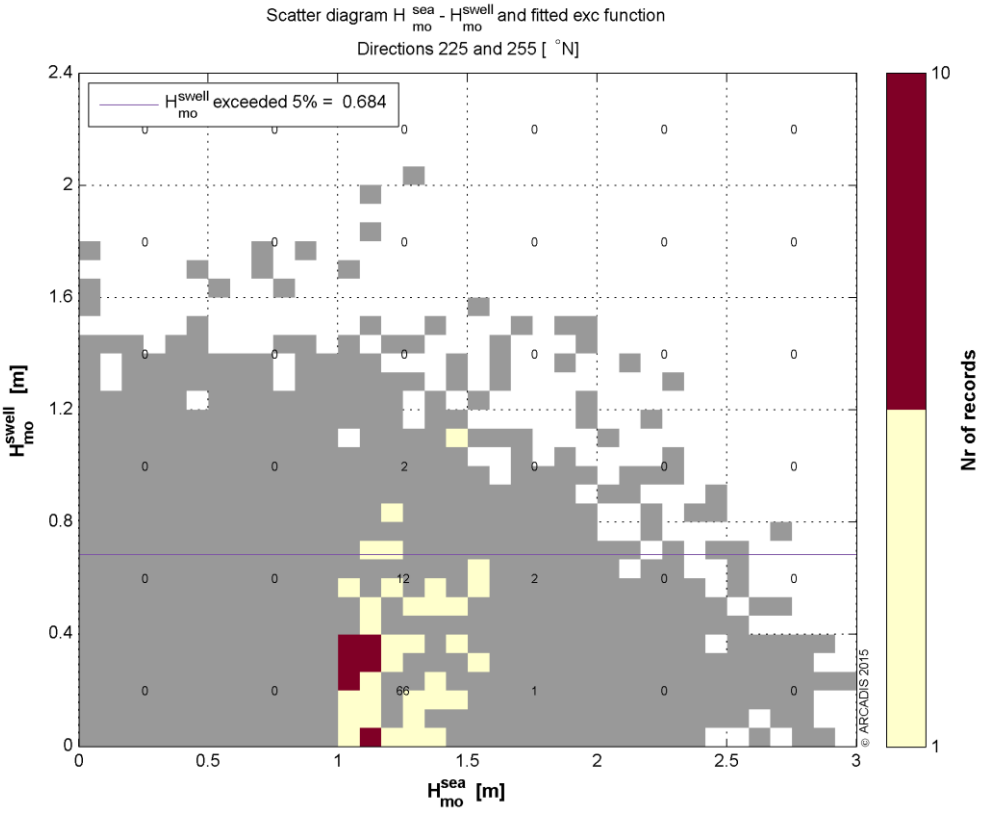
Scatter diagram H sea mo - H swell mo and fitted exc function
Directions 225 and 255 [°N]
H swell mo exceeded 5% = 0.684
H swell mo [m]
H sea mo [m]
Nr of records
© ARCADIS 2015

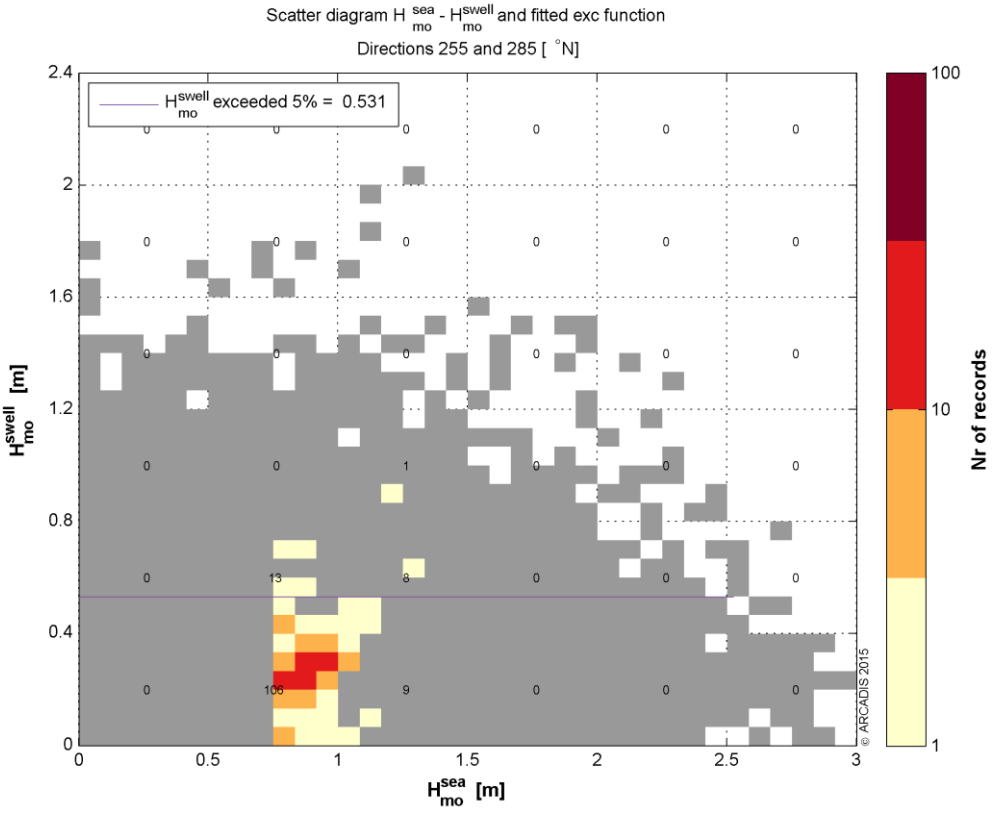
Scatter diagram H sea mo - H swell mo and fitted exc function
Directions 255 and 285 [°N]
H swell mo exceeded 5% = 0.531
H swell mo [m]
H sea mo [m]
Nr of records
© ARCADIS 2015

Appendix 5.4 H_{m0} sea vs T_p swell

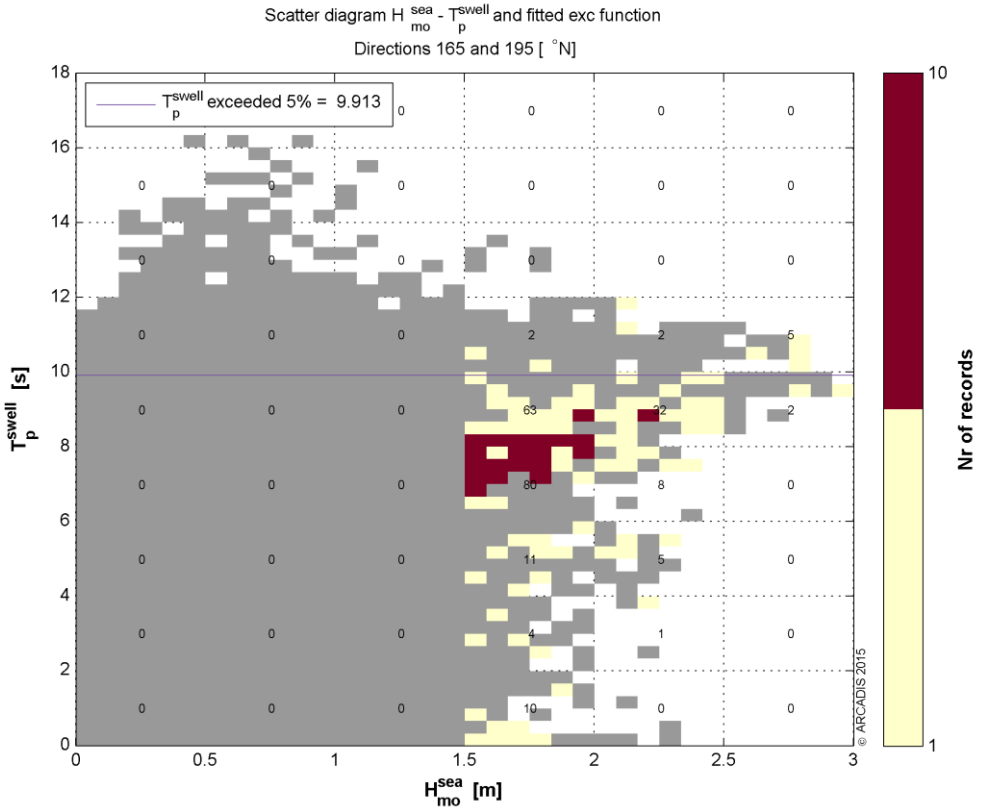

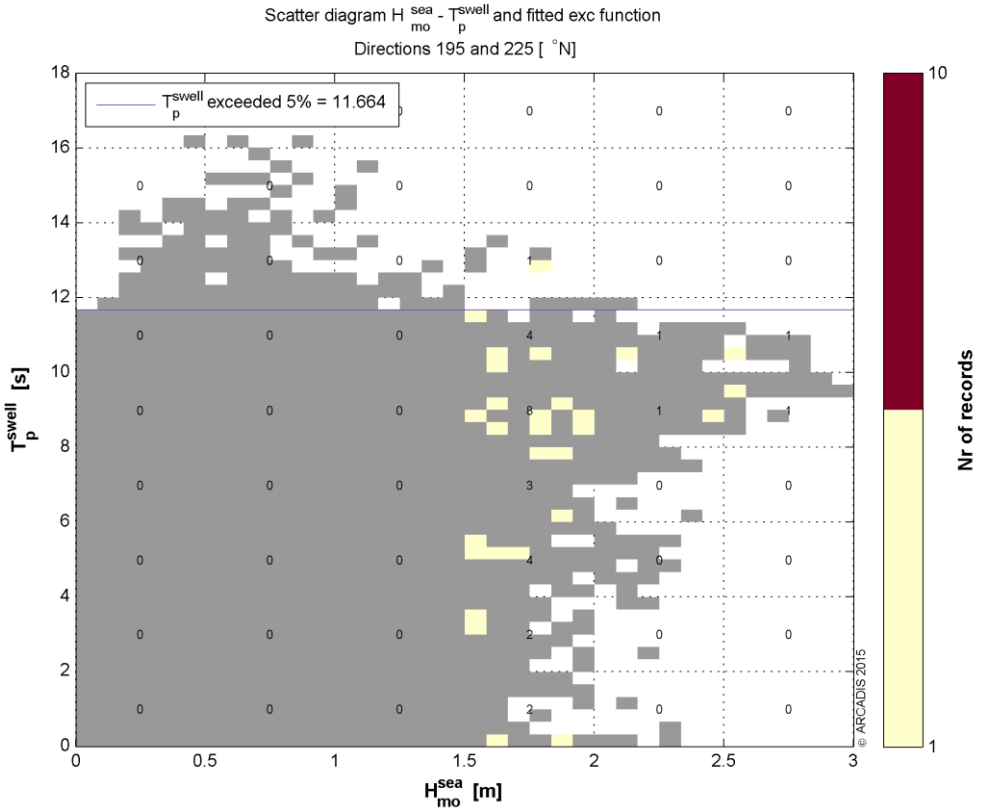

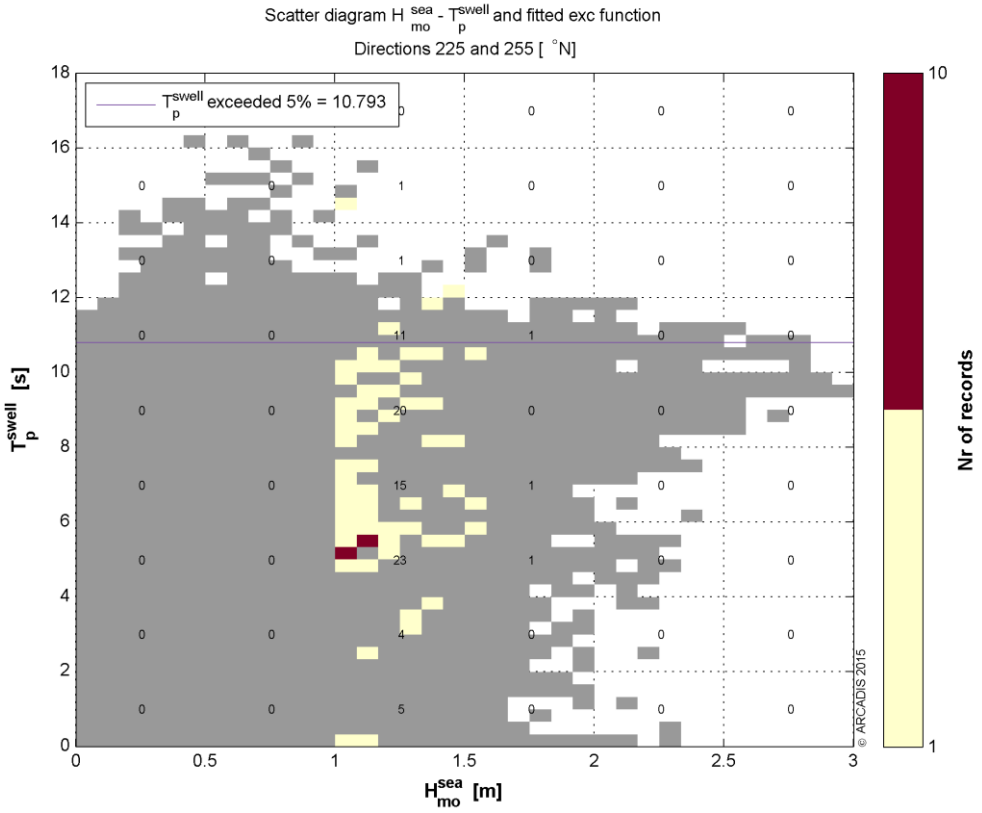
Scatter diagram H sea mo - T swell p and fitted exc function
Directions 225 and 255 [°N]
T swell p exceeded 5% = 10.793
T swell p [s]
H sea mo [m]
Nr of records
© ARCADIS 2015

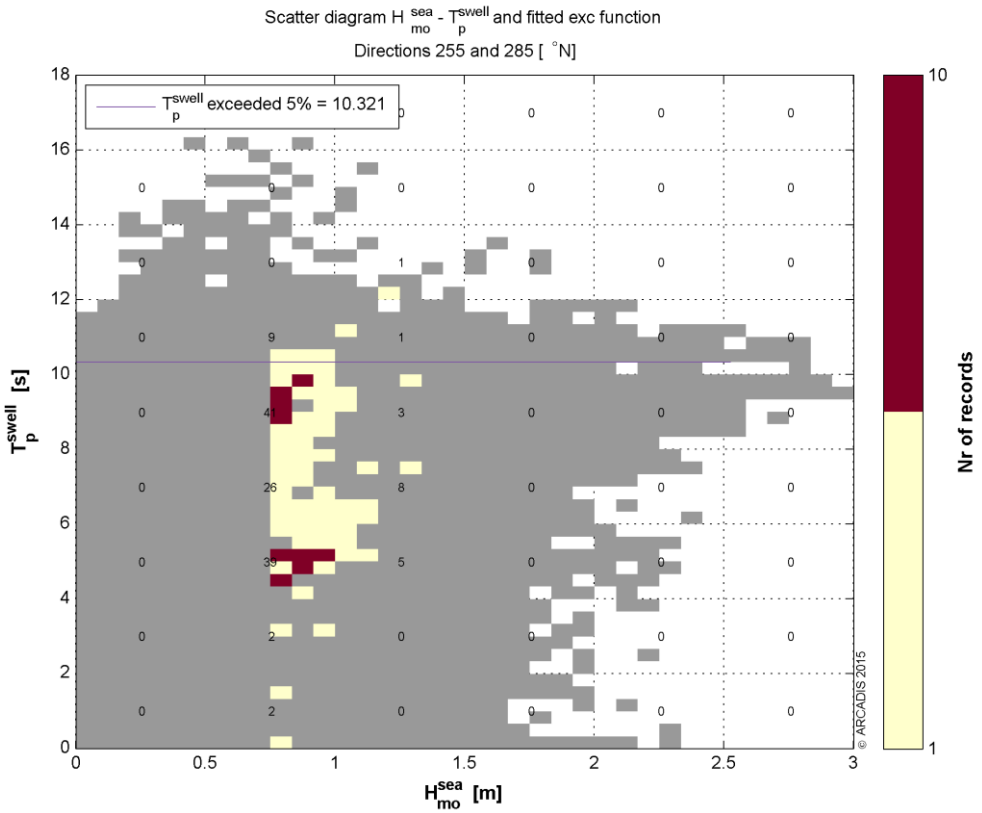
Scatter diagram H sea mo - T swell p and fitted exc function
Directions 255 and 285 [°N]
T swell p exceeded 5% = 10.321
T swell p [s]
H sea mo [m]
Nr of records
© ARCADIS 2015

Appendix 6 Figures of conditions associated to H_{m0} swell extremes

Appendix 6.1 H_{m0} swell vs U_{10}

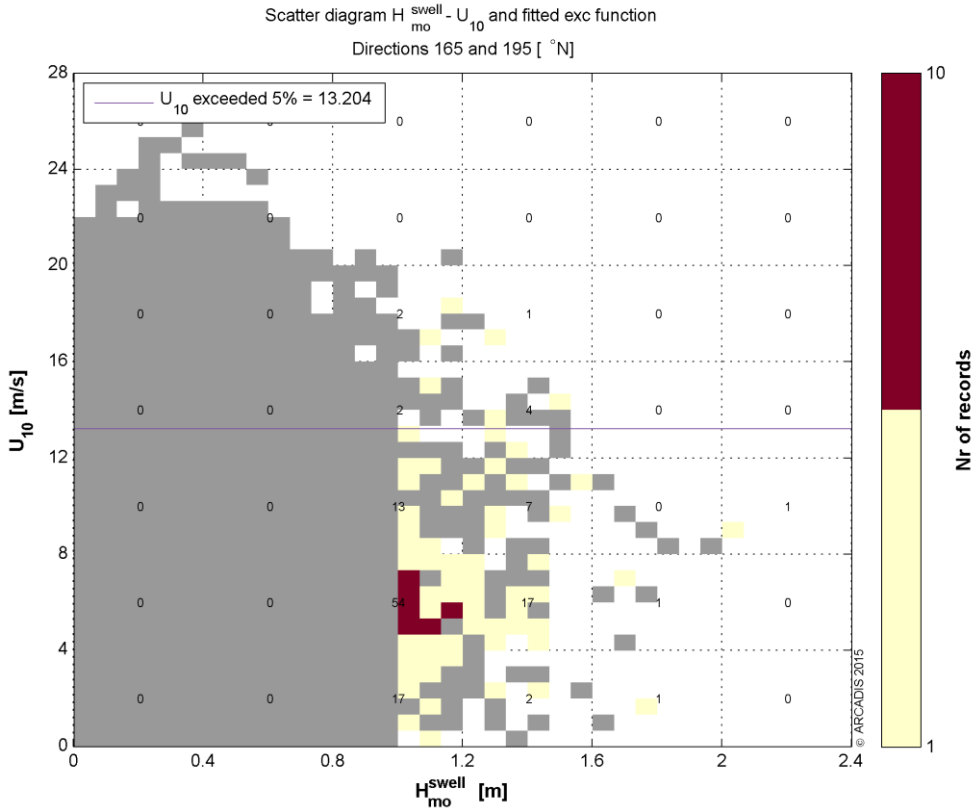

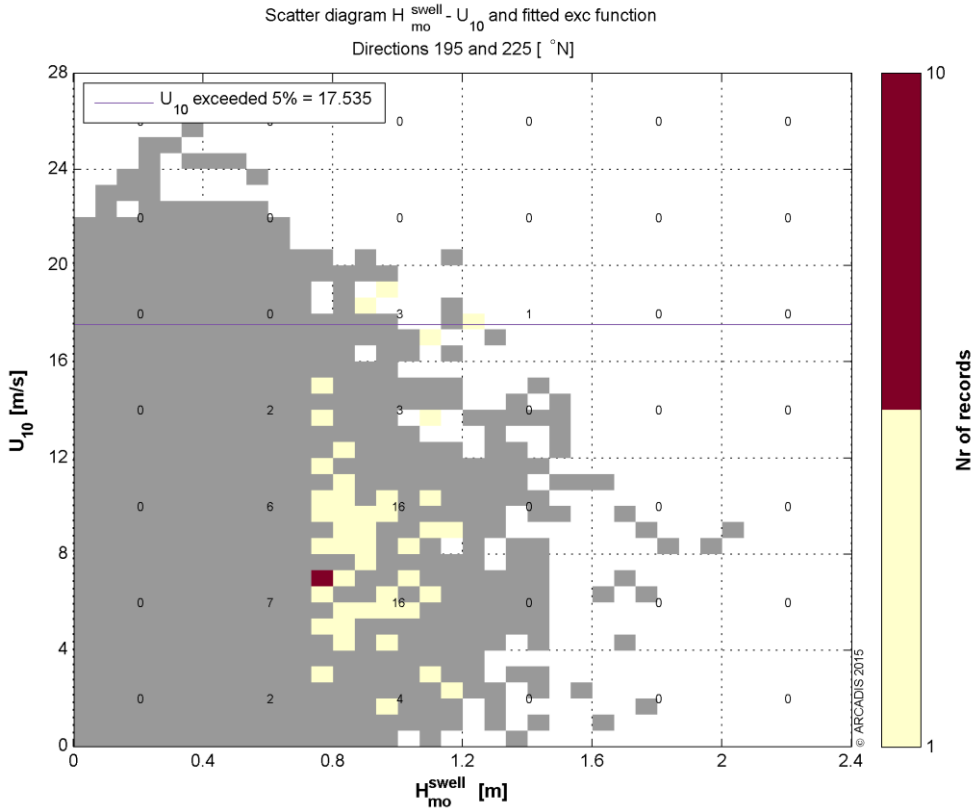

Appendix 6.2 H_{m0} swell vs H_{m0} wind sea

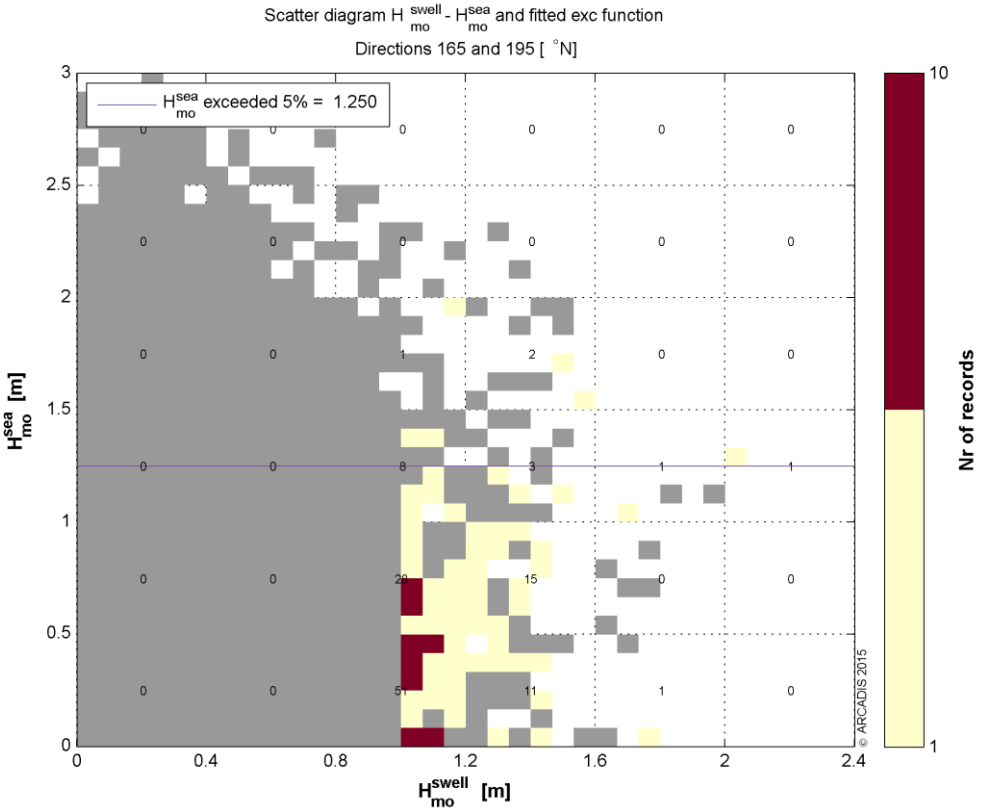

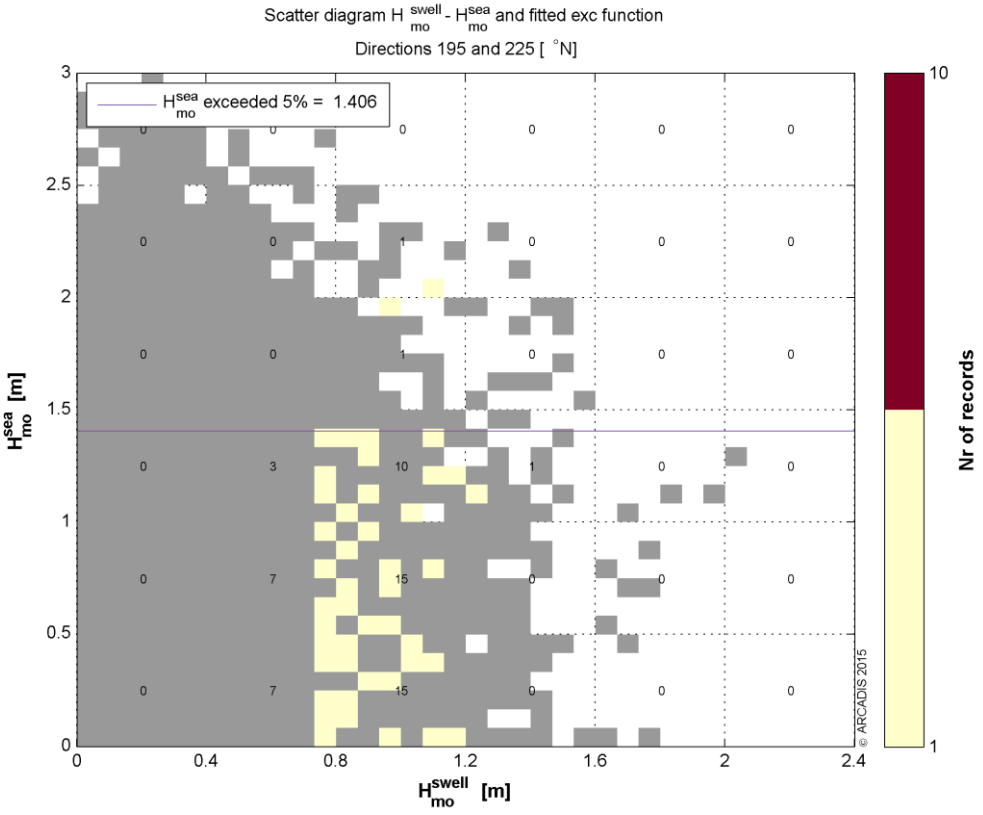

Appendix 6.3 H_{m0} swell vs T_p wind sea

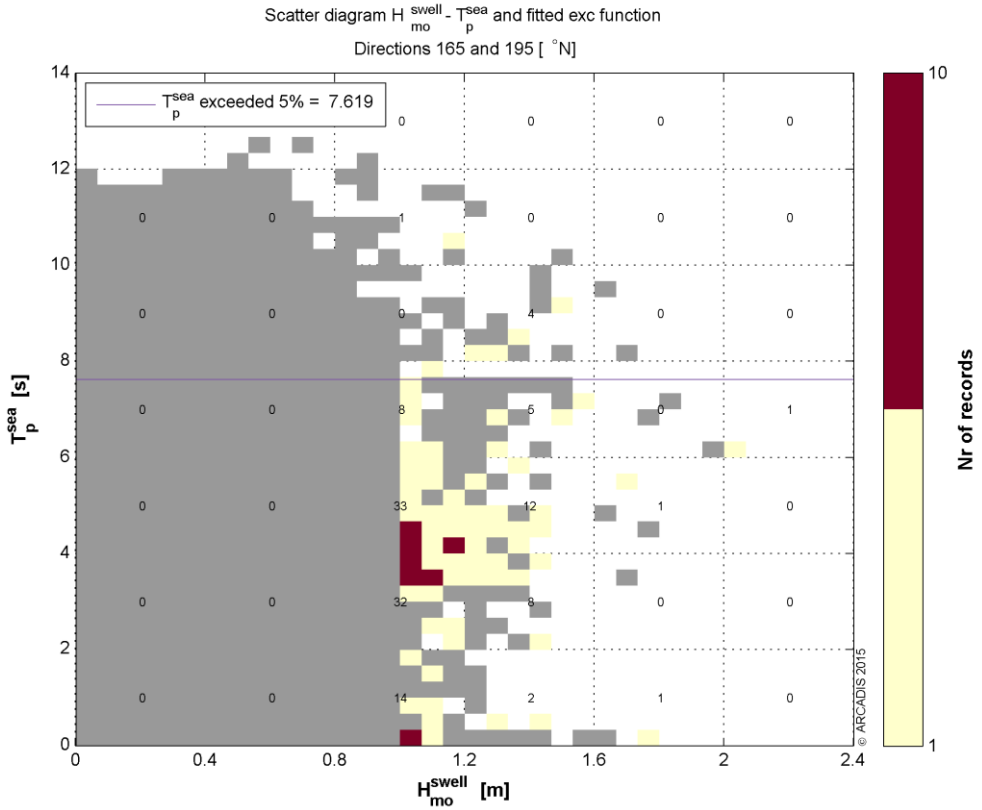

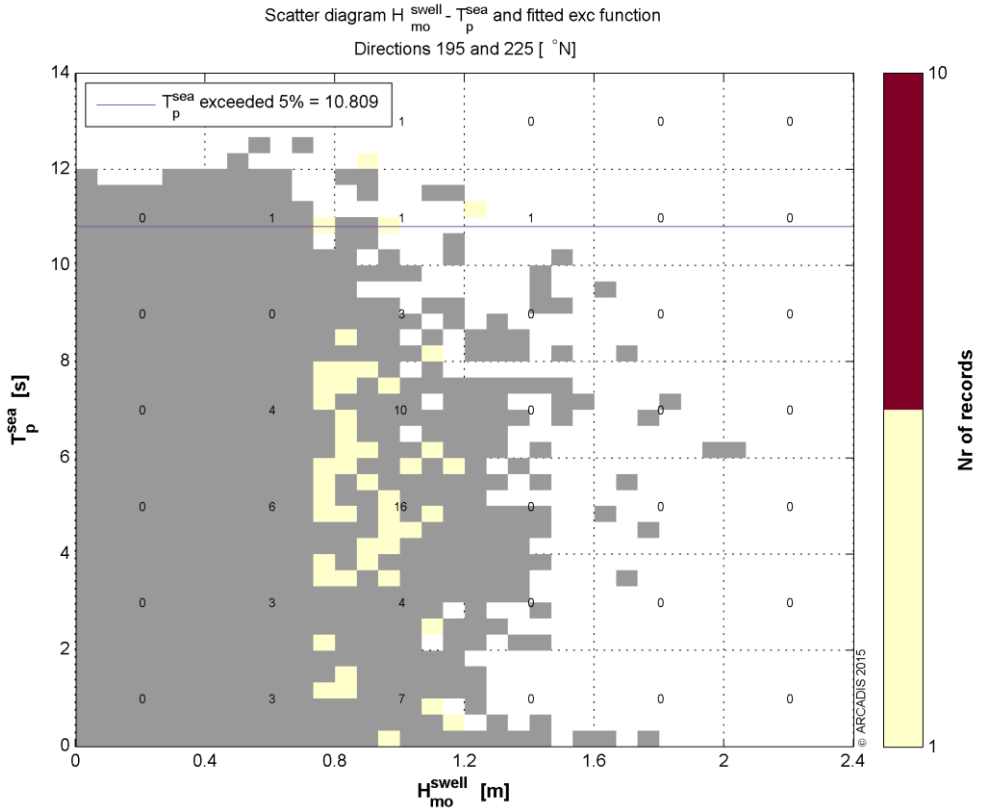

Appendix 6.4 H_{m0} swell vs T_p swell

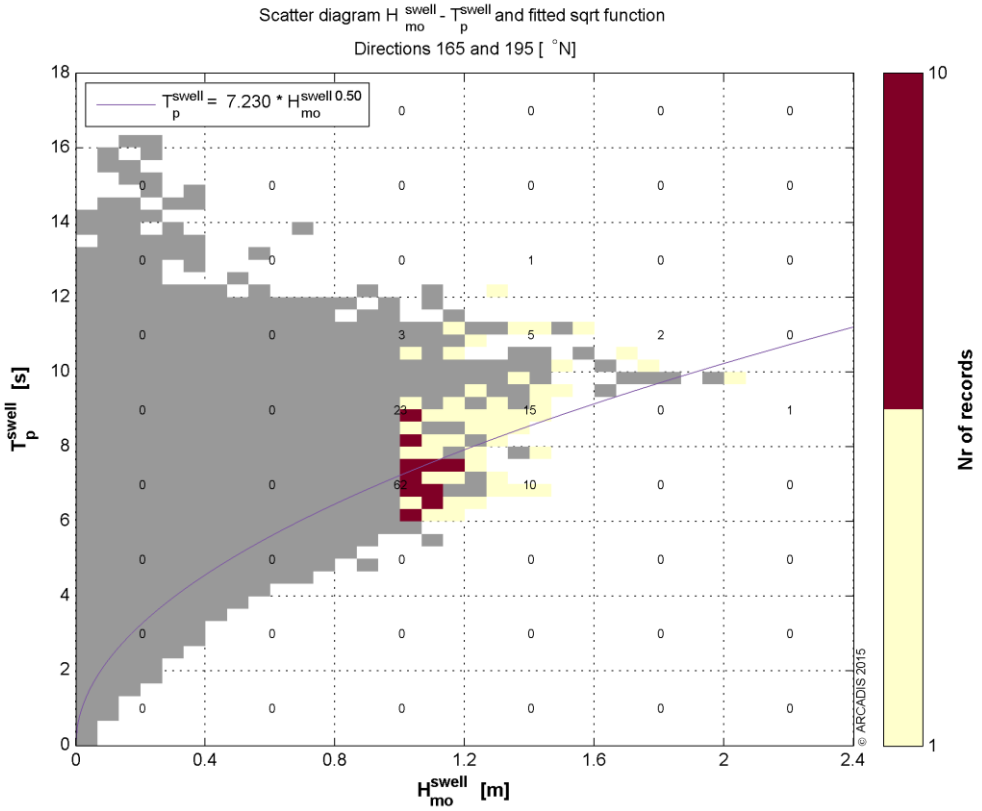

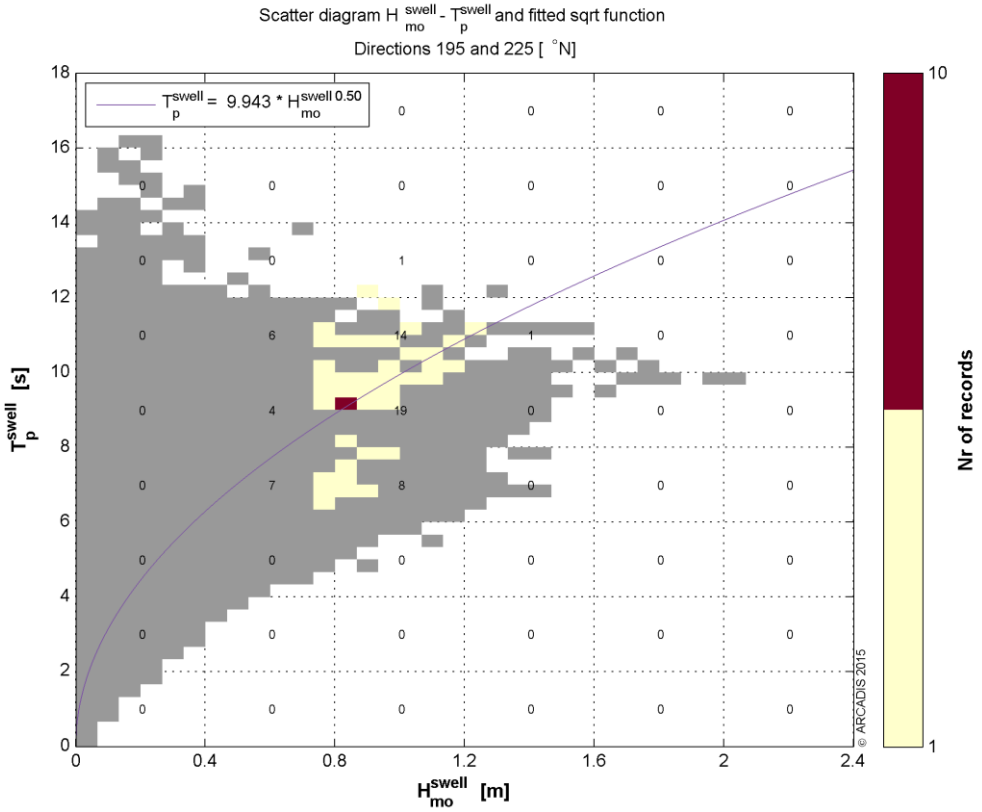

Appendix 7 Figures of H_{m0} vs T_p ranges

Appendix 7.1 H_{m0} wind sea vs T_p wind sea

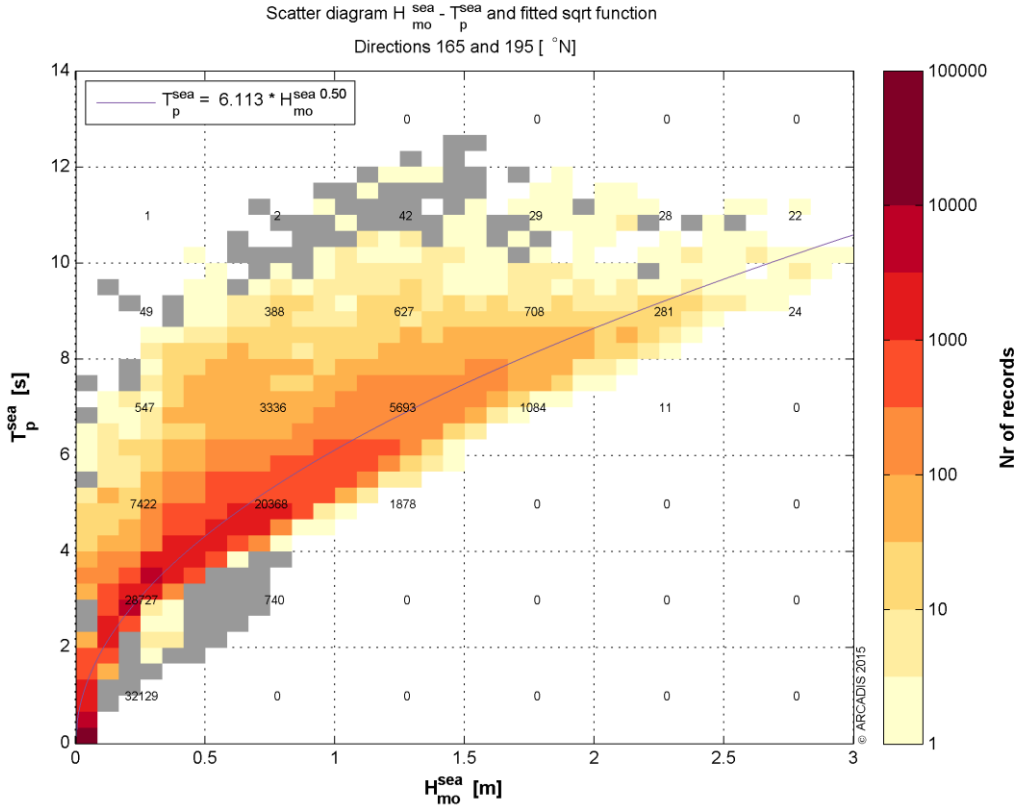

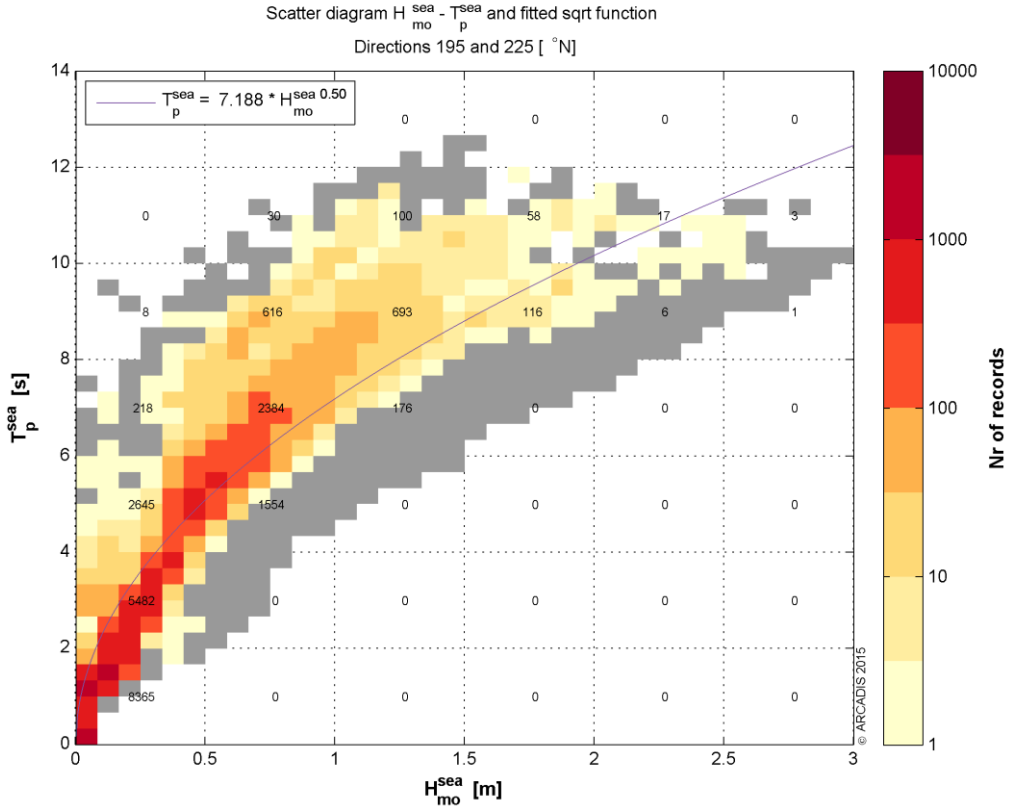

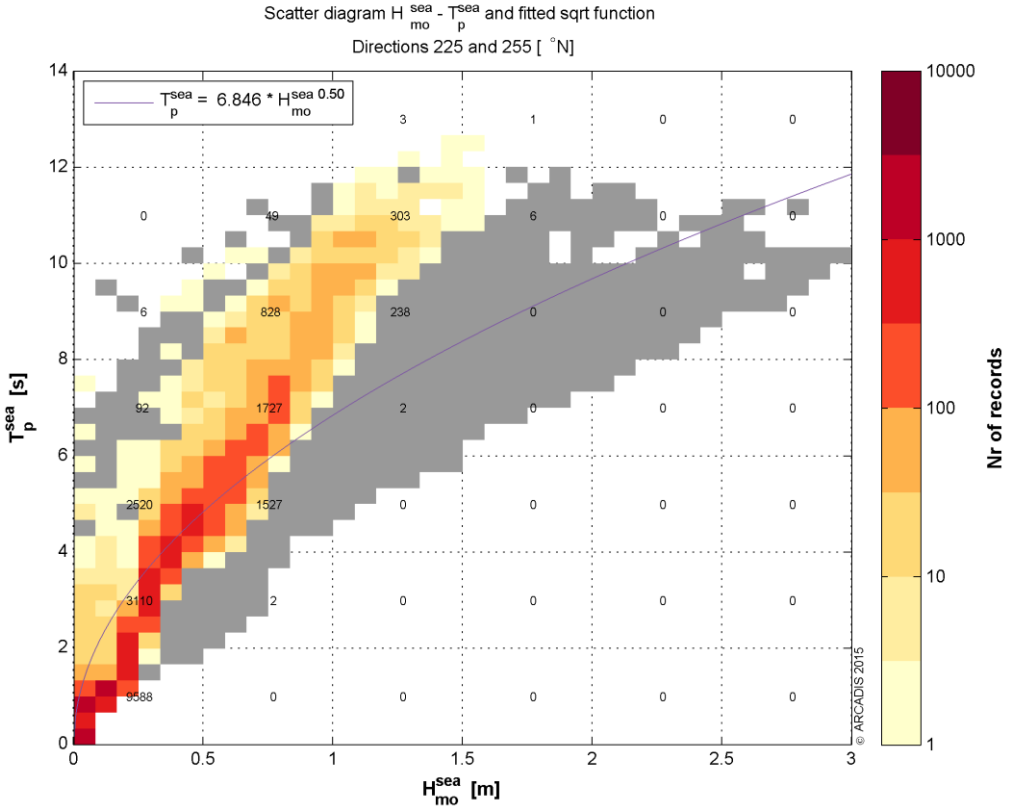
Scatter diagram H sea mo - T sea p and fitted sqrt function
Directions 225 and 255 [°N]
T sea p = 6.846 * H sea 0.50 mo
T sea p [s]
H sea mo [m]
Nr of records
© ARCADIS 2015

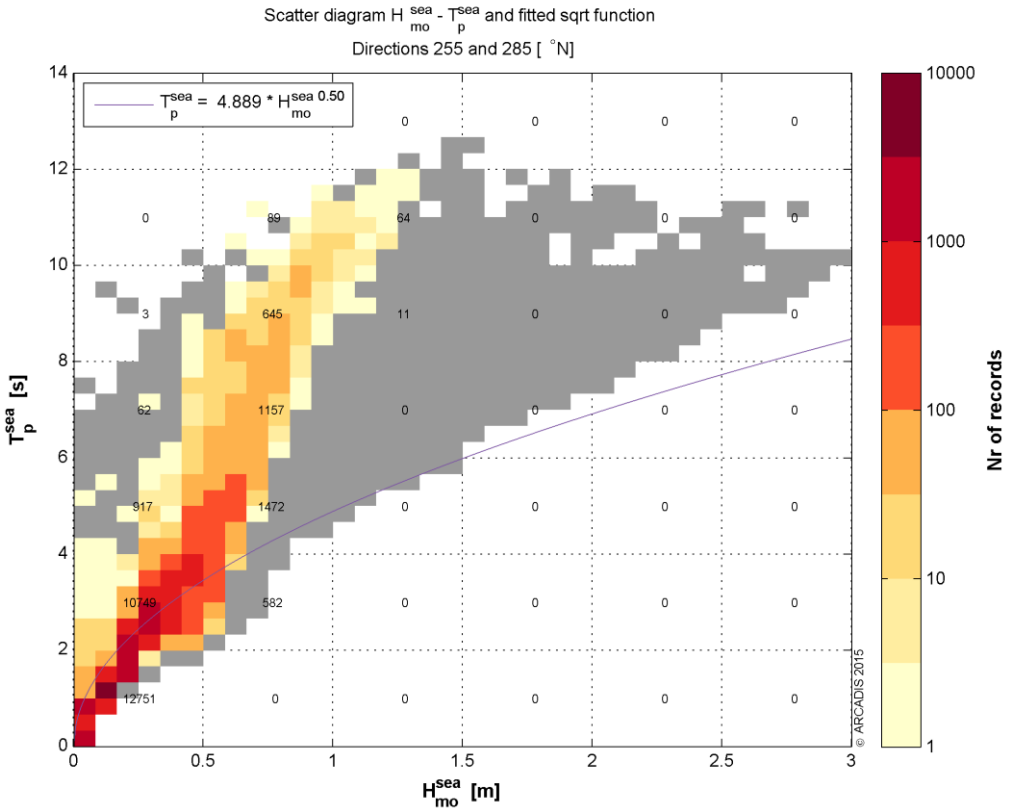
Scatter diagram H sea mo - T sea p and fitted sqrt function
Directions 255 and 285 [°N]
T sea p = 4.889 * H sea 0.50 mo
T sea p [s]
H sea mo [m]
Nr of records
© ARCADIS 2015

Appendix 7.2 H_{m0} swell vs T_p swell

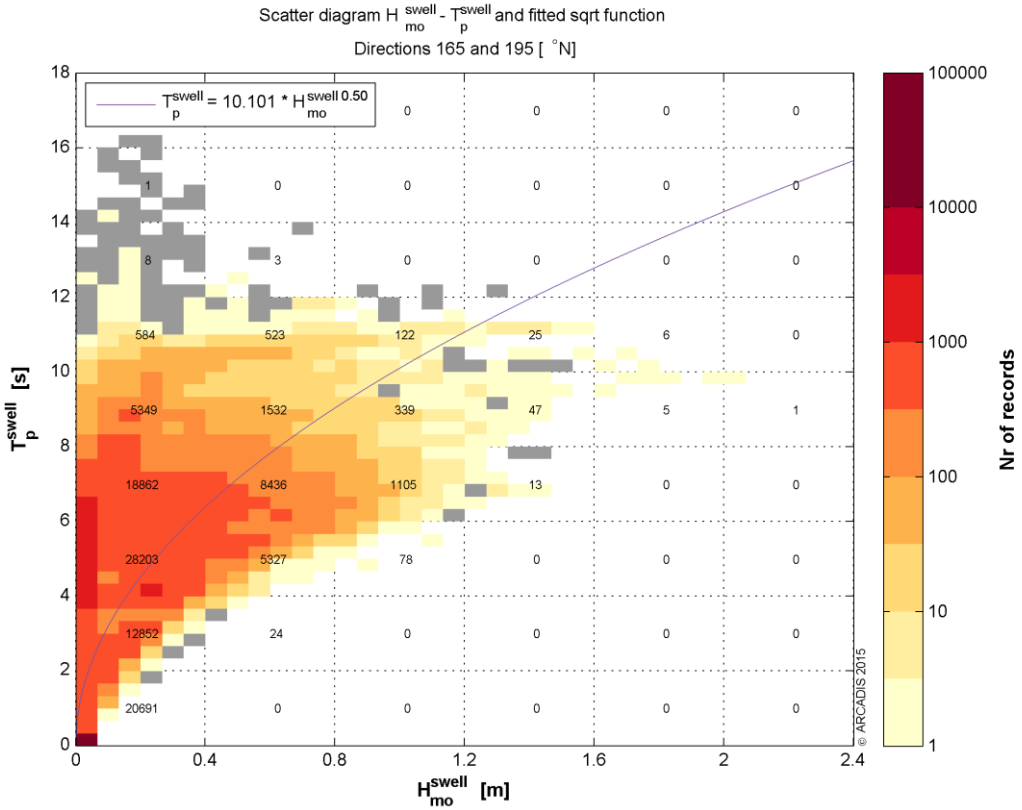

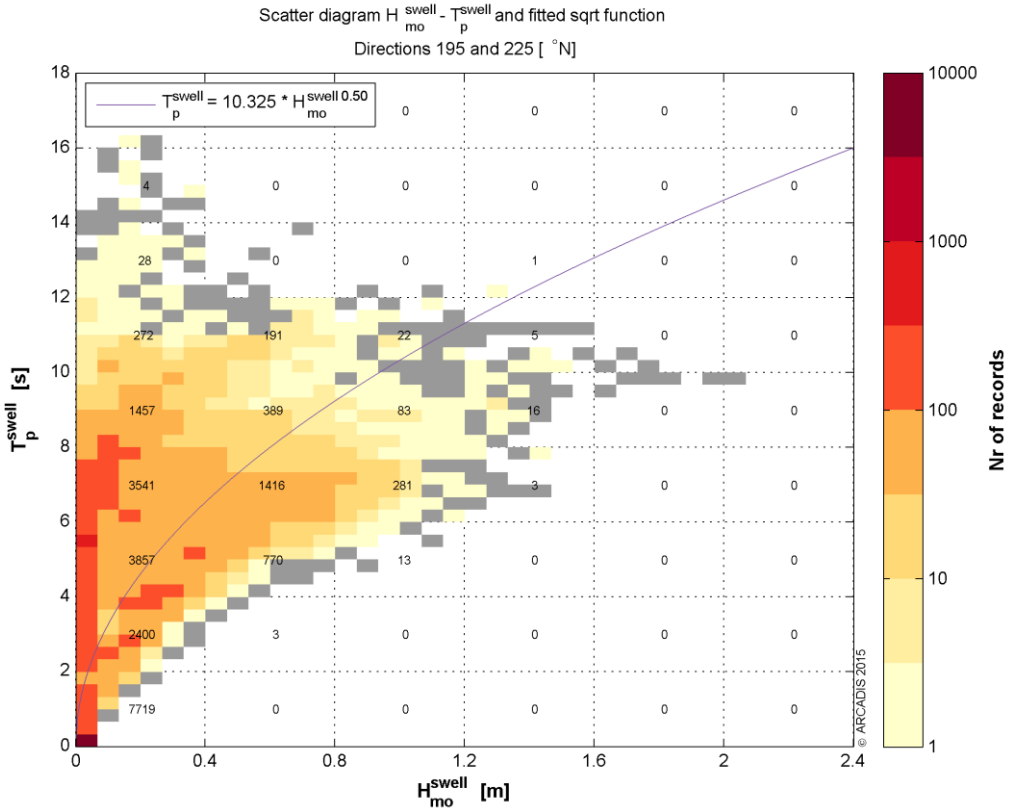

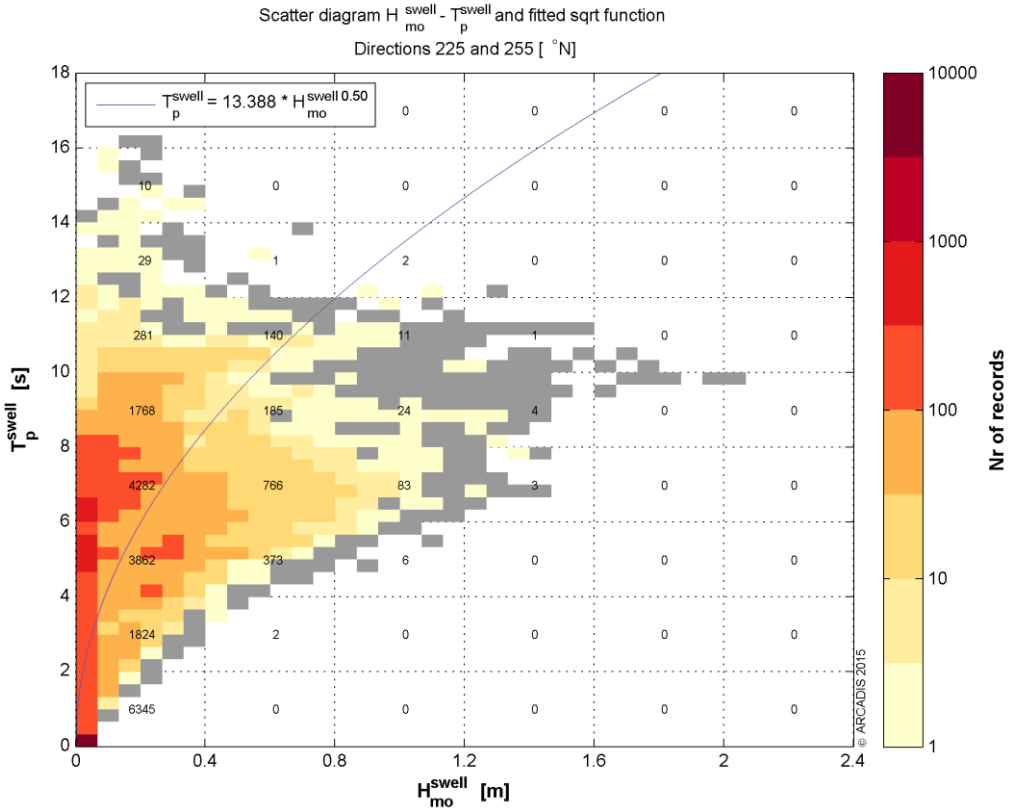
Scatter diagram H mo swell - T p swell and fitted sqrt function
Directions 225 and 255 [°N]
T p swell = 13.388 * H mo swell 0.50
T p swell [s]
H mo swell [m]
Nr of records
© ARCADIS 2015

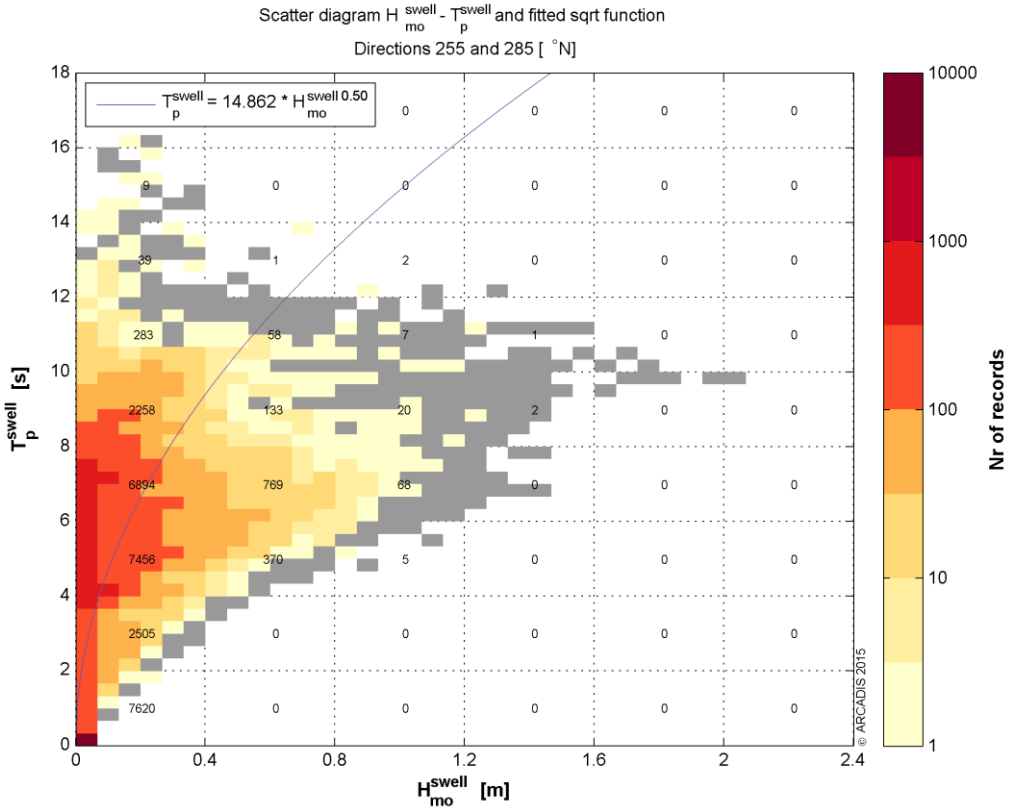
Scatter diagram H mo swell - T p swell and fitted sqrt function
Directions 255 and 285 [°N]
T p swell = 14.862 * H mo swell 0.50
T p swell [s]
H mo swell [m]
Nr of records
© ARCADIS 2015

Appendix 8 Spectra shape for nearshore extreme wave conditions

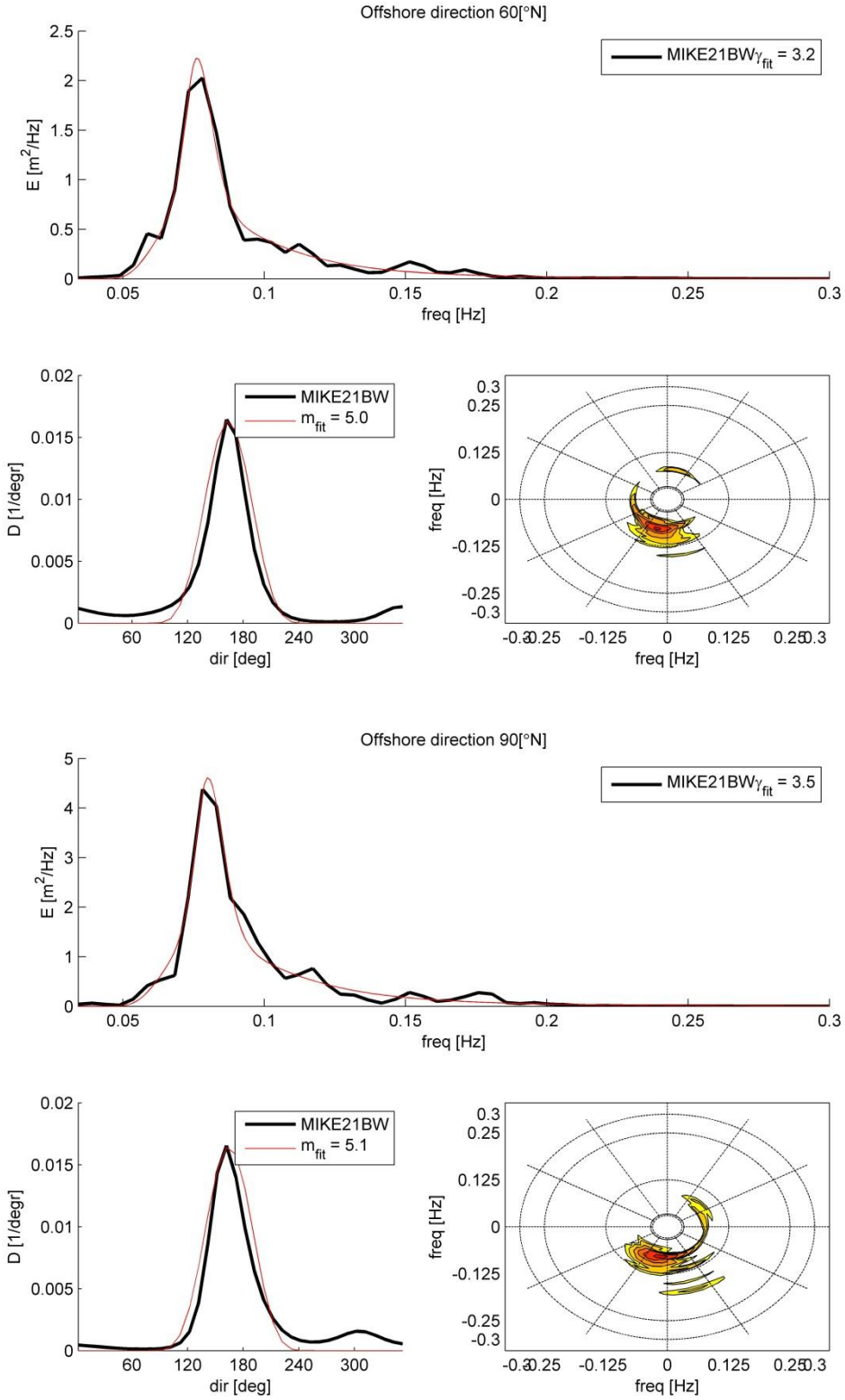

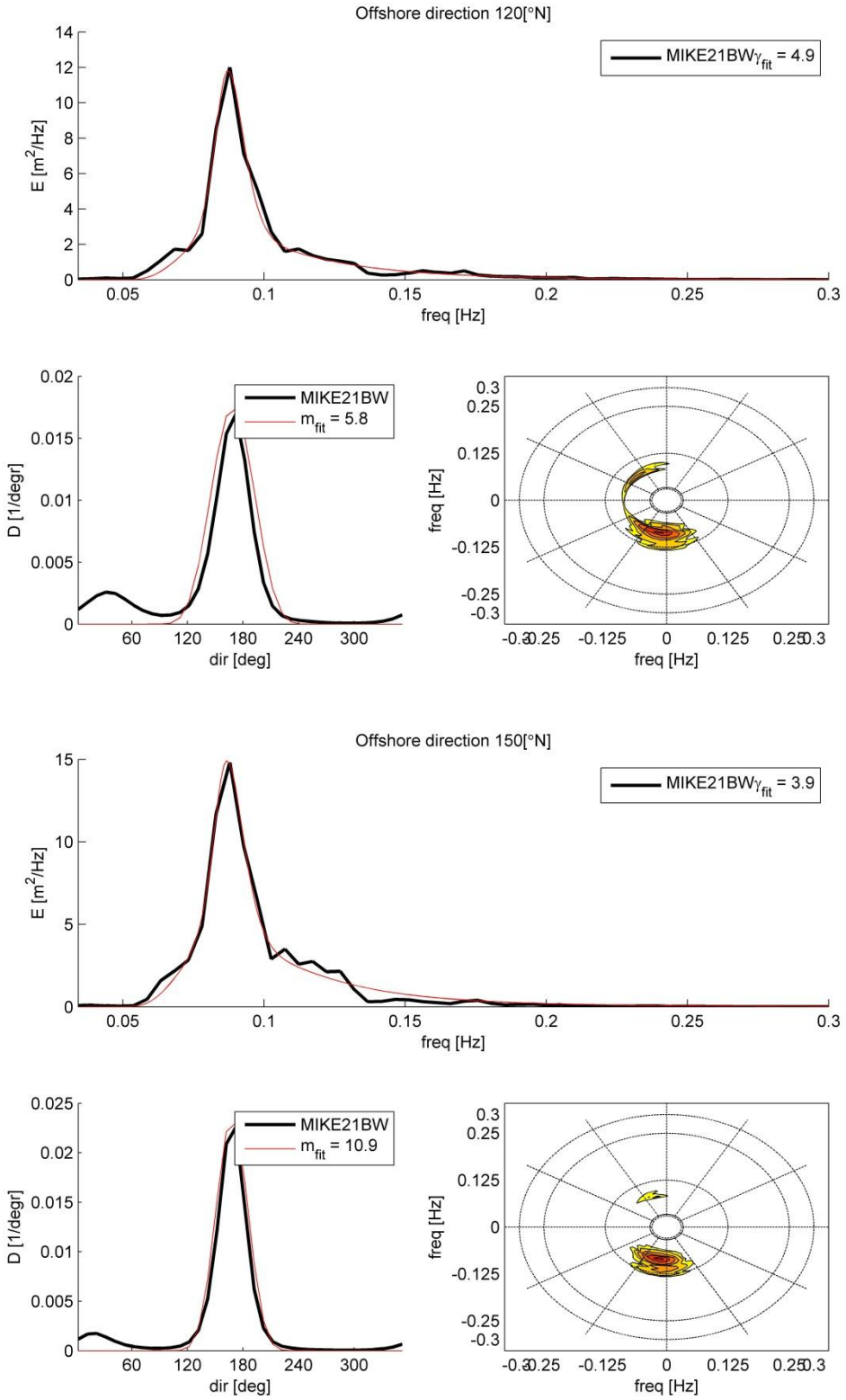
Offshore direction 120[°N]
MIKE21BW γfit = 4.9
E [m2/Hz]
freq [Hz]
MIKE21BW
mfit = 5.8
D [1/degr]
dir [deg]
freq [Hz]
Offshore direction 150[°N]
MIKE21BW γfit = 3.9
E [m2/Hz]
freq [Hz]
MIKE21BW
mfit = 10.9
D [1/degr]
dir [deg]
freq [Hz]

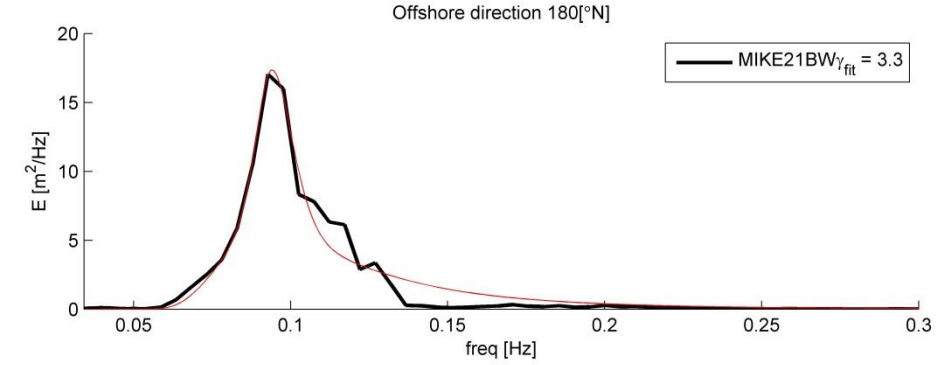
Offshore direction 180[°N]
MIKE21BW γ_{fit} = 3.3
E [m^2/Hz]
freq [Hz]

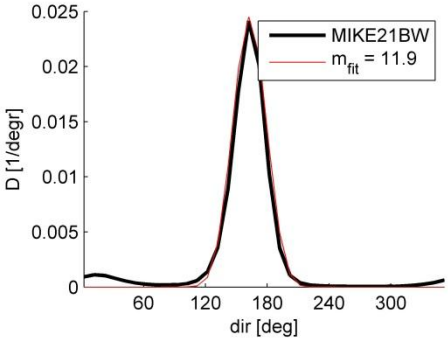
MIKE21BW
m_{fit} = 11.9
D [1/degr]
dir [deg]

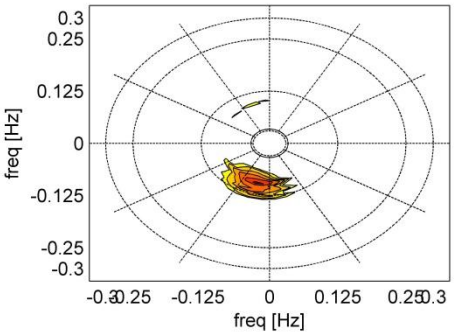
freq [Hz]
freq [Hz]

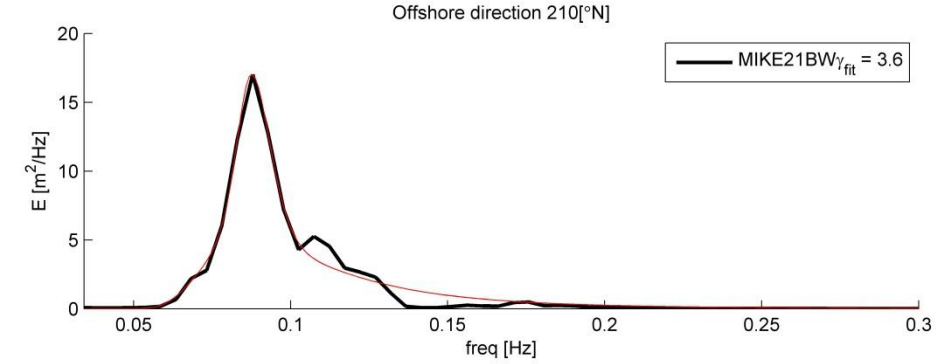
Offshore direction 210[°N]
MIKE21BW γ_{fit} = 3.6
E [m^2/Hz]
freq [Hz]

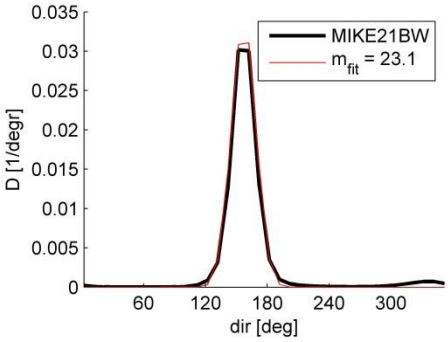
MIKE21BW
m_{fit} = 23.1
D [1/degr]
dir [deg]

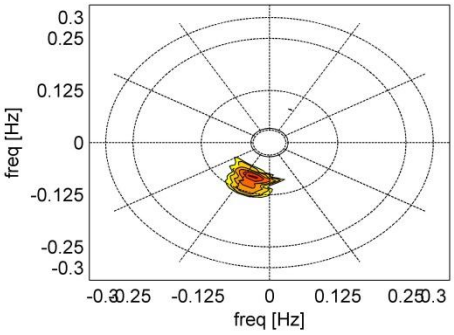
freq [Hz]
freq [Hz]

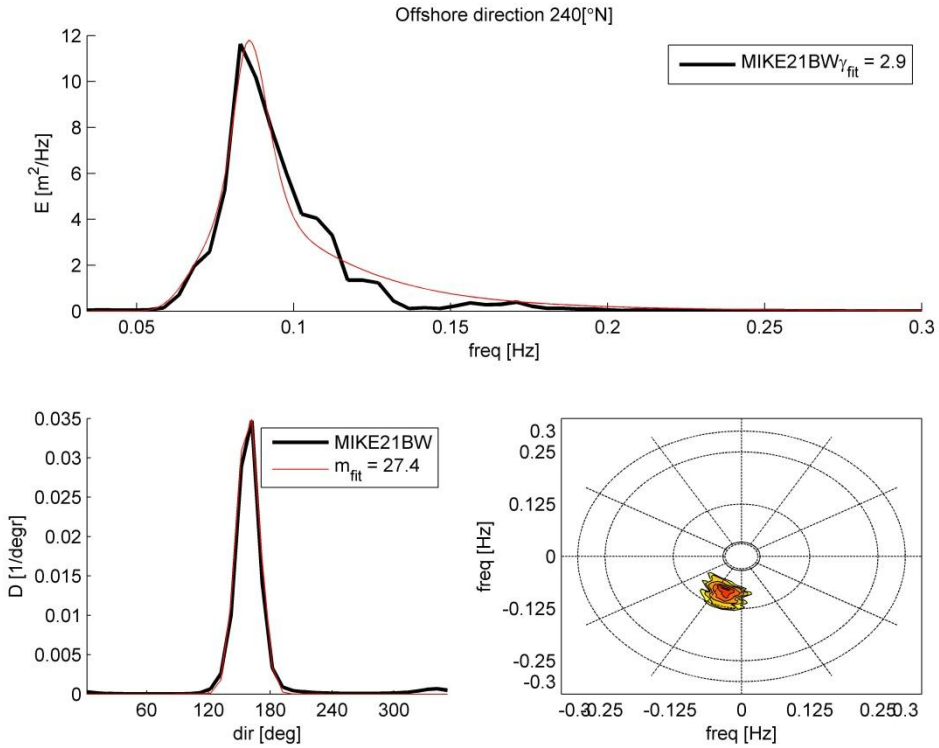
Offshore direction 240[°N]
MIKE21BW γ_{fit} = 2.9
E [m^2/Hz]
freq [Hz]
MIKE21BW
m_{fit} = 27.4
D [1/degr]
dir [deg]
freq [Hz]
freq [Hz]

Appendix 9 Spatial distribution of significant wave height nearby the FSU

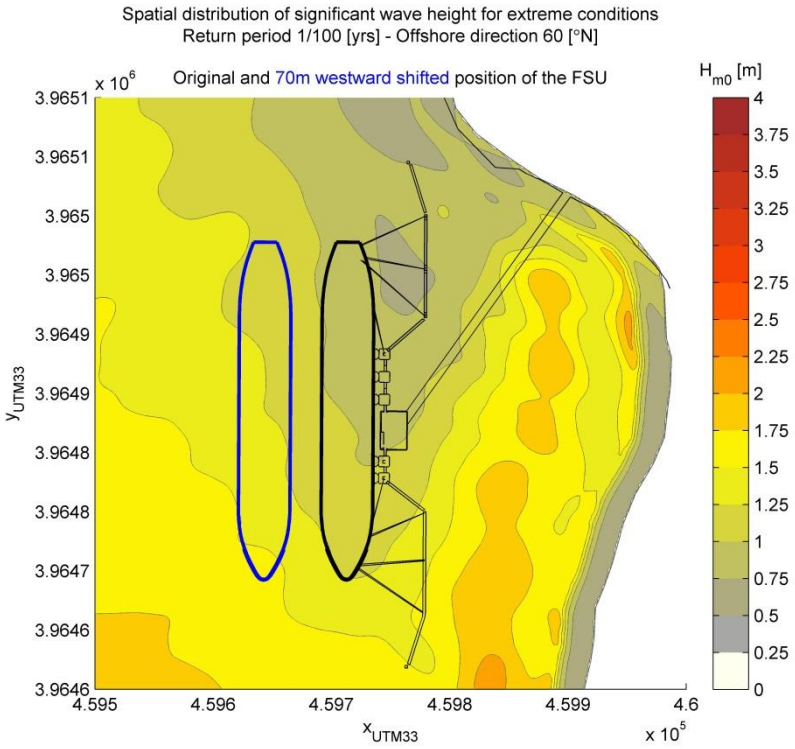

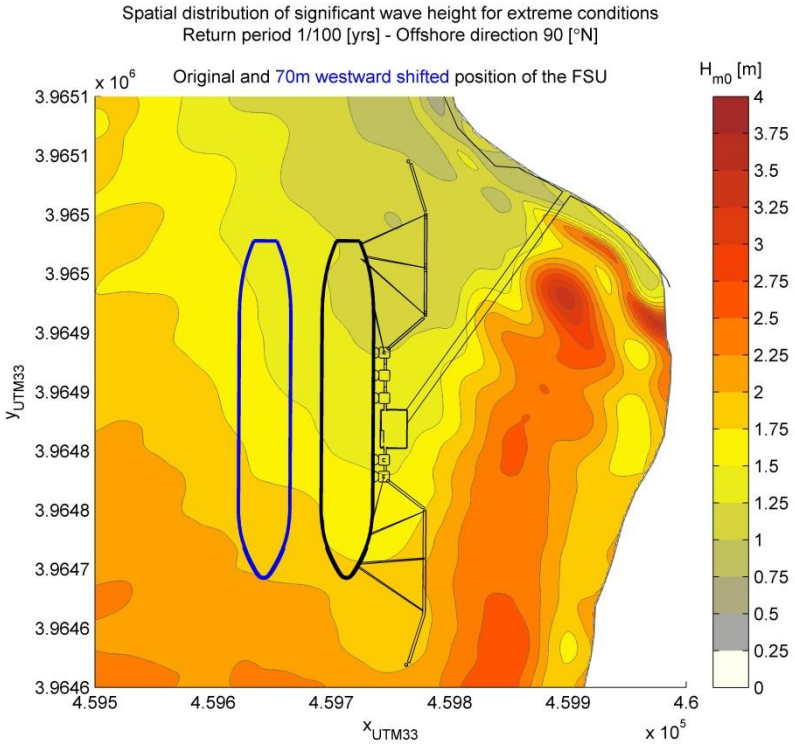

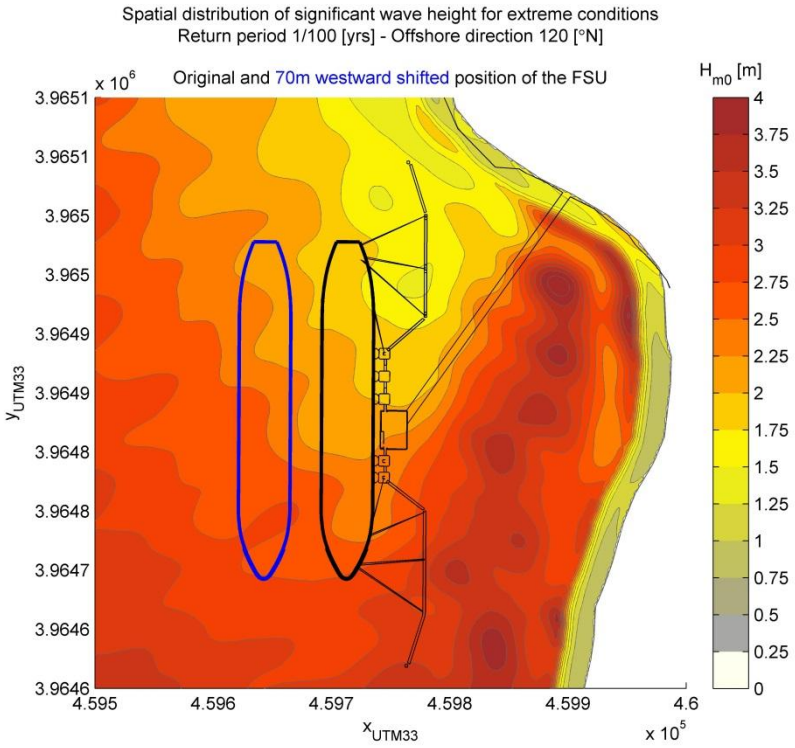
Spatial distribution of significant wave height for extreme conditions
Return period 1/100 [yrs] - Offshore direction 120 [°N]
Original and 70m westward shifted position of the FSU
x 10^6
3.9651
3.9651
3.965
3.965
3.9649
3.9649
3.9648
3.9648
3.9647
3.9646
3.9646
y_UTM33
4.595
4.596
4.597
4.598
4.599
4.6
x_UTM33
x 10^5
H_m0 [m]
4
3.75
3.5
3.25
3
2.75
2.5
2.25
2
1.75
1.5
1.25
1
0.75
0.5
0.25
0

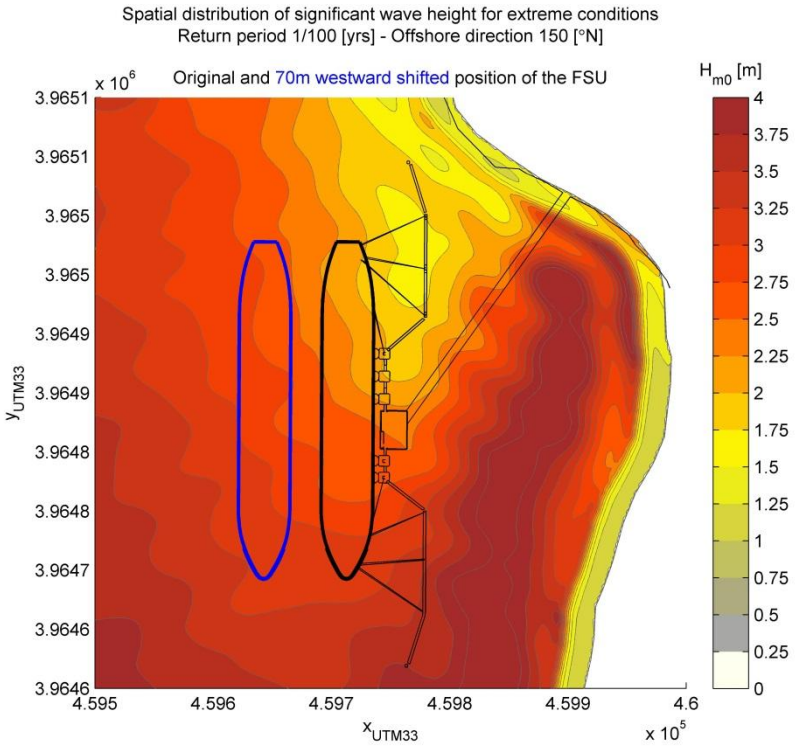
Spatial distribution of significant wave height for extreme conditions
Return period 1/100 [yrs] - Offshore direction 150 [°N]
Original and 70m westward shifted position of the FSU
x 10^6
3.9651
3.9651
3.965
3.965
3.9649
3.9649
3.9648
3.9648
3.9647
3.9646
3.9646
y_UTM33
4.595
4.596
4.597
4.598
4.599
4.6
x_UTM33
x 10^5
H_m0 [m]
4
3.75
3.5
3.25
3
2.75
2.5
2.25
2
1.75
1.5
1.25
1
0.75
0.5
0.25
0

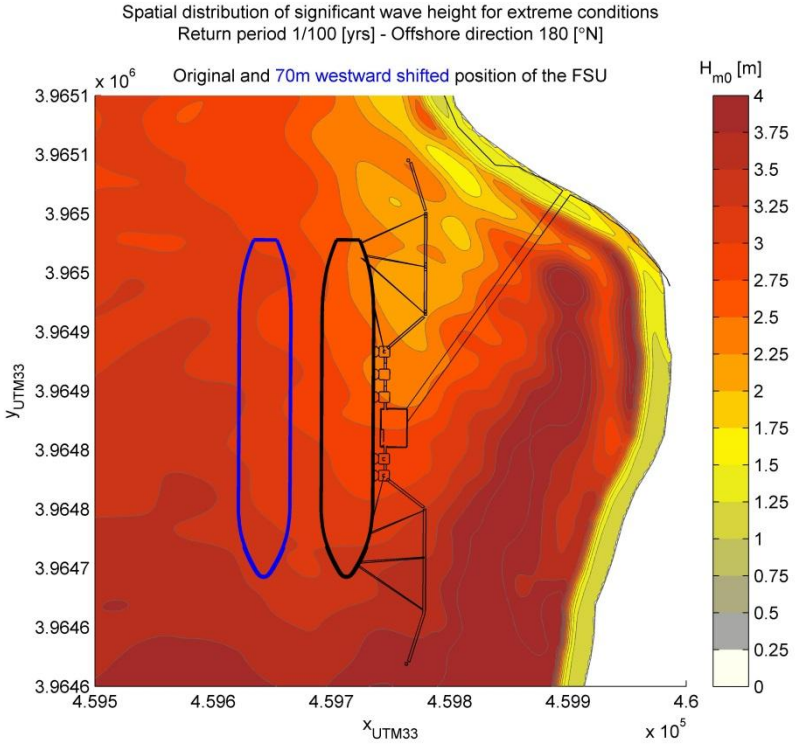
Spatial distribution of significant wave height for extreme conditions
Return period 1/100 [yrs] - Offshore direction 180 [°N]
Original and 70m westward shifted position of the FSU
x 10^6
3.9651
3.9651
3.965
3.965
3.9649
3.9649
3.9648
3.9648
3.9647
3.9646
3.9646
y_UTM33
4.595
4.596
4.597
4.598
4.599
4.6
x 10^5
x_UTM33
H_m0 [m]
4
3.75
3.5
3.25
3
2.75
2.5
2.25
2
1.75
1.5
1.25
1
0.75
0.5
0.25
0

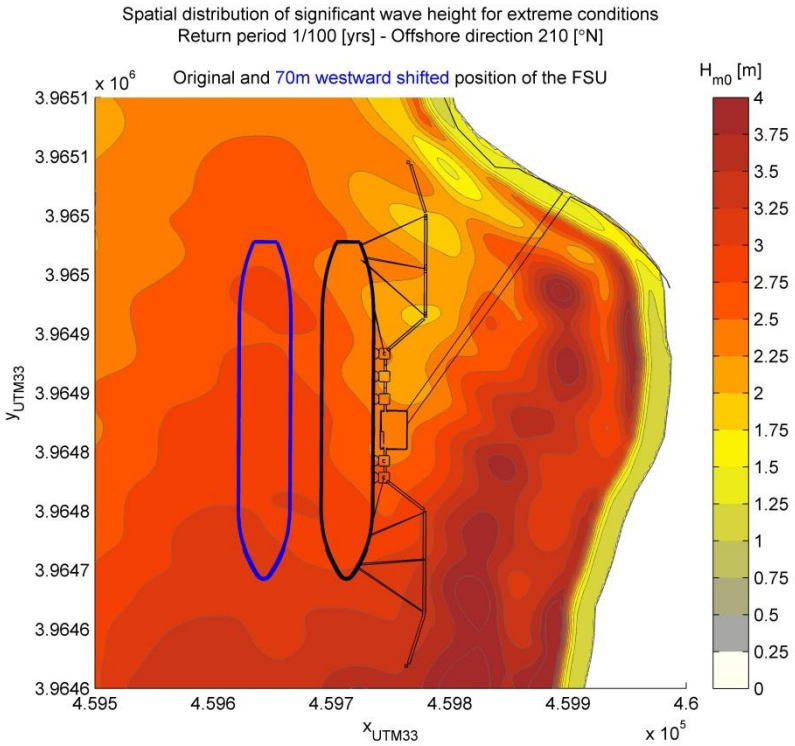
Spatial distribution of significant wave height for extreme conditions
Return period 1/100 [yrs] - Offshore direction 210 [°N]
Original and 70m westward shifted position of the FSU
x 10^6
3.9651
3.9651
3.965
3.965
3.9649
3.9649
3.9648
3.9648
3.9647
3.9646
3.9646
y_UTM33
4.595
4.596
4.597
4.598
4.599
4.6
x 10^5
x_UTM33
H_m0 [m]
4
3.75
3.5
3.25
3
2.75
2.5
2.25
2
1.75
1.5
1.25
1
0.75
0.5
0.25
0

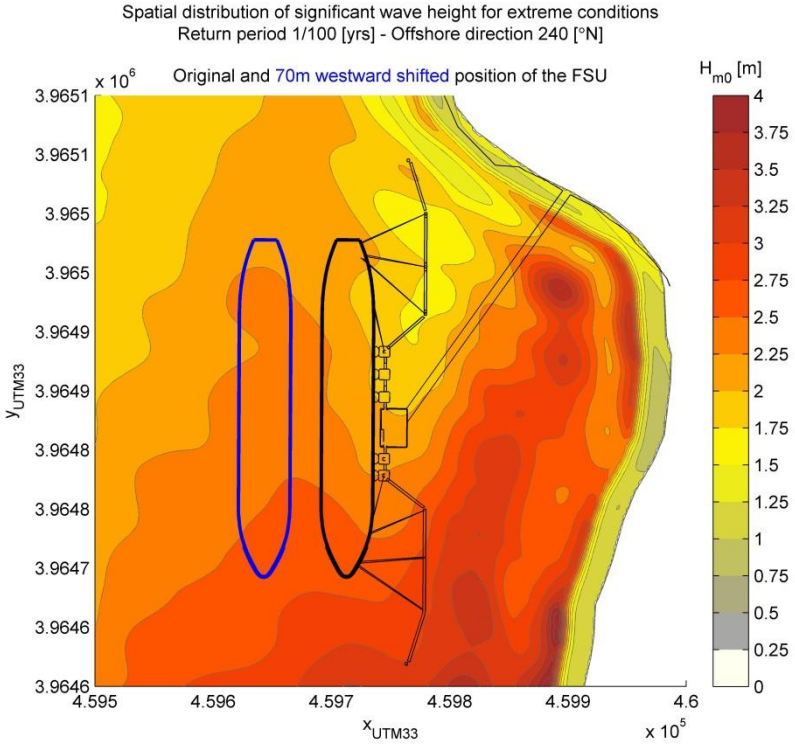
Spatial distribution of significant wave height for extreme conditions
Return period 1/100 [yrs] - Offshore direction 240 [°N]
Original and 70m westward shifted position of the FSU
x 10^6
3.9651
3.9651
3.965
3.965
3.9649
3.9649
3.9648
3.9648
3.9647
3.9646
3.9646
y_UTM33
4.595
4.596
4.597
4.598
4.599
4.6
x 10^5
x_UTM33
H_m0 [m]
4
3.75
3.5
3.25
3
2.75
2.5
2.25
2
1.75
1.5
1.25
1
0.75
0.5
0.25
0

Colophon

NAUTICAL AND RISK STUDIES FOR THE DELIMARA LNG TERMINAL IN MARSAXLOKK PORT, MALTA

ADDITIONAL METOCEAN ANALYSIS

CLIENT:

MARIN

STATUS:

Final

AUTHOR:

Matthijs Bénit (M.Sc.)
Jeroen Adema (M.Sc.)
Jurjen Wilms (B.Eng.)

CHECKED BY:

Gerbrant van Vledder (Ph.D.)

RELEASED BY:

Jaap de Groot (M.Sc.)

21 September 2015
078630641:E

ARCADIS NEDERLAND BV
Hanzelaan 286
P.O. Box 137
8000 AC Zwolle
The Netherlands
Tel +31 38 7777 700
Fax +31 38 7777 710
www.arcadis.nl
Dutch Trade Register 09036504